# Targeting the PI3K/mTOR and ATR/Chk1 Pathways to Improve Radiation Efficacy for Cancer Therapy




## DPhil Thesis

submitted to Oxford University

in fulfilment of the requirements for the degree of

DOCTOR OF PHILOSOPHY

in Radiobiology

HILARY TERM, 2012

by

Emmanouil Fokas, MD

Linacre College
University of Oxford

**Supervisor**

Professor Ruth J Muschel, MD PhD

**Assessment Committee**

Anne Kiltie BM, BCh, MA, DM, MRCP, FRCR

Kaye Williams PhD







The study presented in this thesis was performed at the Department of Oncology, Gray Institute for Radiobiology and Radiation Oncology, Radiobiology Research Institute, University of Oxford, Oxford, GB. This work was supported by grants from Cancer Research UK, the Medical Research Council, the Oxford Cancer Imaging Centre and the NIHR Biomedical Research Centre, Oxford.

*To my father*

# ACKNOWLEDGEMENTS

I would like to thank my supervisor, Professor Ruth J. Muschel, for her continuous help, patience and guidance. I am and will remain grateful to her for giving me the unique opportunity to study for a DPhil in Radiobiology at Oxford University and for everything she has done for me. I have been extremely fortunate to have her as my mentor. I also want to thank Professor W. Gillies McKenna and Professor Thomas B. Brunner for their invaluable support, the encouragement and for the excellent collaboration throughout my DPhil study.

Special thanks go to Dr Remko Prevo for his constant help. A truly great guy to work with, I will most certainly miss his kind and pleasant manner. I thank Dr Tapmeier for being a great "desk mate". Many thanks also to Dr Stanley Liu, Ms Lukxmi Balathasan, Ms Sabira Yameen, Dr Jaehong Im, Dr Veerle Kersemans, Dr Sean Smart, Mr Michael Woodcock, Dr Bart Cornelissen, Dr John Beech, Dr Michio Yoshimura, Dr Sally Hill, Dr Cat Kelly and Dr. Michael Stratford for the helpful contribution. I also want to thank all other colleagues and friends in the Gray Institute for the countless hours of discussions and the good time we spent together. Thanks to Ms Karla Watson and Ms Magda Flieger for their help with the animal work. I have also acknowledged the contributions to the experimental work performed at the beginning of Chapters 3, 4 and 5.

I want to thank my family, especially my lovely mother, which, even though far away, they have always been very close to me in spirit, supporting me with their kind words and love. Last but not least, I would like to express my gratitude to my wife, Sarah J. Moore, for her constant support, encouragement, patience and unconditional love during the last years of my studies.

Even though I probably do not fully appreciate it at the present time, I have the feeling that the last years will most profoundly and positively influence me for the rest of my career. I feel extremely fortunate to have met and worked with some outstanding people at the Gray Institute.

This page was left intentionally blank

# ABSTRACT

The purpose of the present thesis was to better understand the effect of targeting key biological mechanisms in order to improve radiotherapy response. Two important and distinct pathways were targeted using novel agents: (1) the phosphoinoside-3-kinase (PI3K)/Akt/mammalian target of rapamycin (mTOR) pathway; (2) the ataxia telangiectasia-mutated-Rad3-related (ATR)/Chk1 pathway. The role of the PI3K/mTOR signalling pathway in tumour radiosensitivity and tumour microenvironment (TME) was examined using three, recently-developed signalling inhibitors obtained from Novartis Pharma: NVP-BEZ235 (dual PI3K/mTOR inhibitor), NVP-BGT226 (dual PI3K/mTOR inhibitor) and NVP-BKM120 (single PI3K inhibitor). The radiosensitising potential of NVP-BEZ235 and NVP-BGT226 was demonstrated in tumour and endothelial cells. Additionally, a thorough research into the effects of NVP-BKM120 and NVP-BEZ235 on TME showed that oncogenic signalling inhibitors can improve vascular morphology and increase tumour oxygenation and perfusion in tumour xenograft models, resulting in improved radiation response. Furthermore, a highly potent and selective ATR inhibitor, VE-822, that was obtained from Vertex Pharmaceuticals (Europe) Ltd, was tested in pancreatic ductal adenocarcinoma (PDAC) cells and tumour xenograft models. ATR inhibition by VE-822 resulted in sensitisation of tumour cells but not normal cells to radiation and gemcitabine. Similarly, VE-822 strongly enhanced radiation- and chemoradiation-induced tumour growth delay in tumour xenograft models. Importantly, VE-822 did not potentiate radiation-induced gastrointestinal tract epithelial damage. To summarize, the impact of targeting two distinct pathways in combination with radiation and chemoradiation was explored. Inhibition of the PI3K/mTOR and ATR/Chk1 signalling pathways increases response of tumours to radiotherapy they and might be promising

targeting strategies for cancer treatment. These findings have considerable translational implications and future clinical trials should aim to validate these observations.

# Table of Contents


## CHAPTER 1 ..... 1

General Introduction ..... 1

1.1. Introduction ..... 2

1.2 Biological determinants of radiation sensitivity and the therapeutic ratio and side effects ..... 4

1.2.1 Tumour hypoxia ..... 6

1.2.2 Definition of Hypoxia ..... 6

1.2.3 Abnormal tumour vascularity and hypoxia pathogenesis ..... 7

1.2.4 Tumour angiogenesis ..... 9

1.3 Consequences of TME for cancer treatment ..... 11

1.3.1 The impact of tumour hypoxia ..... 11

1.3.2 The impact of tumour vasculature on cancer treatment ..... 12

1.3.3 The mechanical barrier of abnormal tumour vasculature and interstitium ..... 13

1.4 The PI3K/mTOR pathway and indirect antiangiogenic strategies ..... 15

1.4.1 Introduction ..... 15

1.4.2 The PI3K/mTOR pathway: role, structure and signalling in cancer ..... 15

1.4.3 Antiangiogenic therapy ..... 16

1.4.4 The role of PI3K/Akt/mTOR pathway in normal and tumour angiogenesis ..... 18

1.4.5 Indirect targets of tumour angiogenesis and their combination with radiation and/or chemotherapy ..... 21

1.5 The ATR/Chk1 pathway in DNA damage signalling and cancer therapy ..... 26

1.5.1 Introduction ..... 26

1.5.2 The DNA damage response ..... 27

1.5.3 ATR structure and the phosphoinositide 3-kinase related kinase (PIKK) family ..... 28

1.5.4 The ATR/Chk1 checkpoint pathway in cell cycle ..... 28

1.5.5 ATR/Chk1 pathway activation in response to various stimuli ..... 31

1.5.6 Targeting the ATR pathway in combination with chemoradiation for cancer therapy ..... 31
1.5.7 ATR inhibition, replication stress and synthetic lethality ..... 34
1.5.8 Efficacy of Chk1 inhibitors ..... 36
1.6 Pancreatic cancer: clinical and biological evidence and role of radiotherapy ..... 38
1.7 Outline and purpose of the thesis ..... 41
**CHAPTER 2** ..... 44
Materials and Methods ..... 44
2.1 Cell culture ..... 45
2.2 Dual PI3K/mTOR inhibitors treatment ..... 46
2.3 ATR inhibitor preparation and treatment ..... 46
2.4 Biochemical and cellular inhibition of ATR and related kinases ..... 47
2.5 Clonogenic survival assay ..... 47
2.6 Analysis of protein phosphorylation. ..... 48
2.7 Analysis of γH2AX foci ..... 49
2.8 Cell cycle assay ..... 51
2.9 Analysis of apoptosis *in vitro* ..... 52
2.10 Capillary tube formation and endothelial cell migration ..... 53
2.11 Xenograft studies using PI3K and PI3K/mTOR inhibitors ..... 54
2.11.1 Tumour xenograft growth delay assay ..... 54
2.11.2 *In vivo* real-time optical and ultrasound imaging ..... 55
2.11.3 Microscopy, Immunostaining and VEGF ELISA ..... 57
2.12 Xenograft studies using ATR inhibition ..... 60
2.12.1 Tumour xenograft growth delay assay ..... 60
2.12.2 Immunostaining and microscopy ..... 61
2.13 Statistical analyses ..... 63
**CHAPTER 3** ..... 64

BEZ235 and BGT226 enhance tumour and endothelial cell radiosensitivity ..... 64

3.1 Introduction ..... 65

3.2 RESULTS ..... 67

3.2.1 BGT226 and BEZ235 inhibit PI3K and mTOR activity and reduce AKT and S-6 phosphorylation ..... 67

3.2.2 BGT225 and BEZ235 reduce radiation survival of tumour cells with EGFR overexpression or Ras mutation ..... 68

3.2.3 BEZ235 radiosensitises tumour cells under hypoxic conditions ..... 71

3.2.4 BEZ235 induces apoptosis in SQ20B cells and increases necrosis in tumour ..... 72

3.2.5 Radiosensitisation induced by the dual PI3K/mTOR inhibitors is accompanied by persistence of γH2AX foci and cell cycle arrest ..... 73

3.2.6 BEZ235 blocks PI3K/mTOR signalling and sensitises endothelial cells to irradiation ..... 76

3.2.7 BEZ235 increases DNA damage and necrosis in irradiated endothelial cells ..... 77

3.2.8 BEZ235 attenuates tube formation in irradiated endothelial cells ..... 78

3.2.9 BEZ235 attenuates migration in irradiated endothelial cells ..... 79

3.3 DISCUSSION ..... 80

3.4 CONCLUSION ..... 84

**CHAPTER 4** ..... 85

Inhibition of the PI3K/mTOR pathway by NVP-BEZ235 and NVP-BKM120 normalizes tumour vasculature to increase radiation sensitivity ..... 85

4.1 Introduction ..... 86

4.2 RESULTS ..... 88

4.2.1 Dose response of BEZ235 and BKM120 in HT1080 and FaDu xenografts ..... 88

4.2.2 PI3K/mTOR inhibition reduces tumour hypoxia and increase perfusion in a dose-dependent fashion ..... 89

4.2.3 BEZ235 and BKM120 promote vascular normalization and remodelling ..... 92

4.2.4 The effect of BEZ235 on radiation response ..... 96

4.2.5 Hypoxia, perfusion and vascular morphology in irradiated tumours ..... 98

4.3 DISCUSSION ..... 105

4.4 CONCLUSION ..... 109

**CHAPTER 5** ..... 110

Targeting ATR *in vivo* using the novel inhibitor VE-822 results in selective sensitisation of pancreatic tumours to radiation ..... 110

5.1 Introduction ..... 111

5.1 RESULTS ..... 112

5.1.1 VE-822 inhibits Chk1 phosphorylation and sensitises pancreatic cancer cells to radiation *in vitro* ..... 112

5.1.2 VE-822 does not increase normal cell radiosensitivity and chemosensitivity *in vitro* ..... 116

5.1.3 VE-822 enhances residual DNA damage *in vitro* ..... 118

5.1.4 VE-822 disrupts DNA damage-induced cell cycle checkpoint ..... 120

5.1.5 VE-822 increases radiation and gemcitabine-induced apoptosis ..... 121

5.1.6 Efficacy of VE-822 with radiotherapy in pancreatic tumour xenografts ..... 123

5.1.7 VE-822-mediated tumour radiosensitisation *in vivo* is dose-dependent ..... 126

5.1.8 VE-822 increases gemcitabine-mediated radiosensitisation in pancreatic tumour xenografts ..... 128

5.1.9 VE-822 does not increase tissue toxicity *in vivo* ..... 130

5.1.10 The effect of VE-822 on tumour vessel density ..... 132

5.1.11 The effect of VE-822 on tumour proliferation ..... 133

5.2 DISCUSSION ..... 135

5.3 CONCLUSION ..... 137

**CHAPTER 6** ..... 138

Summary and Future Perspectives ..... 138

6.1 Introduction ..... 139

6.1.1 Therapeutic targeting of the PI3K/Akt/mTOR pathway .....139
6.1.2 Therapeutic targeting of the ATR/Chk1 pathway .....151
6.1.3 References .....157

# List of abbreviations

ADME: Absorption, distribution, metabolism, and excretion
AML: Acute myeloid leukemia
ATM: ataxia telangiectasia-mutated
ATR: ATM-Rad3-related
ATRIP: ATR-interacting protein
BCA: Bicinchoninic acid assay
BM: Basement membrane
BMDCs: Bone marrow-derived cells
BRCT: BRCA1 carboxyl-terminal
CEP: Circulating bone marrow-derived endothelial progenitor cells
CI: Confidence interval
$CO_2$**:** Carbon dioxide
CTV: Clinical target volume
DAPI: 4',6-diamidino-2-phenylindole
DDR: DNA damage response
DLL4: Delta-like ligand 4
DMEM: Dulbecco's Modified Eagle Medium
DMF10: Dose modifying factor 10%
DMSO: Dimethyl sulfoxide
DNA: Deoxyribonucleic acid
DNA-PK: DNA protein kinase
DSBs: Double strand DNA breaks
DTPA: Diethylene triamine pentaacetic acid
EC: endothelial cell
EDTA: Ethylenediaminetetraacetic acid
EGFR: Epidermal growth factor receptor
EGFR: epidermal growth factor receptor
ELISA: Enzyme-linked immunosorbent assay
eNOS: endothelial nitric oxide synthase
FACS: Fluorescence-activated cell sorting
FCS: Fetal calf serum
FDA: Food Drug Administration
FGF: Fibroblast growth factor
FITC: Fluorescein isothiocyanate
FTIs: Farnesyltransferase inhibitors
GTV: Gross tumour volume
H&E: Haematoxylin and eosin
HCC: Hepatocellular carcinoma
HDMVC: Human dermal microvascular cells
HDMECs: Human dermal microvascular endothelial cells
HER2: human epidermal growth factor receptor 2
HF: Hypoxic fraction

HIF: Hypoxia inducible factor
HR: Homologous recombination
HRE: Hypoxia responsive element
HRG: histidine-rich glycoprotein
HRP: Horseradish peroxidase
HRR: Homologous recombination repair
HUVEC: Human umbilical venous endothelial cells
ICRU: International Commission on Radiation Units
IFN-γ: Interferon-γ
IFP: Interstitial fluid pressure
Ig: Immunoglobulin
IGRT: Image-guided radiotherapy
IM: internal margin
IMRT: intensity-modulated radiotherapy
ITV: Internal target volume
KGF: keratinocyte growth factor
LeTx: anthrax lethal toxin.
MAPK: mitogen-activated protein kinase,
MLL: mixed lineage leukemia
MRE: Mre11-Rad50-Nbs1 complex
mTOR: mammalian target of rapamycin
NER: Nucleotide excision repair
NOS: Nitric oxide synthase
NSCLC: non-small cell lung cancer
$O_2$: Oxygen
OER: Oxygen enhancement ratio
p.o.: per os
PC: pericyte
PDAC: Pancreatic ductal adenocarcinoma
PDGF: Platelet derived growth factor
PE: Plating efficiency
PHD: prolyl hydroxylase domain protein
PI: Propidium iodide
PI[4,5]P2: phosphatidylinositol 4,5-bisphosphate
PI3K: phosphatidylinositol 3-kinase
PIKK: Phosphoinositide 3-kinase related kinase
PRD: PIK regulatory domain
PTEN: Phosphatase and tensin homologue deleted in chromosome 10
PTV: Planning target volume
Raptor: Regulatory-associated protein of mTOR.
RFC: replication factor C
Rgs5: G-protein signalling 5
Rictor: Rapamycin-insensitive companion of TOR
RNA: Ribonucleic acid

ROI: Region of interest
RPE: R-Phycoerythrin
RS: Replication stress
RTKs: Receptor tyrosine kinases
SD: Standard deviation
SDF-1: stromal cell-derived factor-1
SNPs: Single nucleotide polymorphisms
SPECT: Single photon emission computed tomography
SSBs: Single strand DNA breaks
TBGS: Tocopheryl polyethylene glycol 1000 succinate
TBS: Tris Buffered Saline
TME: Tumour microenvironment
TMZ: Temozolomide
TORC: target of rapamycin complex
TSP-1: Thrombospondin-1
TUNEL: Terminal deoxynucleotidyl transferase dUTP nick end labelling
TUNEL: Transferase dUTP nick end labeling
TV400: time for tumour to reach a volume of 400 $mm^3$
TV600: time for tumour to reach a volume of 600 $mm^3$
UV: Ultraviolet
VDA: Vascular disruptive agents
VEGF: Vascular endothelial growth factor
VEGFR: Vascular endothelial growth factor receptor
VOI: Volume of interest
VOI: Volume of interest
XRT: Radiation

# CHAPTER 1

# General Introduction

# 1.1. Introduction

In the UK, around 309,500 people were diagnosed with cancer in 2008. This equates to around 504 cases for every 100,000 people. In 2009, there were 156,090 deaths from cancer reported in the UK. The death rates from cancer rise with increasing age and the majority of cancer deaths occur in those aged over 65 (77%). Today, millions of people are diagnosed and live with cancer or have had cancer.

Radiotherapy plays a pivotal role in the management of many tumours and approximately 50% of all cancer patients will receive radiotherapy during the course of their illnesses [1]. There are different indications for prescribing radiotherapy including definitive treatment with curative intent, neoadjuvant treatment, alone or in combination with chemotherapy, to downstage the tumour and enhance resectability, adjuvant therapy with the purpose of eradicating microscopic residual disease, and finally as a palliative tool [2]. Significant technical improvements have occurred in recent years that enable accurate targeting and better radiotherapy delivery. New techniques such as three-dimensional conformal RT (3D-CRT), intensity-modulated RT (IMRT) and image-guided RT (IGRT) allow radiation dose escalation and more precise dose deposition in the tumour while limiting its delivery to critical normal structures [3, 4].

Radiotherapy is a localised treatment and the definition of tumour and target volumes is crucial to its successful application that necessitates accurate characterisation of tumour's location and extent [5]. Diagnostic imaging, including computer tomography, ultrasonography, magnetic resonance imaging and, more recently, positron emission tomography (PET) and single-photon emission computed tomography (SPECT) are essential for precise radiotherapy planning. The volumes used for clinical radiotherapy are defined by the International Commission on Radiation Units (ICRU) report 50 and the supplement ICRU 62. There are three main volumes in radiotherapy planning [5]. The first

defines the extent and position of gross tumour and it is known as the gross tumour volume (GTV). The second volume is known as the clinical target volume (CTV) and includes the GTV plus a margin to account for possible subclinical disease spread that cannot be fully imaged. The third volume is known as the planning target volume (PTV) and includes the CTV plus a margin to allow for uncertainties in planning or treatment delivery. The PTV is designed to ensure that radiotherapy dose is actually delivered to the CTV. With the advent of modern radiotherapy techniques, such as IGRT, two recent planning concepts include the internal margin (IM) and the internal target volume (ITV). IM takes into account variations in size, shape, and position of the CTV relative to anatomic reference points; e.g., filling of bladder, movements of respiration. These internal variations results in change in site, size, and shape of the CTV. The ITV encompasses the CTV and IM. Apart from the primary tumour, the adjacent organs at risk (OAR) need to be contoured and planned to consider dose delivery to critical normal tissue structures. Radiotherapy planning highly depends on detailed and high quality imaging [5].

Despite the technological advances, the rate of local recurrence and treatment failure after radiotherapy or even combined chemoradiotherapy remains high for many tumour entities. Indeed, even though radiotherapy can result in high survival rates in certain tumours (head and neck, prostate, early stage non-small cell lung cancer), the outcome for many cancer sites such as advanced non-small cell lung cancer, glioblastoma, sarcoma, bladder cancer and others remains poor [4].

Although different clinical factors such as very late diagnosis and advanced tumour stage, geographical miss during radiotherapy course and incomplete staging can contribute to the poor outcome, it is becoming increasingly clear that biological factors play a crucial role in treatment failure [6, 7]. In recent years, elaborate molecular mechanisms of the way tumours respond to radiation have been uncovered. Accumulating evidence indicates that a

better understanding of the way cancer biology affects and determines radiotherapy efficacy will probably help identifying important molecular targets [7, 8]. Such an approach has the potential of improving the therapeutic outcome by combining novel biological agents with radiotherapy or chemoradiotherapy.

## 1.2 Biological determinants of radiation sensitivity and the therapeutic ratio and side effects

Ionising radiation can affect tumours in many different ways. In 1975 Withers proposed a model which indicated that the probability of local tumour control after fractionated radiotherapy is affected by four main factors [9]. The four "R's" of radiation biology included repair, repopulation, redistribution and reoxygenation. While the first two processes render the tissue more resistant to ionising radiation, the last two tend to make it more sensitive [9]. Later, Steel and colleagues proposed intrinsic cellular radiosensitivity as a fifth 'R' in order to explain the impact that different oncogenic pathway signalling and deficient DNA repair have on radiation-induced cell killing [10].

One of the fundamental concepts in radiation biology is what is termed the therapeutic ratio [11]. The therapeutic ratio is a risk-versus-benefit approach used when a radiotherapeutic regimen is planned and it is highly relevant to the incorporation of novel biological agents to radiotherapy to optimize treatment outcome. Theoretically, all malignant tumours could be eradicated by administering very high doses of radiation. In reality, however, this is impossible as the total dose is limited by the biologic consequences and the adverse effects of radiation to normal tissues. Importantly, a balance needs to be maintained between the probability of efficient tumour control and the probability of radiation-induced toxicity of normal tissues. Hence, the objective of any cancer treatment and, relevant to this thesis, the incorporation of a potential radiosensitising agent to radiotherapy, should aim to improve the likelihood of tumour

control without producing unacceptable normal tissue damage. The concept of therapeutic ratio can be illustrated graphically in Figure 1. Both radiotherapy efficacy and normal tissue damage are correlated to the dose of radiation (or cytotoxic drugs), and this relationship is commonly described by a sigmoid curve.

The maximum tolerated dose (MTD) of new agents needs to be carefully investigated in phase I clinical studies to avoid late side effects of irradiation [12]. Late side effects include skin fibrosis and telangiectasia, cataracts, tooth decay, cardiopulmonary diseases, hypothyroidism, infertility, incontinence, diarrhoea, cognitive and memory deficits, osteoporosis and also increased risk of second cancers. These are induced by vascular damage mediated by inflammatory and coagulation cascades and also oxidative stress, resulting in fibrosis [12, 13]. Cytokines and molecules involved in this process include the transforming growth factor (TGF)-β, thrombin, Rho GTPases, proteinase-activated receptor 1, keratinocyte growth factor (KGF), endothelial nitric oxide synthase (eNOS), the renin-angiotensin system and also mesenchymal stem cells. Several agents that modulate these factors are currently under investigation [13].

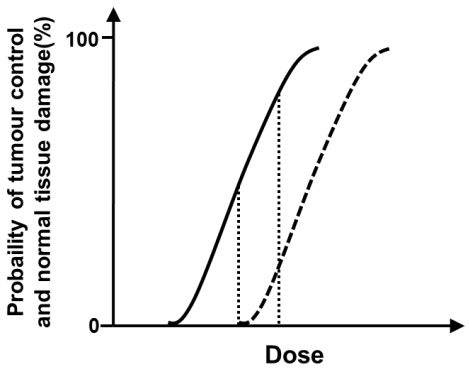



**Figure 1.** The therapeutic ratio is the ratio of the doses of a cancer treatment(s) that produce(s) the same probability of antitumour effect and normal tissue damage. The solid line indicates the local tumour control dose-response curve, and the dotted line represents the normal tissue damage dose-response curve for a given degree of late side effects. The two vertical lines illustrate two dose levels which might be chosen. The dashed line to the left represents a dose level at which no patient experiences the given severity of normal tissue damage. The dotted line to the right represents a dose level at which patients achieve a better local tumour control but at the cost of increased normal tissue damage. Selective radiation sensitisers should lead to a positive therapeutic ratio i.e. inflict more damage to

the tumour cell than to normal tissue, shifting the therapeutic dose-response curve to the left (adapted from [11]).

## 1.2.1 Tumour hypoxia

In 1955 Thomlinson and Gray conducted histological studies in specimens from human lung cancer and showed that cells were consistently growing in cords running parallel to vascularized stroma [14]. In large tumours, they observed a necrotic core surrounded by a viable rim of tumour cells next to a blood vessel. They proposed that the viable rim, found at 170 μm in width, was consisted of hypoxic tumour cells and attributed necrosis to the insufficient oxygen ($O_2$) and nutrient supply of distant cells [14]. Following investigations reported similar findings in cervical and renal cancer [15]. These pioneering studies were the first to demonstrate that tumour cells are exposed to an $O_2$ gradient that decreases gradually from the periphery to the tumour core. There is now overwhelming evidence that hypoxia commonly occurs in animal tumours and a large proportion of human tumours [16-18]. Indeed, the presence of hypoxic tissue areas is a characteristic pathophysiological property of solid tumours, especially in advanced stage, and hypoxia has been documented in a wide range of human malignancies [16, 17].

## 1.2.2 Definition of Hypoxia

Ambient air is 21% $O_2$ (150 mm Hg) but the majority of mammalian tissues exist at 2%-9% $O_2$ (40 mm Hg average). The state of reduced $O_2$ availability or decreased $O_2$ partial pressures below critical thresholds is defined as hypoxia and results in limitations of cellular or organ functions [19]. In tumours, the term hypoxia is used to describe critical $O_2$ levels below which different pathophysiological effects progressively occur. The oxygenation status of tumours can be described by four different parameters including the median tumour $pO_2$ value, the fraction of $pO_2$ values $\leq$2.5 mmHg (hypoxic fraction 2.5; HF 2.5), the fraction of $pO_2$ values $\leq$5 mmHg (HF 5), and the fraction of $pO_2$ values $\leq$10 mmHg (HF 10) [19].

## 1.2.3 Abnormal tumour vascularity and hypoxia pathogenesis

Hypoxia is known to increase both invasion and metastasis, therefore, contributing to more aggressive disease [17]. Over 50% of locally advanced tumours present hypoxic and even anoxic areas, with extreme heterogeneity within the tumour mass [20, 21]. Hypoxia occurs due to the imbalance between oxygen supply and oxygen demand in tissues [17, 21]. Indeed, in normal tissues the supply of oxygen is well matched to the metabolic requirements of the tissue. In contrast, tumour and also stromal cells outweigh the insufficient oxygen supply [17, 19, 21]. This is predominantly due to the inadequate perfusion that is commonly encountered in tumours due to the severe structural and functional abnormalities of tumour vasculature.

Tumour vasculature is characterised by a chaotic, poorly functional vessel architecture and increased interstitial fluid pressure (IFP) that result in oxygen depletion and extracellular acidosis [22-25]. The morphological characteristics of new blood vessels produced within tumours include marked capillary sprouting, convoluted and excessive branching, distorted vessels, erratic blood flow, shunting, lack of proper pericyte coverage, enlarged basement membrane, leakiness and microhaemorrhaging. Poorly connected endothelial cells, loosely-associated vascular smooth muscle cells and an increase in vesiculo-vacuolar organelles all contribute to this hyperpermeable phenotype, and hence, intravascular fluids and plasma proteins can easily extravasate [22-25] (Fig. 1).

Another major factor that can contribute to the development of hypoxia is anaemia, either tumour-associated or therapy-induced, as it is commonly encountered after chemotherapy [26, 27]. Similarly, heavy smokers often have functional anaemia due to the blockade of haemoglobin transportation by carboxyhaemoglobin formation which can also contribute to poor tumour oxygenation [26]. In addition, tumour cells are often perfused by plasma (mostly transiently), whereby only few malignant cells can be adequately supplied

with oxygen, mainly at the arterial end. Organ-specific limitation in oxygen supply can also contribute to hypoxia formation, as it occurs in primary or metastatic liver tumours which receive supply by the portal vein [21, 28].

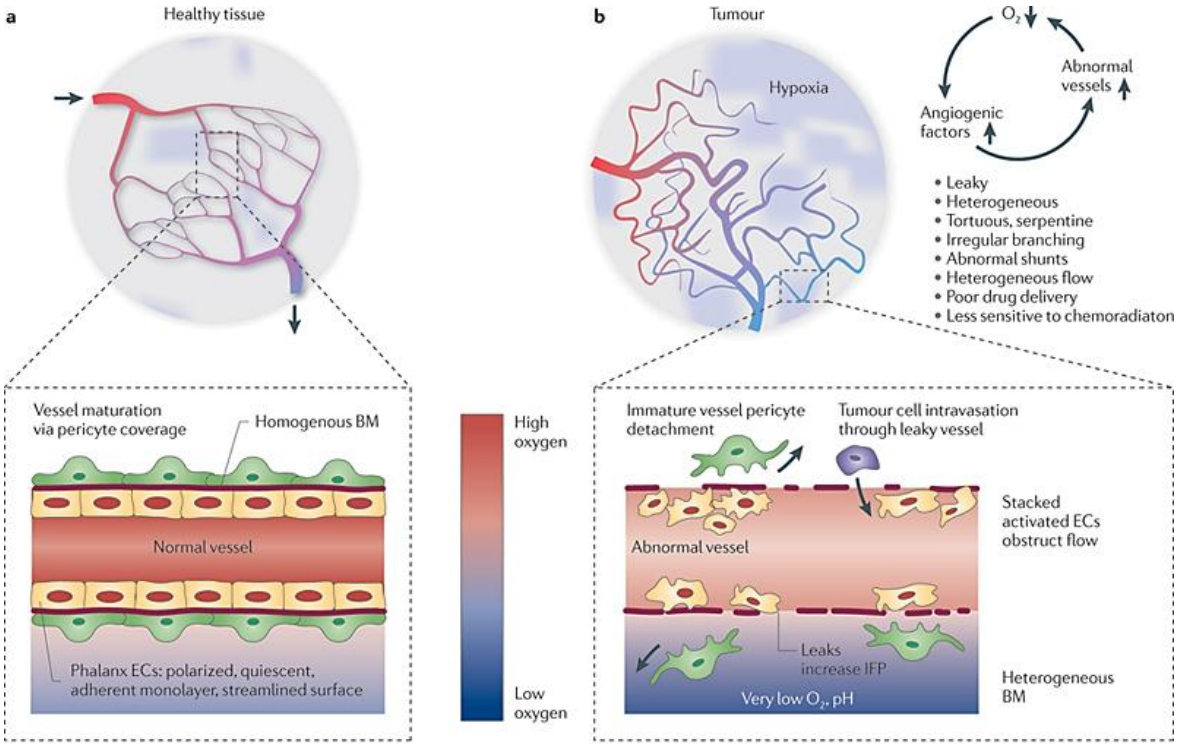



**Figure 2.** Illustration of vasculature in healthy tissues (a) and established tumours (b). In healthy tissues, mature blood vessels have a parallel organisation, are non-tortuous, have a homogenous basement membrane (BM) with endothelial cells (ECs) resembling a "phalanx", and are covered by pericytes. In contrast, in tumours, blood vessels are immature, leaky, tortuous, with immature pericyte detachment, leading to increased interstitial fluid pressure (IFP), resulting in hypoxia. Hypoxia in turns leads to a vicious circle of continuous production of proangiogenic factors that lead to subsequent abnormal angiogenesis. The latter contributes to poor drug delivery and reduced response of tumours to chemoradiation (adapted from [29])

Hypoxic (micro-) regions are heterogeneously distributed within the tumour mass and may be located adjacent to regions with $O_2$ tensions in the range of those found in the normal tissue neighbouring the neoplastic lesion [18]. Perfusion-limited $O_2$ delivery leads to ischemic hypoxia, which is often transient. For this reason, this type of hypoxia is also called "acute" hypoxia, a term that does not take into account the mechanisms underlying this condition. Alternatively, "acute" hypoxia often results as a consequence of transient

flow with plasma only due to the very low $O_2$ content in plasma. Hypoxia in tumours can also be caused by an increase in diffusion distances, so that cells far away (>70 μm) from the nutritive blood vessel receive less oxygen than required. This condition is termed diffusion- limited hypoxia, also known as "chronic" hypoxia. In addition to enlarged diffusion distances, an adverse diffusion geometry (e.g., concurrent vs countercurrent tumour microvessels) can also cause hypoxia [18, 19, 21, 30].

## 1.2.4 Tumour angiogenesis

Abnormal angiogenesis contributes to the pathogenesis of many diseases, including cancer [31]. The abnormal morphology of tumour vasculature was described for the first time by Virchow in the 19$^{th}$ century [32]. Following this, Goldman's studies suggested that angiogenesis was correlated to tumour growth [33]. It was not until over a century later when Judah Folkman demonstrated the vital role of angiogenesis in tumour cell growth and survival [34]. In the pioneering studies that he conducted, Folkman hypothesised that tumour growth was dependent upon angiogenesis and showed that if blood supply is inhibited, tumours are maintained in a quiescent state [34]. Further studies showed that angiogenesis plays an important role in the pathogenesis of cancer and is strongly correlated with tumour aggressiveness, survival and metastases [22].

Similarly to normal tissues, tumours require nutrients and oxygen for sustenance. Under normal circumstances (e.g. wound healing, female reproductive cycle), angiogenesis is switched on only transiently [31]. In contrast, permanent activation of the "angiogenic switch" is a prerequisite for tumour progression, causing normal quiescent vasculature to continually sprout new vessels that support further tumour growth [35]. This angiogenic switch is controlled by pro- (such as vascular endothelial growth factor-A; VEGF-A) and anti-angiogenic factors (such as thrombospondin-1; TSP-1) that are

countervailing [35]. The structural and functional abnormalities encountered in tumour blood vessels occur due to the deregulated angiogenic signalling [23, 24].

Tumour-induced angiogenesis is sustained by the production and secretion of angiogenic factors originating from tumour and stroma cells [23, 24, 31]. The VEGF family of growth factors are master regulators of angiogenesis, encoding ligands that orchestrate new blood vessel formation both in normal and malignant tissues. VEGF signalling occurs via three receptor tyrosine kinases (VEGFR1-3) at multiple levels through complex and diverse processes [36, 37]. The expression of VEGF is often increased in the majority of tumour cells *in vitro* and *in vivo*, as a consequence of genetic (mutant p53, VHL, PTEN-suppressor genes, oncogenic signalling activation) and epigenetic (hypoxia, cytokines, hormones, growth factors, chemokines) mechanisms [23, 38]. The identification of VEGF as a key molecular regulator of normal and pathological angiogenesis has stimulated significant efforts toward effective anti-cancer therapies and will be discussed below.

Additional important regulators of angiogenesis include the Tie-2/angiopoietin receptor tyrosine kinase signalling, the Notch/Delta-like ligand 4 signalling pathway, semaphorins, Eph/ephrins and others [23, 24, 38]. Furthermore, the role of bone marrow-derived cells (BMDCs) in tumour vessel formation (vasculogenesis) has generated considerable interest. The angiogenic process can be enhanced by different types of BMDCs including CD45+ haematopoietic cells of either monocytic or myeloid origin, chemokine receptors such as CXCR4 and its ligand stromal cell-derived factor-1 (SDF1), neutrophils and macrophages. CD45- i.e. nonhaematopoietic BMDCs such as circulating endothelial progenitor cells can also contribute to angiogenesis but the extreme diversity and overlapping of cell surface markers and methods used to characterise these cell types has generated controversy. The in-depth description of the role and mechanism of action of

proangiogenic factors is beyond the scope of this thesis, and they have been described elsewhere [23, 38-41].

## 1.3 Consequences of TME for cancer treatment

### 1.3.1 The impact of tumour hypoxia

Hypoxia plays a pivotal role in the therapeutic outcome since oxygen depletion is associated with resistance to radiotherapy, chemotherapy but also immunotherapy and hormonal therapy [14, 21, 28, 42-44]. This occurs by both direct and indirect effects. The effects of hypoxia *per se*. i.e. direct effects, are mediated by oxygen deprivation. Molecular oxygen "fixes" (i.e., makes permanent) DNA damage produced by oxygen free radicals, which occurs upon interaction of radiation with intracellular water. Hypoxia results in reduced "fixation" of DNA damage after radiotherapy, making radiation less effective (oxygen fixation hypothesis) [42, 45-47]. Thus, because of this so-called "oxygen-enhancement effect," the radiation dose required to achieve the same biologic effect is approximately three times higher in the absence of oxygen than in the presence of normal levels of oxygen [42, 45-47] (OER; Fig. 3). OER values in tumours can vary between 2 and 3.

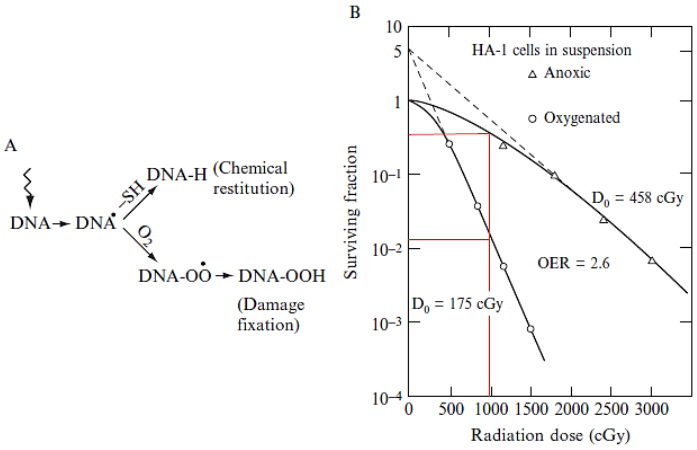



**Figure 3.** Hypoxia results in resistance of tumour cells to radiation. A, Radiation kills cells by the formation of peroxyl radicals that "fix" DNA damage, leading to cell death. In hypoxia, cellular nonprotein sulfhydryls, especially glutathione, can donate an H atom to the radical, thereby restoring it to its undamaged form and this leads to increased DNA

damage repair and decreased cell killing. B, Clonogenic survival of irradiated Chinese hamster HA-1 cells is higher in hypoxia (open triangles) compared to normoxia (open circles), as determined by clonogenic assay (OER=2.6) (adapted from [45]).

Furthermore, the impaired generation of free radicals can decrease cytotoxicity of certain chemotherapy agents such as bleomycin and doxorubicin [48-50]. Hypoxia can also lead to resistance to radiation and chemotherapy indirectly, by modifying the genome and proteome in diverse ways [19, 30, 42, 49, 51]. These can include decreased proliferation [52], altered cell cycle kinetics such as G1/S-phase arrest [45], reduced apoptotic rates [53-55], clonal selection and clonal expansion towards an aggressive phenotype [16] and increased DNA damage repair efficiency [56].

### 1.3.2 The impact of tumour vasculature on cancer treatment

Several studies have indicated that the tumour vasculature can play a role in regulating response to radiotherapy. Irradiation alone has an antivascular effect, both *in vitro* and *in vivo*, but this phenomenon is prominent at high radiation doses [57-60]. Fuks and colleagues previously reported that endothelial cells undergo apoptosis post-irradiation, which determines tumour response to radiotherapy [61, 62]. However, this finding remains highly controversial [63, 64] and a recent elegant study openly questioned this theory [65]. Furthermore, pre-irradiation of the tumour bed before implantation of tumour cells has an antiangiogenetic effect and can lead to delayed tumour growth [66-69]. In addition, radiation of tumour cells can result in the release of proangiogenic factors such as VEGF that promote tumour growth but the extent of this contribution to the tumour radiation response remains unclear [57, 70]. Brown and colleagues have demonstrated that tumour vasculature can affect radiation response. They showed that high doses of radiation ablate tumour vessels that leads to activation of vasculogenesis, via BMDC, that promotes tumour regrowth [67, 71, 72]. Whether vasculogenesis is crucial for tumour relapse post-

irradiation, though, has to be determined yet [73]. Liu *et al*. recently demonstrated the important role of Notch pathway-mediated angiogenesis on radiation outcome. Blockade of DLL4-Notch signalling significantly improved radiation response, leading to extensive tumour necrosis [74]. The combination of specific DLL4–Notch blockade and ionising radiation impairs tumour growth by promoting nonfunctional tumour angiogenesis and extensive tumour necrosis. These data indicate that tumour vasculature can significantly affect radiation response in many different ways.

### 1.3.3 The mechanical barrier of abnormal tumour vasculature and interstitium

Extensive studies have shown that the typical chaotic tumour microvasculature and the significant arteriovenous shunting impair efficient delivery of drugs. Due to the lower mean vascular density in most tumour areas, as compared to normal tissues, the diffusion distances are larger than usual, compromising penetration of drugs via tumour capillaries to cancer cells. This results in drug concentrations that are insufficient to exert a lethal effect, especially for drugs with short half-life [49, 75, 76]. Furthermore, cellular turnover rate is high for cells close to blood vessels and much lower father from the nearest vessels due to the low nutrients available. Therefore, many cytotoxic therapies targeting the S-cell cycle phase population are rendered less effective for the cells with slower division rate that are situation away from microvessels [49, 75, 76].

In addition, the majority of solid tumours present a high IFP due to vessel leakiness, impaired lymphatic functionality and increased contraction of interstitial matrix mediated by tumour-associated fibroblasts and in some cases interstitial fibrosis. Increased IFP results in poorer blood supply and decreased drug extravasation by convection [77-80]. Indeed, the increased intratumoural IFP decreases the hydrostatic pressure gradient between the intravascular and extravascular compartments which essentially become

equilibrated. It is not entirely clear to whether this phenomenon is sufficient to cause tumour vessel collapse but it most certainly reduces transvascular flow [49, 77, 78, 80]. In addition, as cancer and stromal cells proliferate and the tumour mass grows larger, the mechanical stress obliterates the vascular lumen [81, 82]. Previous studies have shown that IFP is almost uniform throughout the tumour interstitium and it is significantly decreased at the interface between normal and tumour tissue. The latter leads to oozing of molecules, including anticancer drugs, out of the tumour into the surrounding tissue, further contributing to treatment failure [77, 83-85].

To summarize, the microenvironment of solid tumours is complex. The past decades significant progress has been made in our understanding of the biology of TME and its role in tumour resistance to chemoradiation. Tumour cells exploit their microenvironment by growth factors and cytokines such as VEGF to stimulate abnormal vessel formation that is leaky and tortuous, causing irregular blood flow. The combination of poor perfusion, raised IFP, and areas of vascular collapse leads to hypoxia within tumours. The latter activates factors such as HIF-1 that serve to make cancer cells more aggressive and also markedly influences the response of malignant tumours to conventional irradiation and chemotherapy. Indeed, severely hypoxic cells require 2-3 times the radiation dose compared to well-oxygenated cells to achieve similar cell killing while the chaotic vascular architecture in combination with the increased hydrostatic pressure in tumour interstitium impairs adequate delivery of chemotherapy drugs. Below, the possibility of exploiting oncogenic signalling to target the pathological TME in order to improve response to cancer treatment will be discussed.

# 1.4 The PI3K/mTOR pathway and indirect antiangiogenic strategies

## 1.4.1 Introduction

One of the most studied oncogenic pathways is the phosphoinositide-3-kinase (PI3K)-Akt-mammalian target of rapamycin (mTOR) cascade. Activation of the pathway mediates a diverse spectrum of different downstream proteins. Accumulating evidence indicates that the PI3K/Akt/mTOR pathway also plays an important role in tumour angiogenesis. Below, a brief summary of the signalling mechanisms of the pathway will be presented. The different modes of angiogenesis targeting and how they affect vascular morphology will also be discussed. In addition, the expanding role of oncogenic signalling on tumour angiogenesis will be reviewed. Special emphasis will be paid to the potential of different oncogenic pathways blockade, as an alternative to the classical antiangiogenic therapies, to alter the TME for the benefit of cancer treatment.

## 1.4.2 The PI3K/mTOR pathway: role, structure and signalling in cancer

The PI3K/Akt/mTOR pathway regulates cell proliferation, apoptosis, cell cycle kinetics, metabolism, invasion [86]. A large amount of evidence has showed that activation of this pathway decreases the response of tumours to radiation [6, 87-94]. The PI3K family of lipid kinases phosphorylate the 3'OH group of phosphatidylinositols. PI3Ks are divided into three major classes according to their structure and function [86, 95, 96]. mTOR is the catalytic subunit of two molecular complexes, TORC1 and TORC2. mTOR is a major effector downstream of Akt and is composed of two complexes, mTORC1 and mTORC2 [97, 98].

The phosphorylation of the key target Akt occurs via several growth factors. Activation of class IA PI3Ks by receptor tyrosine kinases (RTKs)-mediated stimulation occurs via the regulatory subunit, p85 that binds to phosphotyrosine residues on RTKs

and/or adaptors. This will in turn results in relief of the inhibition of the p110 catalytic subunit by p85 that mediates localization of PI3K to its substrate phosphatidylinositol 4,5-bisphosphate (PI[4,5]P2) that resides on the plasma membrane [95, 99, 100]. Oncogenic activation can also stimulate PI3K/Akt/mTOR signalling. These include epidermal growth factor receptor (EGFR) overexpression, PTEN tumour suppressor loss, mutations in Ras oncogene (K-Ras and N-Ras) and others. G-protein coupled receptors can also activate the p110β catalytic subunit. PI3K/Akt signalling can also be activated in response to somatic mutations [97, 100]. In human cancers, somatic activating mutations in PIK3CA commonly target specific areas in the helical (E542 and E545) and kinase (H1047) domains and occur in up to 30% of epithelial cancers. They result in enhanced lipid kinase activity and upregulation of downstream signalling events such as phosphorylation of Akt but whether PIK3CA mutations occur early or late remains unclear [86, 100-102].

## 1.4.3 Antiangiogenic therapy

During the last decades, there has been a progressively increasing interest in modifying tumour vasculature with the purpose of starving the tumour of its nutrients by shutting down its blood supply. Two main strategies have been explored: [1] Vascular disruptive agents (VDA); [2] Antiangiogenic drugs.

VDA, such as the prototype combretastatin A4, aim to induce rapid shutdown of the established tumour vasculature, resulting in extensive cancer cell death in the centre of the tumour [103]. However, their therapeutic efficacy is limited due to the sparing of a relatively intact viable rim at the periphery of the tumour, from which tumour rapidly regrows, possibly via induction of hypoxia. The acute mobilisation of circulating bone marrow-derived endothelial progenitor cells (CEP) has been implicated in resistance to VDA, as they home the peripheral rim, resulting in revascularisation and tumour regrowth [23, 103, 104].

As mentioned previously, the second method consisted of using anti-angiogenic drugs that target new blood vessel formation by blocking the formation of growth factors such as VEGF and others. Different approaches have been explored such as VEGF traps and inhibitors of VEGF kinase activity, anti-VEGF receptor antibodies [105] and more recently drugs that target additional factors such as fibroblast growth factor (FGF), platelet derived growth factors (PDGF) and others [23, 25]. Several anti-angiogenic agents have now been approved for clinical use by Food and Drug Administration (FDA), based on the results of phase II and III trials [106]. The first was the VEGF-specific antibody bevacizumab, in combination with chemotherapy or cytokine therapy, for renal cell cancer, non-small cell lung cancer (non-squamous), metastatic breast cancer, colorectal cancer and recurrent glioblastoma. Furthermore, four multi-targeted pan-VEGF receptor tyrosine kinase inhibitors have been recently approved by FDA: sunitinib and pazopanib for the treatment of metastatic renal cell cancer; sorafenib for metastatic renal cell cancer and advanced, unrespectable hepatocellular carcinoma (HCC); and vandetanib for metastatic and/or unrespectable medullary thyroid cancer [106].

The combination of VEGF-targeting agents with conventional chemotherapy and radiotherapy has drawn considerable attention. Preclinical studies demonstrated that proangiogenic factors such VEGF can in fact be induced after radiation of tumour cells and the combination of VEGF blockade with radiation increased growth delay in tumour models [57, 107, 108]. The promising preclinical data shown after combination of VEGF blockers with various cytotoxic agents was confirmed in the first successful Phase III trial using bevacizumab with chemotherapy for metastatic colorectal cancer [109]. However, the efficacy is generally modest and toxicity is also a concern [105].

It was initially thought that VEGFR blockade enhances radiation efficacy only by promoting tumour vessel regression and sensitisation of endothelial cells to cell death.

However, preclinical work showed that VEGF inhibition reversed the morphological and functional abnormalities of tumour blood vessels [83, 110, 111]. This process now referred as vascular normalization is associated with decrease in IFP and increased blood flow and oxygenation [29, 112]. This window offers an opportunity for improved response to radiation and chemotherapy but it is transient, as prolonged administration of agents results in strong antiangiogenic effect with extensive regression of vessels [29, 112].

It is now becoming increasingly clear that the success of VEGF-targeted therapies is can be limited by the development of resistance [106]. Additionally, recent preclinical studies have showed that VEGF blockers might in fact promote metastasis by exacerbation of hypoxia and activation of compensatory proangiogenic pathways [113]. Therefore, alternative strategies might be required. Below, I discuss why oncogenic signalling targeting might be a meaningful option.

### 1.4.4 The role of PI3K/Akt/mTOR pathway in normal and tumour angiogenesis

The TME has the ability to perpetuate abnormal tumour angiogenesis via hypoxia [114]. The latter results in reduced activity of the prolyl hydroxylase domain proteins (PHD1–3), which act as oxygen sensors [16]. Reduced PHD activity prevents the degradation, via ubiquitination, of HIF-1α and HIF2α, which leads to activation of HIF-driven proangiogenic factors including VEGF that promote angiogenesis [16, 24]. Tumour cell oncogenic signalling can also stimulate new vessel formation in cancers. Indeed, human malignancies often exhibit diverse angiogenesis patterns and in many tumours, activated oncogenic signalling in tumour cells, such as Ras, Akt and Myc, contributes to ongoing neovascularisation by upregulation of proangiogenic factors [23, 106, 115, 116].

There is now sufficient evidence to support the crucial role of PI3K/Akt signalling in normal tissue and tumour angiogenesis. PI3K signalling is essential for

haematopoiesis and angiogenesis in zebrafish [117]. Overexpression of PI3K or Akt using the RCAS retroviral vector system resulted in increased angiogenesis, while forced expression of PTEN or of dominant-negative constructs of PI3K blocked angiogenesis in chicken embryos, providing direct evidence of the importance of PI3K in normal embryonal angiogenesis [118]. Multiple vascular defects, such as reduced branching morphogenesis in the endocardium, dilated vessels in the head, lack of hierarchical order of large and small branches in the yolk sac, impaired development of anterior cardinal veins, and decrease of Tie2 protein level were reported in mice deficient in the p110α catalytic subunit of PI3K [119]. The vascular permeability response to both Ras and VEGF was significantly diminished in mice deficient in p110γ subunit, suggesting that PI3Kγ is necessary and sufficient for vascular permeability [120]. Deletion of endothelial cell-specific p110α subunit resulted in embryonic lethality due to severe defects in angiogenic sprouting and vascular remodelling [121]. Reduced heart size and altered cardiac gene expression was observed in muscle-specific pan-p85α−/− p85β−/− mice [122]. A recent study showed that three prevalent mutants of p110α, E542K, E545K, and H1047R, are oncogenic *in vivo* and these tumours were characterised by increased angiogenesis and activation of the PI3K/Akt pathway [122].

The PI3K/mTOR pathway closely interacts with HIF-1α and VEGF to mediate angiogenesis. HIF-1α expression is regulated by PI3K/mTOR activation in response to growth factors [123]. HIF-1α expression is induced by cobalt and hypoxia through PI3K-dependent mechanism in pulmonary artery smooth muscle cells and airway smooth muscle [124, 125]. HIF-1-dependent gene transcription was blocked by overexpression of a dominant-negative form of Akt and by wild-type PTEN, whereas transcription was stimulated by constitutively active form of Akt. The PI3K inhibitor LY294002 and the mTOR inhibitor rapamycin blocked growth factor- and mitogen-induced secretion of

VEGF and provided a connection of PI3K/PTEN/Akt to mTOR, HIF-1 and VEGF and tumour angiogenesis [123, 126]. Similarly, overexpression of PI3K or Akt led to transcriptional upregulation of VEGF. LY294002 suppressed VEGF expression while overexpression of PI3K or Akt led to increased mRNA level of VEGF [118]. The authors concluded that PI3K signalling is sufficient to induce angiogenesis, and the effect may be partially through increasing HIF-1 and VEGF expression.

In ovarian cancer cells, VEGF transcriptional activation was regulated by PI3K/Akt through HIF-1α expression [127]. Several studies have shown that PI3K/PTEN/Akt/mTOR signalling regulates HIF-1 and VEGF expression in Ras-transformed cells, pulmonary artery smooth muscle cells, osteoblasts, pulmonary vascular endothelial cells, airway smooth muscle cells, mast cells and various types of cancer cells [123-126, 128-130]. Exposure of melanoma cells overexpressing bcl-2 to hypoxia activated phosphorylation of Akt and extracellular signal-regulated kinase (ERK)1/2 proteins, induced VEGF and HIF-1 expression, that was suppressed by PI3K and MAPK inhibitors [131].

Suppression of p110α expression in ovarian cancer cells by small interfering RNA (siRNA) resulted in decreased ovarian tumour growth and angiogenesis and inhibited VEGF expression by decreasing HIF-1α expression in both ovarian cancer cells and tumour tissues [132]. A recent study showed that Akt1 is a major downstream mediator for regulating tumour growth, angiogenesis, and VEGF expression [133]. Inhibition of PI3K activity by LY294002 decreased cancer cell-induced angiogenesis [134]. Overexpression of PTEN or an Akt dominant negative also inhibited angiogenesis and tumour growth that was associated with decreased levels of HIF-1α and VEGF expression in the tumour xenografts [134]. These results suggest that PI3K can regulate tumourigenesis and angiogenesis through HIF-1 and VEGF expression in cancer cells. Different proangiogenic

factors, including VEGF, can be upregulated downstream of oncogenic activation. [106, 115, 135]. Activation of PI3K/Akt upregulated VEGF expression and increased new vessel formation in chicken embryos [118]. Akt is necessary for vascular growth and homeostasis [136]. Loss of PI3K catalytic subunits in endothelial cells results in marked vascular hyperpermeability, implicating PI3K in the maintenance of vascular integrity [137]. PI3K/Akt signalling also activates nitric oxide synthase (NOS) which stimulates VEGF, angiogenesis and vascular permeability when expressed in endothelial cells [138, 139]. PI3K/Akt. PI3K/mTOR increases HIF-1 expression which in turn increases angiogenesis and promotes tumour growth [126]. Sustained endothelial Akt activation in normal tissues resulted in increased blood vessel size and generalized oedema from chronic vascular permeability [140]. These results suggest that PI3K can regulate normal tissue and tumour through HIF-1 and VEGF expression.

### 1.4.5 Indirect targets of tumour angiogenesis and their combination with radiation and/or chemotherapy

The above data show that oncogene-mediated angiogenesis induction demonstrates that separate cancer hallmark capabilities can be driven by the same factors that promote tumour cell proliferative signalling [23, 38, 116]. Targeting of oncogenic signalling and other indirect angiogenesis targets can alter the balance between pro- and anti-angiogenic molecules to modify vascularity and it could be an alternative approach to classical antiangiogenetic drugs as they are designed to block targets upstream of VEGF and also possess a direct cytotoxic effect. Also, there are no reports to date showing that agents such as PI3K and PI3K/mTOR inhibitors can induce a hypoxia-driven metastasis, as it has been described for VEGF blockers, which could consist an additional benefit of these drugs. In table 1, the indirect angiogenesis targets that can alter the TME have been summarised. In table 2, the preclinical evidence in regards to the growth delay effect of

angiogenesis targets combined with cytotoxic treatment (mainly radiation and chemotherapy) is reviewed.

**Table 1.** Alteration of tumour vascularity after inhibition of indirect angiogenesis targets.

| Target | Agent | Vascular morphology | TME effect | Tumour Type |
|---|---|---|---|---|
| PI3K/ Akt/mTOR | BEZ235 | ↓density | ↓IFP, ↓Permeability, | Breast carcinoma [141] |
| | PI-103 | ↓Tortuosity, ↑PVC coverage, ↓density | ↑tumour oxygenation, ↑ perfusion | Fibrosarcoma, SCC [142] |
| | Nelfinavir | ↓Irregularity, ↑PVC coverage, ↓density | ↑tumour oxygenation, ↑ perfusion | Fibrosarcoma, SCC [89, 142] |
| | FTIs | ↓Tortuosity, ↓diameter, ↑PVC coverage ↓density | ↑tumour oxygenation, ↑ perfusion | Prostate carcinoma, bladder carcinoma, glioma, fibrosarcoma, SCC [142-144] |
| | Palomid-529 | ↓Tortuosity, ↓density | ↓Permeability | Glioma [145] |
| | Rapamycin | ↓Tortuosity, ↓density, ↑PVC coverage | ↓Permeability, ↑tumour ↑/↓oxygenation, ↑/↓ perfusion, | Breast, Glioma [146-148] |
| | Everolimus | ↓density | ↓ perfusion, | Glioma [93, 94] |
| EGFR | Gefitinib | ↓Tortuosity, ↑PVC coverage | ↑tumour oxygenation, ↑ perfusion | Fibrosarcoma, SCC [142, 149] |
| | Erlotinib | ↓Tortuosity, | ↑oxygenation, ↓permeability, | SCC, NSCLC [150] |
| EGF | Suramin | ↑density | ↑tumour oxygenation | Glioma [151] |
| HER2 | Trastuzumab | ↓Diameter, ↓density | ↓Permeability | HER2+ breast carcinoma [152] |
| Myc | Omomyc | ↓density | ↓Permeability, ↓oxygenation | Pancreatic islet tumour [153] |
| MAPK | AZD6244 | Only slightly ↓density | ↑oxygenation, ↓ perfusion | NSCLC [154] |
| | LeTx | ↓density | ↓ perfusion | Fibrosarcoma [155] |
| Immune system | Thalidomide | ↓Density | ↓IFP, ↑oxygenation | HCC [156, 157] |
| | IFN-γ | ↑PVC coverage, ↓density | ↑oxygenation, | Glioma [158] |
| | Rgs5 | ↓Diameter, ↓density | ↑tumour oxygenation, ↑ perfusion, ↓permeability | Insulinoma [159] |
| | HRG | ↑PVC coverage | ↑tumour oxygenation, ↑ perfusion, ↓permeability | Fibrosarcoma, pancreatic carcinoma, Breast [160] |
| Cytoskeleton | FAK & | ↓density | ↑tumour oxygenation | Glioma [161] |

| | | | | |
|---|---|---|---|---|
| | β3 integrin | | | |
| Oxygen sensor | PHD2 | ↓Tortuosity, ↑PVC coverage, tight intercellular junctions | ↑tumour oxygenation, ↑ perfusion, ↓permeability | Melanoma, LLC, Pancreatic carcinoma [162] |
| Androgens | Castration | ↓Diameter, ↓tortuosity | ↓Permeability, ↓leukocyte adhesion to endothelium, ↑oxygenation | Shionogi carcinoma [163, 164] |

EGFR, epidermal growth factor receptor; HER2, human epidermal growth factor receptor 2; FTIs, farnesyltransferase inhibitors; mitogen-activated protein kinase, MAPK; IFP, interstitial fluid pressure; mTOR, mammalian target of rapamycin; NSCLC, non-small cell lung cancer; HCC, hepatocellular carcinoma; PI3K, phosphoinositide-3-kinase; PVC, perivascular cell; Rgs5, G-protein signalling 5; HRG, histidine-rich glycoprotein; PHD2, prolylhydroxylase 2; IFN-γ., interferon-γ; anthrax lethal toxin, LeTx.

**Table 2.** Therapeutic effect of combination of agents targeting vasculature with cytotoxic anti-cancer treatment.

| Vascular agent | Cytotoxic treatment | Effect on Delivery | Tumour type | Growth delay effect |
|---|---|---|---|---|
| A4.6.1 | Irinotecan | ↑ | Colon carcinoma | n.s. [165] |
| VEGF neutralising Ab | XRT (2 x 20 Gy, 4 x 10 Gy, 4 x 5 Gy, 8 x 5 Gy) | - | SCC, LLC, Esophageal carcinoma | Supra-additive (varied) [107, 108] |
| Bevacizumab | Topotecan, etoposide | ↑ | Neuroblastoma | Supra-additive [166] |
| Bevacizumab | FDG | ↑ (per vessel) | Rectal carcinoma | N/A [167, 168] |
| ZD6474 | XRT (3 x 2 Gy) | _ | NSCLC | Supra-additive (scheduling) [169] |
| AZD2171 | XRT ( 3 x 2 Gy, 5 x Gy) | - | NSCLC | Supra-additive [170] |
| S247 (αvβ3 integrin inhibitor) | XRT (5 x 2.5 Gy) | - | Prostate, Glioma | Additive [171] |
| SU11657 | XRT (1 x 7.5 Gy) | - | Epidermoid carcinoma | Additive [172] |
| Erlotinib | Cisplatin<br>XRT ( 1 x 6 Gy) | - | SCC | Supra-additive<br>Additive |
| Nelfinavir | XRT (1 x 8 Gy) | - | NSCLC | Supra-additive [89] |
| GDC-0941 | Doxorubicin | ↑ | SCC | Supra-additive [173] |
| BEZ235 | XRT ( 1 x 6 Gy) | - | SCC, Fibrosarcoma | Supra-additive [174] |
| LY2109761 | XRT ( 5 x 2 Gy) | - | Glioma | Supra-additive [175] |
| DC101 | XRT (5 x 5-24 Gy) | - | SCLC, Glioma | Additive |
| DC101 | XRT (3 x 7 Gy) | - | Glioma | Supra-additive (scheduling) [176] |
| Sunitinib | Temozolomide | ↑ | Glioma | N/A [177, 178] |
| Sunitinib | XRT (10 Gy) | - | SCC | Supra-additive [179] |

| Vascular agent | Cytotoxic treatment | Effect on Delivery | Tumour type | Growth delay effect |
|---|---|---|---|---|
| PDGF-D overexpression | Doxorubicin | ↑ | Breast carcinoma | Supra-additive [180] |
| IFN-β | Topotecan | ↑ | Neuroblastoma | Supra-additive [166] |
| Thalidomide | Cyclophosphamide | ↑ | Liver carcinoma | Additive [157] |
| AZD6244 | XRT ( 5 x 2 Gy) | - | NSCLC | Supra-additive (scheduling) [154] |
| Everolimus | XRT ( 5 x 2 Gy) | - | Pancreatic | Additive [94] |
| Rapamycin | XRT (4 x 3 Gy) | - | Glioma | Supra-additive [93] |
| TNP-470 | Cyclophosphamide, cisplatin | ↑ | Lung carcinoma | N/A [181] |
| TNP-470 | Temozolomide | ↓ | Glioma | N/A [182] |
| Axitinib | anti-E-cadherin Ab Viral particles | ↑ | Lung carcinoma, pancreatic tumour | N/A [183] |
| cRGD | Oncolytic virus | ↑ | Glioma | Supra-additive (?) [184] |
| Anginex | XRT (1-2 x 5 Gy) | - | Melanoma, Ovarian carcinoma | Supra-additive (scheduling) [185] |
| Botulinum toxin | XRT (20 Gy) Cyclophosphamide | | Fibrosarcoma, HCC | Additive (?) [186] |
| $^{225}$Ac-E4G10 | Paclitaxel | - | Prostate | Supra-additive [187] |

S247 (αvβ3 Integrin inhibitor); GDC-0941 (PI3K inhibitor) LY2109761 (TGF-b Signalling blocker) cRGD (integrin antagonist) SU11657 (VEGF, VEGFR, PDG, c-KIT inhibitor); DC101 (VEGFR2 inhibitor); ZD6474 (VEGFR2 inhibitor); AZD2171 (VEGFR inhibitor); AZD6244 (MAPK inhibitor); TNP-470 (methionine aminopeptidase-2 inhibitor); Axitinib (VEGFR1-3, c-KIT inhibitor); Sunitinib (VEGFRs, PDGFRs, RET, CSF-1R, flt3 inhibitor); NSCLC (non-small cell lung cancer); SCC (squamous cell carcinoma); LLC (Lewis lung carcinoma); XRT (radiation).

In table 3, the most important clinical trials testing the PI3K (BKM120) and PI3K/mTOR (BEZ235 and BGT225) inhibitors that were used as part of this thesis are presented. Although a high amount of preclinical data on the efficacy of PI3K and/or mTOR targeting in combination with radiation already exist, it is interesting to note that the majority of these clinical studies have not yet tested this combination at the clinical setting. The only study found to use one of these novel agents in combination with radiation so far is the NCT01473901 clinical trial that is currently recruiting patients with refractory/relapsed GBM to receive temozolomide with or without radiotherapy.

**Table 3.** Clinical trials using PI3K and PI3K/mTOR inhibitors (http://clinicaltrials.gov)

| Drug | Phase | Histology | Combination | Aim | Identifier |
|---|---|---|---|---|---|
| BEZ235 | I | Advanced breast, others | +/- trastuzumab | MTD, safety | NCT00620594 |
| | Ib/II | RCC | - | MTD, safety 4-month PFS | NCT01453595 |
| | I | Advanced/metastatic solid tumours | paclitaxel | Safety | NCT01285466 |
| | I | Advanced solid tumours | MEK162 | safety | NCT01337765 |
| | I | Metastatic breast | capecitabine | MTD, safety | NCT01300962 |
| | II | Advanced/recurrent endometrial | - | Efficacy | NCT01290406 |
| | I/II | Advanced solid tumours | Everolimus | DLT, safety, pharmacokinetic profiling of BEZ235 | NCT01508104 |
| | I | ER+, Stage IV breast | letrozole | MTD, safety, PFS, RR | NCT01248494 |
| BKM120 | I | Advanced NSCLC, others | gefitinib | Safety, dosing , pharmacokinetic profiling | NCT01570296 |
| | I | Advanced solid tumours | carboplatin | Safety, dosing, pharmacokinetic profiling, radiographic response | NCT01297452 |
| | I | Advanced CRC | irinotecan | MTD, pharmacokinetic profiling of BKM120 and irinotecan | NCT01304602 |
| | I/II | relapsed/refractory GBM | bevacizumab | Safety, dosing, pharmacokinetics profiling of BKM120 | NCT01349660 |
| | II | recurrent GBM | +/- surgical resection | Pathway modulation, efficacy, pharmacokinetic profiling of BKM120, safety, radiographic response, PFS, OS | NCT01339052 |
| | Ib | refractory GIST | STI571 | Safety, DLT | NCT01468688 |
| | I | ER+, Stage IV breast | fulvestrant | MTD, antitumour effect, pharmacokinetic profiling, | NCT01339442 |
| | I | refractory/relapsed GBM | temozolomide +/- XRT | DLT, ORR, PFS, OR, pharmacokinetic profiling of BKM120 | NCT01473901 |
| | I | Advanced/metastatic breast | paclitaxel | PFS, OS, Time and duration of response, Safety, Pharmacokinetic profiling of BKM120 | NCT01572727 |
| | I | Advanced solid tumours | GSK1120212 | MTD, histology studies, pharmacokinetic profiling of BKM120 and GSK1120212 | NCT01155453 |
| | I | metastastic CRC and PDAC | mFOLFOX6 | DLT, MTD, histology studies, pharmacokinetic profiling of BKM120, OS, PFS | NCT01571024 |
| | I/II | BRAF mutant metastatic melanoma | Vemurafenib | Safety, DLT, PFS, histology studies, biomarkers | NCT01512251 |

| | | | | | |
|---|---|---|---|---|---|
| | I | advanced/metastastic breast/CRC/ PDAC, recurrent GBM | LDE225 | DLT, MTD, histology studies, pharmacokinetic profiling of BKM120, OS, PFS | NCT01576666 |
| BGT226 | I/II | Advanced solid tumours, breast, Cowden syndrome | - | MTD, pharmacokinetic profiling of BGT226 | NCT00600275 |
| | I | Advanced solid tumours | - | DLT, efficacy, biomarkers | NCT00742105 |

CRC, colorectal cancer; PDAC, pancreatic ductal adenocarcinoma; GSIT, gastrointestinal stromal tumours; GBM, glioblastoma multiforme; ER, estrogen receptor; OS, overall survival; PFS, progression-free survival; MTD, maximum tolerated dose; DLT, dose-limiting toxicity; GSK1120212, MEK1/2 inhibitor; ORR, objective response rate; RR, response rate; STI571, MEK1/2 inhibitor; LDE224, smoothened inhibitor; NSCLC, non-small cell lung cancer;

To conclude, the PI3K/Akt/mTOR pathway is activated in the majority of human cancers and plays a key role in tumour survival and response to radiation. Several studies have implicated the pathway in tumour angiogenesis. Accumulating data now suggest that blockade of oncogenic signalling, for example by PI3K/Akt/mTOR inhibitors, might consist a promising strategy since these agents do not only possess anti-tumour effects but they can, dose-dependently, also change tumour vasculature and improve the response to radiation and chemotherapy. In many cases, these changes are related to downregulation of HIF-1α and VEGF. Future studies should investigate the translational importance of these preclinical findings.

## 1.5 The ATR/Chk1 pathway in DNA damage signalling and cancer therapy

### 1.5.1 Introduction

The exploitation of DNA damage to kill tumour cells has been used for many decades. Radiotherapy and chemotherapy consist the backbone of non-surgical treatment of human cancer. However, over a century since Roentgen discovered X-rays, a main question remains unsolved: how do we improve tumour cell killing without enhancing normal tissue toxicity? ATR inhibition seems to provide a promising answer to this crucial

question. In the present chapter, the literature on the ATR structure, its role of ATR in DNA-damage response (DDR) and the potential of ATR inhibition in enhancing radiation and chemotherapy efficacy will be reviewed. Information in regards to the emerging synthetic lethal effect of ATR blockade in oncogene-driven tumours by overloading replication stress will also be provided. Chk1 inhibitors are the closest comparison to ATR inhibition. Therefore, the preclinical and clinical evidence in regards to the efficacy of Chk1 inhibitors will be briefly presented, especially in pancreatic cancer model that is relevant to the present thesis.

## 1.5.2 The DNA damage response

The DDR consists of a series of molecular events and components inflicted by radiation and cytotoxic agents to allow repair and promote cell survival [188]. Compared to normal cells, the DDR in cancer cells is characterized by a divergence due to a multitude of genetic alterations that results in disabled repair, resistance to apoptosis and inefficient response to chemotherapy drugs and radiation [188, 189]. Indeed, many cancers are characterized by a defective DDR, especially a failure to halt the cell cycle. Therefore, targeting various DDR pathways is an important strategy for enhancing the efficacy of DNA-damaging anticancer agents and radiotherapy [189, 190].

The major signal transducers are the ataxia telangiectasia-mutated (ATM) and ATM-Rad3-related (ATR) protein kinases [189]. ATM and ATR are members of the conserved phosphoinositide 3 kinase-related kinases [95]. These two proteins are Ser/Thr-Gln-directed protein kinases that present overlapping substrate specificities. The ATM pathway is activated in response to double-strand breaks (DSBs) and is active during all phases of the cell cycle [189, 191]. ATR acts primarily in S and G2 phases of the cell cycle in an ATM-dependent manner [189, 191]. The DDR detectors, such as the Mre11-Rad50-Nbs1 (MRN) complex and replication protein A (RPA)-coated single-stranded DNA

(ssDNA), act upstream of the signal transducers, recruiting them to sites of DNA damage [189, 192]. For the purpose of the present thesis, we will only focus on the role of ATR in DDR and how this can be exploited therapeutically in cancer therapy.

## 1.5.3 ATR structure and the phosphoinositide 3-kinase related kinase (PIKK) family

ATR is a member of the phosphoinositide 3-kinase related kinase (PIKK) family [95]. PIKKs exhibit sequence homology particularly in their kinase, FAT (named after the kinases FRAP, ATM, and TRRAP) and FATC domains [95, 193] (Fig. 1). The kinase region is bordered by the FAT domain on the N-terminal side and the FATC domain on the C-terminal side. The PIK regulatory domain (PRD) is a poorly conserved regulatory domain of least ATR, ATM, and the mammalian target of rapamycin (mTOR). ATR is a large molecule with 2644 aa and a molecular weight of 300 kD [194]. The ATR-interacting protein (ATRIP) binds to the N-terminus of ATR. ATRIP is likely a subunit of ATR holoenzyme as loss of ATR or ATRIP results in no phenotypic difference [194].

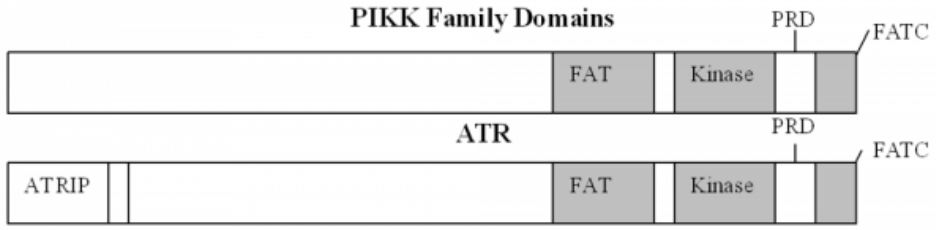



**Figure 4.** The structural domains of ATR and the PIKK family. The shaded domains share the highest degree of sequence homology and illustrate the similarity of PIKK family members. ATRIP (ATR-interacting protein), FAT (FRAP, ATM, TRRAP), PRD (PIK regulatory domain), FATC (FAT domain at the carboxyl terminus) (adapted from [195]).

## 1.5.4 The ATR/Chk1 checkpoint pathway in cell cycle

ATR is activated in response to replication stress, ultraviolet light, chemotherapeutic drugs and radiation [194, 196]. These agents result in stalled polymerases during replication at sites of DNA damage, prompting helicases to

continuously unwind the DNA, leading to long stretches of ssDNA [197]. Notably, ssDNA is most abundant during DNA synthesis, due to the activated replicative helicases, even though recent evidence suggests that SSBs are also generated at resected DSBs, upon exposure of telomeric overhand and also during NER [197].

There are two components (stabilizing proteins) that coat ssDNA. First, RPA recruits ATRIP which is binds to ATR, bringing the kinase to the lesion site [198]. Second, the 9-1-1 complex, a heterotrimeric ring, is loaded by Rad17 and the four small replication factor C (RFC) subunits onto RPA-coated ssDNA [199]. 9-1-1 is loaded onto DNA with 5'-recessed ends. These including stalled replication forks at sites of damage, recombination sites, and nucleotide-excision repair sites [200]. Following this, the BRCT I and II domains of the allosteric activator TopBP1 are recruited, which upon interaction with the phosphorylated serine317 on chromatin-bound Rad9 will finally activate ATR [199-202].

Chk1 is the immediate downstream target that is phosphorylated on Ser317 and Ser345 by activated ATR [203]. Chk1 phosphorylation leads to diminished replication and slowed cell cycle progression, thereby allowing time for repair to occur. Upon its phosphorylation, Chk1 phosphorylates Cdc25A phosphatase, leading to its degradation via ubiquitylation [196]. This results in G2-cell cycle phase arrest as Cdc25A cannot remove inhibitory phosphorylation of Cdk1/cyclin B kinase [196, 204]. In addition, phosphorylation of the ATR/Chk1 complex can lead to intra-S phase checkpoint activation. ATR signalling acts by inhibiting the firing of replication origins via Chk1-mediated phosphorylation of Cdc25A [196, 204]. This cannot de-phosphorylate and activate the Cdk2/cyclin A complex that is required for progression of S-phase. ATR/Chk1 pathway enables slowing of elongation of replication forks, protecting from replication stress-induced genomic instability [194, 196]. Other substrates phosphorylated in response

to ATR activation include claspin [205] and the Tim/Tipin complex [206], which bring ATR and Chk1 together. A study showed that BRCA1 (breast cancer suppressor protein 1) was phosphorylated by ATR following damage by IR or hydroxyurea but whether this process plays a role remains unclear [207]. Figure 1 illustrates the role of ATR/Chk1 signalling pathway in DDR [196] (Figure 5).

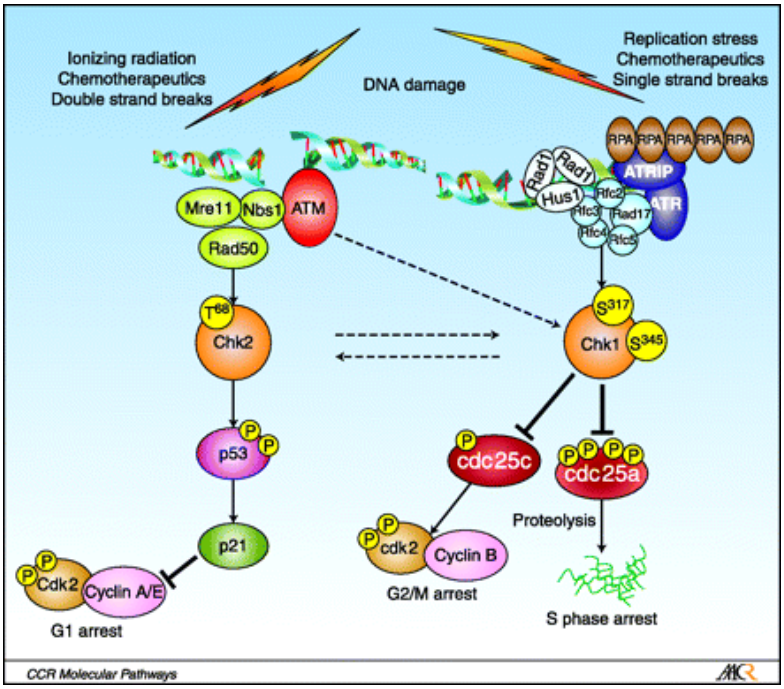



**Figure 5.** DNA damage results in activation of ATM and ATR kinases that result in phosphorylation of Chk2 and Chk1 serine/threonine kinases, respectively. These checkpoint kinases are key transducers of the DNA damage signal, leading to phosphorylation of several substrates involved in DDR. Chk1 and Chk2 have distinct roles and are activated in response to SSBs and DSBs, respectively; upon exposure of cells to different DNA damage-inducing factors such as ionising radiation, chemotherapeutic agents, replication stress-inducing factors and others The ATM/Chk2/p53 pathway primarily modulates the G1 checkpoint. After the cell passes this restriction point, the levels of ATR, Chk1 and Cdc24a increase. If DNA damage is detected, then Chk1/Chk2 are activated, Cdc25a is phosphorylated and becomes destabilized, leading to a p53-independent S arrest. The same cascade can also results in an intra-S phase arrest in response to stalled replication forks. The G2/M checkpoint prevents entry into mitosis for cells with unrepaired DNA lesions and this checkpoint is mediated by both cascades and will lead to suppression of the promitotic activity of cyclin B/Cdc2. SSBs result in activation of the ATR/Chk1 pathway via recruitment of the ATR/ATRIP complex via binding to the RPA that coats ssDNA. In parallel, ATR phosphorylates Chk1 resulting in activation of several downstream effectors involved in cell cycle control, DNA repair, DNA replication process, apoptosis and transcription process (adapted from [208]).

## 1.5.5 ATR/Chk1 pathway activation in response to various stimuli

ATR is activated in response to replication stressors leading to the formation of SSBs [194]. However, Fernandez-Capetillo and colleagues have shown that SSBs can lead to DSBs and ATM activation and vice versa, in response to genotoxic stimuli such as radiation and hydroxyurea [209]. Activation of the G2/M checkpoint in response to IR is not only dependent on ATM but also on ATR but can be independent of Chk2 [209]. Hence, there is significant crosstalk between ATR and ATM pathways. This study showed that the traditional model placing ATM and ATR in distinct checkpoint responses was incomplete and provided indirect evidence on how ATR targeting can enhance radiation-induced DNA damage and tumour cell killing. In addition to DNA damaging agents, replication can be stalled in fragile sites [210]. These consist chromosomal regions that replicate late during the S phase [211]. Fragile sites present an increase in the sister chromatid exchanges and deletions after treatment with the replication inhibitor aphidicolin, that is further exacerbated after ATR/Chk1 blockade [210]. Shortened telomeres, as occurs in senescent human fibroblasts also lead to activation of the ATR/Chk1 pathway, which has also been implicated in telomere maintenance and senescence in human and mouse cells via the 9-1-1 complex [212, 213].

## 1.5.6 Targeting the ATR pathway in combination with chemoradiation for cancer therapy

Radiation and chemotherapy result in a variety of DNA lesions that, if left unrepaired, they will ultimately lead to cell killing by mitotic catastrophe and/or apoptosis [188, 189]. The efficacy of chemoradiation greatly depends on the ability of DNA repair mechanisms to reverse the damage imposed. An important feature of a potential radiosensitising target is its selectivity i.e. the ability to sensitise cancer cells without aggravating normal tissue toxicity [7].

ATR represents an attractive therapeutic target for cancer therapy. As described above, ATR is activated in response to replication stress, protecting the genome from accumulated genomic instability and ensuring cell survival [194, 214]. Several cancer types are defective in DNA repair pathways such as the G1 checkpoint due to mutation in p53 or related components like ATM [215]. In pancreatic cancer, which consists the main focus of the present thesis in relation to targeting ATR, 50-70% of PDAC harbour mutations in ATM and p53-mediated signalling [216, 217]. Approximately 50-70% of PDAC harbour mutations in ATM and p53-mediated signalling In contrast normal tissues present proficient DNA repair capacity. Tumour cells are expected to rely on the S and G2 checkpoints to arrest the cell cycle and provide for repair and survival after radiation and chemotherapy and on alternative repair pathways such as ATR/Chk1 [209, 218-223]. Thus, targeting ATR can selectively sensitise cancer cells but not normal cells, similarly to the synthetic lethality concept [214, 224, 225]. Upon replication stress, ATR inhibition will prompt conversion of SSBs to DSBs, which will further augment DNA damage. Effective blockade of ATR can potentiate replication stress and target related processes such as homologous recombination (HR) to augment replication damage in response to cytotoxic therapy [214, 221, 224]. In normal cells, ATR/Chk1-independent activation of p38 collaborates with Chk1 to prevent mitotic entry after replication fork stalling [226]. In contrast, tumour cells rely entirely on the ATR/Chk1 pathway and therefore blockade of this pathway with hydroxyurea enhances cancer cell death without harming normal cells [226]ATR inhibition by overexpression of a kinase-dead mutant leads to significant radiosensitisation of cancer cells [35, 36].

A variety of strategies have been tested to inhibit ATR for cancer therapy. The prototype ATR inhibitor caffeine sensitises cells to radiation and genotoxic drugs but it can also block ATM at concentrations similar to those that inhibit ATR, therefore lacking

specificity [227]. Schisandrin B, initially discovered from the fruit *Schisandra chinesis*, is another nonspecific ATR inhibitor that inhibited Chk1 phosphorylation in response to ultraviolet (UV) light and sensitise A549 cells to UV radiation. However, schisandrin B also blocks ATM, although in higher concentrations [228]. Therefore, it is expected to also sensitise normal cells, leading to increased toxicity.

The use of ATR inhibition has been explored in combination with various chemotherapeutic drugs such as antimetabolites. Gemcitabine, an antimetabolite often used in pancreatic cancer and more recently in lung cancer, acts by blocking the enzyme ribonucleotide reductase and acts as a nucleoside analogue that is incorporated into the DNA, leading to chain termination [229]. Gemcitabine acts as a nucleoside analogue that is incorporated into DNA during replication, resulting in replication fork stalling and SSBs. Gemcitabine activates the ATR/Chk1 pathway affecting tumour survival [230]. Downregulation of ATR/Chk1 pathway sensitises cancer cells to gemcitabine [231]. Similar effects have been observed with the antimetabolites cytarabine and 5-fluorouracil [232, 233].

ATR has also been shown to increase response of tumour cells to topoisomerase poisons. These agents catalyse the breaking and rejoining of the phosphodiester backbone to promote the unwinding of DNA during replication and transcription and they therefore block the relegation step, generating both SSBs and DSBs [234]. ATR inhibition but not ATM or Chk2 inhibition by siRNA enhanced the cytotoxic effect of the topoisomerase I inhibitors camptothecin and SN-38 [235]. Additionally, a dominant-negative ATR allele also sensitised GM847 human fibroblasts to topotecan and camptothecin [236].

Platins act by covalently binding to DNA to form intra- and inter-strand crosslinks that block replication and lead to DSBs formation [237]. ATR inhibition by siRNA has been shown to sensitise tumour cells to cisplatin, carboplatin and oxaliplatin, both *in vitro* and

*in vivo* [238]. Interestingly, ATR mediated cisplatin resistance in a p53 genotype-specific manner [220].

ATR inhibition can also sensitise cells to alkylating agents such temozolomide (TMZ) and the nitrogen mustard melphalan. Alkylating agents act by adding an alkyl group to the guanine base of DNA, resulting in interference with DNA replication [239]. In a preclinical study, colorectal cancer cells were strongly sensitised by inhibition of ATR but not ATM silencing using siRNA [240]. Notably, ATR acted as an upstream activator of Akt in the response to TMZ [240]. Similarly, ATR has been implicated in the response of mismatch repair-proficient cells after treatment with TMZ but not mismatch repair-deficient cells [241]. Similarly, ATR blockade in GM847 SV40-transformed fibroblasts and U2OS human osteosarcoma cells by expressing the kinase-dead ATR sensitised them profoundly to melphalan [238]. ATR has also been targeted by creating DLD1-ATR Seckel cells whereby ATR mutant knock-in cells express very low levels of ATR and results in profound sensitisation to chemotherapeutics [242].

## 1.5.7 ATR inhibition, replication stress and synthetic lethality

The concept of synthetic lethality is complex [243]. Multiple DNA repair pathways are required for cancer cells to be able to replicate their DNA and divide. Malignant cells can rely to DNA damage repair pathways other than the one that led to its initial mutability. Because lesions in DNA repair machinery are repaired by multiple pathways that promote survival of tumour cells, blockade of all routes to DNA damage repair can be lethal to the malignant cells. The most characteristic example is in breast or ovarian cancers that present a mutation of BRCA1 or 2, which promote repair of DSBs [244]. Since replicating DNA requires repair of these DNA lesions, these cancers have become reliant on another DNA repair component, Poly-ADP-ribose-polymerase (PARP), for

replication fork progression. Studies have shown that inhibition of PARP1 in these tumour cells leads to overwhelming DSBs formation during replication, and ultimately cell death [245]. Curtin and colleagues have shown that PARP inhibitors can effectively sensitise tumour cells to radiation and chemotherapy [246]. The exploitation of these unique features of tumour cells is currently the subject of intense investigation by many groups that employ synthetic lethality screening to develop novel compounds with antineoplastic activity [243].

During each cell division and even more, upon exposure to genotoxic events, cells undergo replication stress, which is normally repaired by ATR [194, 214]. Fernandenz-Capetillo and colleagues have hypothesised that inhibition of the ATR/Chk1 pathway will promote tumour cell killing due to accumulation of mediated by oncogenic signalling [224]. In contrast, normal cells are not expected to be affected by ATR inhibitors because they present the minimal levels of replication stress. One of the hallmarks of cancer cells is the upregulation of Ras oncogene that occurs in 50-70% of the pancreatic cancer, promoting survival. In line to the hypothesis by Capetillo, ATR inhibition exacerbated the levels of replication stress to promote cell killing Ras activation in combination with complete ATR suppression resulted in substantial tumour cell killing [247]. Similarly, ATR suppression resulted in regression of Ras- and Myc-driven tumours. Additionally, ATR inhibition using a mouse model of ATR-Seckel syndrome prevented the development of Myc-induced lymphomas or pancreatic tumours that presented high levels of replication stress. Chk1 inhibitors suppressed tumour growth in these tumours while no response was observed in K-RasG12V pancreatic adenocarcinomas that were characterised by lack of replication stress. Importantly, overexpression of the Myc oncogene increased the degree of replication stress [248]. A similar study by the same group and by Brown and colleagues explored a genetic system to conditionally reduce ATR expression to 10%

(hypomorphic suppression) of normal levels in adult mice. In this model normal tissues such as the bone marrow and intestinal epithelium were minimally affected, even at long term. In contrast, tumour growth was significantly reduced in fibrosarcomas expressing H-rasG12V and acute myeloid leukemias (AMLs) driven by mixed lineage leukemia (MLL)-eleven nineteen leukemia (ENL) gene and N-rasG12D MLL-ENL and N-rasG12D [249].

Accumulating evidence also points to a synthetic lethal interaction between ATR and ATM/p53. ATR deficiency in the same mouse model of ATR-Seckel syndrome presented impairment of DNA replication during embryogenesis and accelerated ageing that was aggravated after p53 deletion due to replication stress accumulation [250]. ATR inhibition was particularly toxic for p53-deficient tumour cells and this toxicity can be exacerbated by replication stress-generating conditions such as cyclin E overexpression [219]. Accordingly, Reaper *et al*. recently demonstrated that ATR inhibition by VE-821 leads to extensive cell death in cancer cells with defective ATM-p53 signalling and also enhances the response to chemotherapy and radiation [251].

## 1.5.8 Efficacy of Chk1 inhibitors

To date, no selective ATR inhibitors to be used *in vivo* have been reported. In contrast, several Chk1 inhibitors have been developed including UCN-01, AZD7762, XL844, PF-00477736, CBP501, and SCH 900776 [191]. Except SCH900776 that is a selective Chk1 inhibitor, the rest are known to block both Chk1 and Chk2 kinases [191]. Chk1/2 inhibitors are known to sensitise tumour cells to radiation and chemotherapy, both *in vitro* and *in vivo* [191]. Preclinically, AZD7762 has been investigated in the treatment of pancreatic cancer. AZD7762 sensitised pancreatic tumour cells to radiation and gemcitabine, both *in vitro* and *in vivo* [252]. Radiosensitisation by AZD7762 was associated with G2 cell cycle checkpoint abrogation and was associated with persistent γH2AX expression and inhibition of Rad51 focus formation [252]. Importantly, AZD7762

has been previously shown to be selective for tumour cells but not normal fibroblasts [253]. Clinical studies have been conducted using the prototype Chk1/Chk2 inhibitor UCN-01 in combination with chemotherapy [254-258]. However, the responses to date have been very modest, in up to 10% of patients. More trials using new Chk1 inhibitors such as AZD7762 and SCH900776 have been recently initiated and the results are awaited with great interest.

To summarize, ATR is an apical kinase in the DNA-damage induced checkpoint pathways with broad functions and major physiological importance in DNA repair, cell-cycle regulation and apoptosis. Based on the traditional model, ATM/Chk2 and ATR/Chk1 networks are activated by different types of DNA lesions, signalling through two independent pathways. However, significant crosstalk between ATM and ATR activation routes can occur, indicating that this model has probably been oversimplified. The emerging concept of exploring ATR inhibition to overload replication stress in oncogene-driven tumours is promising but warrants further investigation. Several preclinical studies have shown that ATR can increase the effectiveness of different types of chemotherapeutic agents and radiation *in vitro* and *in vivo*, which could improve the therapeutic outcome in cancer therapy. Importantly, preclinical evidence suggests that targeting ATR might be selective for tumour but not normal cells, making this an attractive target. Although inhibitors targeting Chk1 kinase have been produced for *in vivo* use, no ATR inhibitors have yet been developed to explore the potential of ATR blockade in clinical studies. Several factors could account for the paucity of potent, selective candidate pharmaceuticals that inhibit ATR [212, 222]. This may be a result of the difficulties in obtaining active ATR protein to support drug discovery efforts. This can also be attributed to the large size of ATR protein (2644 aa) that makes it challenging to express it in bacteria for subsequent use in kinase assays, when conducting in a high-throughput screen.

Another reason could be the lack of ATR crystal structure that is important for the development of targeting compounds. The advent of new drugs that will enable highly potent and selective inhibition of ATR is awaited with great interest [212, 222].

## 1.6 Pancreatic cancer: clinical and biological evidence and role of radiotherapy

Pancreatic cancer is one of the most lethal solid malignancies and pancreatic ductal adenocarcinoma (PDAC) accounts for the majority (>90%) of pancreatic malignancies [259]. Pancreatic adenocarcinoma is characterised by a high propensity for local invasion, distant metastases and perineural, vascular and lymphatic invasion are often detected in resected tumour specimens [259]. In addition, lymph-node metastases are present in 50–75% of resected cases and more than 80% of patients with PDAC present with irresectable disease. The prognosis for these patients is very poor and the overall 5-year survival rate among patients with PDAC is <5% [260].

The causes of pancreatic cancer remain unknown but several environmental factors have been implicated such as tobacco use, alcohol and coffee intake. Others factors include a history of diabetes or chronic pancreatitis, chronic cirrhosis, a high-fat, high-cholesterol diet, and previous cholecystectomy [261]. Approximately 5 to 10% of patients with pancreatic cancer present a family history of the disease and a subgroup high-risk kindred carry germ-line mutations of genes involved in DNA damage repair such as BRCA2 and the partner and localiser of BRCA2 (PALB2) [261].

Biology studies have shown that PDAC can be formed as a result of accumulation of gene mutations of the pancreatic ductal epithelium that evolve from premalignant lesions (pancreatic intraepithelial neoplasia; PIN grade 1A-B) to dysplasia (PIN grades 2-3) and finally fully invasive PDAC [216, 262]. Mutations include inactivation of the tumour-suppressor genes *TP53* (50-70% of patients) and deleted in pancreatic cancer 4

(DPC4, also known as the SMAD family member 4 gene [SMAD4] in 50% of patients), activation of the K-Ras oncogene (90% of patients) and inactivation of the tumour-suppressor gene CDKN2A (which encodes the inhibitor of cyclin-dependent kinase 4 [INK4A] in 95% of patients) [216, 262]. An important study that analysed the genetic profile of 24 PDAC samples showed that the genetic basis of this disease is extremely heterogenous and genetic abnormalities can be organised in 12 abnormal cancer pathways [217]. Another characteristic example of PDAC is desmoplasia i.e a dense stroma composed primarily of pancreatic stellate cells (myofibroblasts) that is regulated by growth factors such as transforming growth factor β1 (TGFβ1), platelet-derived growth factor (PDGF), fibroblast growth factor (FGF), integrins, SPARC (secreted protein, acidic, cysteine-rich), and hedgehog pathway elements and others [263]. Desmoplasia acts as a mechanical barrier, impairing sufficient drug delivery [264] and also results in resistance to radiation [265], resulting in treatment failure. In addition, desmoplasia and stromal cells plays important role in tumour formation, progression, invasion, and metastasis [263].

The clinical picture of patients with PDAC depends on the location of the tumours [259]. The majority of tumours are found in the head of the pancreas and cause obstructive cholestasis. Obstruction of the pancreatic duct can result to pancreatitis. At presentation, most patients have systemic manifestations of the disease such as weight loss, fatigue, anorexia, anaemia and often dysglycaemia. Less commonly patients develop deep and superficial venous thrombosis, panniculitis and gastric outlet obstruction. Jaundice, peripheral lymphadenopathy, hepatomegaly and ascites are encountered in patients with advanced or metastatic disease. Diagnosis is mainly established by helical computed tomography (CT) with intravenous administration of contrast material and more recently positron-emission tomography (PET). Endoscopic ultrasonography is also used in case of suspected but invisible mass (on CT) and for obtaining biopsy specimens. Endoscopic

retrograde cholangiopancreatography (ERCP) is carried to guide ductal brushing and lavage and for stent positioning in case of obstructive jaundice. CA 19-9 is often used as a diagnostic marker and for therapeutic monitoring [259].

The management of patients with PDAC depends on the stage and the extent of the disease at the time of primary diagnosis. Surgical resection is the most important therapeutic modality for patients with PDAC but the majority of patients already have an advanced or even metastatic disease at the time of diagnosis that precludes surgery [266]. Several novel compounds targeting oncogenic signalling, angiogenesis and metastases have failed to demonstrate a substantial benefit in patients with PDAC. Accumulating evidence indicates that patients with potentially resectable disease might be eligible to surgical resection if they undergo multimodality treatment including chemoradiation to improve resectability and reduce recurrence [267]. Indeed, neoadjuvant treatment can downstage patient, increase resectability and improve local control in a subset of patients with irresectable PDAC [268]. A recent study showed improved overall survival with the addition of radiotherapy to gemcitabine in patients with localised unresectable PDAC, with acceptable toxicity [269]. However, more trials are required before this approach becomes widely accepted and hence, patients should not be treated with neoadjuvant chemoradiation outside of clinical trials. In the adjuvant setting, chemotherapy after R0-resection and chemoradiation should also be applied as part of clinical trials. In patients with R1-resection, chemoradiation should be considered [268].

Radiotherapy for PDAC should always be combined with chemotherapy, preferably gemcitabine-based. Even though palliative analgesic treatment of the pancreas with hypofractionated radiotherapy only (20 Gy in 5 fractions) has been used in the UK, this approach is not evidence based and has not been supported by any relevant studies [270]. To minimise gastrointestinal and haematological toxicity, radiotherapy should be

conventionally fractionated i.e 1.8-2 Gy/fraction to a total dose of 50 to 55 Gy, even though a hypofractioned regimen (10 x 3 Gy) has been reported as a safe regimen. Treatment planning should be 3D-conformal and IMRT is desirable to improve conformity and decrease normal tissue exposure to radiation. Common toxicities encountered in patients with PDAC that undergo radiotherapy or combined chemoradiation include gastroduodenal ulcers, bleeding, diarrhoea, renal and hepatic toxicity and also haematotoxicity, especially in gemcitabine-incorporating regimens [271]. Recommended dose limits for critical organs are: liver: 50% of the volume ≤30 Gy; kidneys: no more than maximally 50% of the volume of kidney should receive >20 Gy and no more than 30% of contralateral kidney volume should receive >20 Gy; spinal cord: ≤45 Gy. There is no consensus to date as to whether the regional lymphatics should be included in the target volume. Special attention should be paid in regards to the irradiated volume as the tolerance of gemcitabine based concurrent chemoradiation depends on the total treatment volume in PDAC [270].

To summarise, PDAC remains one of the most lethal cancers. Despite the technological advances and the better understanding of the biological background of this disease, the prognosis remains poor due to the low resectability. The use of radiotherapy, especially in combination with chemotherapy, can downstage the disease and improve resectability in the patient subset with potentially resectable, non-metastatic disease but it should be conducted as part of clinical trials.

## 1.7 Outline and purpose of the thesis

The aim of the present thesis was to better understand the biological consequences of targeting key biological mechanisms with the purpose of improving radiotherapy response. Two important and distinct pathways were targeted using novel agents to investigate their potential to improve radiation sensitivity, both *in vitro* and *in vivo*: (1) the

PI3K/Akt/mTOR pathway; (2) the ATR/Chk1 pathway. Below, an overview of the contents of this thesis is given. In the present chapter, **Chapter 1**, the biological basis of hypoxia, factors that determine radiation outcome, the pathophysiology of tumour angiogenesis and how the abnormal TME adversely affects response to radiotherapy and patient outcome are discussed. In addition, the role of the PI3K/Akt/mTOR signalling pathway in tumour growth and response to radiotherapy is examined. The different strategies available for targeting tumour vasculature are presented together with the possibility of exploiting indirect antiangiogenic strategies, such as oncogenic signalling inhibition to alter the TME to increase radiation efficacy. Furthermore, the structure and the role of ATR/Chk1 pathway in DNA damage response, the effects of ATR downregulation in cancer cells, its relevance to the concept of synthetic lethality and the potential of combining ATR inhibition with radiation and chemotherapy for clinical use are investigated. Highly relevant to the present thesis, the clinical and biological profile of pancreatic cancer are summarised together with the role that radiotherapy plays in the multimodal therapy of this disease. In **Chapter 2**, the materials and methods relevant to the preclinical studies are described.

In the next two chapters, the role of PI3K/mTOR signalling pathway in tumour radiosensitivity was examined using three, recently-developed signalling inhibitors obtained from Novartis Pharma: NVP-BEZ235 (dual PI3K/mTOR inhibitor; BEZ235), NVP-BGT226 (dual PI3K/mTOR inhibitor; BGT226) and NVP-BKM120 (single PI3K inhibitor; BKM120). Relevant to the PI3K/Akt/mTOR pathway, two separate preclinical studies were conducted. In **Chapter 3**, the radiosensitising effect BEZ235 and BGT226 was investigated in tumour and endothelial cells i.e. in cell culture. A series of assays relevant to radiosensitisation were conducted to better elucidate the impact of these agents on the molecular mechanisms of tumour and endothelial cells. In **Chapter 4**, a thorough

research was conducted into the effects of oncogenic signalling inhibitors on tumour vasculature and oxygenation. The effect of BKM120 and BEZ235 on tumour microenvironment was investigated in tumour xenograft models via different imaging methods and histology. Clinically applicable drug scheduling was also performed during that study with the purpose of improving the response to radiation. In **Chapter 5**, the impact of ATR/Chk1 pathway inhibition in radiosensitising tumour cells was analysed using a novel ATR inhibitor, VE-822, that was obtained from Vertex Pharmaceuticals. For this project, pancreatic cancer was the main focus for reasons that are explained in detail in the relevant chapter below. The influence of ATR inhibition on tumour cell response to radiation and gemcitabine chemotherapy was tested using VE-822, a novel ATR inhibitor developed by Vertex Pharmaceuticals. Several *in vitro* assays were performed to better understand the mechanism of action of ATR inhibition. The radiochemosensitising potential of VE-822 was thoroughly investigated in different pancreatic tumour xenograft models. Special emphasis was paid in evaluating the selectivity of VE-822 for tumour cells. Hence, the effect of VE-822+radiation combination treatment was also examined in normal fibroblasts, endothelial cells and more importantly on the murine intestinal epithelium. The latter is of particular importance as gastrointestinal epithelial tract toxicity, limits the therapeutic potential of radiotherapy in patients with PDAC. In the final **Chapter 6**, the findings of the preclinical studies are summarised and the impact and clinical implications that inhibition of the PI3K/mTOR and ATR/Chk1 pathways might have in future cancer therapy is discussed.

# CHAPTER 2

# Materials and Methods

# 2.2. MATERIALS AND METHODS

## 2.1 Cell culture

T24 (bladder), HT1080 (fibrosarcoma), FaDu (hypopharyngeal) and MiaPaCa-2 (PDAC) cancer cells were obtained from ATCC. PSN-1 (PDAC) cells were obtained from Merck & Co, Inc. as previously [272] . SQ20B laryngeal squamous cell carcinoma cells were obtained from Dr. Ralph Weichselbaum (University of Chicago, Chicago, IL). Cells were cultured in DMEM containing 4.5 g/L glucose (Invitrogen, Paisley, UK) supplemented with 10% fetal bovine serum (HyClone, Loughborough, UK), penicillin (100 units/ml), and streptomycin (100 mg/ml; Invitrogen, Paisley). Normal human fibroblast cells (MRC5 and HFL-1) and the primary pancreatic cancer cell line (the PancM cell line; passage 17) were cultured in similar conditions, as for tumour cells above. Human dermal microvascular endothelial cells (HDMECs/HDMVC) and human macrovascular endothelial cell (HUVEC) were purchased from Lonza and were maintained in EGM-2 medium (Lonza, Slough, UK) supplemented with EGM-2 SingleQuots at 37° C in water saturated 5% CO2/95 % air. The HT1080-HRE-luc was kindly provided from Professor Pugh, Oxford University [142]. The HT1080 cell line contains an endogenous mutant allele of N-Ras oncogene.

FaDu cells were transfected with a HIF-Hypoxia Reporter Element (HRE) using the Cignal Lenti HIF Reporter luciferase (SABiosciences, Crawley, UK), according to the manufacturer's instructions. To generate the stable HIF-1-HRE reporter cell line, (FaDu-HRE-luc), FaDu cells were infected with a lentivirus harbouring a HIF-HRE driving expression of the firefly luciferase gene. For that purpose, 10.000 FaDu cells were plated on a 96-well plate and were cultured overnight. The following day, cells were exposed for 24 h to a 100 μL solution containing: 25 μL HIF-HRE Lenti reporter plus 74 μL DMEM medium supplemented with 10% fetal bovine serum (HyClone, Loughborough, UK),

penicillin (100 units/ml), and streptomycin (100 mg/ml; Invitrogen, Paisley, UK) together with 1 µL of polybrene (Invitrogen, Paisley, UK). Following this, medium was washed away and was replaced with Lenti reporter-free medium. In order to obtain a stable pooled cell line, FaDu-HRE-luc cells were continuously exposed to 1 µg/ml puromycin (Sigma, Dorset, UK). To assess HIF-HRE luciferase activity activity, D-luciferin (150 µg/ml; Gold BioTechnology, St Louis, MO) was added to the 10% DMEM medium, and the cells were incubated for 2 minutes. Luminescence readings were then captured with the use of a Xenogen IVIS 200 imaging system (Calliper Life Sciences Ltd, Preston Brook, UK) using a 5 sec exposure and analysed with the Living Image 3.0 software (Calliper Life Sciences Ltd, Preston Brook, UK).

## 2.2 Dual PI3K/mTOR inhibitors treatment

BGT226 and BEZ235 dual PI3K/mTOR inhibitors were obtained from Novartis Pharma AG, Basel, Switzerland. The drugs were added to mid-log phase cell cultures. After treatment, medium was replaced with drug-free medium. For the control group, equal amounts of dimethyl sulfoxide (DMSO) were used.

## 2.3 ATR inhibitor preparation and treatment

The ATR inhibitors VE-821 and VE-822 were obtained from Vertex Pharmaceuticals, Abingdon, UK, under material transfer agreement. In the control group, DMSO was used at a concentration equivalent to the dose used in the VE-822-treated cells. VE-822 was added to mid-log phase cell cultures and drug-free medium replaced the compound-containing medium after the specific treatment time. For the *in vivo* studies, VE-822 was dissolved in 10% Vitamin E d-alpha tocopheryl polyethylene glycol 1000 succinate (TBGS; provided by Vertex Pharmaceuticals, Abingdon, UK). The drug was administered orally via gavage, in a volume of 200 µl.

## 2.4 Biochemical and cellular inhibition of ATR and related kinases

Biochemical enzyme studies against ATR, ATM, DNA-PK, mTOR and PI3K, along with broad kinase selectivity profiling was carried out by Vertex Pharmaceuticals as previously described [251]. Cellular inhibition of ATR, ATM and DNA-PK was assessed by Vertex Pharmaceuticals using previously reported methods [251]. The kinase selectivity profile of VE-822 (0.4 and 2 μm) was screened against the indicated human (h), rat (r), mouse (m) and fission yeast (y) kinases using the Millipore Kinase Profiler service, at ATP concentrations equal to each enzyme's ATP Km. Details of this can be found at https://www.millipore.com/drugdiscovery/svp3/kpservices. The biochemical and cellular inhibition studies for VE-822 were entirely performed and analysed by Vertex Pharmaceuticals.

## 2.5 Clonogenic survival assay

The effect of BEZ235 (50 nmol/l) and BGT226 (5 nmol/l) on tumour cell survival after irradiation was assessed by clonogenic assay. For experiments testing the efficacy of the ATR inhibition, VE-822 (80 nM) was administered 1 h before XRT and was washed away 17 h after XRT. For chemotherapy, cells were exposed to increasing concentrations of gemcitabine (10, 20 and 50 nM) for 24 h before addition of VE-822 (80 nM) for another 18 h. Gemcitabine was washed away immediately before addition of VE-822.

In all clonogenic survival experiments, cells were plated from single-cell suspensions and allowed to adhere to culture dishes before irradiation and/or inhibitor exposure. Cells were irradiated with J. L. Shepherd Mark I Irradiator (J. L. Shepherd & Associates, San Fernando, CA) at a dose rate of 1.7 Gy/min. Colonies were stained and counted 2-3 weeks after irradiation. Colony counting performed using an Oxford Optronics Colcount (Oxford Optronics, Oxford, UK). In some cases, primary cells formed

diffuse colonies and colonies were counted manually. The surviving fraction was derived using the following formula:

$$(\#\,Colonies/\#\,of\ cells\ plated)_{irradiated}/(\#\,Colonies/\#\,of\ cells\ plated)_{unirradiated}$$

Different PI3K/mTOR inhibitor-radiation schedules were also tested (see "Results", Chapter 3). In HUVEC and HDMVC, BEZ235 (50 nmol/l) was added 1 h before radiation and medium was replaced by basal medium containing 1.5% FCS and a constant concentration of VEGF (10 ng/ml) at 1 h post-irradiation [273].

The clonogenicity was also assessed in tumour cells cultured in hypoxia after treatment with one of the PI3K/mTOR inhibitors, BEZ235 (50 nmol/l). For the clonogenic assays performed in hypoxia, tumour cells were incubated in 0.5% $O_2$ using an InVivo2 300 chamber (Ruskin Technology, South Wales, UK), for 6 hours before irradiation under hypoxic conditions using tightly sealed chambers. The target $O_2$ level was achieved within 6 h of gassing and maintained during irradiation, as confirmed by an OxyLite oxygen probe (Oxford Optronix, Oxford, UK). Tumour cells irradiated under hypoxia were exposed to normoxia at 1 h post-irradiation. As standard, BEZ235 was added 1 h prior to irradiation and was washed away 17 h after irradiation. Experiments were performed three times in triplicates.

## 2.6 Analysis of protein phosphorylation.

SQ20B, T24 and FaDu cells were lysed after treatment with BEZ235 and BGT226 at the different times and concentrations indicated. Cell lysis was performed with reducing Triton lysis buffer following washing once with PBS. Samples were boiled, sheared, clarified by centrifugation at 14,000 rpm and they were finally stored at −80°C. Protein concentration in lysates was determined by the Bicinchoninic acid assay. For blotting, Invitrogen precast gels were used to separate and blot equal amounts of protein onto nitrocellulose membranes (GE-Amersham, London, UK). Blockade of the membranes was

performed using a mixture of TBS with 0.1% Tween 20 and 5% non-fat powdered milk (both from Sigma, Gillingham, UK). Before the addition of primary antibody, blocking was also done using 5% bovine serum albumin (BSA) for probing with phospho-specific antibodies. Phospho-mTOR (ser-2448), phospho-Akt (ser-473) and phospho-S6 (ser-235/236) primary antibodies (Cell Signalling, Hitchin, UK) were used at 1:1,000 dilution. β-actin clone AC-15 (Sigma, Gillingham, UK) was used at 1:4,000 dilution. Antibody binding was detected using the enhanced chemoluminescence kit (GE-Amersham, London, UK). Exposed film was digitised and figures were assembled using Adobe Photoshop and Microsoft PowerPoint.

For experiments using the ATR inhibitor, MiaPaCa-2, PSN-1 and HFL-1 cells were treated with VE-822 (80 nM) and/or gemcitabine (20 nM) for 1 h before XRT (6 Gy), lysates were obtained at 2 h post-XRT, after rinsing cells with cold PBS and using reducing Triton lysis buffer. Additionally, female Balb/C nude mice bearing PSN-1 tumours (volume ~ 300 $mm^3$) were treated with VE-822 (60 mg/kg; day 0 and 1), and/or gemcitabine (100 mg/kg; day 0), and/or XRT (6 Gy; day 1). Gemcitabine (day 0) was administered 24 h before irradiation. VE-822 was administered 2 h after gemcitabine (day 0) and 2 h before XRT (day 1). We aimed to give VE-822 for only 2 days in order to examine the blockade of Chk1 phosphorylation *in vivo* at 2 hours post-XRT, similarly to the *in vitro* experiment. Tumours were harvested 2 h post-XRT, snap frozen, homogenised and prepared in the same buffer used in cells. Immunoblotting was conducted as described above.

## 2.7 Analysis of γH2AX foci

Residual DNA damage in irradiated FaDu and SQ20B cells was assessed by measuring residual γH2AX foci. Cells were plated into 96-well plates at a density of 10,000 cells per well and incubated overnight at 37°C with 5% $CO_2$. Cells in the mid-log

phase were pretreated with either BGT226 (5 nmol/l) or BEZ235 (50 nmol/l) for 1 h before radiation (4 Gy) using an IBL 637 caesium irradiator at a dose rate of 1.1 Gy/min (CIS Bio International, Gif-sur-Yvette, France). Cells were exposed to PI3K/mTOR inhibitor for up to 24 h post-irradiation. Cells were also treated separately with the BEZ235 (50 nmol/l) and radiation (4 Gy), as above, and a time-course analysis of residual γH2AX foci was performed at 6, 24 and 48 h post-irradiation.

The number of residual γH2AX foci was also measured in HUVEC, as above, at 24 h post-irradiation (4 Gy). HUVEC were pretreated with BEZ235 (50 nmol/l) for 1 h before irradiation. Following irradiation of HUVEC, medium was replaced by basal medium containing 1.5% FCS and 10 ng/ml VEGF-A.

For analysing the impact of ATR inhibition on the number of residual foci, VE-822 (80 nM) was added 1 h before XRT (6 Gy). The residual DNA damage was assessed by 53BP1 and γH2AX in PSN-1 and MiaPaCa-2 cells at 24 h post-XRT with 6 Gy. Homologous recombination repair (HRR) was analysed by Rad51 at 6 h post-XRT. The analysis for residual γH2AX, 53BP1 and Rad51 foci was performed using immunofluorescence.

Cells were plated into 96-well plates at a density of 10,000 cells per well and incubated overnight at 37°C with 5% CO2 to allow cells to attain growth in mid-log phase before drug and XRT treatment. Cells were fixed with 3% paraformaldehyde in PBS at the different time points after XRT as indicated. Following that, cells were exposed to 0.1% Triton diluted in PBS containing 1% BSA (Sigma, Gillingham, UK) for 1 h at 4°C, for permeabilisation and blockade. Subsequently, cells were incubated with a primary mouse monoclonal antibody to γ-H2AX (Millipore, Watford, UK), a primary rabbit monoclonal antibody to 53BP1 (Cell Signalling, Hitchin, UK) or rabbit anti-human Rad51 antibody (Santa Cruz, Wembley, UK) at 1:1,200 dilution overnight at 4°C. Thereafter, cells were

washed using PBS (5 min each time) and were incubated with a secondary antibody for 1 h at room temperature. More specifically, a goat anti-mouse Alexafluor 488 conjugated secondary antibody (Invitrogen, Paisley, UK) 1:1,200 was used for γ-H2AX while Rad51 and 53BP1 were detected using a goat anti-rabbit Alexa-568 antibody (1:1,200; Invitrogen, Paisley, UK). Cells were again washed with PBS (5 min each time) before stained for 10 min with 4′,6-diamidino-2-phenylindole (DAPI; 0.5 μg/ml) diluted in PBS. The DAPI was replaced with 200 μm PBS before detection of foci by an IN Cell Analyser 1000 automated epifluorescence microscope (GE Healthcare, London, UK). For the latter, the following excitation and emission filters (Chroma) were used: DAPI excitation filter, 360 nm (D360_40x); emission filter, 460 nm (HQ460_40M); dichroic mirror, 61002bs. Alexafluor 488 excitation filter, 480 nm (HQ480_40x); emission filter, 535 nm (HQ535_50M); Dichroic mirror, 61002bs. The number of foci and nuclei was quantitated by the IN Cell Analyser Workstation software (v3.5).

## 2.8 Cell cycle assay

FaDu, SQ20B and HUVEC cells were plated into T25 tissue culture flasks (Falcon, Seaton Delaval, UK) and incubated overnight to allow cells to reach mid-log phase. Tumour cells were treated with BEZ235 (50 nmol/l) for 1 h before irradiation using an IBL 637 caesium irradiator at a dose rate of 1.1 Gy/min (CIS Bio International, Gif-sur-Yvette, France) and medium was replaced 17 h post-irradiation.

HUVEC cells were plated in growth-factor depleted medium overnight. Cells were treated with BEZ235 (50 nmol/l) 1 h before irradiation with a single dose of 4 Gy. Following irradiation, HUVEC medium was replaced by basal medium containing 1.5% FCS and a constant concentration of VEGF (10 ng/ml).

PSN-1 and MiaPaCa-2 cells were treated with VE-822 (80 nM) for 1 h before XRT (6 Gy) until cells were harvested. In the chemotherapy-incorporating groups, gemcitabine (10 nM) was added for 24 h, medium was washed and VE-822 (80 nM) was added.

A mixture of 0.5% Trypsin/EDTA (Life Technologies-Bethesda Research Laboratories, Gaithersburg, MD) was used to trypsinise cells, followed by centrifugation at 1,200 rpm. Following this, cells were washed with PBS, resuspended in 1 ml ice cold 70% ethanol for 5 min and centrifuged again at 1,200 rpm (10 min). Thereafter, cells were incubated with a mixture of 200 μg/ml RNaseA diluted in PBS with 50 μg/ml propidium iodide (PI; Sigma, Gillingham, UK), for 30 min at room temperature (in dark room). Cell cycle was analysed 24 h post-irradiation in the experiments using PI3K/mTOR inhibitors and at 12 h and 24 h post-irradiation in the experiments using VE-822, by the Becton Dickinson FACSort machine (BD, Oxford, UK) with the Modfit LT analysis software.

## 2.9 Analysis of apoptosis *in vitro*

FaDu, SQ20B and HUVEC cells were plated into T25 tissue culture flasks (Falcon, Seaton Delaval, UK) and incubated overnight to allow cells to reach mid-log phase. Tumour cells were treated with PI3K/mTOR inhibitor for 1 h before irradiation. Medium was replaced 17 h post-irradiation. HUVEC cells were plated in growth-factor depleted medium overnight. Cells were treated with BEZ235 (50 nmol/l) 1 h before irradiation with a single dose of 4 Gy. In tumour cells, fresh medium was replaced 17 h post-irradiation. Similarly to the cell cycle assay, following irradiation, HUVEC medium was replaced by basal medium containing 1.5% FCS and a constant concentration of VEGF (10 ng/ml).

To test the effect of ATR inhibition on apoptosis, PSN-1 cells were pretreated with for 24 h with gemcitabine (50 nM) prior to addition of VE-822 (80 nM) for 1 h before until 18 h after XRT (6 Gy).

Cells were allowed to grow and were finally trypsinised at 24 and 48 h post-irradiation (PI3K/mTOR inhibitors) or at 48 h post-irradiation (ATR inhibitor). Cells were trypsinised using 0.5% Trypsin/EDTA (Life Technologies-Bethesda Research Laboratories) and centrifuged at 1,200 rpm. Subsequently, cells were washed with PBS and centrifuged at 1,200 rpm for 10 min. Apoptosis was analysed by flow cytometry after staining cells with Annexin V-FITC kit (eBioscience) in combination with PI (50 μg/ml; Sigma) mixed with PBS for 30 min, using the Becton Dickinson FACSort machine (BD, Oxford, UK). Data analysis was made by the FlowJo 7.5 analysis software (Tree Star, Oregon Corporation, Ashland, OR).

## 2.10 Capillary tube formation and endothelial cell migration

HUVEC and HDMVC in mid-log phase were plated in growth factor-depleted medium overnight and treated with BEZ235 (50 nmol/l) for 1 h, before irradiation with 4 Gy. Cells were trypsinised immediately after irradiation and 40.000 cells/well were plated onto 24-well plates, previously coated with Matrigel (300 μl per well; BD, Oxford, UK), and incubated in basal medium containing 1.5% FCS and a constant concentration of VEGF (10 ng/ml). Once tubules began to form in the control group, cells were stained with calcein (BD, Oxford, UK), according to the manufacturer's instructions. Three randomly selected digital photomicrographs (magnification x10 for HUVEC and x4 for HDMVC) were obtained from each well. The length of capillary-like tubular structures was measured with the ImageJ software and was normalised to the control group. Experiments were performed twice in quadruplicates.

For the ATR inhibition experiment, HDMEC in mid-log phase were exposed to VE-822 (80 nM) for 1 h before XRT (6 Gy) until 8 h post-XRT and tube formation was analysed. The impact of VE-822 on gemcitabine-induced toxicity was also assessed in

endothelial cells. For that purpose, HDMECs were pretreated with 50 nM gemcitabine for 24 h, gemcitabine was washed away, 80 nM VE-822 was added and tube formation was assessed 9 h later. Tube formation was conducted and analysed as above.

For the migration assay, cells were treated with BEZ235 as for the tube formation assay and were trypsinised immediately after irradiation and plated onto the top chamber of 24-well plates (60,000 HUVEC/well and 30,000 HDMVC/well) with 8 μm matrigel-coated inserts (BD, Oxford, UK). Basal medium (500 μl) containing 1.5% FCS and a constant concentration of VEGF (10 ng/ml) was added to the lower compartment and cells were incubated for 18 h and allowed to migrate towards the VEGF-containing medium, according to the manufacturer's instructions. Cells were finally scraped off at the upper side of the membrane with a cotton swab and migrated cells were stained with calcein fluorescent dye (BD, Oxford, UK). Three randomly selected digital photomicrographs were obtained from each well. The number of migrated endothelial cells (lower side of the membrane) per field (magnification x10) was counted by microscopy. Immunofluorescent images were acquired using the Leica DMRBE microscope with a Hamamatsu camera (c47742-95; Leica Microsystems Ltd, Milton Keynes, UK). The results represent the mean number of migrated cells, normalised to the control group, as calculated from three random fields in quadruplicates.

## 2.11 Xenograft studies using PI3K and PI3K/mTOR inhibitors

### 2.11.1 Tumour xenograft growth delay assay

All animal experiments were carried out in accordance with U.K. Home Office regulations. FaDu-HRE-luc and HT1080-HRE-luc cells ($1 \times 10^6$ in 100 μL serum-free medium) were inoculated s.c. in athymic Balb/c nude mice (Harlan, Wolverhampton, UK). In HT-1080 study, two different doses were tested for BKM120 (30 and 15 mg/kg) and

BEZ235 (20 and 10 mg/kg) p.o., via oral gavage. Only the high dose was applied in FaDu-HRE-luc experiment, based on the dose-dependent inhibition of PI3K signalling.

For the first series of experiments (non-radiation) testing both cell lines, mice were divided into cohorts of four mice per drug per dose. A placebo cohort that received vehicle (NMP/PEG300; provided by Novartis Pharmaceuticals, Basel, Switzerland) was included as well. Drug administration was commenced once tumours reached a volume of 100 $mm^3$ and were given daily for 1 week. At the end of the experiments, the mice were sacrificed and the tumours were fixed in 3% neutral-buffered formalin. For the second series of experiment performed (radiation) using FaDu-HRE-luc xenografts, BEZ235 (20 mg/kg) administration was started once tumours reached a volume of 100 $mm^3$ and was given daily, throughout the experiment.

A single dose (6 Gy) was applied at day 7 with a 300 kV orthovoltage irradiator Philips RT 250 (Philips Medical Systems, Nijmegen, The Netherlands) at a dose rate of 2.63 Gy/min, by copper shielding. Mice were anaesthetised using Ketamine/Xylazine at 1:1 dilution (obtained from Parke-Davis Veterinary, Merthyr Tydfil, UK and Bayer, Cambridge, UK, respectively). The source-to-target distance was 30 cm. Tumour size was measured with callipers using the formula $V= (a \times b^2) /2$, where a and b are the largest and the smallest perpendicular diameters, respectively.

## 2.11.2 *In vivo* real-time optical and ultrasound imaging

Mice were anesthetised with 2% isofluorane (Baxter, Caxton Way, UK) and then placed inside the chamber of a Xenogen IVIS 200 imaging system (Calliper Life Sciences Ltd., Cheshire, UK). The mice were injected with D-luciferin (150 mg/kg body weight; Gold BioTechnology, St. Louis, MO) intraperitoneally, 5 min before imaging. The parameters for image acquisition were f/stop = 1, bin = Med, and exposure time = 5 sec. We quantified the intensity of the signal by measuring the total number photons *per*

*se*cond within the tumour region of interest (ROI) by using Living Image 3.0 software (Calliper Life Sciences Ltd., Cheshire, UK). Tumour hypoxia, represented by photon flux, was normalised to the untreated (control) group.

Evaluation of tumour blood flow was performed with the use of a Vevo 770 Micro-Ultrasound platform equipped with a RMV-704 probe (VisualSonics, Toronto, ON) by contrast microbubbles for image enhancement (Vevo MicroMarker Contrast Agent Kit; VisualSonics, Toronto, ON) that has the benefit of obtaining a direct kinetic analysis of microbubble influx i.e. vessel functionality compared to CD31-RPE [142]. Mice were anaesthetised (inhalational isofluorane 2%) throughout ultrasound imaging. A fresh vial of lyophilized microbubble powder was prepared by injecting 0.7 ml of sterile saline into the fresh vial. Microbubbles were administered as a bolus (50 μL) via injection with a 27-gauge hypodermic needle into a lateral tail vein. The ultrasound transducer probe was placed vertically, over the centre of the tumour. Before injection of microbubbles, an image sequence of the tumour was acquired (contrast mode) over 40 seconds (550 frames), to account for the background intensity and the video was recorded on a cine clip. In addition, an additional B-mode image sequence of the tumour baseline was acquired at a frequency of 40 MHz. The same procedure was repeated again upon injection of the microbubbles, immediately after beginning image recording. For each tumour, the ROI was contoured with the Vevo770 Ultrasound Platform (VisualSonics, Toronto, ON). Subsequently, the percentage of green contrast signal (microbubbles) within the ROI area i.e. the percentage of blood flow within the tumour was analysed using the ImageJ software (NIH, Bethesda, MD). Relative blood flow was determined by dividing tumour blood flow for the treatment groups by the tumour blood flow for the vehicle group, at day 1, and then multiplying by 100%. Moreover, an analysis of the microbubble contrast kinetics was also made using the Vevo 770 software (v.2.23; VisualSonics, Toronto, ON).

The slope and magnitude of microbubble influx (contrast kinetic curve) were assessed for each of the different groups. The ROI (drawn around the tumour) and the acquired cine clip (550 frames; 40 seconds) were evaluated for change in tumour contrast intensity, also by accounting for the baseline intrinsic contrast, to obtain the percentage of contrast kinetic change.

For Power Doppler, tumour blood flow was evaluated using the Vevo770 Mirco-Ultrasound platform (VisualSonics, Toronto, ON) with the RMV 704 probe, immediately after image recording using the microbubbles. Similarly to the microbubbles, mice were kept under anaesthesia with inhalational isofluorane (2%) during ultrasonography. A single-element transducer with 40 MHz centre frequency was used. The following settings were used: a 50dB Power Doppler gain, a wall filter of 2.3 mm/s, and a scan speed of 2.0 mm/s. Imaging of the tumour in B-mode was initially performed to determine the size of the tumour. Thereafter, three-dimensional power Doppler images were acquired through computer-controlled translation of the transducer over the whole length of the tumour. Three-dimensional images of blood volume were created with the VisualSonics image analysis software. Blood flow was assessed as the percentage of blood volume in each tumour and was normalised to the control group (day 0).

## 2.11.3 Microscopy, Immunostaining and VEGF ELISA

After mice were killed by cervical dislocation, excised tumours were immediately placed in 4% paraformaldehyde and incubated overnight at 4°C, then transferred to 25% glucose (in PBS) and incubated for an additional 24 hours at 4°C, followed by snap freezing in isopentane (Sigma, Gillingham, UK) cooled on dry ice and stored at −80°C until cryosectioning using the microtome cool-cut HM355S (Microm International, Walldorf, Germany; 10-μm sections).

The vascular network was visualized using anti-CD31-RPE-conjugated antibody (Biolegend, Cambridge, UK) at the end of each treatment. The mice were subjected to i.v. injection of 100 µL anti-CD31-RPE-conjugated antibody 10 min before tumour harvesting. After mice were killed by cervical dislocation, their tumours were immediately excised, and a central portion of each tumour was directly sectioned (approximately 5-mm-thick sections) and immediately imaged by confocal microscopy (Leica Microsystems Ltd, Milton Keynes, UK). Confocal z-stacks were taken at 1-µm intervals, at ×10 magnification, on multiple randomly chosen fields using the 543-nm laser, to excite phycoerythrin that was conjugated to the anti-CD31 antibody. Three-dimensional vascular reconstructions were created using Amira ResolveRT software (Visage Imaging GmbH, Berlin, Germany) and the three-dimensional morphology of the vascular network was assessed using the Trace3D software (kindly provided by Dr Paul Barber, University of Oxford) [142].

To assess hypoxia by immunostaining, the mice were injected intraperitoneally with the nitroimidazole hypoxic cell marker EF5 (10 µL/g of body weight of a 10 mM solution in 0.9% saline; kindly provided by Dr Cameron Koch, University of Pennsylvania, PA) at 2 hours before tumour harvesting. Antigen retrieval was made by incubating slides with a mixture of 10 mM sodium citrate with 0.05% Tween-20 (pH 6.0) at 90°C, for 20 minutes. Thereafter, sections were pretreated with blocking buffer for 30 minutes. Immunohistochemistry for EF5 was performed with a mouse monoclonal anti-EF5 antibody directly conjugated to Cy3 fluorophore (clone Elk3-51, 75µg/ml; kindly provided by Dr C. Koch, University of Pennsylvania, PA). Slides were incubated with the antibody for 24 hours at 4°C. The Vectashield aqueous mounting media (Vector Laboratories, Peterborough, UK) that contains 4′,6-diamidino-2-phenylindole (DAPI) was used to mount stained sections. Cross-sections of FaDu tumours from the non-radiation

experiment were also stained for Haematoxyllin/Eosin (Sigma, Gillingham, UK). For that purpose, tissue sections were rehydrated in 100% alcohol twice for 5 min, then in 95% alcohol for 2 min and 70% alcohol for 2 min. Following that, sections were washed in PBS and were stained using Harris haematoxylin solution (Sigma, Gillingham, UK) for 1 min. After that, sections were washed in running tap water for 5 min. Subsequently, sections were differentiated in 1% acid alcohol for 30 sec following washing in running tap water for another 5 min. Sections were counterstained in eosin solution (Sigma, Gillingham, UK) for 1 min. Finally, sections were dehydrated using 90 % alcohol followed by 2 changes of 100% alcohol, 5 min each and finally washed in xylene for 5 min. Sections were covered with cover slips using mounting medium (Vector Laboratories, Peterborough, UK).

For immunohistochemical analysis of phospho-Akt (Ser473) and phosphor-mTOR (Ser 2448) expression, 10 μm sections were subjected to antigen retrieval, as above. Endogenous peroxidase activity was blocked by treatment with 1% hydrogen peroxide in PBS for 30 min at room temperature. A blocking step with normal rabbit serum (Vector, Burlingame, CA) was used. The following primary antibodies were applied overnight in a moist chamber at 4°C: phospho-mTOR (ser-2448) and phospho-Akt (ser-473) antibodies (both from Cell Signalling, Hitchin, UK) were used at 1:1,000 dilution. The following day, tissue sections were incubated with a secondary anti-rabbit antibody. The final reaction product was revealed by exposure to 0.03% diaminobenzidine (Sigma, Gillingham, UK), and nuclei were counterstained with Mayer's haematoxylin (Sigma, Gillingham, UK).

Immunofluorescence staining for blood vessels and pericytes was performed by incubating thin (10 μm) tissue sections 4°C overnight with one of the following antibodies: rabbit anti-NG2 (1:100; Chemicon, Hampshire, UK) and rat anti-mouse CD31 (1:50, BD, Oxford, UK). This was followed by exposure to TSA biotin system (Perkin-Elmer, Waltham, MA) and then by streptavidin-conjugated fluorophores Alexa Fluor 488 and 546

(Invitrogen, Paisley, UK). Immunofluorescent images were acquired using the Leica DMRBE microscope with a Hamamatsu camera (c47742-95; Leica Microsystems Ltd, Milton Keynes, UK). VEGF levels were measured by the Quantikine VEGF ELISA kit (R&D Systems, Wiesbaden, Germany).

## 2.12 Xenograft studies using ATR inhibition

### 2.12.1 Tumour xenograft growth delay assay

Animal experiments involving mice were performed according to the guidelines of University of Oxford and within the limits of the Project Licence issued by the Home Office, United Kingdom, and in accordance with the guidelines for the welfare and use of animals in cancer research. MiaPaCa-2 cells and PSN-1 cells ($1 \times 10^6$ in 100 μL serum-free medium mixed with equal amount of Matrigel) were inoculated s.c in female Balb/c nude mice (Harlan, Wolverhampton, UK)., in front of the right hind leg. When the xenograft tumours reached a volume of ~ 80 $mm^3$, the mice were randomized into control or experimental groups.

For tumour irradiation, mice were anaesthetized using intraperitoneal anaesthesia (Ketamine/Xylazine 1:1 dilution; obtained from Parke-Davis Veterinary, Merthyr Tydfil, UK and Bayer, Cambridge, UK, respectively) and were placed in a specialized brass jig to expose the tumour while shielding the remainder of the body. Tumour xenografts were irradiated with X-rays produced by a Gulmay RS320 with 300 kV energy (Gulmay Medical Ltd., Surrey, UK). Tumour size was measured with callipers using the formula $V= (a \times b^2) / 2$, where a and b are the largest and the smallest perpendicular diameters, respectively.

VE-822 was administered at a dose of 60 mg/kg by oral gavage on one of three alternate schedules; either daily on days 0 through to 5 (total of six days dosing), daily on days 0 through to 3 (total of 4 days dosing) or on days 1, 3 and 5. Radiation was given

either on day 0 (6 Gy) or days 1 through to 5 (total of 5 days dosing; 2 Gy). Gemcitabine was dosed at 100 mg/kg by intraperitoneal (i.p.) injection on day 0. Radiation was given 2 hours after initiation of VE-822 treatment. Gemcitabine doses were chosen based on prior tumour growth delay experiments (data not shown).

## 2.12.2 Immunostaining and microscopy

After completion of the experiments, tumours were harvested, snap frozen and were stored at -80º C. Specimens were cut to 10-µm sections using the microtome cool-cut HM355S (Microm International, Walldorf, Germany). Sections were pretreated with 0.3% hydrogen peroxide in PBS for 20 min, followed byris-NaCl-blocking buffer (TNB) for 30 min and subsequent overnight exposure to a primary antibody mixed with TNB, in cold room. Immunofluorescence staining for blood vessels was made using a rat anti-mouse CD31 antibody (1:50; BD, Oxford, UK) and for proliferation by using a rabbit monoclonal Ki67 antibody (1:500, clone SP6; Dako, Cambridge, UK). Bound antibody was labelled with HRP conjugated rabbit anti-Rat IgG (1:100, Dako, Cambridge, UK) and anti-rabbit antibody. Staining was completed using the TSA biotin system (Perkin-Elmer, Waltham, MA) and streptavidin-conjugated fluorophores Alexa Fluor 549 (1:1000; Invitrogen, Paisley, UK).

Vessel density was quantified as the number of blood vessels/field in five random viable fields (10× objective) per tumours (n=4-5 per group). Proliferation was measured as the percentage of Ki67-positive area in relation to the DAPI-positive signal (tumour surface area) in five random viable fields (10× objective) per tumours (n=4-5 per group) using ImageJ software (version 1.38). Immunofluorescent images were acquired using the Leica DMRBE microscope with a Hamamatsu camera (c47742-95; Leica Microsystems Ltd, Milton Keynes, UK).

The effect of radiation and/or VE-822 on gut epithelium was determined by measuring changes in morphology [32] and apoptosis [33] of small intestine after treatment with the ATR inhibitor. Briefly, athymic nude mice bearing PSN-1 tumours xenografts were treated with either vehicle or 60 mg/kg VE-822 p.o. at day 0, 2 and 4. Mice (n=3) were irradiated at day 0 using abdominal radiation (6 Gy), 2 hours after VE-822 initiation. At day five, mice were sacrificed and the small intestine was removed, washed, and fixed in 3% formalin/PBS for histological examinations. Cross-sections of the small intestine were stained for H&E (Sigma, Gillingham, UK; as above) and TUNEL (apoptosis), according to the manufacturer's instructions (Apoptag; Millipore, Watford, UK). For that, slides were washed twice with PBS for 10 min and were fixed in pre-cooled (−20 °C) fixative (2 ethanol:1 acetic acid) for 5 minutes. Slides were then rinsed in PBS for 5 min (2 times) and the equilibration buffer was applied to slides for 10 sec at room temperature. Slides were washed once in PBS and following this, terminal deoxynucleotidyl transferase (TdT) was applied on the slides in a humid chamber for 1 h at 37 °C. Thereafter, the enzyme reaction reaction was stop by incubating slides with the working strength stop/wash buffer for 10 min. Slides were rinsed again in PBS, for 10 min (2 times). The fluorescent TUNEL antibody was finally applied and slides were incubated for 1 h at room temperature in the dark. Slides were finally counterstained with DAPI for 5 min. Slides were washed in PBS for 15 minutes (2 times) in the dark and slides were mounted with mounting medium. Villus length was measured using the ImageJ software (version 1.38). The loss of villus tip loss and the number of apoptotic cells per villus-crypt unit were estimated manually. Approximately 100 crypt-villus units were scored per group. The experiment was performed twice.

## 2.13 Statistical analyses

The values were expressed as means ± standard deviation (SD). The significance of differences between the means was measured by two-tailed t-test or one-way ANOVA (to compare the mean value of more than two samples) using the GraphPad Prism program version 4.0 (GraphPad Software, La Jolla, CA). In the case of one-way ANOVA, the Bonferroni test was used. A value $p<0.05$ was considered statistically significant. In chapters 3 and 4, error bars in the graphs display the standard deviation (SD). In chapter 5, error bars in the graphs represent the 95% confidence interval (95% CI).

# CHAPTER 3

# BEZ235 and BGT226 enhance tumour and endothelial cell radiosensitivity

## Published in: Radiat Oncol. 2012 Mar 27;7:48.

Emmanouil Fokas[1]*, Michio Yoshimura[1]*, Remko Prevo[1], Geoff Higgins[1], Wolfgang Hackl[2], Sauveur-Michel Maira[2], Eric J. Bernhard[1], W. Gillies McKenna[1] and Ruth J. Muschel[1]

[1]Gray Institute for Radiation Oncology and Biology, Oxford University, Oxford, United Kingdom;
[2]Novartis Pharma AG, Novartis Campus, CH-4057 Basel, Switzerland

**Contribution to experimental work:** Michio Yoshimura has conducted the experiments shown in Fig. 1A-B and partly C-D, partly 2B-C and finally 5B. Remko Prevo has assisted with the experiments shown in Fig 1C-D and 2C. Novartis Pharmaceuticals provided the dual PI3K/mTOR inhibitors. The rest of experiments have been performed and analysed by Emmanouil Fokas.

# 3.1 Introduction

Clinical trials have shown that the combination of radiotherapy with chemotherapy can improve local tumour control and, in some cases, overall survival compared to radiotherapy alone. Despite the proven benefit of chemoradiotherapy, local recurrences are not uncommon and normal tissue toxicity is often exacerbated. It now becomes increasingly apparent that better and less toxic radiosensitisers are needed [7].

The PI3K/Akt/mTOR pathway controls tumour cell proliferation, growth, and survival after DNA damage [114]. Activation of this pathway is frequent in many cancers and can occur through diverse mechanisms such as amplification of the EGFR gene, mutations of the Ras oncogene, PI3K mutations and loss of PTEN [7, 87, 114]. This pathway consists of EGFR/Ras/PI3K/Akt and is a prime target for inhibition in the context of radiotherapy [274-276]. Inhibition of the EGFR/Ras/PI3K/Akt pathway can increase susceptibility to radiation-induced tumour killing [87, 88, 91, 277-279]. Inhibition of Ras, PI3K and Akt reduce tumour clonogenic survival after radiation at clinically relevant doses [87, 88, 91, 274, 275, 280]. A phase III randomized clinical trial evaluated the addition of cetuximab, an EGFR inhibitor, to radiotherapy and demonstrated improved overall survival in the combined modality arm over radiation alone [281].

The kinase mTOR consists of TORC1 and TORC2, two functionally distinct multiprotein complexes [282]. TORC1 includes mTOR and raptor (regulatory-associated protein of mTOR). TORC2 is composed of mTOR and rictor (rapamycin-insensitive companion of TOR) and regulates the activity of Akt [282]. Rapamycin is a very potent antifungal and immunosuppressive agent that exerts powerful antiproliferative effects on malignant cells. Several studies have demonstrated the antitumour efficacy of mTOR inhibitors rapamycin and related compounds (“rapalogs”) in cancer therapy [7]. mTOR inhibitors have radiosensitising potential in tumour and vascular cells [93, 94]. Inhibition

of TORC1 activity alone can result in TORC2-mediated feedback phosphorylation of Akt on Ser473 [282, 283]. S6 is a ribosomal protein that is phosphorylated upon activation of the p70/S6 kinase in response to various growth factors and mitogens. The phosphorylation of S6 protein is associated with an increase in translation of mRNA transcripts that encode proteins which play a role in cell cycle progression [282, 283].

Preclinical studies have demonstrated antitumour activity for the PI3K/mTOR inhibitor BEZ235 in a variety of models especially those with PI3K mutation or K-Ras mutation. In chapter 3, the radiosensitising potential of dual PI3K/mTOR (both mTORC1 and mTORC2) inhibitors BEZ235 and BGT226 in tumour cells with EGFR overexpression or Ras mutation was examined. Two inhibitors were tested to get a better insight of the efficacy of each compound and test whether comparable results will be obtained. Both dual PI3K/mTOR inhibitors are issued from the same chemical space (imidazo-quinolines). BGT226 displays more prolonged effects on target in cells, likely due the slow kinetics on target (high affinity, slow release). Additionally, the effect of PI3K/mTOR inhibition in the radiation response of endothelial cells was investigated. A substantial body of evidence has demonstrated that the PI3K/mTOR pathway is involved in angiogenesis and functions downstream of VEGF-A to promote endothelial cell survival [6, 284]. In addition, VEGF-A can act downstream of the PI3K/mTOR as well since activation of oncogenic signalling in tumour cells will cause release of VEGF-A from them that will in turn activate the VEGF-VEGFR complex in endothelial cells, promoting angiogenesis [6]. Therefore the impact of one the inhibitors, BEZ235, on VEGF-mediated Akt signalling, survival and *in vitro* angiogenesis in irradiated tumour and endothelial cells was studied. I also chose to analyse the effect of BEZ235 on endothelial cells in response to irradiation because vascular damage consists one of the major causes of radiation-induced side effects. Radiation can initiate an inflammatory response and also activate

coagulation cascades that lead to vessel injury, capillary bleeding, formation of micro-thrombus subsequent ischemia and fibrosis [7]. Hence, by conducting experiments with BEZ235 in endothelial cells I expected to gain a better insight on the potential side effects that this drug could, in theory, induce in normal tissues exposed to radiotherapy.

## 3.2 RESULTS

### 3.2.1 BGT226 and BEZ235 inhibit PI3K and mTOR activity and reduce AKT and S-6 phosphorylation

The inhibitory effect of these novel compounds on PI3K and mTOR signalling was investigated to establish their minimum inhibitory concentrations. To this end, the phosphorylation of PI3K pathway downstream targets by Western blotting was analysed after treatment of SQ20B cells with BGT226 and BEZ235 in increasing concentrations (Fig. 1A). BGT226 and BEZ235 were able to attenuate phosphorylation of Ser473 Akt, Ser2448 mTOR, and Ser235/236 S6 in SQ20B cells at concentrations of 5 nmol/l and 50 nmol/l, respectively (Fig. 1A). BEZ235 (50 nmol/l) reduced phosphorylation of all three targets within 1 h of exposure. Inhibition persisted mainly for the first 12 h and started returning to baseline levels at 24 h. Inhibition of pAkt by BGT226 (5 nmol/l) was relieved after 16 h (Fig. 1B). BGT226 did not reduce mTOR or Akt phosphorylation as efficiently as BEZ235, both in unirradiated and irradiated tumour cells (Fig. 1C and 1D). The increase of mTOR and, even more prominently, Akt phosphorylation observed at 24 h in the cells exposed to BGT226 (5 nM) could be attributed to different factors such as insufficient drug concentration, drug stability and/or a rebound feedback activation of Akt by mTOR, which can occur as a compensatory mechanism, as discussed in “Discussion”. More specific information from Novartis Pharmaceuticals was requested regarding the stability of BGT226 *in-vitro* but no specific information was obtained.

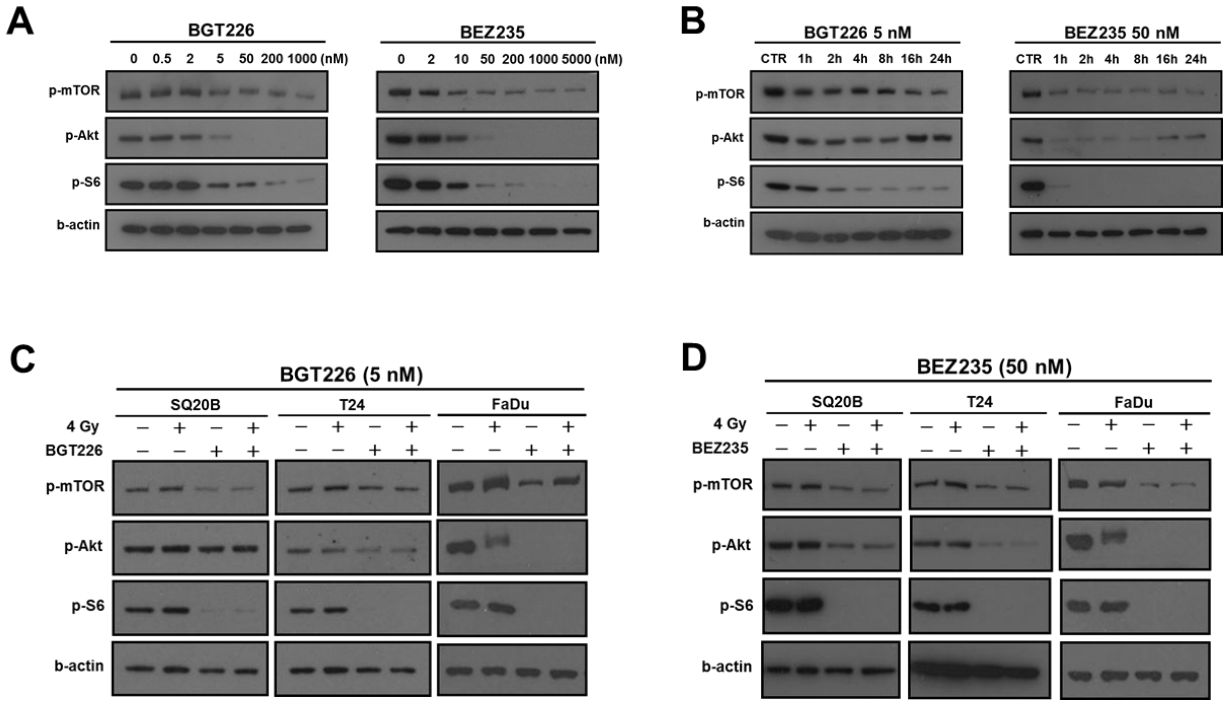



**Figure 1.** BGT226 and BEZ235 attenuate oncogenic signalling. SQ20B cells were exposed to the indicated drugs for 1 h and evaluated by Western blotting for phosphorylation of mTOR (Ser2448), Akt (Ser-473) and S6 protein (ser-235/236). β-actin was used as a loading control. ***A***, Dose response of the PI3K/mTOR pathway in SQ20B cells after 1 h exposure to the indicated drug. ***B***, Time-course of PI3K/mTOR inhibition to indicated drugs at maximal effective doses. ***C- D***, Response of PI3K/mTOR pathway 1 h after 4 Gy. Cells were treated with 5 nmol/l BGT226 (C) or 50 nmol/l BEZ235 (D) for 1 h before and 1 h after irradiation. P-Akt, phosphor-Akt; p-mTOR, phosphor-mTOR; p-S6, phosho-S6; (Figure 1A-D are partly courtesy of Drs Michio Ushimura and Remko Prevo, Gray Institute).

## 3.2.2 BGT225 and BEZ235 reduce radiation survival of tumour cells with EGFR overexpression or Ras mutation

SQ20B and FaDu are derived from head and neck cancers with overexpression of EGFR. T24 is a bladder cancer cell line with mutated H-Ras. Experiments were conducted in order to assess the optimal drug incubation time for colony forming assays with BEZ235 (50 nmol/l) and BGT226 (5 nmol/l) in SQ20B and T24 cells in the absence of radiation. Exposure of cells to the drugs for 18 h did not alter plating efficiency (PE) significantly (Fig. 2A). Therefore, for subsequent clonogenic assays, cells were pretreated with either compound for 1 h before irradiation and total incubation time was limited to 18

h. BGT226 and BEZ235 treatment for 18 h resulted in significant reduction in clonogenic survival after irradiation in all three cell lines (Fig. 2B). To quantify the effect, the radiation dose required to reduce the surviving fraction to 10% was calculated (dose modifying factor 10%; DMF10). The ratio of DMF10 in control cells to BGT226-treated cells was calculated to be 2.6 for SQ20B, 1.6 for FaDu and 1.7 for T24. In BEZ235-treated cells, the DMF10 was 2.5 for SQ20B, 1.5 for FaDu and 1.7 for T24. Thus, there is significant radiosensitisation of these three cell lines by these inhibitors.

To understand the mechanisms of radiosensitisation, the BGT226- and BEZ235-induced enhancement of radiation response in the post-irradiation setting was studied. BGT226 (5 nmol/l) or BEZ235 (50 nmol/l) were added to the culture medium of SQ20 and T24 cells immediately or 6 h after exposure to radiation, for a total exposure time of 18 h. Treatment with drug immediately after irradiation was similar to giving the drug before (Fig. 2C) but if given 6 h after exposure, no radiosensitising effect was observed (Fig. 2D). The latter indicates that blockade of the PI3K/mTOR pathway early before or after irradiation is necessary for sensitising tumour cells to radiation damage.

**A**

**Plating efficiency**

| Cell line | Concentration of the compounds | Mean plating efficiency (%) |
|---|---|---|
| SQ20B | DMSO | 49.8% |
| | BEZ235 50nM | 43.0% |
| | BGT226 5nM | 47.1% |
| T24 | DMSO | 48.0% |
| | BEZ235 50nM | 45.9% |
| | BGT226 5nM | 52.2% |
| FaDu | DMSO | 40.1% |
| | BEZ235 50nM | 36.8% |
| | BGT226 5nM | 37.1% |

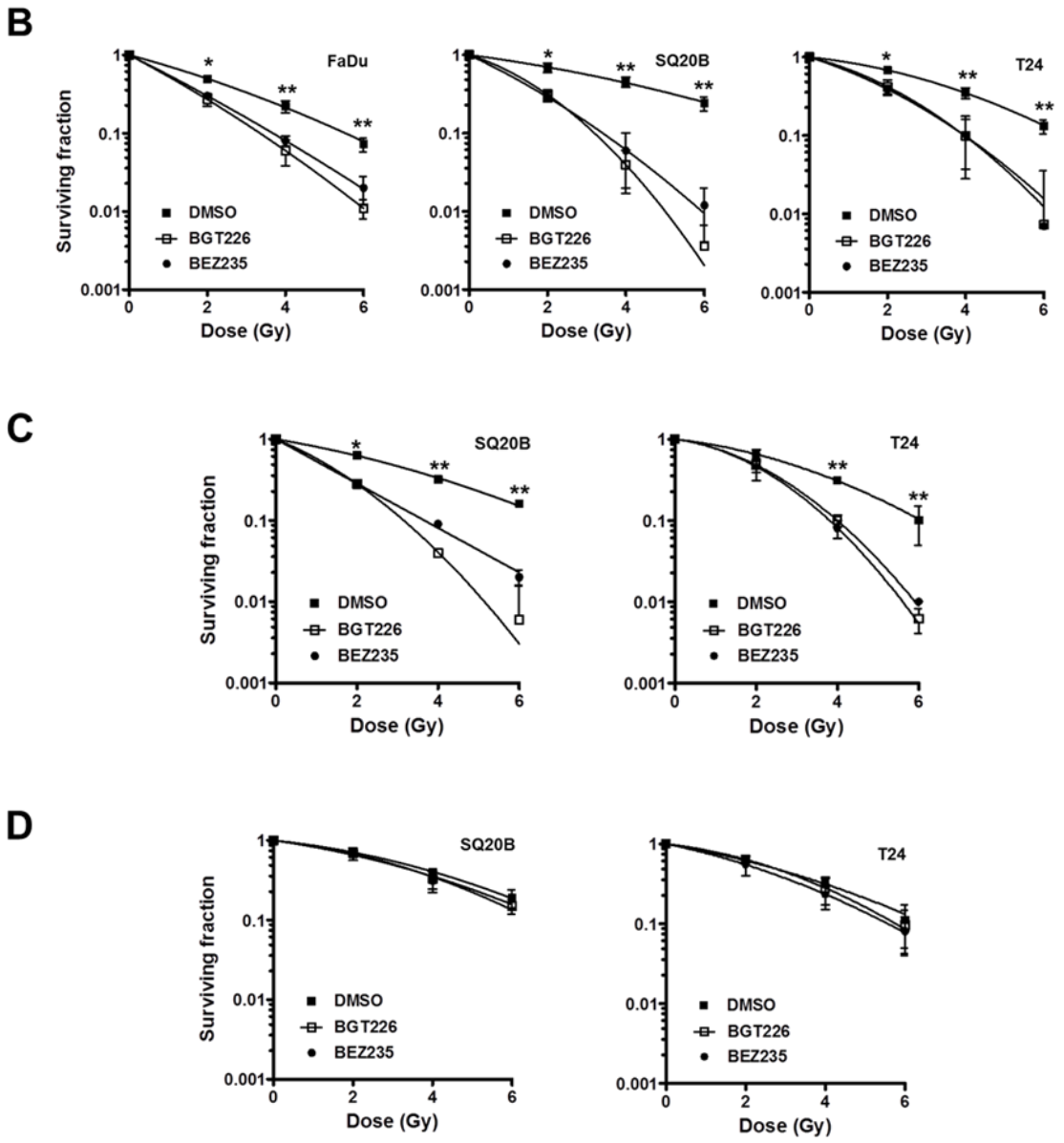
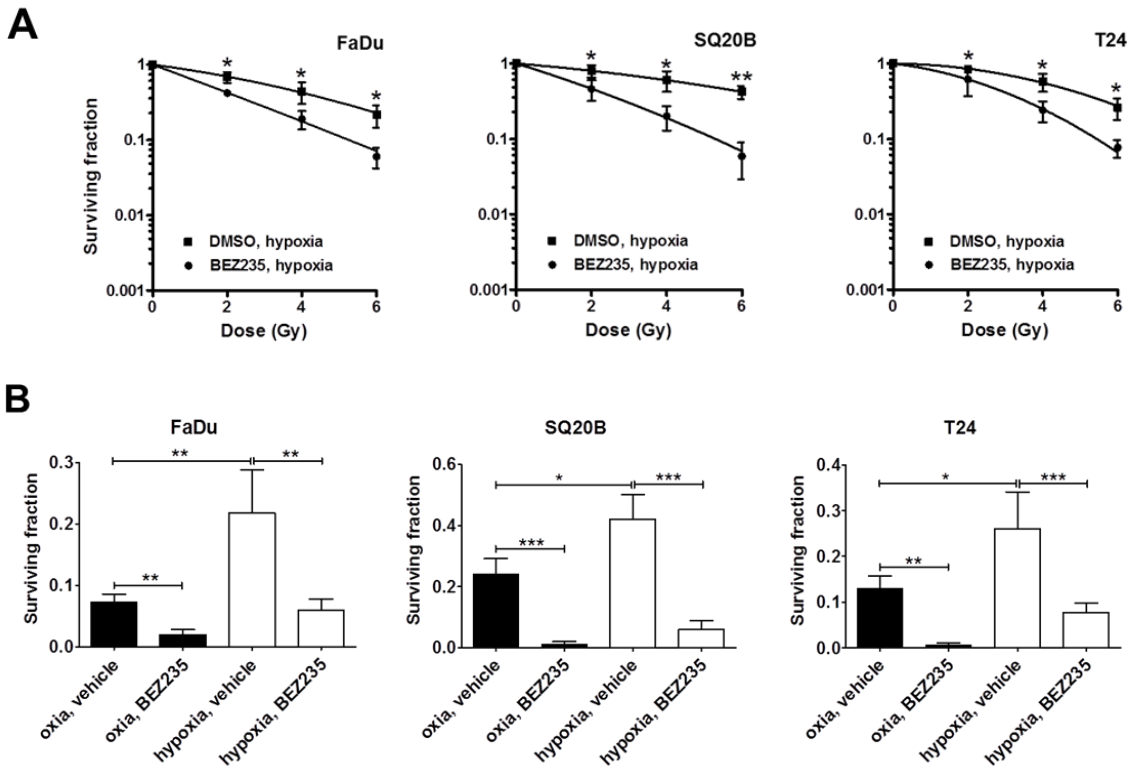



**Figure 2.** BGT226 and BEZ235 reduce clonogenic survival after radiation. ***A,*** Plating efficiency of SQ20B and T24 cells after exposure to indicated drugs for 1 h before up to 17 h post-irradiation (n=3). ***B,*** Clonogenic survival of indicated cell lines after 18 h treatment with BEZ235 (50 nmol/l) and BGT226 (5 nmol/l), as described in "Methods". ***C-D,*** The effect of timing of BEZ235 and BGT226 administration on tumour cell radiosensitivity. Clonogenic survival assays of SQ20B and T24 cells treated as indicated. BEZ235 (50 nmol/l) and BGT226 (5 nmol/l) were added ***(C)*** immediately or ***(D)*** 6 h following irradiation (n=3). *, $P < 0.05$; **, $P < 0.01$ over DMSO-treated control (Fig. 2A, C and D are partly courtesy of Dr Michio Yoshimura, Gray Institute).

## 3.2.3 BEZ235 radiosensitises tumour cells under hypoxic conditions

Because hypoxic cells can be up to three fold more radioresistant, as compared to normoxic cells [43], I asked whether the radiosensitising effect of BEZ235 can still be seen under hypoxic conditions (Fig. 3A-B). Tumour cells were treated with one of the inhibitors, BEZ235 (50 nmol/l) for 1 h before up to 17 h after irradiation under hypoxic conditions (0.5% oxygen). Treatment with BEZ235 in the absence of irradiation did not result in profound toxicity in hypoxia. Indeed, a moderate decrease in plating efficiency was observed in BEZ235- compared to the DMSO-treated cells: 29%/34%, 35%/41% and 34%/40% in FaDu, SQ20B and T24 cells, respectively. Addition of BEZ235 reduced survival significantly for all three cell lines in hypoxia post-irradiation (Fig. 3A). All cell lines showed increased radioresistance under hypoxic conditions, as compared to normoxia, confirming the hypoxic effect in our experimental settings (Fig. 3B). These results show that PI3K/mTOR inhibition can radiosensitise tumour cells in normoxic as well as hypoxic conditions.



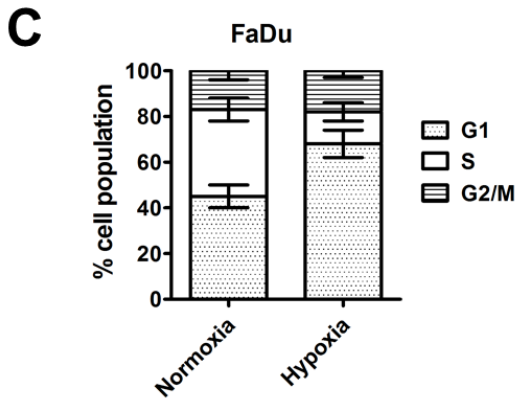



**Figure 3.** BEZ235 radiosensitises tumour cells under hypoxic conditions. ***A,*** clonogenic survival curves of cells treated with 50 nmol/l BEZ235 and irradiation under hypoxic conditions. Cells were incubated in hypoxia (0.5% $O_2$) for 6 h. BEZ235 was then added at 1 h prior to irradiation and left for 17 h upon and the medium was replaced. Cells were transferred to normoxia at 1 h post-irradiation. ***B,*** clonogenic survival of cells after irradiation with 6 Gy and treatment with 50 nmol/l BEZ235 in oxic and hypoxic (0.5% $O_2$) conditions, as described above (A) and in Fig. 1. C, cell cycle of FaDu cells at 24 h, after exposure to oxic and hypoxic (0.5% $O_2$) conditions, as described above (A) and in Fig. 1C. Note the increase in G1 phase population in the hypoxic cells. *Columns/points*, mean of three independent experiments; *bars*, SD. *, $P < 0.05$; **, $P < 0.01$; *, $P < 0.001$ over DMSO-treated control.

## 3.2.4 BEZ235 induces apoptosis in SQ20B cells and increases necrosis in tumour

Apoptosis was analysed in FaDu and SQ20B cells upon administration of BEZ235 (50 nmol/l), in combination with irradiation (4 Gy) (Fig. 4A-B). There was no increase in apoptosis in FaDu cells after treatment with BEZ235 alone or after irradiation, at either time point while necrosis was increased, especially at 48 hours post-irradiation. In contrast, BEZ235 increased both apoptosis and necrosis at 48 h after irradiation in SQ20B cells but this increase was not statistically significant ($p>0.05$). Radiation alone enhanced necrosis at 48 h post-irradiation in FaDu and SQ20B cells (Fig. 4A-B). The addition of BEZ235 to radiation did not significantly ($p>0.05$) increase apoptosis in either cell line compared to BEZ235 alone.

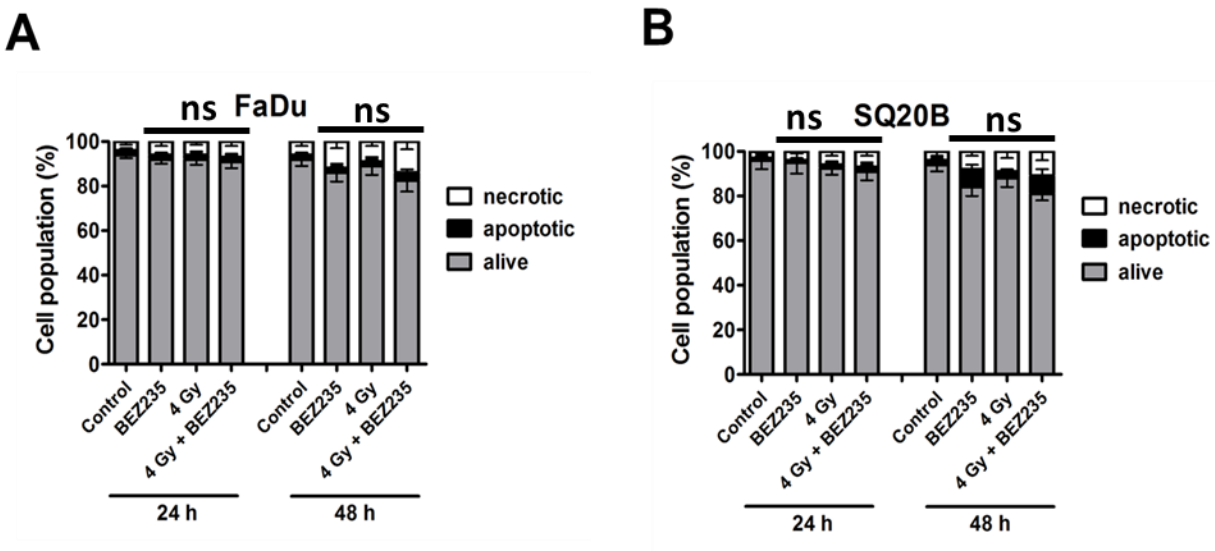
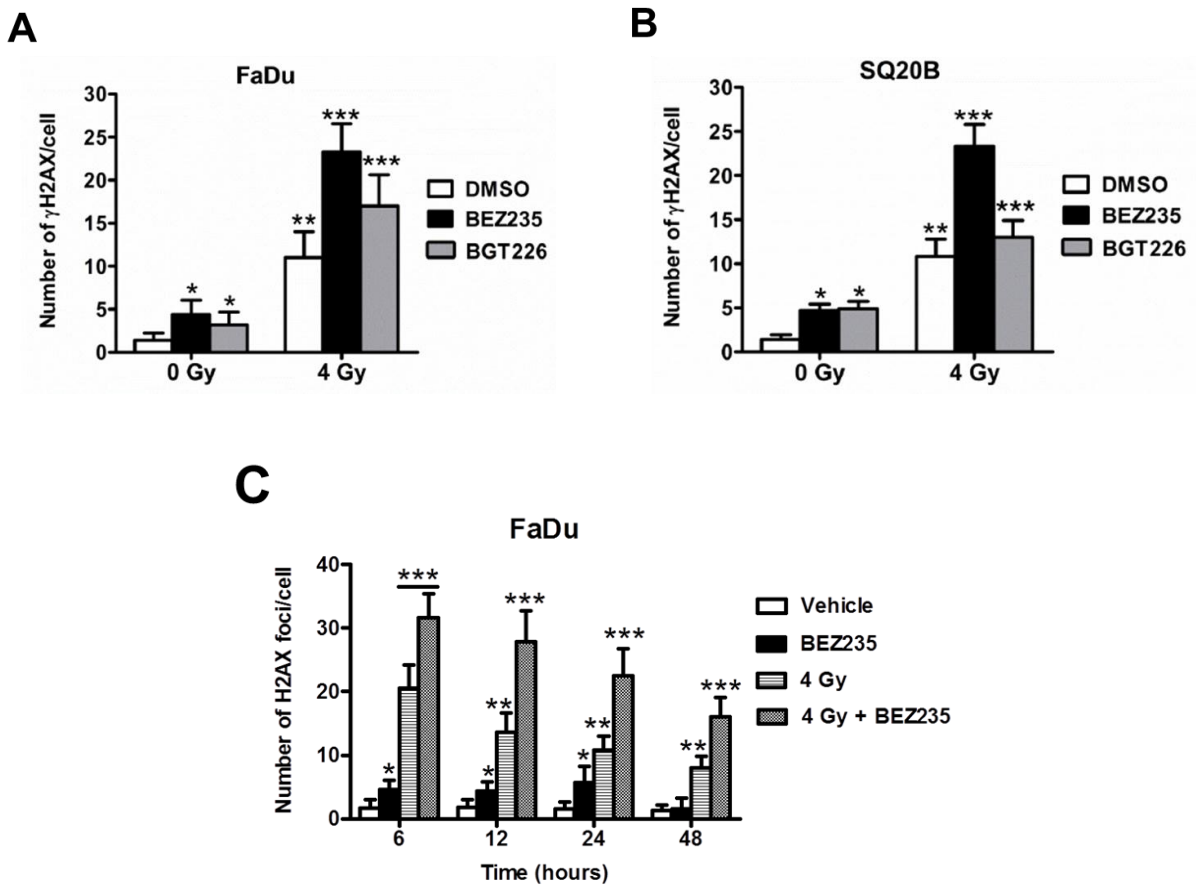



**Figure 4.** Evaluation of apoptosis in irradiated tumour cells. ***A-B***, Cells were treated with BEZ235 (50 nmol/l). 4 Gy was given after 1 h of drug treatment, with the drug maintained for an additional of 17 h. Apoptosis was assessed by flow cytometry for Annexin V combined with propidium iodide, at 24 and 48 h post-irradiation (n=2). ns, not significant (compared to the control group at each time point and for each of the different populations i.e. necrotic, apoptotic and alive). Columns, mean of two independent experiments; bars, SD.

## 3.2.5 Radiosensitisation induced by the dual PI3K/mTOR inhibitors is accompanied by persistence of γH2AX foci and cell cycle arrest

To gain insight into the molecular mechanisms of radiosensitisation of both compounds, the effect of these drugs on the DNA damage response was investigated by measuring the number of γH2AX foci at different time points post-irradiation (4 Gy). A higher number of residual γH2AX foci was detected after treatment with BGT226 (5 nmol/l) and BEZ235 (50 nmol/l) as compared with radiation alone, at 24 h post-irradiation (Fig. 5A-B). I confirmed the higher number of foci after treatment of cells with BEZ235 at different time points post-irradiation in tumour cells (Fig. 5C-D). Although the number of foci is lower in FaDu cells after radiation alone, the trend at 12, 24 and 48 h is similar for both FaDu and SQ20B cells and reveals approximately twice as many foci in the combination group, as compared to radiation alone.

The impact of PI3K/mTOR inhibition on cell cycle distribution was also investigated (5E-F). Treatment with BEZ235 (50 nmol/l) for 1 h before irradiation up to 17 h after led to an increased percentage of cells in G1 phase while the S phase population decreased, indicating a G1 block. Irradiation of FaDu cells led to a G2 block that was substantially increased after treatment with the inhibitor (Fig. 5E). Similar effects were obtained from SQ20B cells even though the increase in G2 phase delay in the combination group was less dramatic (Fig. 5F). Therefore PI3K/mTOR inhibition alone had an antiproliferative effect and resulted to G1 cell cycle arrest. The profound G2 block observed in the combination group underlines their radiosensitising potential.



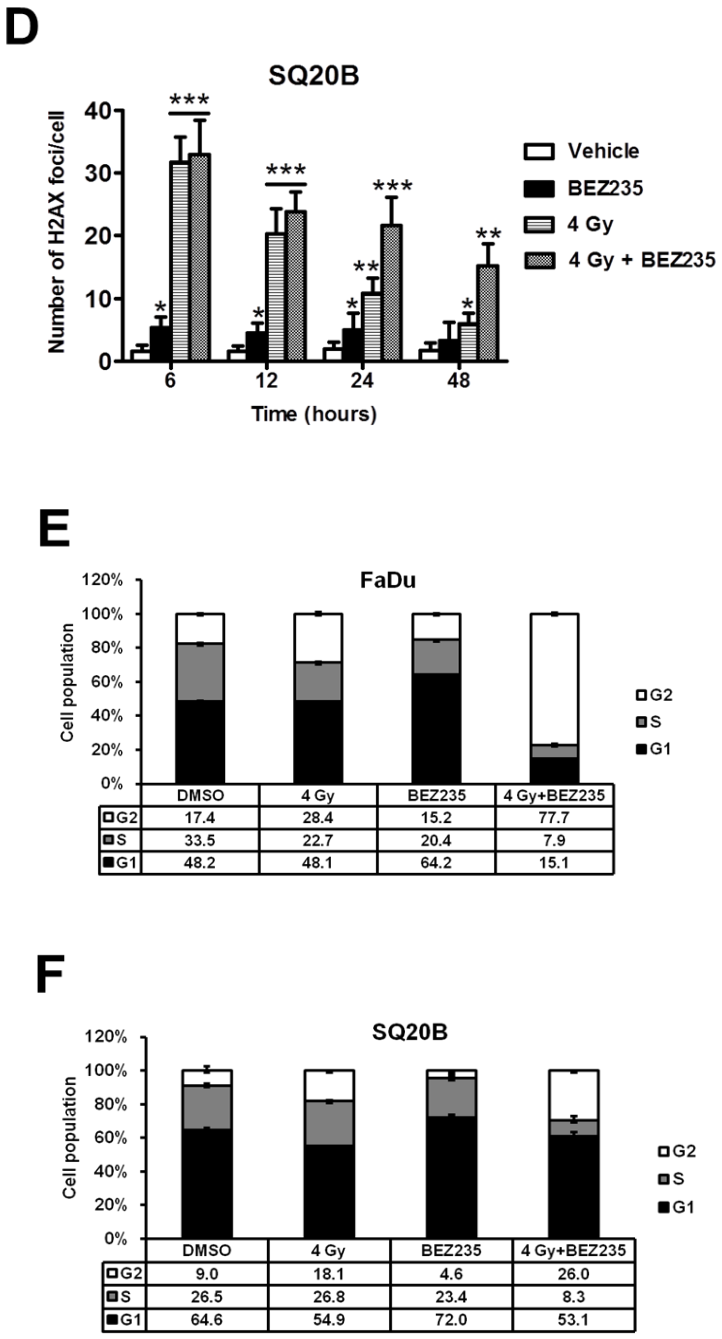



**Figure 5.** Evaluation of residual DNA damage and cell cycle distribution in irradiated tumour cells**.** ***A-B***, γH2AX foci at 24 h post-irradiation. Indicated cell lines were exposed to 5 nmol/l BGT226 or 50 nmol/l BEZ235 for 1 h followed by irradiation with 4 Gy. Drugs were left until staining was performed. Residual γH2AX foci were counted 24 h later. ***C-D***, Time-course of γH2AX foci in irradiated tumour cells treated with BEZ235. FaDu and SQ20B cells were exposed to 50 nmol/l BEZ235 for 1 h followed by irradiation with 4 Gy. Drugs were left up to a maximum of 24 h. Residual γH2AX foci were counted at the indicated time points. ***E-F***, Cells were treated as in (A) and cell cycle distribution was determined by flow cytometry after exposure to propidium iodide 24 h post-irradiation (n=3). *, $P < 0.05$; **, $P < 0.01$; ***, $P < 0.001$ over DMSO-treated control.

## 3.2.6 BEZ235 blocks PI3K/mTOR signalling and sensitises endothelial cells to irradiation

Next the effect of the dual PI3K/mTOR inhibitors in endothelial cells was studied. To this end, the effect of irradiation and VEGF on the PI3K signalling pathway in HUVEC using BEZ235 (50 nmol/l) was determined. In endothelial (HUVEC) cells, Akt was phosphorylated 1 h after irradiation (4 Gy) or exposure to VEGF-containing medium (10 ng/ml) (Fig. 6A; +VEGF). HUVEC exposed to growth factor-depleted medium did not show Akt phosphorylation (Fig. 6A; -VEGF). Pre-treatment of HUVEC with BEZ235 led to complete abrogation of PI3K/Akt/mTOR signalling in irradiated and unirradiated HUVEC (Fig. 6A). Treatment of HUVEC cells with BEZ235 (50 nmol/l) for 1 h before up to 1 h after irradiation significantly reduced clonogenic survival in HUVEC (Fig. 6B). A similar decrease in clonogenicity was observed in HDMVC, cells that more closely resemble tumour microvascular cells (Fig. 6B). The mean plating efficiencies in the control- and BEZ235-treated groups were 42.3% and 24% respectively. Hence, the decrease in clonogenicity observed in irradiated endothelial cells pretreated with BEZ235 can be partially attributed to the cytotoxic effect of the dual PI3K/mTOR inhibitor. For the clonogenic survival assay in endothelial cells, drug concentrations similar to those used in the clonogenic experiments performed in tumour cells were used to better understand how the two different types of cells would react to the same concentration of BEZ235. Also, in the absence of VEGF, endothelial cells growth was severely impaired and hence endothelial cells were only grown in growth factor depleted medium overnight and not for longer period.

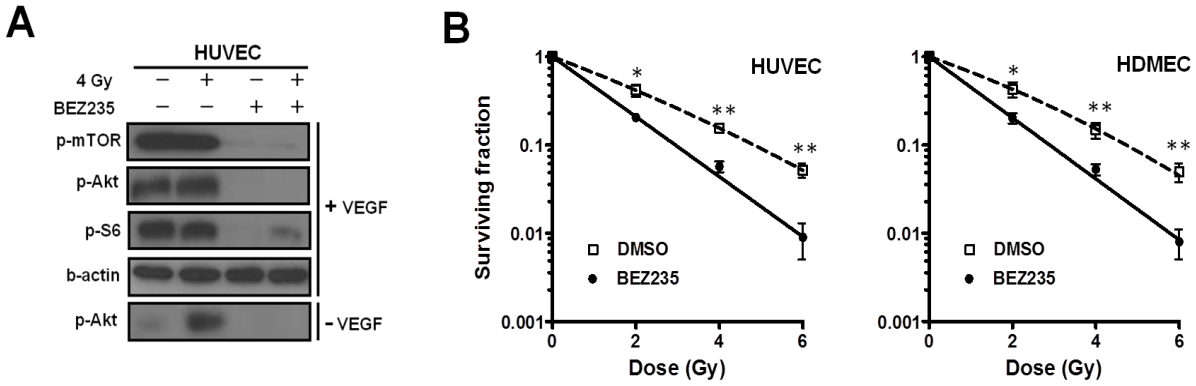



**Figure 6.** PI3K/mTOR inhibition affects downstream signalling and clonogenic survival in irradiated vascular endothelial cells. ***A,*** HUVEC were starved overnight and were treated with 50 nmol/l BEZ235 for 1 h before irradiation (4 Gy). Following irradiation, medium was replaced by either basal medium containing 1.5% FCS and 10 ng/ml VEGF (+VEGF) or growth factor-depleted medium (-VEGF). Cell lysates were collected 1 h post-irradiation and subjected to Western blot analysis. ***B***, Clonogenic survival of HUVEC and HDMVC treated with BEZ235 (50 nmol/l) for 1 h before irradiation to 1 h post-irradiation (n=3). *, $P < 0.05$; **, $P < 0.01$ over DMSO-treated control.

## 3.2.7 BEZ235 increases DNA damage and necrosis in irradiated endothelial cells

DNA damage was analysed in irradiated cells pretreated with BEZ235 (50 nmol/l) in response to VEGF (10 ng/ml), as described in Materials and Methods. BEZ235 resulted in enhanced persistence of γH2AX foci 24 h after exposure to 4 Gy irradiation (Fig. 7A). In addition, BEZ235 treatment only slightly increased apoptosis and necrosis at 24 and 48 h and enhanced radiation-induced necrosis, especially at 24 h post-irradiation (Fig. 7B). Radiation alone increased necrosis 48 h after radiation (Fig. 5B).

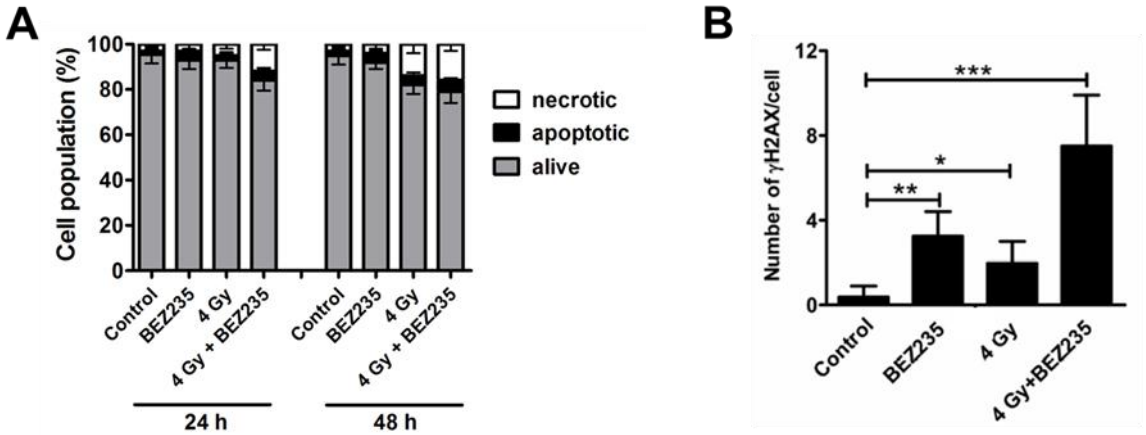
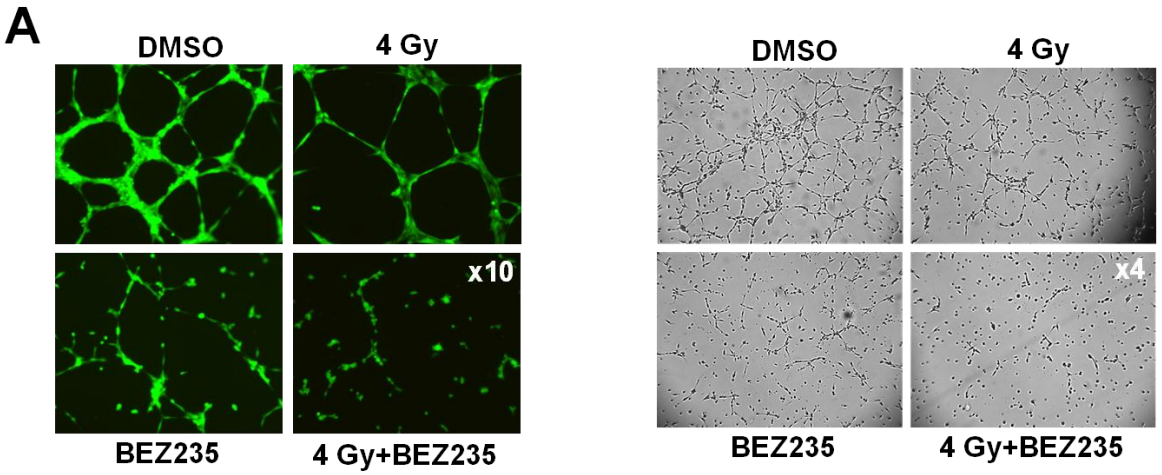


**Figure 7**. PI3K/mTOR inhibition enhances DNA damage in irradiated HUVEC. ***A***, apoptosis assessment in HUVEC treated with BEZ235 and/or radiation. Previously starved HUVEC were treated with BEZ235 (50 nmol/l) for 1 h before irradiation. The medium was removed immediately following irradiation and was replaced by basal medium containing 1.5% FCS and a constant concentration of VEGF (10 ng/ml). Annexin V-PI flow cytometry was used to identify cells in apoptosis or necrosis 72 h after irradiation. ***B***, mean γH2AX foci number in HUVEC cells treated with BEZ235 (as above) and radiation at 24 h post-irradiation (n=3). *, P < 0.05; **, P < 0.01; ***, P < 0.001 over DMSO-treated control.

## 3.2.8 BEZ235 attenuates tube formation in irradiated endothelial cells

To determine whether Akt/mTOR inhibition affects the formation of vascular networks by endothelial cells, a tube formation assay was performed as described in Materials and Methods. BEZ235 (50 nmol/l) or irradiation alone (4 Gy) decreased length of tube formation in both HUVEC and HDMVC and resulted in shorter tubular structures with fewer interconnection branching points (Fig 8A-B). The combination of BEZ235 with irradiation further potentiated the reduction (Fig. 8A-B).



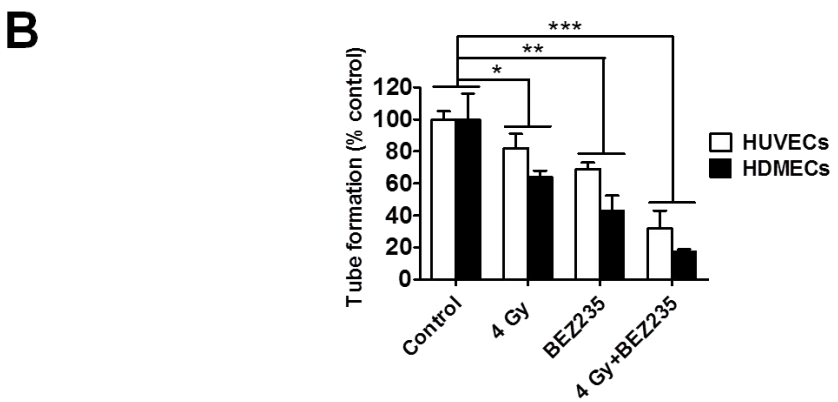



**Figure 8.** PI3K/mTOR inhibition attenuates tubule formation in irradiated HUVEC and HDMVC. Cells were exposed to BEZ235 (50 nmol/l) for 1 h, before irradiation with 4 Gy. Cells were trypsinised immediately after irradiation and were incubated in basal medium containing 1.5% FCS and a constant concentration of VEGF (10 ng/ml). ***A,*** representative images of capillary tubule formation in HUVEC (left) and HDMVC (right) in response to BEZ235 (50 nmol/l). ***B,*** quantification of tubule formation as measured by the length of capillary-like tubular structures and normalised to the control group (4 power fields per sample). *, P < 0.05; **, P < 0.01; ***, P < 0.001 over DMSO-treated control.

## 3.2.9 BEZ235 attenuates migration in irradiated endothelial cells

Cells were treated in a similar way as in the tube formation assay and were allowed to migrate to the lower compartment of a transwell chamber. BEZ235 (50 nmol/l) and irradiation (4 Gy) significantly reduced migration of HUVEC and HDMVC (Fig. 9A-B). Addition of BEZ235 to radiation revealed inhibition of endothelial cells migration (Fig 9A-B). Therefore, dual PI3K/mTOR inhibition can enhance the antivascular effect of radiation in culture.

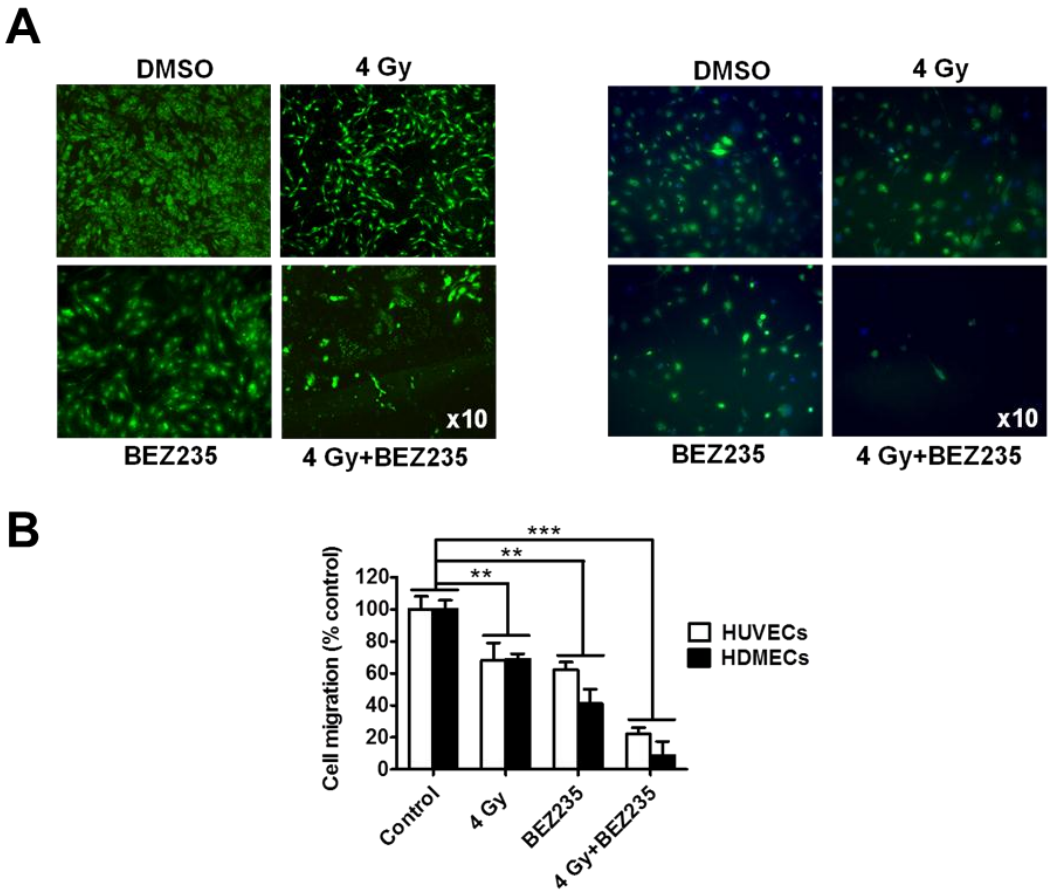


**Figure 9.** PI3K/mTOR inhibition attenuates migration in irradiated HUVEC and HDMVC. Cells were exposed to BEZ235 (50 nmol/l) for 1 h, before irradiation with 4 Gy. Cells were trypsinised immediately after irradiation, were incubated in basal medium containing 1.5% FCS and a constant concentration of VEGF (10 ng/ml) and were allowed to migrate through a membrane to the lower compartment of a migration chamber. ***A,*** representative images of HUVEC (left) and HDMVC (right) migration 18 h post-irradiation. ***B,*** endothelial cell migration of indicated cells (treated as above). The number of migrated cells per power field (10X) was counted (12 fields per group) and normalised to the control group (n=3). *, $P < 0.05$; **, $P < 0.01$; ***, $P < 0.001$ over DMSO-treated control.

## 3.3 DISCUSSION

Previous studies have identified increased PI3K/Akt/mTOR signalling as a mediator of enhanced tumour survival after radiation-induced DNA damage [87-89, 278]. In the present study, the effects of the drugs were studied in SQ20B and FaDu cells (with overexpression of EGFR) and T24 cells (with mutated H-Ras). The cell lines were chosen with the purpose of investigating the impact of the drugs in cells with activation of the PI3K signalling at different levels of the cascade. The number of possible activation points in the PI3K survival pathway can lead to the prediction that inhibition at the level of PI3K is likely to be more effective in a wider range of tumours than inhibition at the level of the EGFR. Inhibition at the level of PI3K is expected to be effective against effective against tumours with activation either of EGFR (upstream of PI3K), Ras (upstream of PI3K), or PI3K, whereas blockade of EGFR signalling might not affect the sensitivity of a tumour with activation of survival signalling at a point downstream of the EGFR. This was one reason for testing the pharmacological inhibition of PI3K/mTOR as a strategy for tumour radiosensitisation.

Moreover, deregulation of mTOR signalling has also been implicated in response to radiation [282]. Rapalogs have antiproliferative effects *in vitro* but their efficacy in tumours with PI3K/Akt and mTOR activation has been limited. There is extensive crosstalk between the two signalling networks [282, 283]. mTOR can affect PI3K/Akt

signalling through the S6K-IRS1 feedback loop and induce Akt phosphorylation by mTORC2 [282, 285]. Because rapalogs inhibit only the mTORC1 complex, paradoxical activation of Akt can limit their therapeutic potential. Here is shown that PI3K/mTOR dual inhibitors effectively block downstream targets and result in radiation sensitisation in tumour cell lines and in endothelial cells. Interestingly, PI3K/mTOR inhibition resulted in decreased clonogenicity in cells radiated in hypoxia. These data indicate that dual PI3K/mTOR inhibition might prevent PI3K pathway reactivation and further enhance radiation-induced cell killing.

Several preclinical studies have found promising activity for the dual PI3K/mTOR inhibitor BEZ235 against various tumours [286, 287] especially those with mutations in PI3K. In the present study, dual inhibitors led to radiosensitisation of tumour cells and of endothelium. The efficacy of these compounds should apply to tumour cells with a wide spectrum of oncogenic lesions because the Ras/EGFR/PI3K/mTOR pathway is activated in many types of cancer. Both BGT226 and BEZ235 enhanced the radiosensitivity of SQ20B cells and T24 cells when added before or immediately after radiation but not after 6 h. These findings may support scheduling strategies for future clinical trials testing the radiosensitising potential of these compounds.

To determine whether radiosensitisation was associated with inhibitor-mediated cell cycle redistribution, we analysed cycle distribution in cells pretreated with one of the dual inhibitors, BEZ235. Treatment of FaDu and SQ20B cells with BEZ235 alone resulted in growth arrest in the G1 phase. This is similar to the observation reported in several studies investigating BEZ235 and other PI3K inhibitors [286, 288-290]. Importantly, when cells were irradiated after BEZ235 pretreatment, the percentage of SQ20B and FaDu cells in G2 phase was increased by approximately 3-fold and 4.5-fold, respectively. This finding concurs with our previous report on PI3K inhibitor, PI-103 where a ~2-fold increase in G2

phase population arrest was recorded [88]. Notably, rapalogs are known to induce a $G_2$ block when combined with irradiation [282].

The effect of dual PI3K/mTOR inhibition in apoptosis was also investigated. BEZ235 increased necrosis but not apoptosis in FaDu cells. In contrast, BEZ235 enhanced both apoptosis and necrosis in SQ20B cells but this was not significant. In the combination group, there was no increased apoptosis in either cell line and only a slight increase in necrosis was observed at 48 h post-irradiation. Previous studies have demonstrated increased apoptosis after treatment with BEZ235 in some tumour cell lines and lack of apoptosis induction in others. For instance there was no apoptosis induction in glioma or melanoma cell lines; there is however in lung cancer, sarcoma and leukemia and lack of apoptosis induction in others [92, 290, 291]. It appears that apoptosis plays a minor role in the radiation response of cells to BEZ235.

Hypoxic cells are 2 to 3-fold more resistant than oxic cells to radiation and tumour hypoxia is associated with treatment failure following radical radiotherapy [43]. Hence, the efficacy of BEZ235 in the context of hypoxia was studied. As expected, hypoxia resulted in increased radioresistance of FaDu, SQ20B and T24 cells. Importantly, PI3K/mTOR inhibition by BEZ235 led to significant sensitisation of hypoxic cells to radiation and therefore this drug can be an attractive adjunct for radiotherapy.

BEZ235 and BGT226 enhanced persistence of residual γH2AX foci after irradiation. γH2AX foci were also moderately increased in cells treated with BEZ235 alone, which could be attributed to the potentially toxic effect of the compounds, leading to enhanced DNA damage even in the unirradiated cells. Selective inhibition of the PI3K pathway using siRNA leads to significant radiosensitisation of tumour cells. Therefore, the radiosensitising effect of PI3K/mTOR inhibitors cannot be wholly attributed to inhibition of other targets ("off-target" effect). Previous evidence has demonstrated that inhibition of

the PI3K pathway can affect formation of γH2AX foci, even in the absence of radiation [88]. These indicate that PI3K/mTOR plays a role in DNA repair after the initial injury. Our results are in accordance to the work of Konstantinidou et al. [92]. Similar findings have been also been described before for different PI3K inhibitors [88] .

The PI3K/Akt/mTOR intercept node is involved in endothelial signalling response to upstream effectors such as VEGF [6]. Chronic Akt activation in endothelial cells recapitulated the salient features of tumour vasculature [140]. In VEGF-stimulated porcine aortic endothelial cells and HUVEC, VEGFR2 recruited the p110/p85 complex and increased their proliferation [9]. PI3K/Akt/mTOR activation can occur upon exposure to radiation in endothelial cells [6]. Overexpression of Akt in endothelial cells resulted in abnormal vascular remodelling with embryonic lethality [136]. Here BEZ235 blocked VEGF- and irradiation-induced activation of Akt phosphorylation and significantly enhanced cell death in vascular and microvascular endothelial cells. Furthermore, BEZ235 reduced VEGF-mediated migration and tube formation and enhanced the antivascular effect of radiation in endothelial cells. A moderate increase in apoptosis and necrosis in BEZ235-treated endothelial cells. BEZ235 increased radiation-induced necrosis, especially at 24 h post-irradiation. These findings are in accordance with previous reports showing that PI3K and/or mTOR blockade can exert an antivascular activity [6, 15, 94]. The mTOR inhibitor rapamycin decreased VEGF-mediated growth of endothelial cells and activation of Akt/mTOR signalling after irradiation and enhanced the antivascular efficacy of radiotherapy [6, 93, 94]. The fact that dual inhibition of PI3K/mTOR pathway can increase the antivascular effect of radiation in endothelial cells is an important finding. First, PI3K/mTOR inhibition by BEZ235 alone can result in alterations in tumour blood vessel morphology and functionality but this appears to be a dose-dependent effect and can affect the efficacy of radiotherapy significantly, as recently demonstrated [174]. Secondly, the

enhanced radiosensitisation of endothelial cells conferred by BEZ235 would imply that dual PI3K/mTOR inhibition could, in theory, enhance normal tissue damage and therefore special caution is required before proceeding with clinical studies using these agents in combination with radiation.

## 3.4 CONCLUSION

In summary, in the present study it was shown that PI3K/mTOR dual inhibitors are effective radiosensitisers in tumour cells with EGFR overexpression or oncogenic Ras mutation. BEZ235 sensitised tumour cells to radiation under both normoxic and hypoxic conditions. The antivascular activity reported represents a clear advance in understanding the properties of dual PI3K/mTOR inhibition. Altogether, these data indicate that direct inhibition of PI3K/mTOR activity may be of benefit when combined with radiotherapy.

# CHAPTER 4

# Inhibition of the PI3K/mTOR pathway by NVP-BEZ235 and NVP-BKM120 normalizes tumour vasculature to increase radiation sensitivity

## Published in: Cancer Research 2011, 1;72(1):239-48.

Emmanouil Fokas[1], Jaehong Im[1], Sally Hill[1], Sabira Yameen[1], Michael Stratford[1], John Beech[1], Wolfgang Hackl[2], Maira Sauveur-Michel[2], Eric J. Bernhard[1], W. Gillies McKenna[1], Ruth J. Muschel[1]

[1]Gray Institute for Radiation Oncology and Biology, Oxford University, Oxford, United Kingdom;
[2]Novartis Institutes for Biomedical Research, Oncology Disease Area, Novartis Pharma AG, Basel, Switzerland

**Contribution to experimental work:** Sabira Yameen performed the staining shown in Fig. 1A-B and Fig 12. Jaehong Im assisted E. Fokas with acquirement of the images shown in Fig. 4A. Sally Hill assisted E. Fokas with the subcutaneous implantation of the tumour cells in female Balb/c nude mice. John Beech assisted E. Fokas with the acquirement of the image shown in Fig 3A. The rest of the experiments and analyses were performed by E. Fokas.

# 4.1 Introduction

Radiotherapy is an important tool in cancer therapy. Both intrinsic and extrinsic factors can influence the sensitivity of tumour cells to radiation [7]. The sensitivity of the cancer cell itself (intrinsic component) is an important determinant of the efficacy of radiotherapy [292] and is adversely affected by the activation of oncogenic signal transduction cascades such as the PI3K/Akt pathway [90, 293]. Inhibition of this cascade can enhance radiosensitivity of tumour cells leaving the normal cells unaffected, providing an attractive concept for improving therapeutic outcome [88].

Hypoxia is the main extrinsic factor that can reduce radiosensitivity. This occurs both because oxygen contributes to fixation of DNA damage and also through less well understood mechanisms by which hypoxia signalling leads to activation of cytokine signalling and alteration in DNA damage repair mechanisms that promote tumour cell survival after DNA damage [43]. As a consequence, reduction in hypoxia has been sought as a means to improve the efficacy of radiation therapy. Manipulation of tumour angiogenesis may be one way to achieve this goal [31, 112].

The vasculature of solid tumours is morphologically aberrant leading to leaky immature vessels [22, 294]. This, in conjunction with impaired lymphatic drainage, creates an abnormal TME characterized by elevated interstitial fluid pressure, poor perfusion and hypoxia [23]. These factors can lead to decreased delivery of chemotherapy and a reduced response to radiation and ultimately treatment failure [24].

Angiogenesis is regulated by molecular pathways with the vascular endothelial growth factor (VEGF) network playing an important role in tumour angiogenesis. While the main goal in using anti-angiogenic agents in cancer therapy was to impair tumour angiogenesis, treatment with some of these agents such as VEGFR2 inhibitors resulted in the transient formation of a more regularized vascular system [110, 111] termed “vascular

normalization" that increased radiation efficacy due to reduced hypoxia [112]. The difficulty in clinical application of this strategy, however, is that the induction of vascular normalization is transient and with greater exposure to the anti-VEGFR2 agents the vasculature becomes diminished and hypoxia increases, potentially counteracting the previously beneficial effect [113].

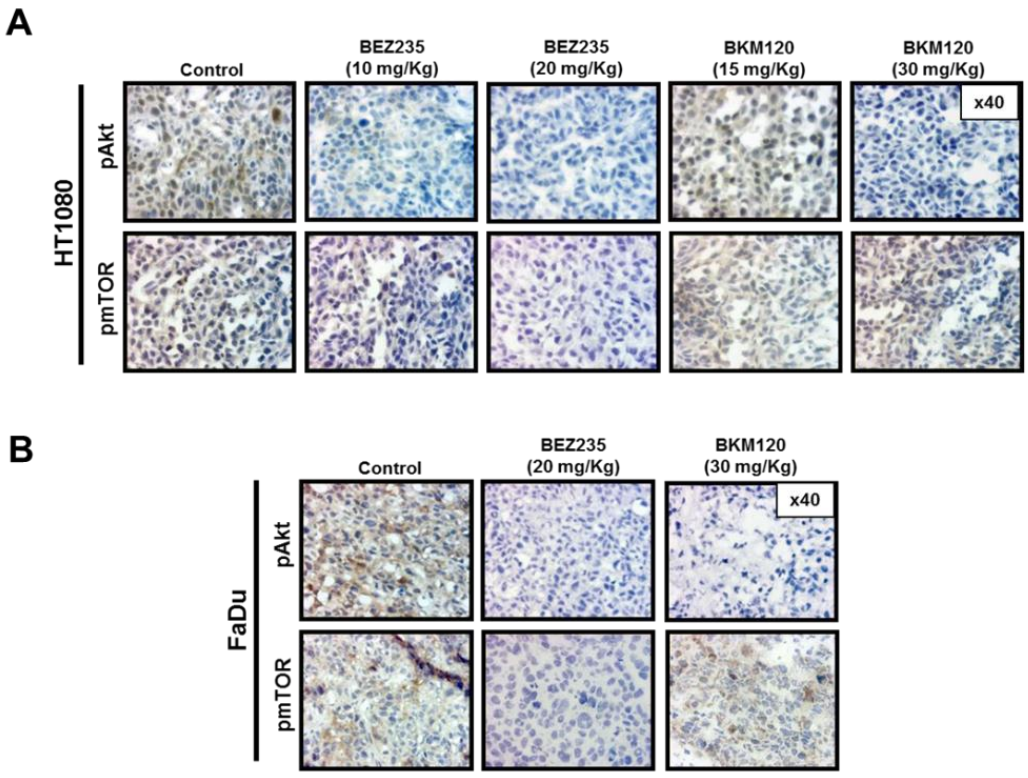
The possibility of inhibiting oncogenic signalling in cancer cells as an alternative strategy to modulate tumour vasculature has been previously investigated. Inhibition of the Ras-EGFR-PI3K-Akt signalling at multiple points in this pathway led to vascular normalization accompanied by improved tumour oxygenation and perfusion [142]. Cerniglia et al. observed similar effects using the EGFR inhibitor erlotinib that resulted in improved delivery of cisplatin and synergistic inhibition of tumour growth [30]. Importantly, inhibition of this pathway appeared to result in more durable induction of vascular normalization than with agents targeting VEGF signalling [142].

The potential of the dual PI3K/mTOR inhibitor BEZ235 and the single PI3K inhibitor BKM120 to improve radiotherapy by inducing vascular normalisation was examined and the results are presented. In that study, it was asked whether vascular normalisation induced in this way 1) would be durable and 2) would act in combination with radiation in delaying tumour regrowth. The contributions of vascular normalisation and hypoxia and intrinsic cell radiosensitivity to demonstrate the contribution of vascular normalisation to the improved response to radiation was distinguished.

# 4.2 RESULTS

## 4.2.1 Dose response of BEZ235 and BKM120 in HT1080 and FaDu xenografts

The biologically effective doses for HT1080 xenografts were established using immunostaining for pAkt as an indicator of PI3K activity and pmTOR for mTOR activity. Tumours were examined after the mice had received seven daily oral doses (Fig. 1A). BEZ235 at 20 mg/kg reduced both pAkt and pmTOR staining. At 10 mg/kg pmTOR staining was still apparent and pAkt staining was reduced but also still apparent. BKM120 at the higher dose resulted in the almost complete blockade of pAkt phosphorylation with partial reduction at the lower dose. Phosphor-mTOR was not affected at either dose of BKM120. Following this, the effective doses were tested on mice bearing FaDu xenografts with equivalent results (Fig. 1B). Despite the high degree of signalling inhibition, the growth of the treated tumours was equivalent to that of controls, (Fig. 1C-D). H&E staining in FaDu tumours revealed decreased cellularity in the drug-incorporating groups.



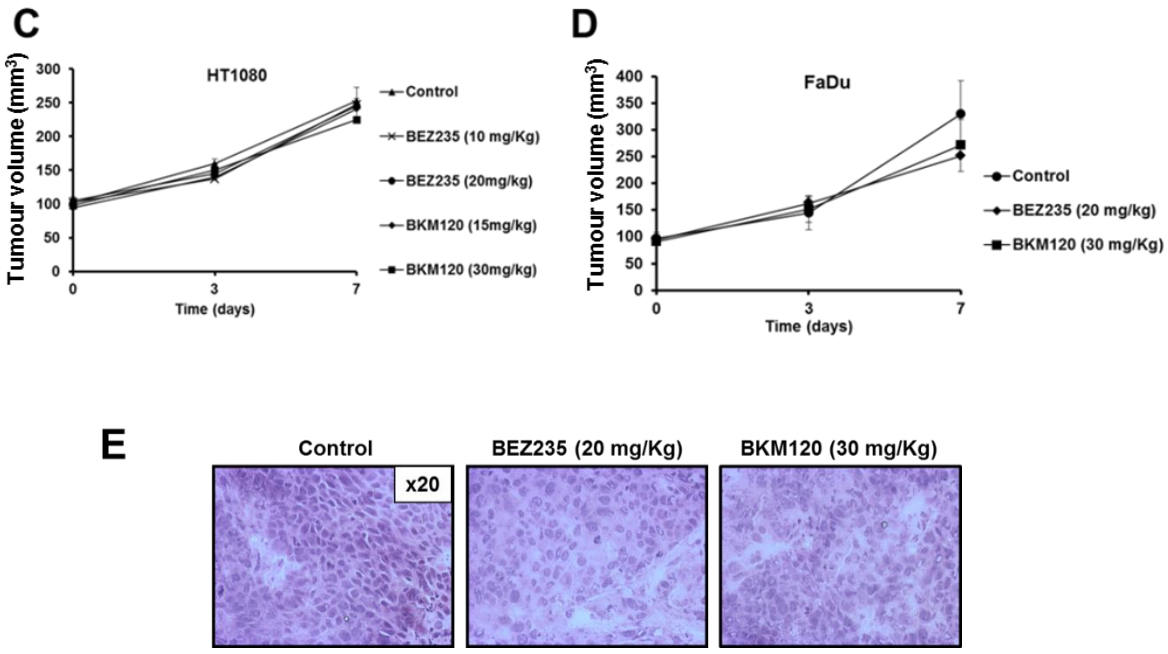
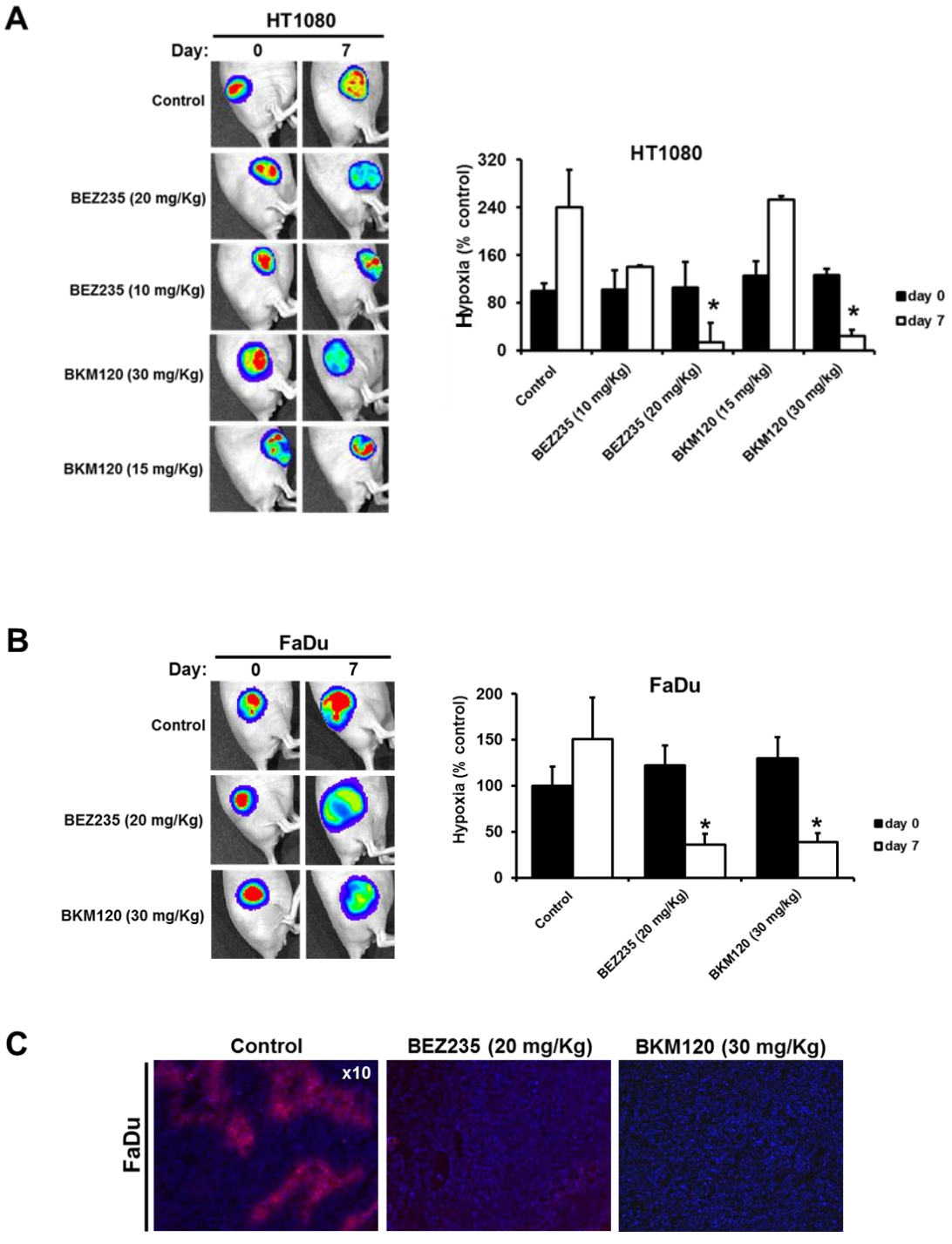



**Figure 1.** Immunohistochemical analysis of HT1080 and FaDu tumours from mice treated with signalling inhibitors. Evaluation of the effects of BKM120 and BEZ235 on p-Akt and p-mTOR in (A) HT1080 and (B) FaDu tumours. Sections were stained with the indicated antibodies. Magnification (X40). C, HT1080 and D, FaDu tumour growth after treatment with the signalling inhibitors. E, Haematoxyllin/Eosin staining in FaDu tumours treated as indicated. *Points*, mean; *bars*, SD. *p<0.05 over vehicle-treated control (Immunohistochemical staining is courtesy of Mrs Sabira Yameen).

## 4.2.2 PI3K/mTOR inhibition reduces tumour hypoxia and increase perfusion in a dose-dependent fashion

Bernhard and colleagues have previously shown that inhibition of the RAS-PI3K pathway led to reductions in tumour hypoxia and increased perfusion using a different series of drugs [16]. Here it is shown that these physiological changes occur only at drug doses giving substantial inhibition of pAkt. The effect of these drugs was evaluated in mice bearing tumours derived from cell lines bearing the hypoxia reporter HRE-luciferase, FaDu-HRE-Luc and HT1080-HRE-Luc. It has been previously demonstrated that the level of luciferase expression correlated with hypoxia as measured by EF5 staining [16]. After 7 days of treatment with the indicated drugs luciferase was again assessed using bioluminescence. Fig 2A shows that hypoxia was reduced in the HT1080 tumours only at

the higher doses that led to substantial pAkt reduction. Treatment of FaDu tumours also led to decreased hypoxia, independently confirmed by EF5 staining (Fig. 2B-C). A moderate but significant decrease in VEGF levels was found in FaDu tumours (Fig. 2D).



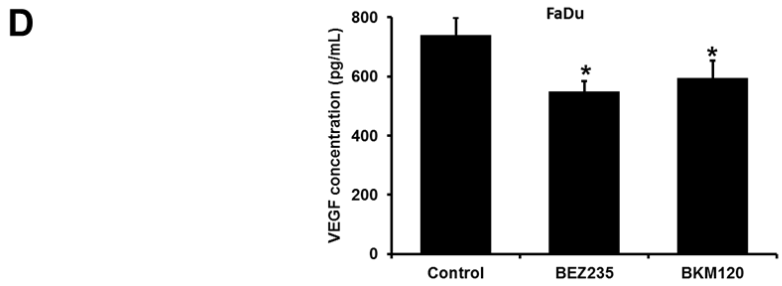
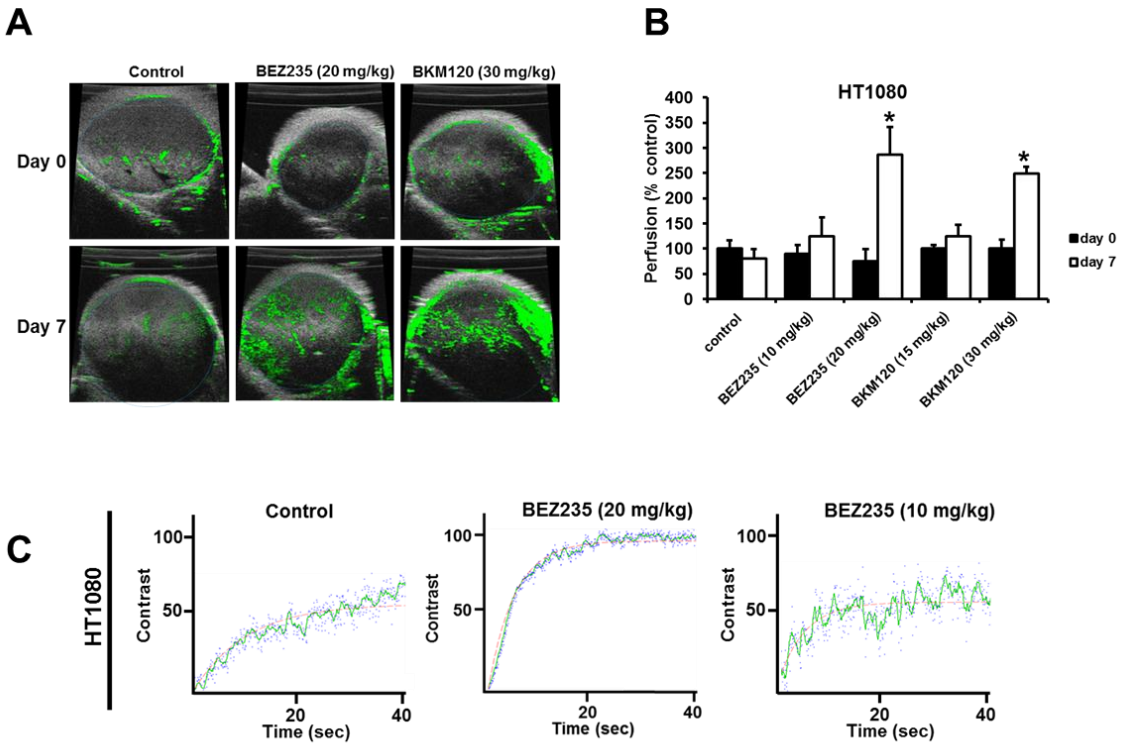



**Figure 2.** BEZ235 and BKM120 reduce hypoxia *in vivo*. Hypoxia was monitored by bioluminescent imaging of the luciferase signal. Representative images and hypoxia measurements from (A) HT1080 and (B) FaDu tumours at day 0 and 7 treated with BEZ235 or BKM120, as indicated. C, immunostaining for EF5 in FaDu tumours confirmed reduction in hypoxia. D, assessment of VEGF concentration in FaDu xenograft model. VEGF concentration was measured using VEGF ELISA at day 7 in FaDu tumours treated as indicated. *Columns/points*, mean; *bars*, SD*, $p<0.05$ over vehicle-treated control. Magnification (X40).

Similarly, perfusion measured by Doppler ultrasound using microbubbles was increased in the HT1080 tumours treated by doses sufficient to cause a substantial decrease in pAkt levels, but not at the lower doses (Fig. 3A-C). The improvement in perfusion was confirmed in FaDu tumours (Fig. 3D-F).



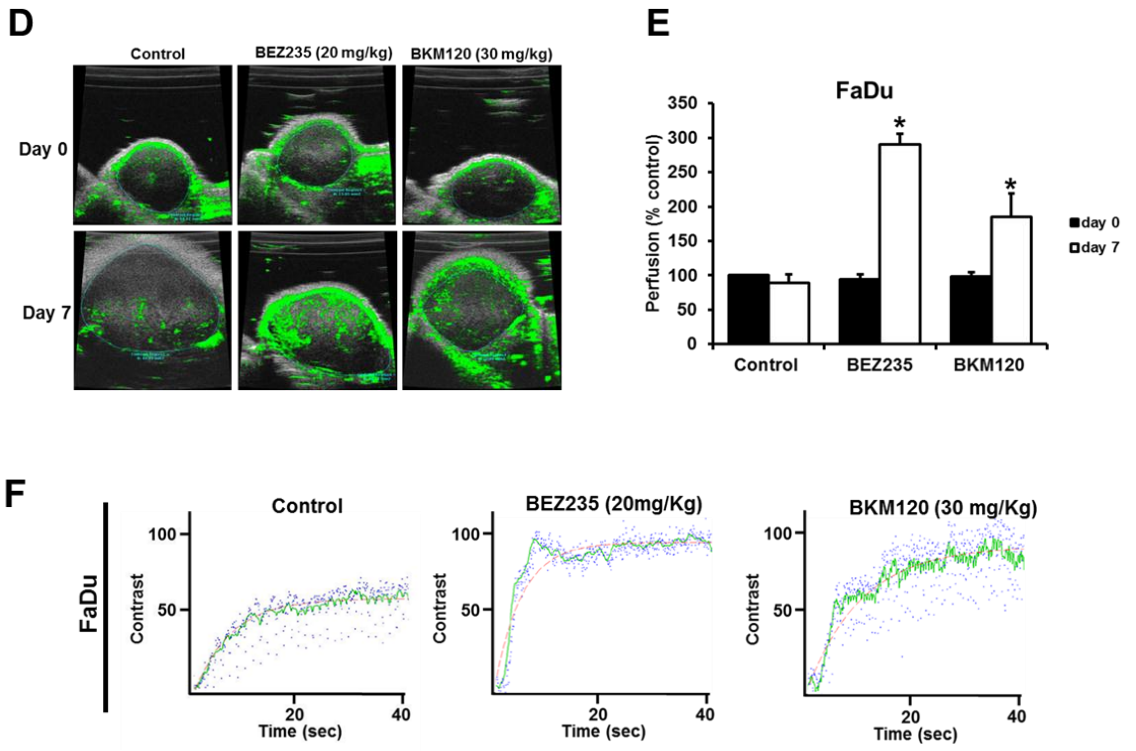



**Figure 3.** Ultrasound analysis of the effects of PI3K/Akt/mTOR inhibition on tumour blood flow. A, representative images show perfusion as depicted by microbubbles (*green signal*), that is proportional to perfusion within the region of interest (ROI). B, perfusion was evaluated from the ROI (blue line) in HT1080 at day 0 and 7 after treatment with BEZ235 or BKM120, as indicated. D-E, representative images of blood perfusion and perfusion measurements in the FaDu model. C and F, microbubble contrast kinetics in HT1080 (C) and FaDu tumours (F) treated with signalling inhibitors. Representative images of the curves generated from the dynamic imaging sequence of the relative changes in contrast signal intensity over time from A, HT1080 and B, FaDu xenografts. *Columns*, mean; *bars*, SD*, $p<0.05$ over vehicle-treated control.

## 4.2.3 BEZ235 and BKM120 promote vascular normalization and remodelling

Vascular remodelling consistent with vascular normalisation underlies the increased perfusion. *Ex vivo* confocal/multiphoton images from sections of the tumours were reconstructed to reveal the vascular structure and Trace 3D software was applied to quantify the vascular characteristics [16]. Increased average vascular diameter, decreased branching (increased length between branch points) and decreased tortuosity were induced only after treatment that had reduced pAkt immunostaining (Fig. 4A-B).

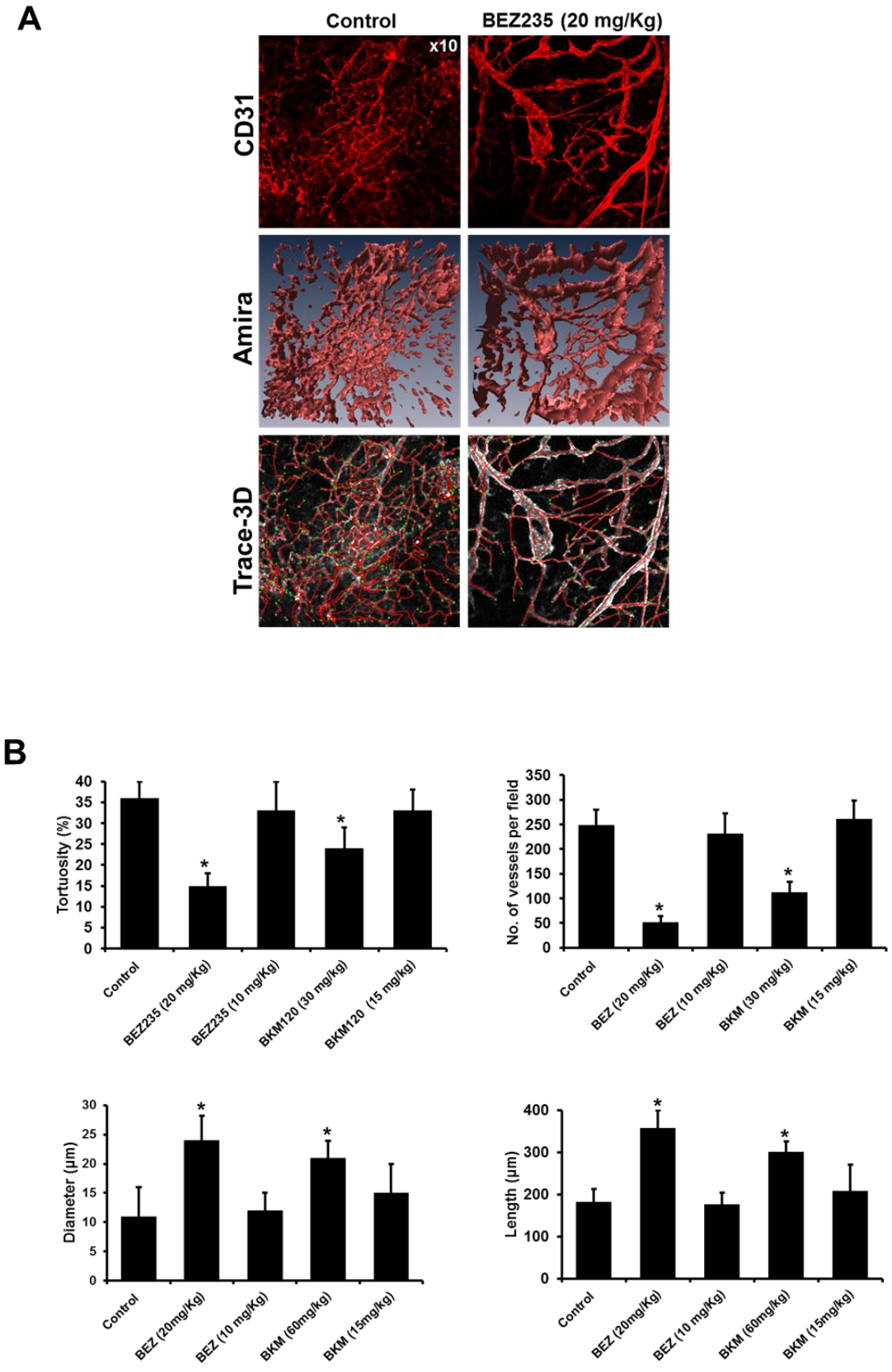
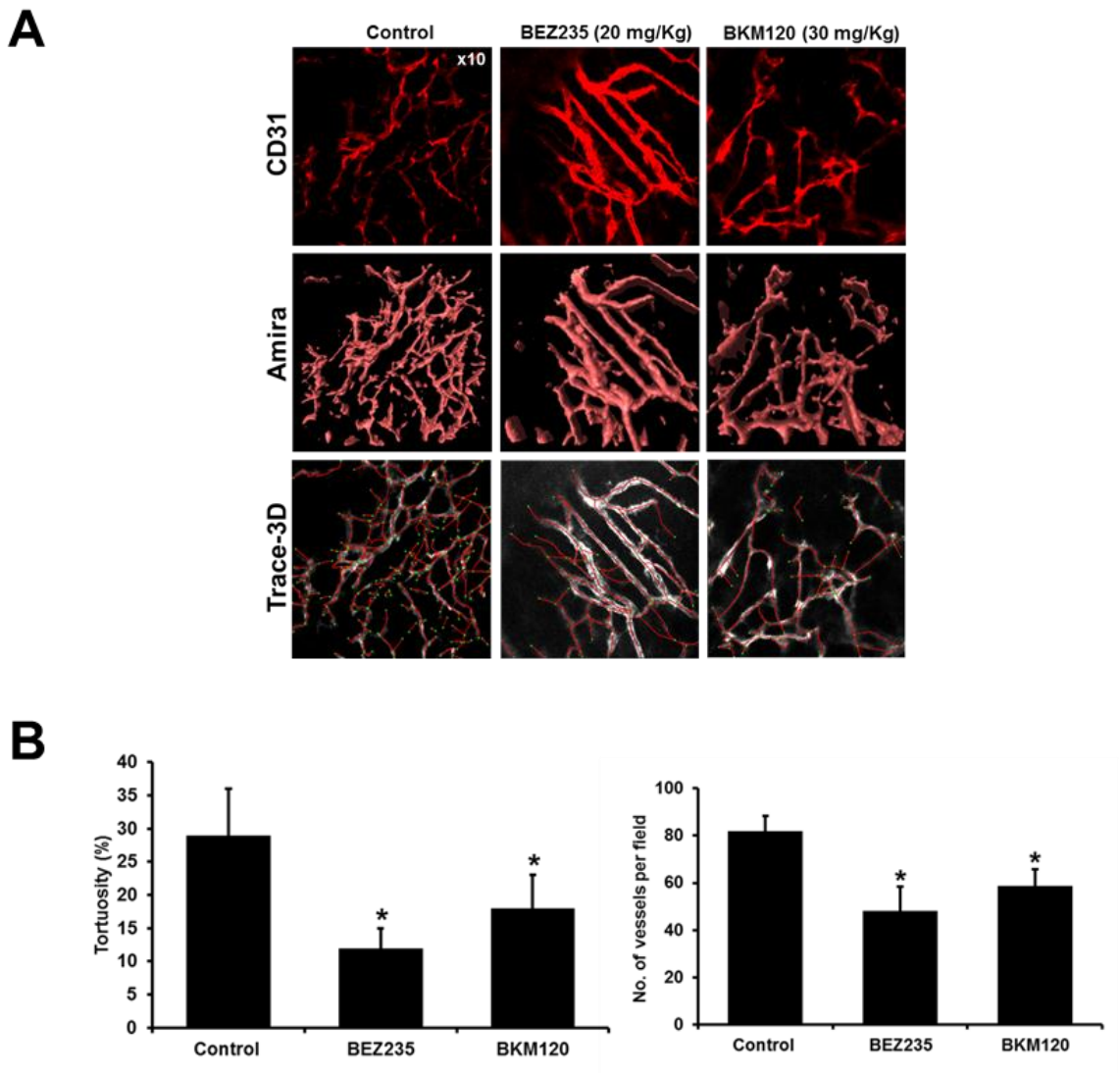



**Figure 4.** BEZ235- and BKM120-induced vascular remodelling and normalisation. HT1080-bearing mice were treated as indicated and CD31-PE was injected i.v. 1 min before sacrifice (day 7). A, representative images from a single 1-µm optical section of

tumour vasculature (upper; X10 magnification), AMIRA software 3D reconstructions (middle) and Trace3D software vascular tree tracings (lower) in HT1080 tumours. B, Trace3D software enabled calculation of vessel density, vessel diameter, length and tortuosity in HT1080 model. *Columns*, mean; *bars*, SD*, $p<0.05$ over vehicle-treated control.

The changes in vascular morphology in FaDu tumours were also investigated using the same method. Analysis of the three-dimensional morphology revealed changes similar to those observed in HT1080 tumours. Therefore, the vascular remodelling effect of BKM120 and BEZ235 was confirmed in FaDu tumours (Fig. 5A-B).



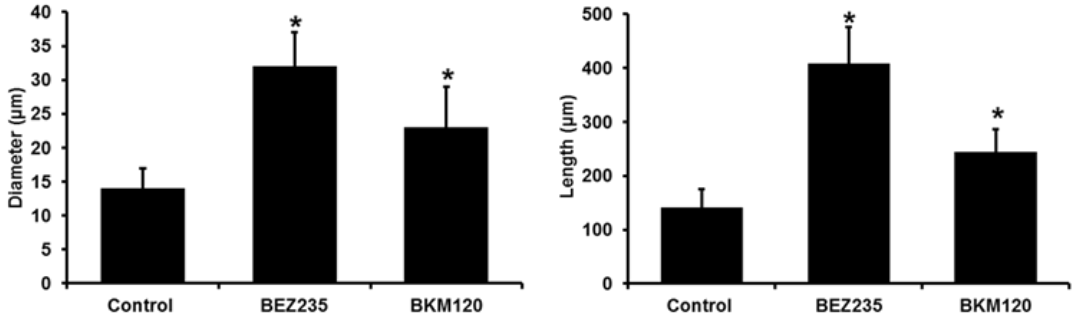
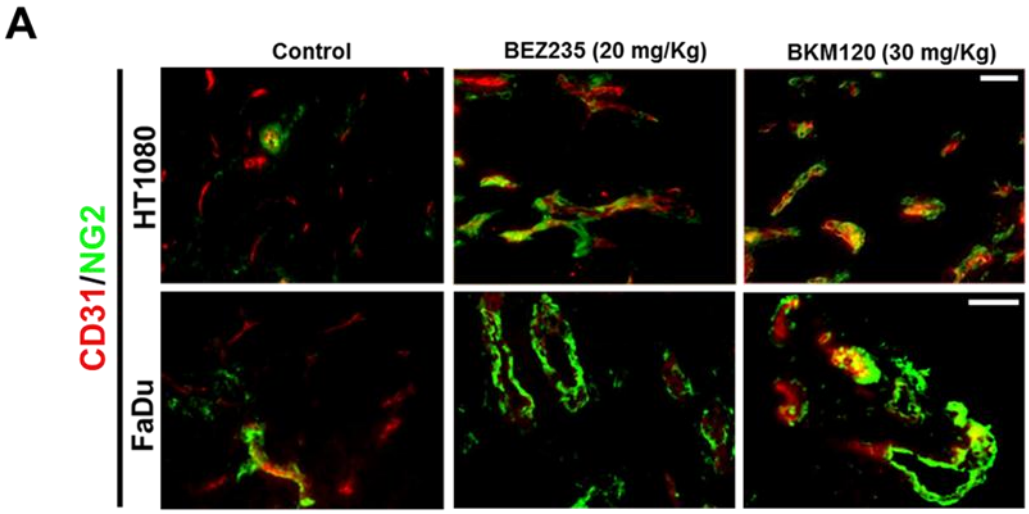



**Figure 5.** Vascular remodelling in FaDu tumours after PI3K/mTOR inhibition. A, representative images of CD31-stained blood vessels (upper; X10 magnification), 3D reconstructions of vascular morphology (AMIRA; middle) and computed tracings (Trace3D; lower) upon treatment as indicated. B, measurement of vessel density, diameter, length and tortuosity. *Columns*, mean; *bars*, SD*, $p<0.05$ over vehicle-treated control.

Vasculature in the treated tumours had significantly increased pericyte coverage, as assessed by NG2 staining, characteristic of a more mature vessel morphology (Fig. 6A-B). NG2 is a well characterised marker of vascular maturation and has been extensively used for demonstrating changes in vascular architecture upon treatment with antiangiogenic drugs. Thus changes in vascular morphology, decreased hypoxia and increased perfusion appeared to be dependent on PI3K inhibition.



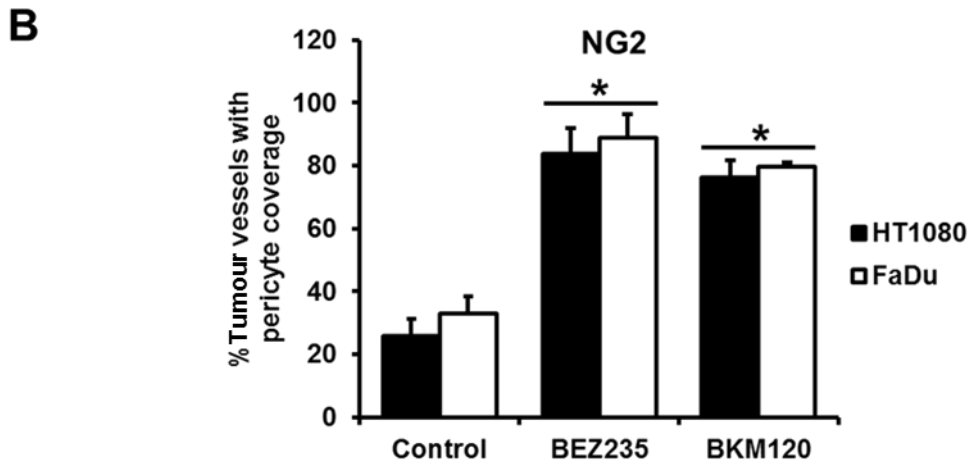



**Figure 6.** BEZ235 and BKM120 increase pericyte coverage of tumour blood vessels. A, HT1080 and FaDu tumours were double immunostained using anti-CD31 (red) and anti-NG2 (green). Scale bar, 20 µm. B, quantification of pericyte coverage in HT1080 and FaDu tumours confirmed improve pericyte recruitment after treatment with BEZ235. *Columns*, mean; *Bars*, SD*, $p<0.05$ over vehicle-treated control.

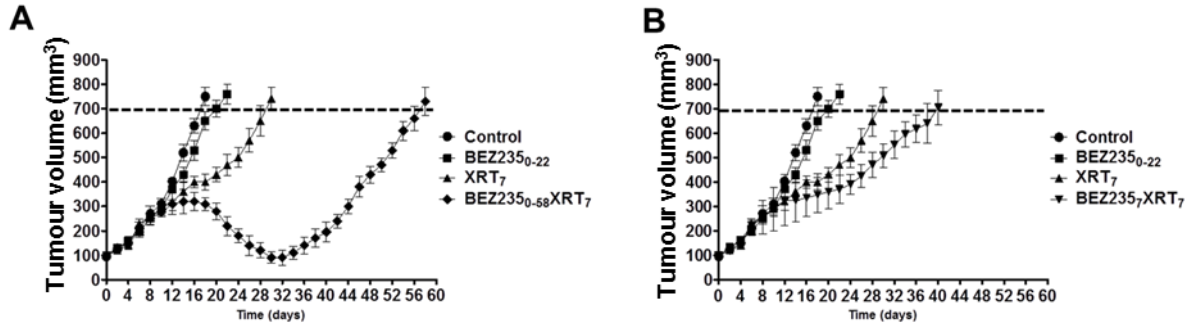
## 4.2.4 The effect of BEZ235 on radiation response

Because hypoxic tumours are substantially less responsive to radiation therapy, we hypothesized that treatment with PI3K inhibition should lead to better radiation response. As the drug with dual PI3K and mTOR inhibition led to the greatest magnitude of vascular modification, we tested the treatment with the dual inhibitor for the ability to enhance the efficacy of radiation therapy using a tumour regrowth delay assay (Fig. 7A). Mice bearing FaDu tumours were treated with BEZ235 (20 mg/kg) for 7 days prior to irradiation with a single dose of 6 Gy. BEZ235 was continued to be administered daily throughout the course of this experiment. In unirradiated mice treated with vehicle or BEZ235, tumours reached the maximum permitted volume (between 700 and 750 $mm^3$) at days 18 (control) and 22 ($BEZ235_{0\text{-}22}$), respectively. The median time to reach this volume was increased by 12 days by radiation alone ($XRT_7$). In contrast, radiation combined with BEZ235 delayed tumour growth by 58 days ($BEZ235_{0\text{-}58}XRT_7$), a strongly supra-additive growth delay. In order to be able to compare the growth delay between the different groups, we compared the time it took for the tumour xenografts to reach a volume of 700 $mm^3$. In this group,

BEZ235 administration was maintained after XRT in order to examine whether the changes observed in the TME will remain persistent or not.

Because inhibition of PI3K or PI3K/mTOR can sensitise tumour cells to radiation, independently of changes in oxygenation, we asked whether some component of the radiosensitisation could be attributed to this effect by treating mice with a single dose of BEZ235 only on the day of irradiation (Fig. 7B). In addition BEZ235 has been shown to inhibit ATR, ATM and DNA-dependent protein kinase (DNA-PK), all of which would be expected to lead to radiosensitisation [19]. Thus, the latter should be taken into consideration when interpreting our findings. This schedule did not alter tumour oxygenation or perfusion. It did however lead to a supra-additive growth delay of 40 days compared to 30 of radiation alone. Thus the drug must lead to alteration in the intrinsic radiosensitivity of the tumour independent of oxygenation changes. .

An additional schedule was tested whereby daily administration of BEZ235 was initiated 3 days after irradiation and was continued throughout the experiment (Fig. 7C). This treatment was not significantly different from XRT alone. This schedule was chosen to account for any possible antiproliferative effects of BEZ235, especially upon long-term administration. Thus we could conclude that radiosensitisation by BEZ235 was partially due to enhanced oxygenation when administered prior to radiation but also affected by direct radiosensitisation of the tumour cells themselves (Fig. 7D).



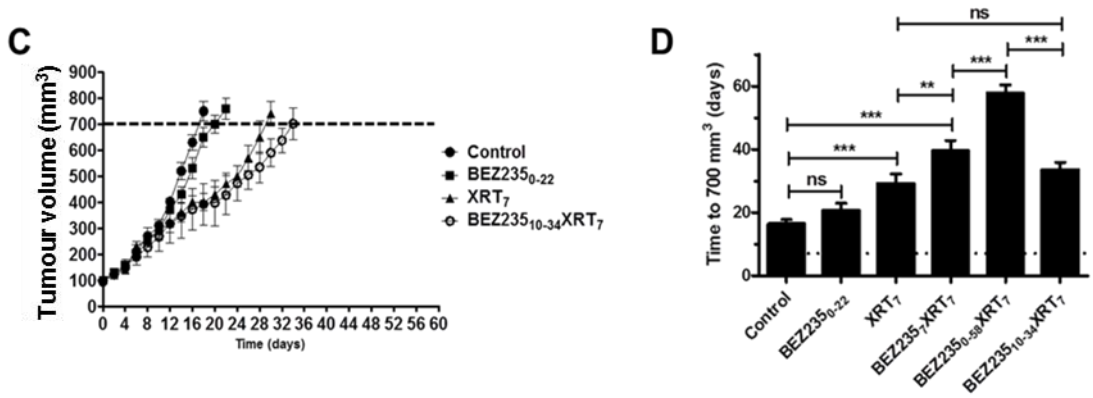
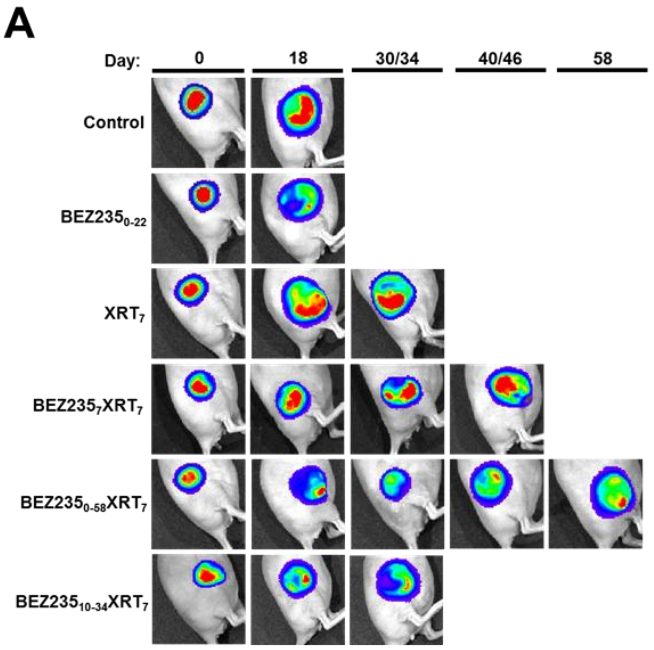


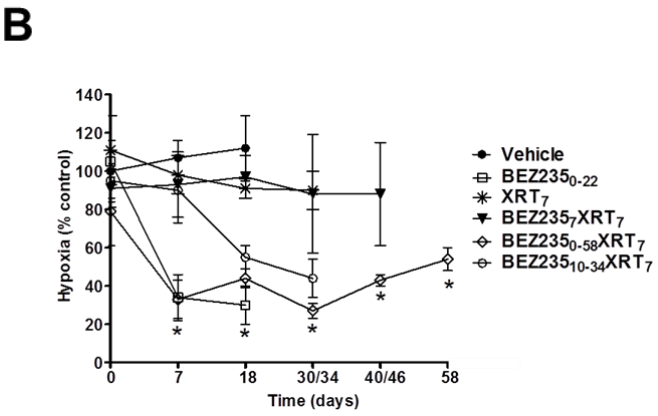

**Figure 7.** Therapeutic efficacy of BEZ235 (20 mg/kg) and radiation in FaDu-HRE-luc xenograft model. A-C, When tumours reached a volume of ~100 $mm^3$ cm, mice were treated with either vehicle (*control*), BEZ235 (on days 0-22; $BEZ235_{0\text{-}22}$), 6 Gy (on day 7; $XRT_7$), BEZ235 single dose at the day of irradiation ($BEZ235_7XRT_7$), BEZ235 pre-treatment followed by 6 Gy and continued throughout the course of experiment (BEZ235 on days 0-58 and 6 Gy on day 7; $BEZ235_{0\text{-}58}XRT_7$) and 6 Gy followed by BEZ235 (6 Gy on day 7 and BEZ235 on days 10-34). Points, mean of tumour volume ($mm^3$) of each treatment group (n=4-5); bars, SD. D, Pretreament with BEZ235 results in supra-additive tumour growth delay effect. *Columns*, mean time of each treatment group to reach 700 $mm^3$; *bars*, SD. *, $p<0.05$; **, $p<0.01$; ***, $p<0.001$.

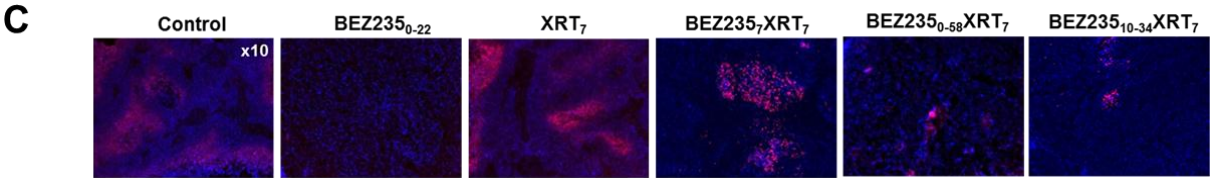
## 4.2.5 Hypoxia, perfusion and vascular morphology in irradiated tumours

We monitored tumour hypoxia using luciferase during the radiation-induced growth delay experiments described above (Fig. 8A-B). Tumours in the $XRT_7$ and $BEZ235_7XRT_7$ group did not show changes in hypoxia when compared to control and remained hypoxic until they reached their maximum size (day 30 and 40, respectively). Mice in the $BEZ235_{0\text{-}22}$ group had a dramatic decrease in hypoxia after 7 days of treatment that persisted until the tumours reached their maximum size. A similar decrease in hypoxia was observed in the treated, radiated $BEZ235_{0\text{-}58}XRT_7$ group. With time, as these tumours regrew hypoxia increased, but did not reach the initial pretreatment level by the time of sacrifice (day 58). $BEZ235_{10\text{-}34}XRT_7$ tumours also showed a persistent decrease in hypoxia. EF5 staining at the time of sacrifice confirmed that the luciferase measurements correlated with hypoxia (Fig. 8C). Thus the decrease in hypoxia persisted throughout the

time of the experiment regardless of radiation. VEGF levels were decreased in tumours treated with BEZ235 for prolonged time (Fig. 8D).



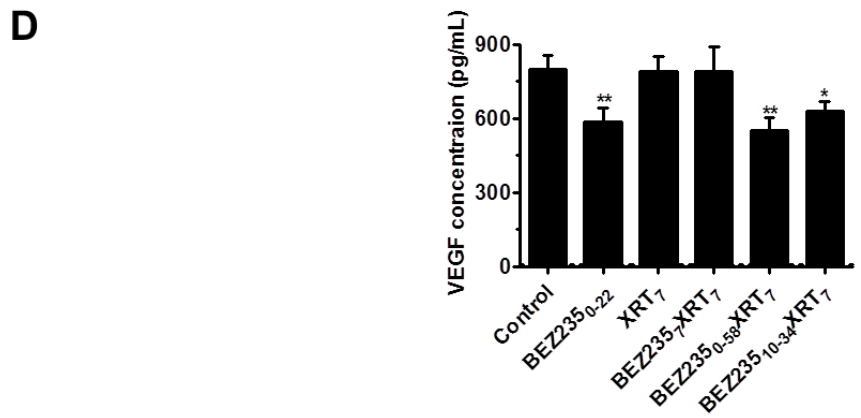
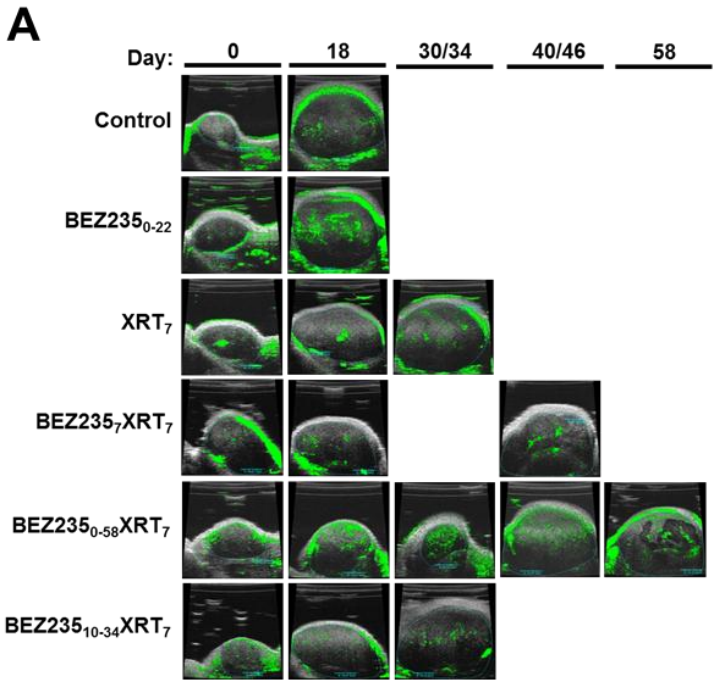
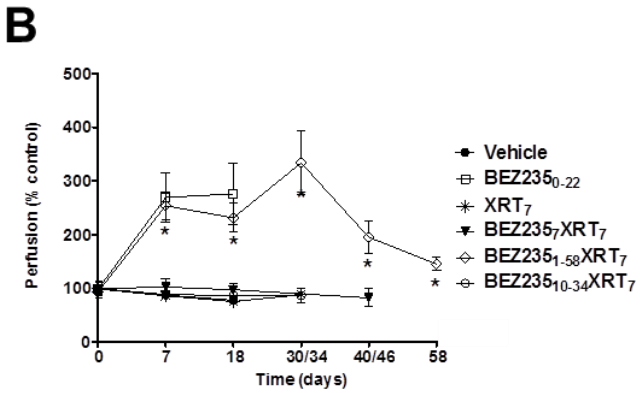
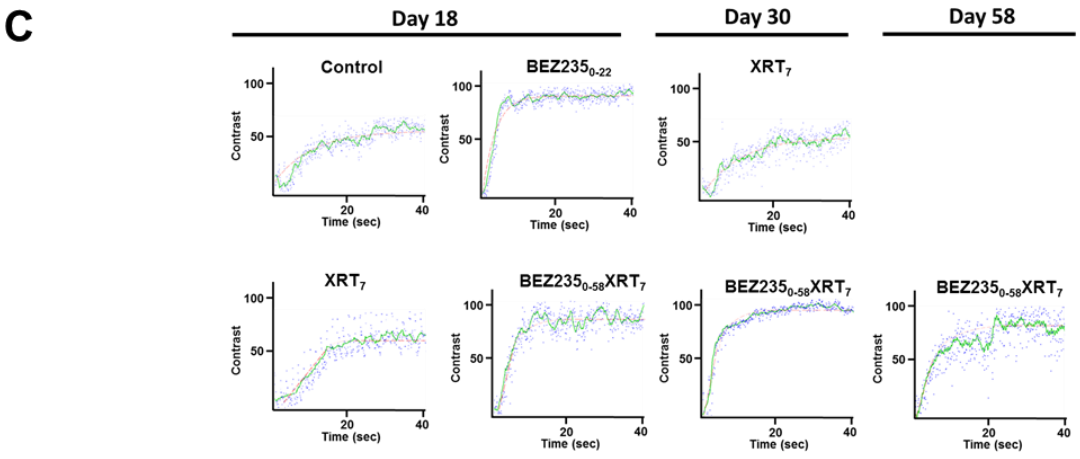



**Figure 8.** Monitoring of hypoxia in irradiated FaDu-HRE-luc xenograft model. Tumours were treated using BEZ235, radiation or the different schedules (as described in "Results"). A, representative images of the luciferase signal and (B) their corresponding measurements are shown. C, immunohistochemical staining for EF5 confirmed reduction in hypoxia in FaDu xenografts (as described in "Results"). D, VEGF concentration was measured by VEGF ELISA. *Columns/points*, mean; *bars*, SD. *, $p<0.05$; **, $p<0.01$ over vehicle-treated control.

Tumour perfusion was also throughout the experiment (Fig. 9A-D). There was no significant alteration in the level of perfusion in the control, $XRT_7$ or $BEZ235_7XRT_7$ groups during the course of the experiment. As expected, both the $BEZ235_{0-22}$ tumours and the $BEZ235_{0-58}XRT_7$ tumours had increased perfusion that persisted until sacrifice. Again, as the experiment progressed, the level of perfusion began to decrease with time but still remained significantly above the control. Some of the decrease may be due to areas of necrosis observed by ultrasound monitoring at this time. In contrast to the finding regarding hypoxia, no significant improvement in perfusion was observed in the $BEZ235_{10-34}XRT_7$ tumours.


A
Day:
0
18
30/34
40/46
58
Control
BEZ235$_{0-22}$
XRT$_7$
BEZ235$_7$XRT$_7$
BEZ235$_{0-58}$XRT$_7$
BEZ235$_{10-34}$XRT$_7$


B
Perfusion (% control)
Time (days)
Vehicle
BEZ235$_{0-22}$
XRT$_7$
BEZ235$_7$XRT$_7$
BEZ235$_{1-58}$XRT$_7$
BEZ235$_{10-34}$XRT$_7$


C
Day 18
Day 30
Day 58
Control
BEZ235$_{0-22}$
XRT$_7$
XRT$_7$
BEZ235$_{0-58}$XRT$_7$
BEZ235$_{0-58}$XRT$_7$
BEZ235$_{0-58}$XRT$_7$
Contrast
Time (sec)

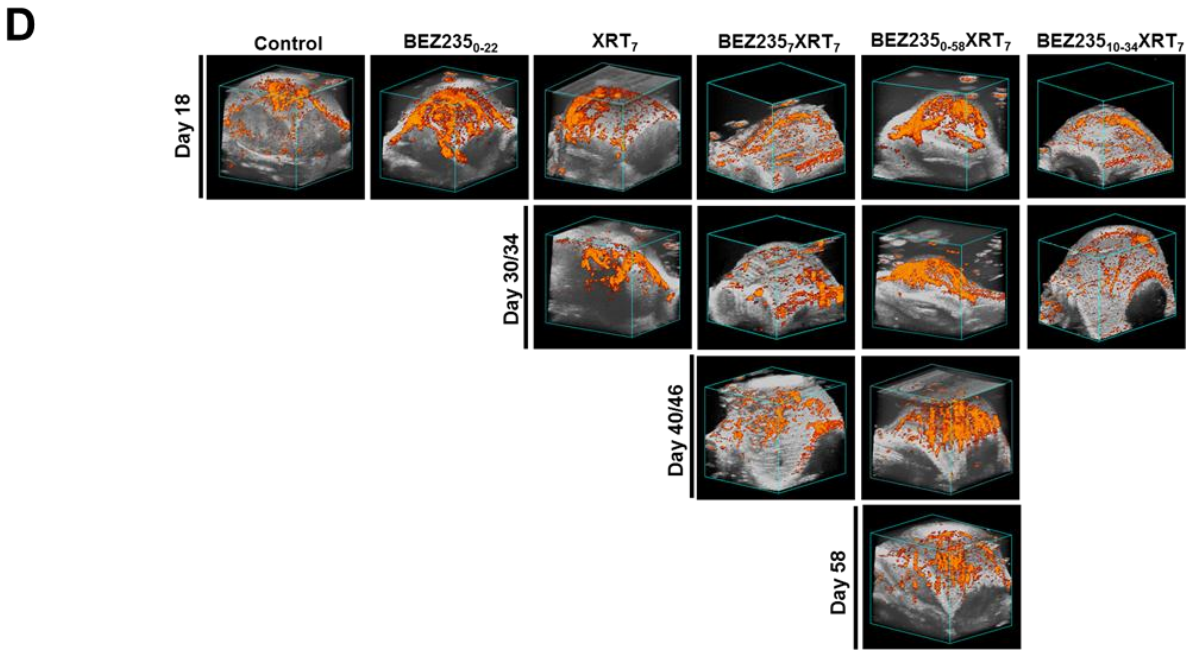



**Figure 9.** Monitoring of perfusion in irradiated FaDu-HRE-luc xenograft model. Tumours were treated as described in "Results". A, representative images of the perfusion for the different times points are shown. B, measurement of microbubble perfusion signal from the ROI. *Points*, mean; *bars*, SD. *p<0.05 over vehicle-treated control. C, representative images of the raw contrast kinetics in FaDu tumours. D, three-dimensional reconstruction of Doppler measurements in the different groups.

Vascular morphology was determined in the tumours after sacrifice. Mice in the control group had typically chaotic tumour vasculature (day 18). Mice from the $XRT_7$ and $BEZ235_7XRT_7$ (day 30 and 40, respectively) treatment groups also had typical tumour vasculature composed of irregular networks. Importantly, the $BEZ235_{0-22}$ group displayed normalised tumour vasculature at the end of the treatment (day 22). The $BEZ235_{0-58}XRT_7$ tumours also showed improved vascular morphology (day 58) consistent with vascular normalisation, but to an extent lower than the BEZ235-only group. Indeed, even though the vessels retained a larger diameter, increased tortuosity and vessel density were observed compared to BEZ235-only group (Fig. 10A-B). Thus irradiation appears to have a distinctive modifying effect on tumour vasculature in the presence of the drug. In line with the perfusion findings, $BEZ235_{10-34}XRT_7$ tumours showed no improvement in vascular morphology.

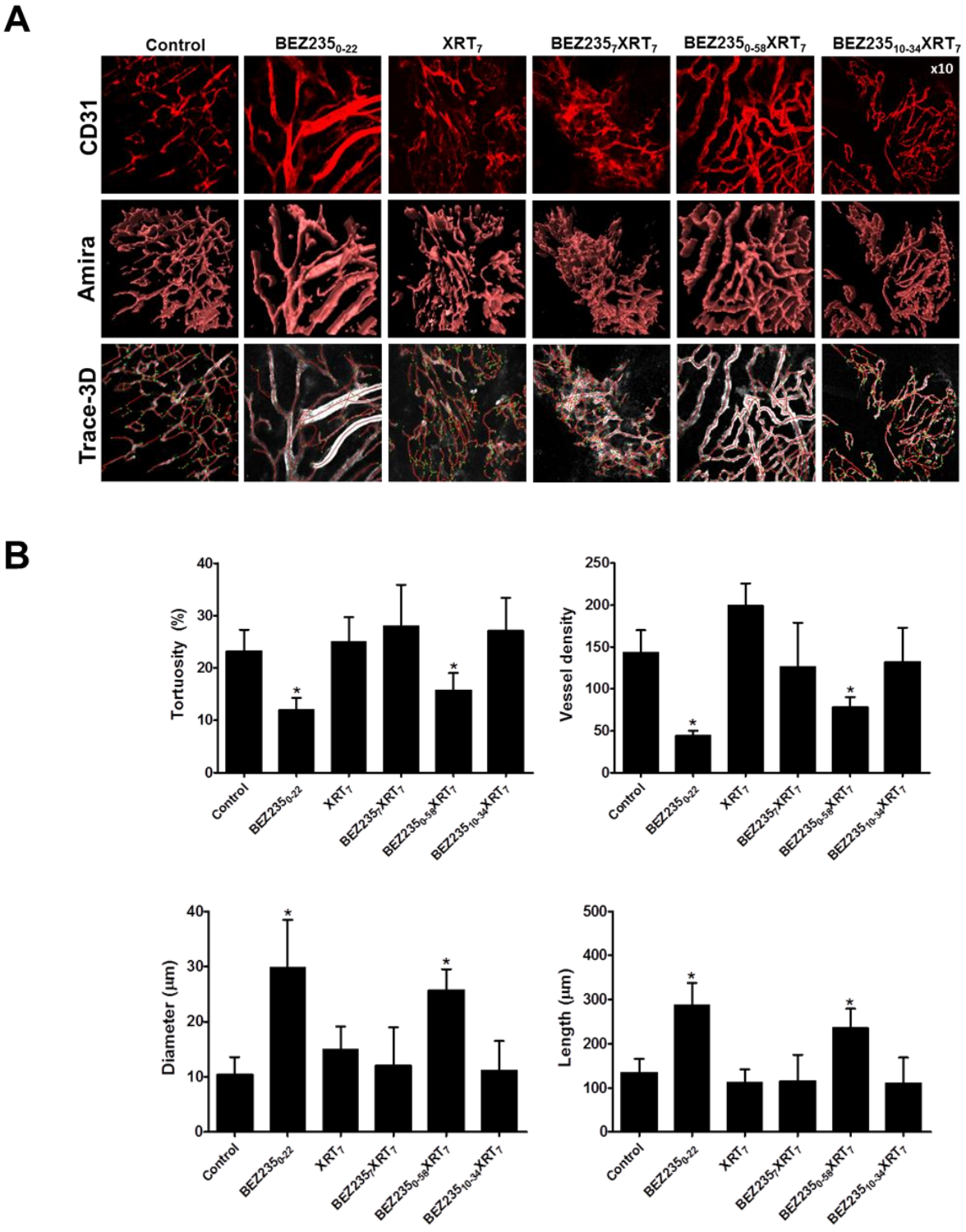



**Figure 10.** The impact of signalling inhibitors on tumour vasculature in irradiated FaDu xenografts. A, representative images of blood vessels (CD31; upper), 3D reconstructions of vascular morphology (AMIRA; middle) and computed tracings (Trace3D; lower). B, measurement of vessel tortuosity, density, diameter and length. Columns, mean; Bars, SD. *, $p<0.05$ over vehicle-treated control.

Pericyte analysis revealed improved pericyte coverage in the $BEZ235_{0\text{-}22}$ group while a less prominent but significant increase was also observed in the $BEZ235_{0\text{-}58}XRT_7$ tumours (Fig. 11).

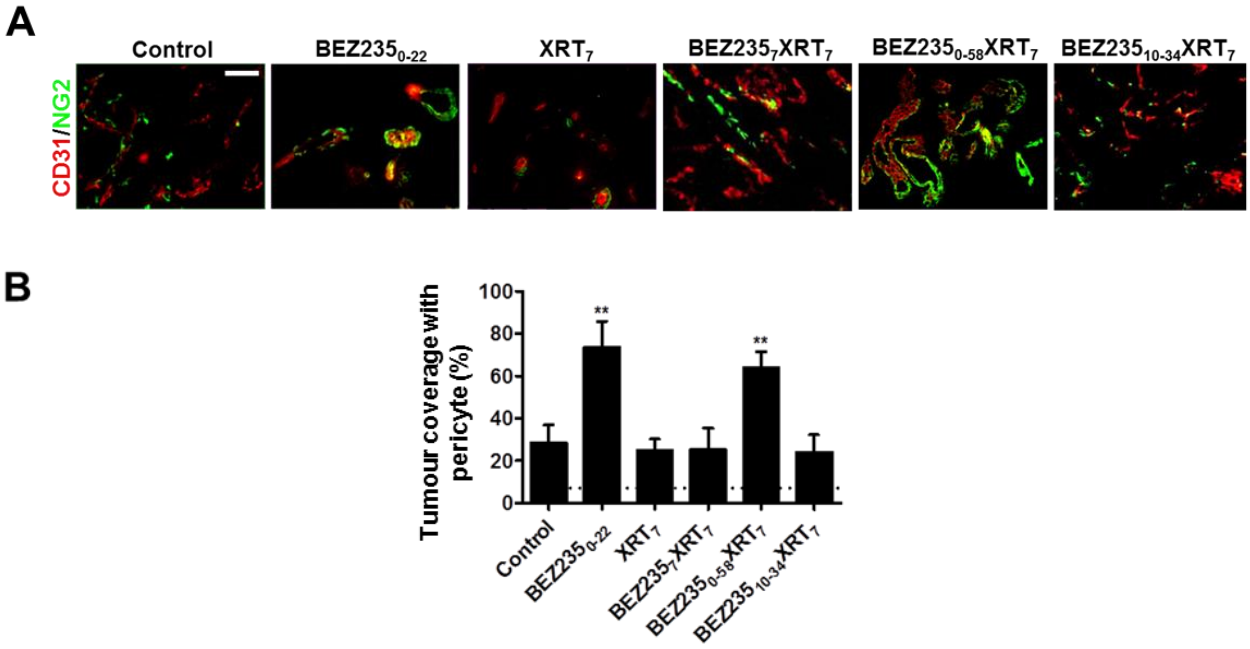



**Figure 11**. BEZ235 results in increased pericyte coverage of tumour blood vessels in irradiated FaDu xenografts. A, FaDu tumours were double immunostained using anti-CD31 (red) and anti-NG2 (green). Scale bar, 20 μm. B, quantification of pericyte coverage in FaDu tumours treated as indicated in "Results". *Columns*, mean; *Bars*, SD. **, $p<0.01$ over vehicle-treated control.

The phosphorylation status of Akt and mTOR were examined in those tumours. Immunohistochemical analysis of Akt and mTOR phosphorylation confirmed blockade of the pathway targets after prolonged treatment with BEZ235 (Fig. 12), at the time of sacrifice.

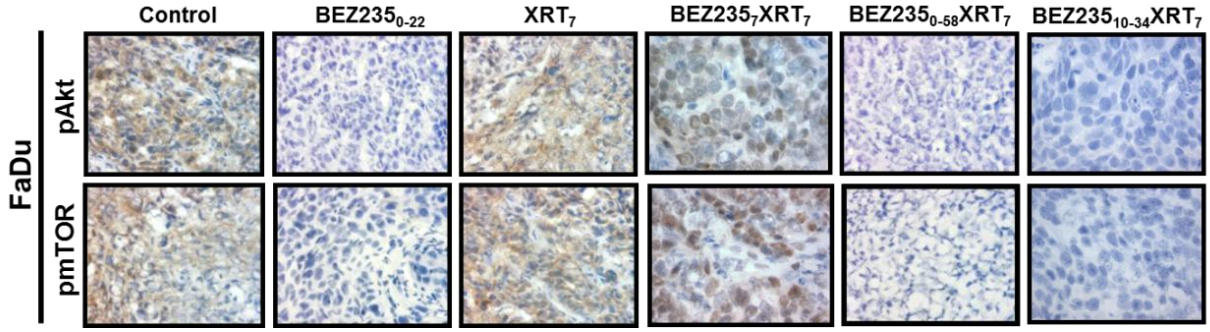


**Figure 12.** Immunohistochemical analysis of irradiated FaDu tumours. Evaluation of the effects of BEZ235 (20 mg/kg) on p-Akt and p-mTOR in irradiated FaDu xenografts. Sections were stained with the indicated antibodies. Magnification x40 (Staining was performed from Sabira Yameen).

## 4.3 DISCUSSION

Vascular remodelling plays an important role in controlling tumour microenvironment and its regulation evolves as a promising approach for cancer therapy [114]. This study shows that that inhibition of the PI3K/Akt/mTOR pathway markedly normalises the tumour vasculature. BKM120 and, more potently, BEZ235 significantly remodelled vascular morphology towards well-organized, longer vessels with large diameter that were enriched with pericytes, resembling those in normal tissues. These changes were accompanied by improved tumour perfusion and oxygenation and improved response to radiotherapy but only at drug doses that showed substantial inhibition of pAkt, highlighting the potential of signalling in this pathway in modulating vascular remodelling and altering the TME. These data are in line to previous work on oncogenic signalling inhibitors of the Ras/PI3K/Akt pathway [89, 142]. Cerniglia et al. have recently shown that EGFR inhibitor erlotinib modulated tumour microenvironment in a similar way [30].

It was hypothesised that the improvement in tumour blood flow and oxygenation as observed in treated tumours at day 7 should result in enhanced response to radiation *in vivo*. BEZ235 leads to radiosensitisation of tumours derived from cell lines with Kras mutations. However this work did not distinguish between the effects on radiosensitisation of the tumour cells themselves and effects on the TME [92]. Administration of BEZ235 only on the day of irradiation ($BEZ235_7XRT_7$) resulted in an additional 10 days growth delay over $XRT_7$ alone which is significantly lower than the 28 days growth delay observed in the $BEZ23_{0\text{-}58}XRT_7$ ($p<0.001$). Moreover, BEZ235 administration initiated three days post-irradiation ($BEZ235_{10\text{-}34}XRT_7$) had essentially no effect on growth delay.

These results indicate that (a) PI3K/mTOR inhibitors function by increasing both the intrinsic and the extrinsic sensitivity of cancer cells to irradiation (b) alteration of TME can substantially improve response to radiotherapy, underlying the importance of tumour oxygenation for radiotherapy. These findings demonstrate that the benefit of PI3K/mTOR inhibition might be enhanced by precise treatment scheduling. These experiments utilized the tumour growth delay assay which can under some circumstances yield different results from tumour control assays. Relevant to this study, Baumann and colleagues found a growth delay similar to the anti-epidermal growth factor receptor (EGFR) antibody cetuximab after radiation but the tyrosine kinase inhibitors BIBIX1382BS and erlotinib failed to improve local tumour control in the FaDu model [295-297]. However in these experiments the drugs were first administered on the same day as radiation was initiated, a dosing schedule that would not have maximized the effect of decreased hypoxia. Undoubtedly, the local tumour control remains an important and relevant parameter in determining the therapeutic effect of irradiation when combined with different drugs [298]. Nevertheless, the impressive growth delay of 38 days observed in the $BEZ235_{0\text{-}58}XRT_7$ group, as compared to $XRT_7$, indicates a substantial response to radiotherapy.

The effects of PI3K/Akt/mTOR inhibition on the cancer vasculature and radiation outcome resemble the transient changes reported from Jain and colleagues after anti-VEGFR treatment [299, 300]. Blockade of the VEGF pathway normalized blood vessel and improved oxygenation, providing a window for combination with radiotherapy [301]. Dings et al. showed that radiotherapy was most effective when administered after treatment with bevacizumab in ovarian, breast and melanoma models [302]. Bevacizumab and continuous delivery of interferon-β presented changes consistent with normalization and increased radiation response in an orthotopic glioma model [34].

However, the vascular remodelling that occurs after antiangiogenic therapy is only transient, lasting approximately 5 days [301]. In contrast, the present data suggest that PI3K/mTOR could further extend this normalisation window. Even though irradiation did not alter vascular density in our study, we observed areas of leakage in previously irradiated vessels. Importantly, no improvement in vascular morphology was observed in the $BEZ235_{10\text{-}34}XRT_7$ arm. We are tempted to speculate that this can be attributed to the effect of irradiation on endothelial cells, at least in part, or to compensatory mechanisms of the tumours cells. Radiation can lead to endothelial cell damage which could result to partial vessel collapse and rebound hypoxia [303-305]. Interestingly, FaDu tumours grown in preirradiated tissues presented a better response to the VEGFR inhibitors, indicating that irradiated blood vessels are more susceptible to these drugs than unirradiated vessels [68]. Whether PI3K/mTOR inhibitors could potentially have similar effects on tumours grown in preirradiated tumour bed remains to be investigated.

Increased perfusion in normalised tumour vessels might have been expected to increase tumour growth rate. However, no alteration in tumour growth was seen with BEZ235 or BKM120. This could be attributed to the antiproliferative effect of the signalling inhibitors that counterbalance increased tumour growth from the increased perfusion, or perhaps improved oxygenation renders the tumour less aggressive.

How could inhibition of PI3K/mTOR pathway result in improvement of vascular functionality? One explanation could be that both BKM120 and BEZ235 caused a moderate down-regulation of VEGF expression, at the doses which normalised blood vessels. This is in accordance to the reports from Qayum et al. and Cerniglia et al. with the signalling inhibitors erlotinib and nelfinavir, respectively [30, 142]. In contrast, antiangiogenic agents aim at inducing a complete inhibition of VEGF. Anti-VEGF therapy

can induce tumour hypoxia, leading to increased invasion and metastasis in tumour models [83, 112].

A second possible explanation could be the involvement of the PI3K/ mTOR pathway in endothelial signalling [30, 115, 306]. Activation of PI3K/Akt signalling upregulated VEGF and promoted vessel formation in chicken embryos [36]. Promising preclinical activity has been demonstrated for BEZ235 while blockade of neovascularization and downregulation of VEGF and HIF-1 have been reported [286-290]. BEZ235 inhibited VEGF-induced permeability and vascular leakage and reduced interstitial fluid pressure [141]. These data complement the findings of the current study.

Moreover, Akt overexpression in endothelial cells resulted in embryonic lethality due to abnormal vascular remodelling [136]. Transient expression of myrAkt was capable of altering the normal response to oxygen-induced remodelling without causing vascular malformations Therefore, physiological levels of Akt signalling modulate microvascular patterning [136]. Phung et al. demonstrated that Akt is chronically activated in tumour-associated endothelial cells but not in normal tissues. Sustained endothelial activation of Akt in otherwise healthy tissues induced vascular malformations and recapitulated the abnormal structural and functional features of tumour blood vessels [140]. These changes were reversible upon inactivation of Akt, providing a rationale for Akt inhibition to decrease angiogenesis and excessive vascular permeability in cancer [140]. In the present work, vessel normalisation was accompanied by global inhibition of Akt and mTOR phosphorylation, indicating a direct correlation between PI3K/Akt/mTOR signalling and vascular architecture. It is unclear whether the cancer cell, the host vasculature or both are the target for these TME effects. If it is the cancer cell then stratification for PI3K-AKT signalling would be warranted. However, if it is the host vessels then the effect may be

more universal. These data suggest that decreased hypoxia might be used as a surrogate marker to demonstrate PI3K inhibition in tumours.

## 4.4 CONCLUSION

The results of the present study provide evidence that inhibition of the PI3K/mTOR signalling by BKM120 and BEZ235 displays significant effects on tumour microenvironment by remodelling blood vessels and enhancing tumour perfusion and oxygenation. BEZ235-induced changes promoted a substantial response to radiotherapy and showed a supra-additive effect in delaying tumour regrowth, as compared to other drug-radiation combinations. This is the first study to analyse in detail the effect of different scheduling of PI3K/mTOR inhibition on radiation efficacy. Modulation of oncogenic signalling could be potentially used as a therapeutic approach for cancer therapy.

# CHAPTER 5

## Targeting ATR *in vivo* using the novel inhibitor VE-822 results in selective sensitisation of pancreatic tumours to radiation

Emmanouil Fokas[1], Remko Prevo[1], John R. Pollard[2], Philip M. Reaper[2], Peter A. Charlton[2], Bart Cornelissen[1], Katherine A. Vallis[1], Ester M. Hammond[1], W. Gillies McKenna[1], Ruth J. Muschel[1,3] and Thomas B. Brunner[1,3]

[1]Gray Institute for Radiation Oncology and Biology, Oxford University, Oxford, United Kingdom

[2]Vertex Pharmaceuticals (Europe) Ltd, Abingdon, Oxfordshire, UK

**Contribution to experimental work:** Vertex Pharmaceuticals (Europe) Ltd provided the structure shown in Fig 1A conducted the experiments shown in Tables 1 and 2. Remko Prevo conducted the experiments shown in Fig 1B, partly 1C, 2A, partly 3 A-C and also 6A. The rest of the experiments were conducted by E. Fokas.

## Manuscript submitted, in review

This work was partly supported by grants from Vertex Pharmaceuticals (Europe), Ltd.

# 5.1 Introduction

With a five-year survival rate of 5%, pancreatic ductal adenocarcinoma (PDAC) is one of the most lethal malignancies [216, 260]. Most patients have locally advanced (LAPC) or metastatic disease at the time of diagnosis [216]. Chemoradiation was shown to increase resectability and to enhance local tumour control [267, 268] at the cost of gastrointestinal toxicity [270]. Several trials with targeted agents such as inhibitors of angiogenesis, metastasis and oncogenic signalling had disappointing results [307]. Therefore, targeting factors mediating survival after DNA damage in cancer but not normal cells are highly relevant.

Radiation (XRT) and chemotherapy induce chromosomal DNA lesions resulting in activation of the ataxia telangiectasia-mutated (ATM) and ATM-Rad3-related (ATR) protein kinases in response to double strand DNA breaks (DSBs) and single stranded DNA breaks (SSBs), respectively [189, 308, 309]. Defects in the DNA damage response (DDR) such as ATM and p53 deletion/mutation are common in human tumours [310] and occur in up to 70% of patients with PDAC [216, 217, 311, 312]. They might lead to a differential response in DNA repair signalling between normal and tumour cells that could be exploited to increase killing of cancer cells with DNA damaging agents without increasing normal cell toxicity [189, 243]. Defects in one component of the DDR may result in tumour cells relying on the remaining intact DDR pathways, such as ATR, for survival upon DNA damage [218, 221, 223, 250, 251, 313-315]. Additionally, oncogenic mutations that often occur in human malignancies induce replication stress that can create a selective sensitivity to inhibition of ATR in cancer cells [247, 248, 313, 316]. Finally, hypoxia may further drive dependence on ATR in tumours [317]. Thus, targeting ATR could markedly potentiate the efficacy of DNA damaging agents without harming normal tissues.

In the present study, *in vitro* and *in vivo* data for VE-822 [27], a close analogue of VE-821 [27], with a marked increase in potency against ATR and good pharmacokinetic (PK) properties are presented. With VE-822, it is shown that ATR inhibition profoundly sensitise tumours, both *in vitro* and *in vivo*, to radiation and chemoradiotherapy. During radiotherapy treatment of patients with PDAC, the small intestine, especially the duodenum, is partially exposed to radiation and the latter consists an important dose-limiting factor [5]. Thus, in that study the impact of VE-822 on radiation-induced intestinal damage was also assessed.

# 5.1 RESULTS

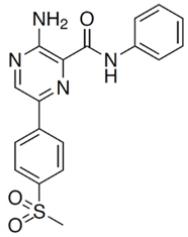
## 5.1.1 VE-822 inhibits Chk1 phosphorylation and sensitises pancreatic cancer cells to radiation *in vitro*

An extensive biochemical and cellular characterization of the highly selective ATR inhibitor VE-821 was recently reported (Fig 1A). VE-822 [15, 35] is a close analogue of VE-821 that has increased potency against ATR. Furthermore, VE-822 has absorption, distribution, metabolism and excretion (ADME) properties that support *in vivo* studies [15, 27]. Importantly, VE-822 retains the excellent biochemical and cellular ATR selectivity profile of VE-821. Most notably VE-822 has >100-fold cellular selectivity for ATR over the closely related PIKKs ATM and DNA-PK (Table 1 and Table 2).

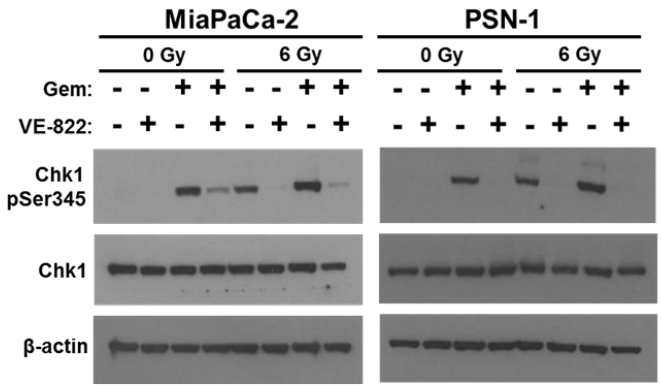
ATR is the major kinase leading to phosphorylation of Chk1. First, I showed that VE-822 (80 nM) blocks Chk1 phosphorylation (Ser 345) after gemcitabine (100 nM), XRT (6 Gy) or their combination in PDAC (Fig. 1B). We then showed that treatment with VE-822 results in marked radiosensitisation of PDAC cells; decreases in clonogenic survival of irradiated MiaPaCa-2, PSN-1 and primary PancM cells (all three cell lines are p53-mutant; K-Ras mutant) were observed with co-treatment with XRT and VE-822 (Fig. 1C). Gemcitabine is the standard chemotherapeutic agent in PDAC. Combined VE-822

and gemcitabine reduced cell survival ~3-fold in PSN-1 and MiaPaCa-2 cells and less in primary PancM tumour cells (Fig. 1D), and this was markedly improved with addition of XRT (Fig. 1E). Importantly, the plating efficiencies of tumour cells in the control and VE-822 groups were comparable. For radiation experiments, the plating efficiencies in the DMSO and VE-822 groups were 49%/42.7%, 66.4%/60.2% and 15.7%/14.9% in MiaPaCa-2, PSN-1 and PancM cells, respectively. For radiation experiments, the plating efficiencies in the DMSO and VE-822 groups were 62%/59%, 67%/61% and 19.3%/16.8% in MiaPaCa-2, PSN-1 and PancM cells, respectively. We did not assess the plating efficiency for VE-822 concentrations larger than 80 nM in our studies. We conducted our *in vitro* experiments using 80 nM VE-822 as at this drug concentration cells were strongly sensitised to XRT and gemcitabine without a profound decrease in plating efficiency, as assessed by the clonogenic survival assay.

**A**




**B**



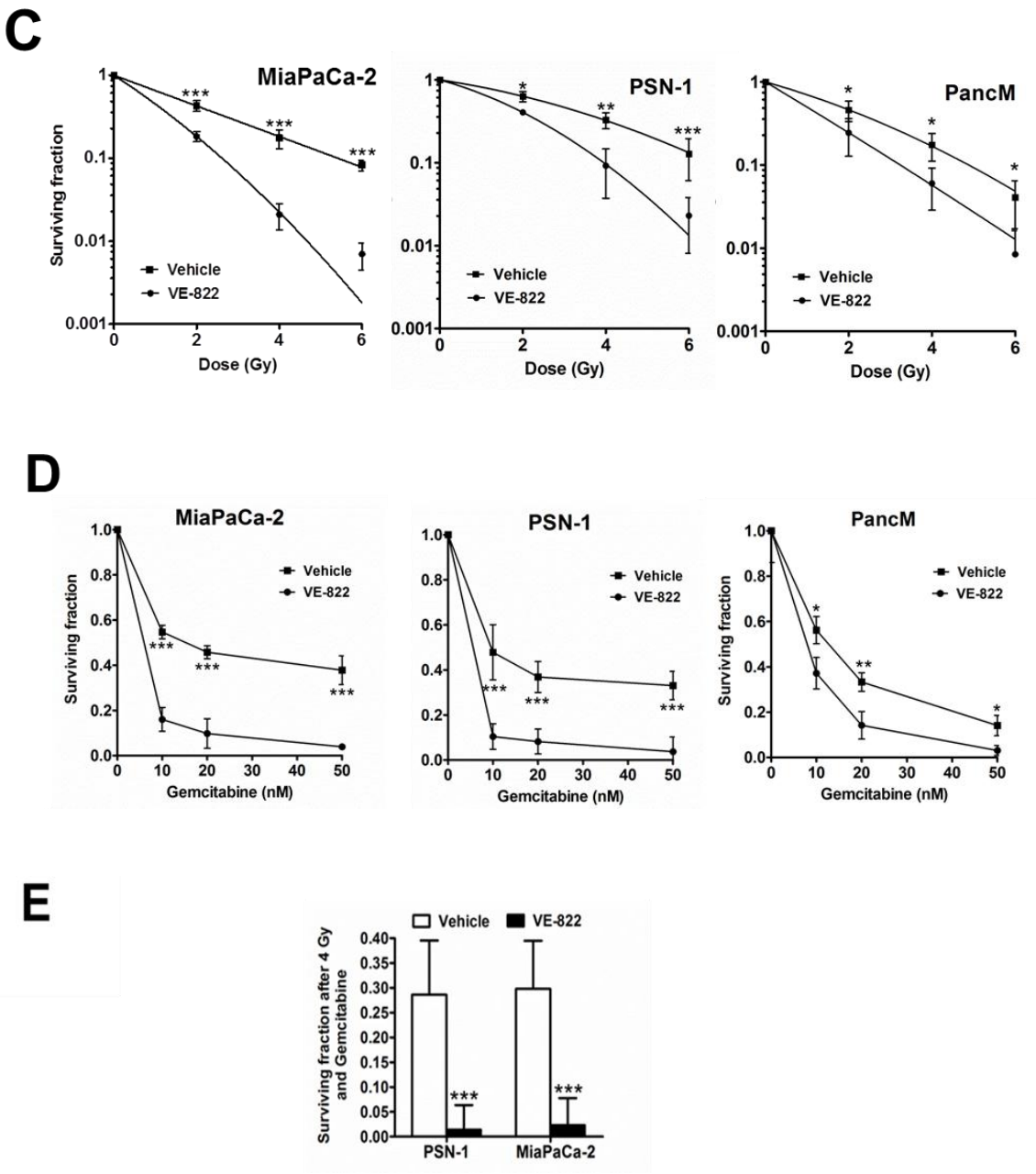



**Figure 1.** VE-822 attenuates ATR/Chk1 signalling pathway and reduces survival in tumour cells in response to XRT and gemcitabine. ***A,*** chemical structure of VE-821. ***B***, Chk1 phosphorylation was examined by immunoblot in lysates from MiaPaCa-2 and PSN-1 cells 2 hours after XRT (6 Gy) or 4 hours after gemcitabine. Treatment with VE-822 (80 nmol/l) was initiated either 2 h before XRT or 1 h after gemcitabine. Blots were also stained with β-actin and total Chk1, as indicated. ***C,*** clonogenic survival of MiaPaCa-2, PSN-1 and Panc-M after XRT was assessed after exposure to VE-822 (80 nM) for 1 h before until 18 h post-XRT. ***D***, clonogenic survival of pancreatic tumour cells treated as indicated. Cells were exposed to gemcitabine for 24 h before addition of 80 nM VE-822 for another 18 h. Gemcitabine was removed immediately before addition of VE-822. ***E,*** assessment of the triple combination of VE-822 with gemcitabine and XRT. MiaPaCa-2 and PSN-1 cells were pretreated with 10 nM and 5 nM of gemcitabine, respectively, for 24 h. Gemcitabine was washed away, VE-822 (80 nM) was added for 1 h before until 18 h

after XRT with 4 Gy. Clonogenicity was measured 14-21 days post-irradiation/gemcitabine. *Datapoints/columns*, mean; *bars*, 95% CI. (n=3). *, P < 0.05; **, P < 0.01; ***, P < 0.001 over DMSO-treated control.(Western blot is courtesy of Dr Remko Prevo).

**Table 1.** Summary of the binding affinity (Ki) and half maximal inhibitory concentration (IC50) of the two ATR inhibitors, VE-821 and VE-822.

| Kinase | VE-821 | | VE-822 | |
|---|---|---|---|---|
| | Ki (μM) | Cell IC50 (μM) | Ki (μM) | Cell IC50 (μM) |
| **ATR** | 0.013 | 0.71 | <0.0002 | 0.019 |
| **ATM** | 16 | >10 | 0.034 | 2.6 |
| **DNA-PK** | 2.2 | >10 | >4 | 18.1 |
| **mTOR** | >1 | - | >1 | - |
| **PI3Kγ** | 3.9 | - | 0.22 | - |

IC50, half maximal inhibitory concentration; Ki, absolute inhibition constant.

**Table 2.** Summary of the kinase activity of the ATR inhibitor VE-822.

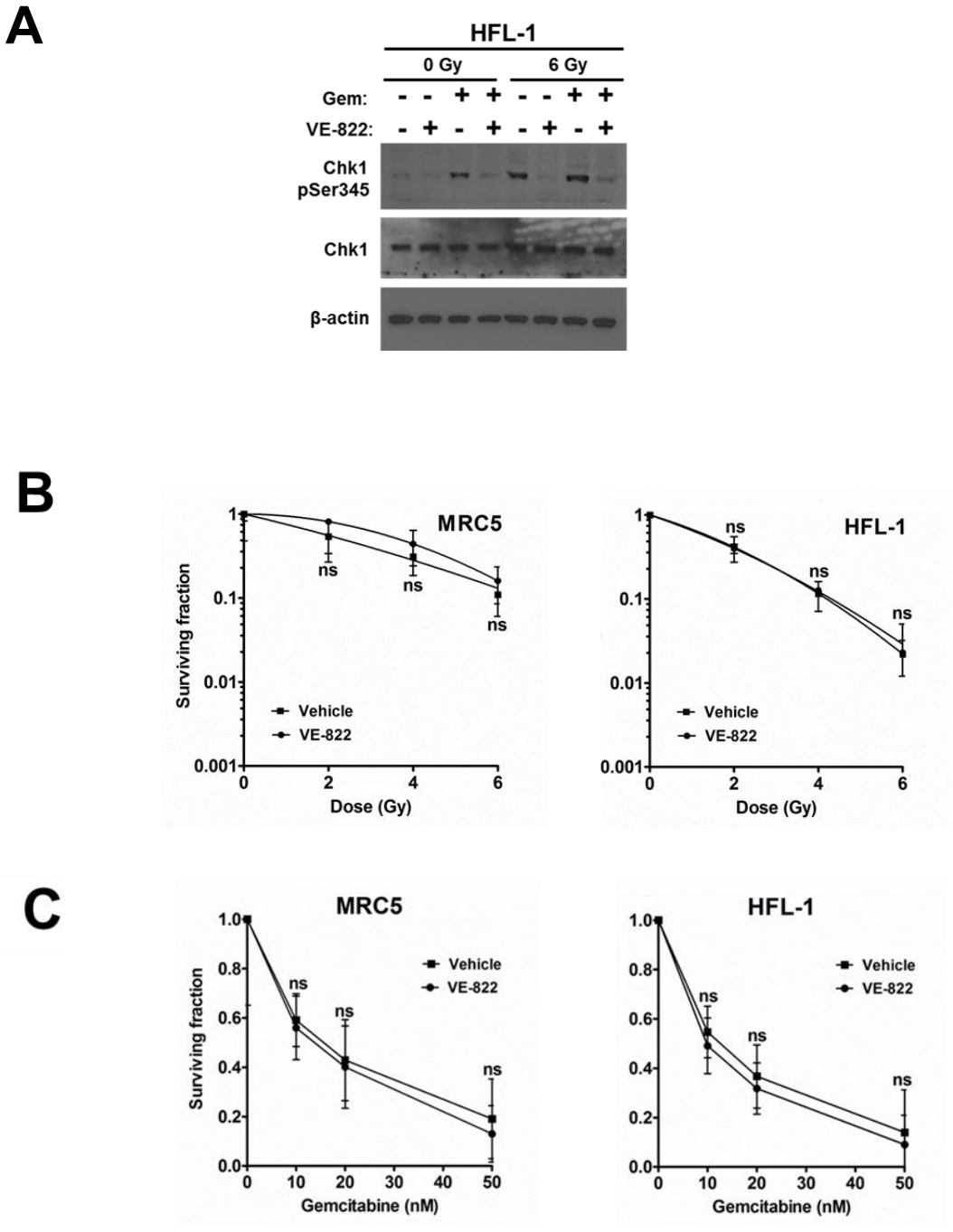
| Kinase | % Inhibition | |
|---|---|---|
| | @ 0.4 μM | @ 2 μM |
| Abl(h) | 11 | 34 |
| ALK(h) | 2 | 4 |
| AMPK(r) | 0 | 20 |
| ASK1(h) | 0 | 0 |
| Axl(h) | 27 | 75 |
| Blk(m) | 2 | 36 |
| BTK(h) | 4 | 6 |
| CaMKII(r) | 0 | 1 |
| CDK1/cyclinB(h) | 0 | 6 |
| CDK5/p35(h) | 0 | 16 |
| CHK1(h) | 15 | 52 |
| CK1(y) | 0 | 8 |
| c-RAF(h) | 0 | 10 |
| EGFR(h) | 0 | 0 |
| EphB4(h) | 0 | 10 |
| Fes(h) | 0 | 0 |
| FGFR3(h) | 0 | 10 |
| Flt1(h) | 50 | 83 |
| Fyn(h) | 9 | 27 |
| IGF-1R(h) | 0 | 2 |

| | | |
|---|---|---|
| IKKα(h) | 17 | 36 |
| IR(h) | 0 | 0 |
| JNK1α1(h) | 6 | 8 |
| Lck(h) | 42 | 64 |
| Lyn(h) | 13 | 53 |
| MAPK1(h) | 12 | 19 |
| MEK1(h) | 12 | 6 |
| MKK6(h) | 15 | 28 |
| MKK7β(h) | 0 | 0 |
| MSK1(h) | 0 | 0 |
| MST2(h) | 18 | 43 |
| mTOR(h) | 0 | 37 |
| NEK2(h) | 0 | 2 |
| PAK2(h) | 7 | 6 |
| PDGFRα(h) | 0 | 9 |
| PKCβII(h) | 5 | 7 |
| PKCι(h) | 0 | 1 |
| PKCθ(h) | 0 | 0 |
| PRAK(h) | 0 | 0 |
| PRK2(h) | 59 | 82 |
| Ret(h) | 22 | 42 |
| RIPK2(h) | 6 | 26 |
| ROCK-II(h) | 0 | 13 |
| Ros(h) | 0 | 4 |
| Rsk3(h) | 17 | 49 |
| SAPK2b(h) | 2 | 11 |
| SGK(h) | 0 | 0 |
| Tie2(h) | 0 | 44 |
| TrkA(h) | 13 | 32 |
| ZAP-70(h) | 0 | 0 |

## 5.1.2 VE-822 does not increase normal cell radiosensitivity and chemosensitivity *in vitro*

HFL-1 normal fibroblasts were treated as in Fig. 1B and analysed phosphorylation of Chk1. VE-822 blocked Chk1 phosphorylation (Ser 345) after exposure to gemcitabine, radiation or their combination (. 2A). The impact of VE-822 on XRT- and gemcitabine-induced killing of normal cells was also evaluated. Application of VE-822 did not alter the clonogenic survival of MRC5 and HFL-1, two normal fibroblast cell lines, after treatment with increasing doses of XRT or gemcitabine (Fig. 2B-C). To further assess the impact of

VE-822 on normal cells *in vitro*, HDMEC were exposed to VE-822, gemcitabine and XRT, and were allowed to form capillary tubes (Fig. 2D-E). VE-822 did not enhance the reduction of tube formation after treatment with XRT or gemcitabine (Fig. 2D-E). Similar results were obtained with VE-822 in unirradiated HDMECs. These data underline the tumour-specificity of VE-822-enhanced cytotoxicity of XRT and gemcitabine.



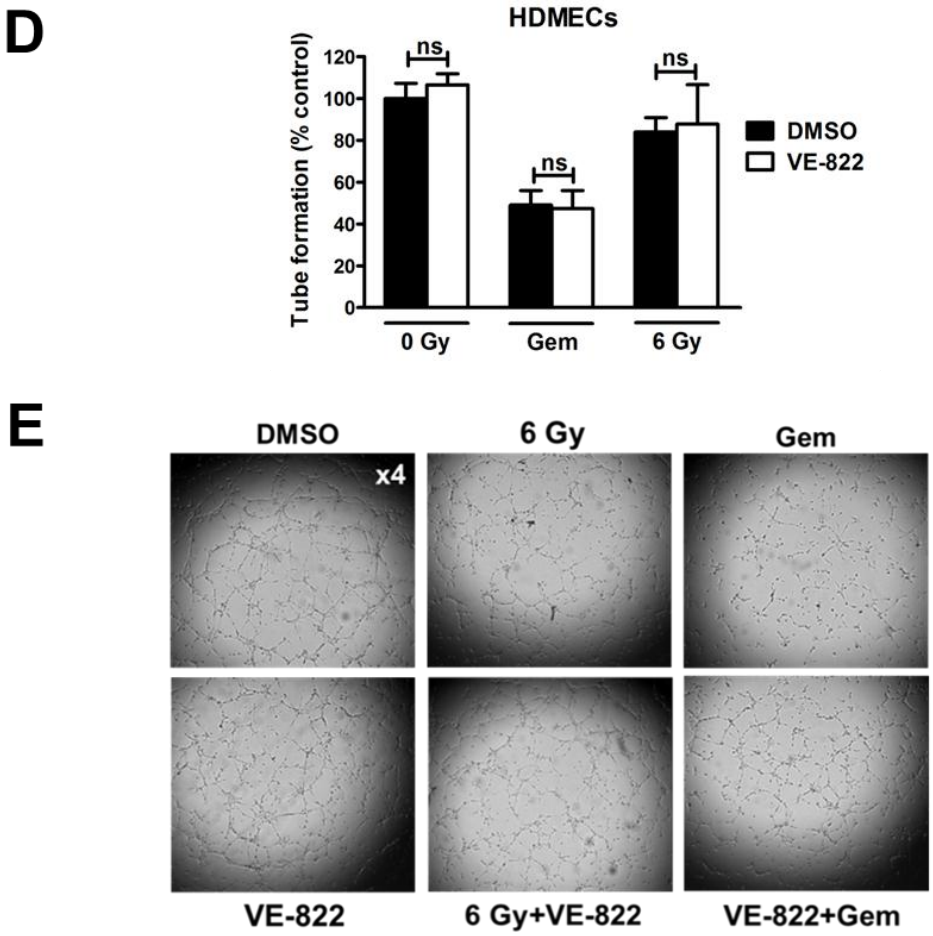



**Figure 2.** VE-822 attenuates ATR/Chk1 signalling in normal cells without enhancing radiation- and gemcitabine killing in normal cells. A, Chk1 western blot in HFL-1 normal cells treated as tumour cells in Fig 1B. ***B,*** clonogenic survival of MRC5 and HFL1 normal cells treated as tumour cells in Fig. 1C. ***C,*** clonogenicity of cells treated as tumour cells in Fig. 1D. ***D,*** quantification of tube formation counted by number of branches and normalised to the control group (4 power fields per sample). HDMVCs were pretreated with 50 nM gemcitabine for 24 h. Gemcitabine was washed away and 80 nM VE-822 was added 1 h before XRT (6 Gy). Tube formation was analysed 8 h post-XRT. Representative images of capillary tube formation in HDMVCs are shown on ***F***. *Data points/columns,* mean; *bars,* 95% CI. (n=3). ns, not significant. *, $P < 0.05$; **, $P < 0.01$ as compared to control (Fig. 2A and 2B-left panel are courtesy of Dr Remko Prevo).

## 5.1.3 VE-822 enhances residual DNA damage *in vitro*

To confirm modification of the DDR by VE-822, the number of γH2AX, 53BP1 and Rad51 foci was investigated in PSN-1 and MiaPaCa-2 cells (Fig. 3). VE-822 increased XRT-induced residual γH2AX and 53BP1 foci compared to XRT alone (Fig. 3A-B). VE-822 significantly decreased Rad51 foci, a homologous recombination repair (HRR) marker, after XRT. This is consistent with inhibition of HRR leading to unrepaired damage

(Fig. 3C). In the unirradiated cells, VE-822 alone resulted in no increase in γH2AX or 53BP1 foci (between 2-3 foci both in the VE-822- and DMSO-treated group) and Rad51 foci (no foci either in the VE-822- or DMSO-treated group) respectively.

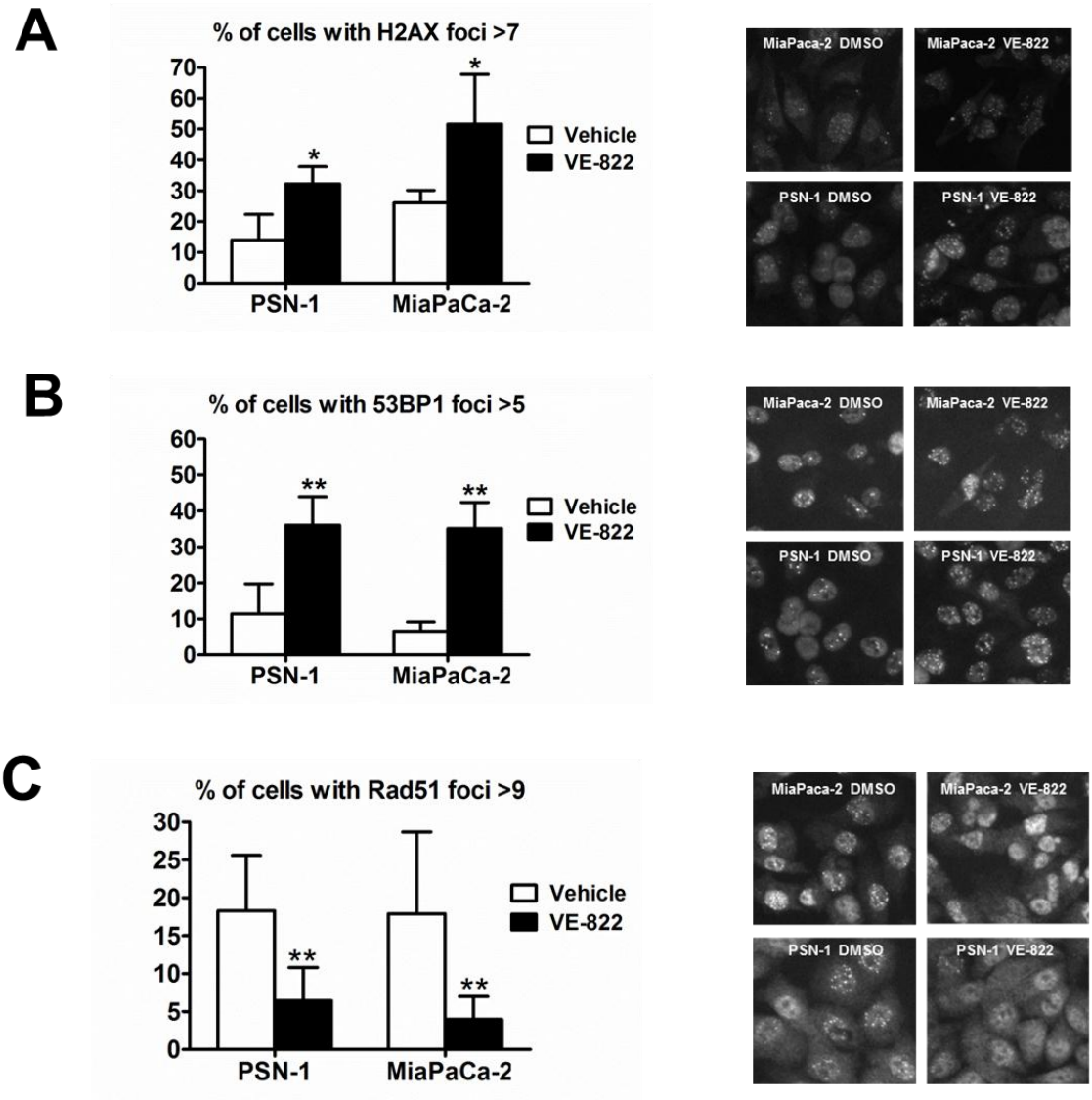
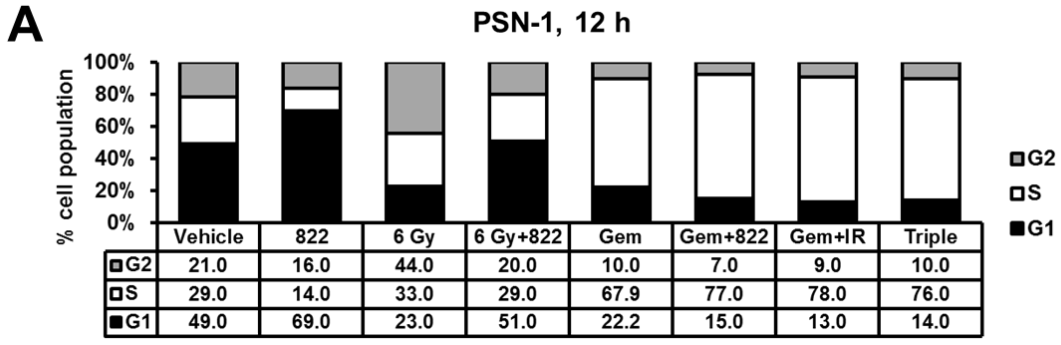



**Figure 3.** Effect of VE-822 on 53BP1, γH2AX and Rad51 foci formation. ***A-B***, VE-822 (80 nM) was added to cells 1 h before radiation (XRT) with 6 Gy. Cells were fixed at 24 h post-irradiation, stained for γH2AX and 53BP1 foci and the percentage of cells with more than 7 and 5 foci per cell was quantitated, respectively. ***C,*** Rad51 foci were analysed at 6 h post-XRT. The percentage of cells with more than nine foci per cell was quantitated. Representative images are shown on the right. *Columns*, mean; *bars*, 95% CI. (n=3). *, P< 0.05; **, P<0.01 over DMSO-treated control. (The images are courtesy of Dr Remko Prevo).

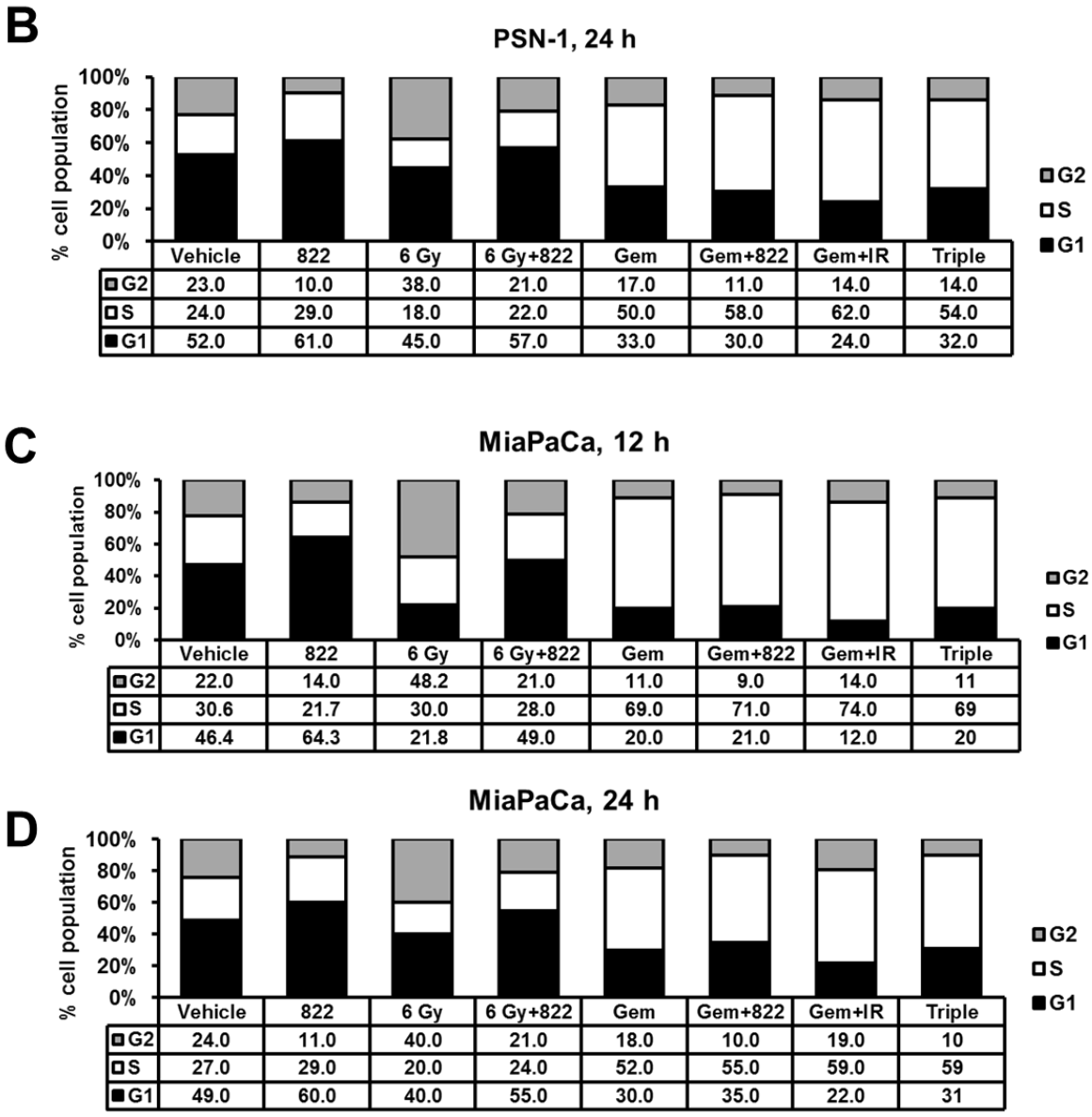
## 5.1.4 VE-822 disrupts DNA damage-induced cell cycle checkpoint

The impact of ATR inhibition on cell cycle distribution after irradiation (6 Gy) and gemcitabine treatment (50 nM) was examined. PSN-1 and MiaPaCa-2 cells were pre-treated with VE-822 (80 nM) at 1 h prior to radiation and their cell cycle profile was examined at 12 h and 24 h post-irradiation (Fig. 4A-D). In unirradiated cells, VE-822 alone increased the proportion of cells in the G1 phase, including the sub-G1 phase population. As anticipated, radiation alone caused an increase in the proportion of cells in the G2/M and S-phase. VE-822 addition to cells treated with radiation abrogated the increase in G2/M and S-phase.

Gemcitabine pretreatment for 24 h induced a profound S-phase arrest. Only a minimal increase in G2-phase was found in radiation+gemcitabine cells while addition of VE-822 to gemcitabine revealed a more rapid transit of cells from S to G1-phase only in MiaPaCa-2 cells at 24 h (Fig. 4D). Taken together, these data indicate that VE-822 abrogates radiation-induced G2 phase delay, likely through inhibition of the ATR/Chk1 checkpoint.




| | Vehicle | 822 | 6 Gy | 6 Gy+822 | Gem | Gem+822 | Gem+IR | Triple |
|---|---|---|---|---|---|---|---|---|
| G2 | 21.0 | 16.0 | 44.0 | 20.0 | 10.0 | 7.0 | 9.0 | 10.0 |
| S | 29.0 | 14.0 | 33.0 | 29.0 | 67.9 | 77.0 | 78.0 | 76.0 |
| G1 | 49.0 | 69.0 | 23.0 | 51.0 | 22.2 | 15.0 | 13.0 | 14.0 |




| | Vehicle | 822 | 6 Gy | 6 Gy+822 | Gem | Gem+822 | Gem+IR | Triple |
|---|---|---|---|---|---|---|---|---|
| G2 | 23.0 | 10.0 | 38.0 | 21.0 | 17.0 | 11.0 | 14.0 | 14.0 |
| S | 24.0 | 29.0 | 18.0 | 22.0 | 50.0 | 58.0 | 62.0 | 54.0 |
| G1 | 52.0 | 61.0 | 45.0 | 57.0 | 33.0 | 30.0 | 24.0 | 32.0 |

| | Vehicle | 822 | 6 Gy | 6 Gy+822 | Gem | Gem+822 | Gem+IR | Triple |
|---|---|---|---|---|---|---|---|---|
| G2 | 22.0 | 14.0 | 48.2 | 21.0 | 11.0 | 9.0 | 14.0 | 11 |
| S | 30.6 | 21.7 | 30.0 | 28.0 | 69.0 | 71.0 | 74.0 | 69 |
| G1 | 46.4 | 64.3 | 21.8 | 49.0 | 20.0 | 21.0 | 12.0 | 20 |

| | Vehicle | 822 | 6 Gy | 6 Gy+822 | Gem | Gem+822 | Gem+IR | Triple |
|---|---|---|---|---|---|---|---|---|
| G2 | 24.0 | 11.0 | 40.0 | 21.0 | 18.0 | 10.0 | 19.0 | 10 |
| S | 27.0 | 29.0 | 20.0 | 24.0 | 52.0 | 55.0 | 59.0 | 59 |
| G1 | 49.0 | 60.0 | 40.0 | 55.0 | 30.0 | 35.0 | 22.0 | 31 |

**Figure 4.** Effect of VE-822 on cell cycle distribution in pancreatic tumour cells. MiaPaCa-2 and PSN-1cells were exposed to 80 nM VE-822 for 1 h before irradiation (6 Gy) and left for the duration of the experiment. Gemcitabine (10 nM) was added 24 h pre-irradiation and was replaced with gemcitabine-free medium 1 h before irradiation. The cell cycle distribution was analysed by flow cytometry for propidium iodide at 12 h and 24 h post-irradiation. The G1 phase also contains the sub-G1 population. *Columns,* mean; *bars,* SD. (n=3). *, $P < 0.05$; **, $P < 0.01$; ***, $P < 0.001$ over DMSO-treated control.

## 5.1.5 VE-822 increases radiation and gemcitabine-induced apoptosis

We analysed apoptosis at 48 h post-XRT by combined Annexin V-FITC/PI staining to differentiate necrotic (late apoptotic) from early apoptotic cells (Fig. 5). VE-

822 alone had little effect on apoptosis in PSN-1 cells. XRT and gemcitabine increased apoptosis only slightly in PSN-1 cells consistent with apoptosis rarely being the cause of death in p53-mutant cells. Combinations of VE-822, XRT, and / or gemcitabine enhanced early and late apoptosis with the strongest effect in the triple combination group. Interestingly, in the VE-822 alone group, the percentage of early apoptosis was higher than in the combination groups (VE-822 plus gemcitabine and/or XRT) while late apoptosis was negligible.

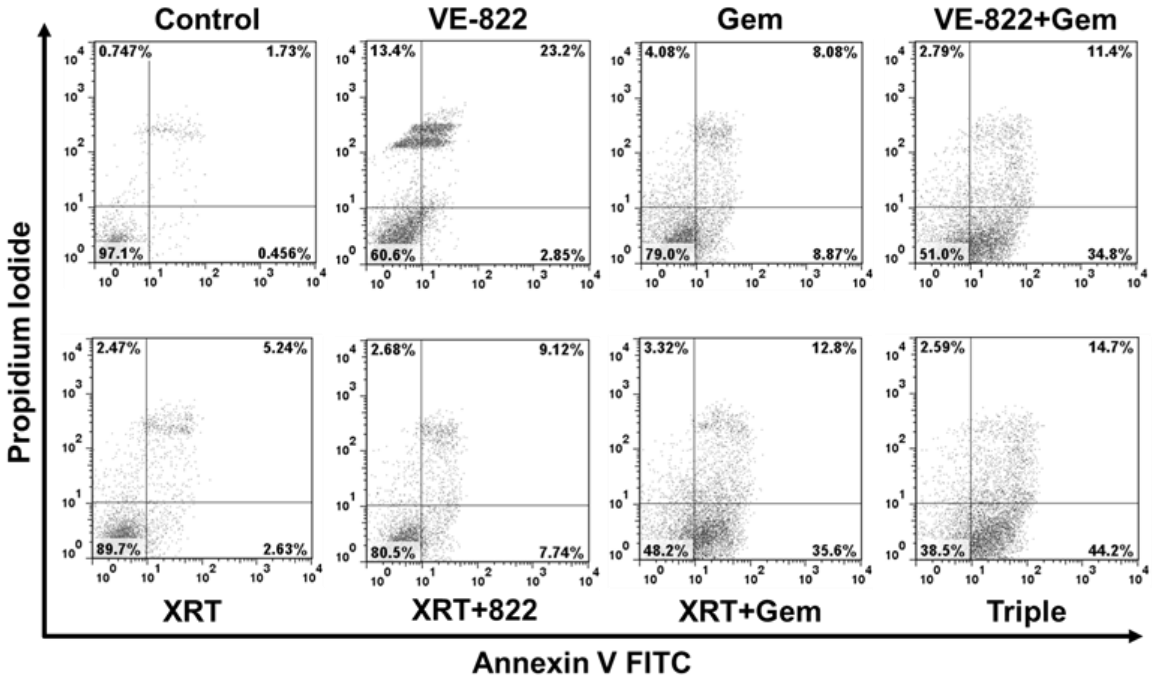



**Figure 5.** Effect of VE-822 on apoptosis of pancreatic tumour cells. PSN-1 cells were exposed to 80 nM VE-822 for 1 h before until 18 h post-irradiation (XRT; 6 Gy). Gemcitabine (10 nM) was added 24 h pre-XRT and was replaced with gemcitabine-free medium immediately before addition of VE-822. Cells were stained with Annexin V-FITC plus propidium iodide and samples were analysed by flow cytometry for PI (y-axis) and Annexin V (x-axis) at 48 h after XRT. Representative scattergrams are shown with percentages of cells undergoing apoptosis only (lower right quadrant) versus those undergoing late apoptosis and necrosis (upper right quadrant). Gem, gemcitabine; Triple, VE-822+Gemcitabine+XRT.

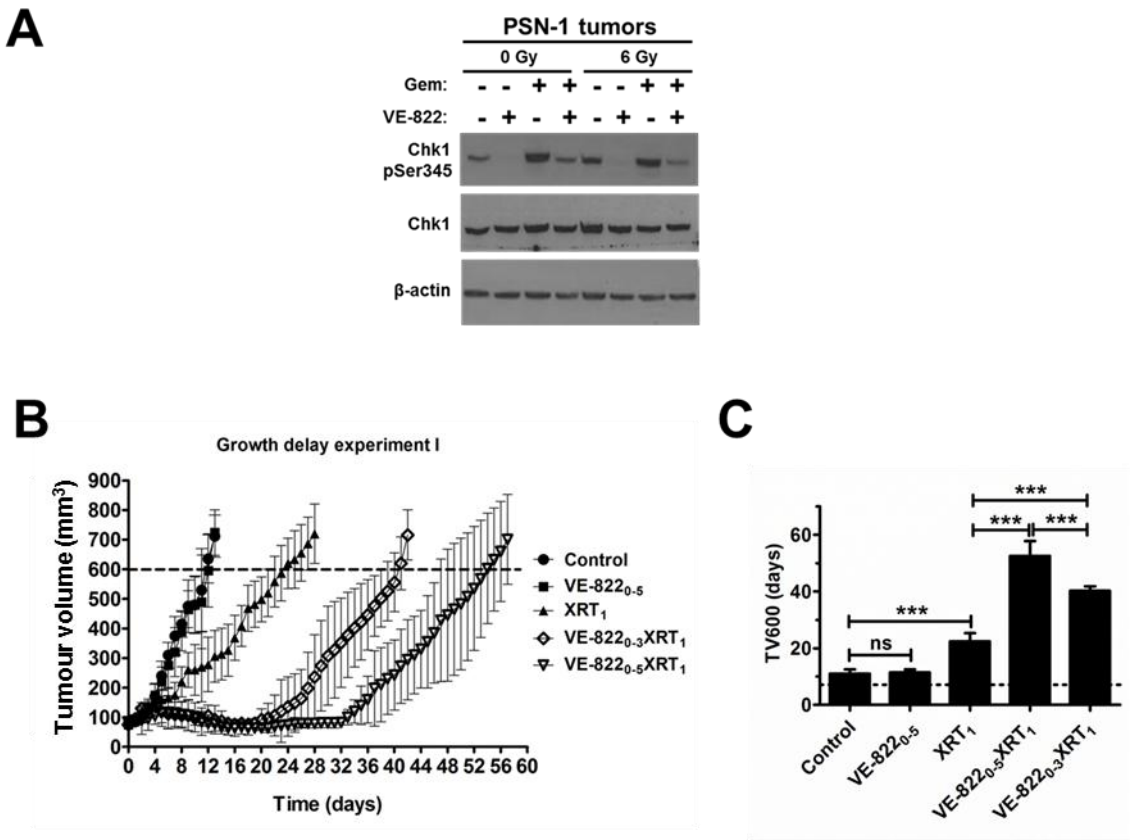
## 5.1.6 Efficacy of VE-822 with radiotherapy in pancreatic tumour xenografts

To verify that VE-822 inhibits ATR *in vivo*, mice bearing subcutaneous PSN-1 tumours were treated with VE-822 (60 mg/kg; day 0 and 1), gemcitabine (100 mg/kg; day 0) and/or XRT (6 Gy; day 1), as described in "Methods". Tumours were then harvested 2 h post-XRT (Fig. 6A). VE-822 inhibited S345 Chk1 phosphorylation in PSN-1 tumours treated with gemcitabine, XRT and gemcitabine+XRT, which is consistent to the *in vitro* observations.

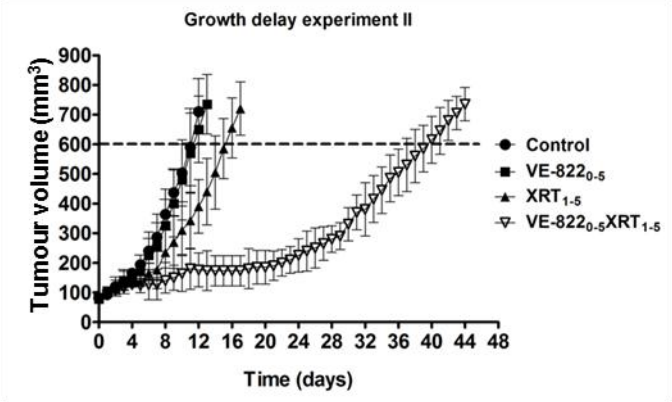
Since VE-822 has the potential to radiosensitise cancer cells, we asked whether mice with irradiated PSN-1 PDAC xenografts would show a better response to radiotherapy (**Growth delay experiment I**; Fig. 6B-C). Below, the subscripts indicate the days of treatment in each group. The time it took for tumours to grow to 600 $mm^3$ (TV600) was chosen as a reference volume in order to be able to compare the growth delay in the different groups. The TV600 in the $XRT_1$ group was significantly longer than vehicle or VE-$822_{0-5}$ ($p<0.001$). Combined with XRT, VE-822 was administered for either 6 days (VE-$822_{0-5}XRT_1$), or 4 days (VE-$822_{0-3}XRT_1$). The TV600 in both VE-$822_{0-3}XRT_1$ and VE-$822_{0-5}XRT_1$ TV600 were significantly longer than $XRT_1$ ($p<0.001$). Similarly, VE-$822_{0-5}XRT_1$ was significantly longer than VE-$822_{0-3}XRT_1$ ($p<0.001$). These data confirm the radiosensitising potential of VE-822 and indicated a better radiosensitisation with prolonged combination.

Clinically radiation is typically delivered in fractions around 2 Gy for PDAC. Therefore, five daily fractions of 2 Gy ($XRT_{1-5}$) were tested in combination with VE-822 in PSN-1 tumours (**Growth delay experiment II**; Fig. 6D-E). $XRT_{1-5}$ only significantly delayed tumour growth compared to control/VE-$822_{0-5}$ ($p<0.001$). Combined treatment (VE-$822_{0-5}XRT_{1-5}$) delayed regrowth significantly compared with $XRT_{1-5}$ ($p<0.001$).

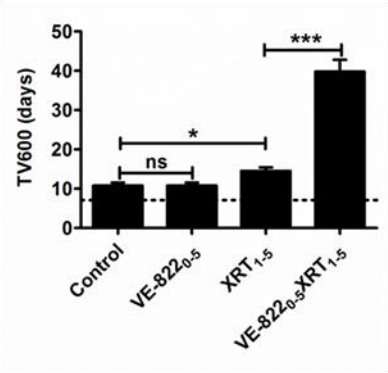
The efficacy of VE-822 was also tested in a different tumour cell line, MiaPaCa-2 (**Growth delay experiment III**; Fig. 6F-G). Administration of the ATR inhibitor alone (VE-$822_{0\text{-}5}$) resulted in no statistical change in tumour growth, as compared to the control (Fig. 6B). Six Gray to the tumour ($XRT_1$) resulted in a significant tumour growth delay compared to control and VE-$822_{0\text{-}5}$ ($p<0.01$). Strikingly, in the combined group (VE-$822_{0\text{-}5}XRT_1$; n=4), only 2/4 tumours regrew while one tumour was stable at 60 $mm^3$, and another showed complete response. The TV600 for the two tumours that presented regrowth was significantly longer than TV600 in $XRT_1$ ($p<0.001$). No weight loss was recorded in any of the three experiments (Fig. H-J). Taken together, VE-822 can safely sensitise tumours supra-additively to single XRT dose and most relevantly also to fractionated XRT.



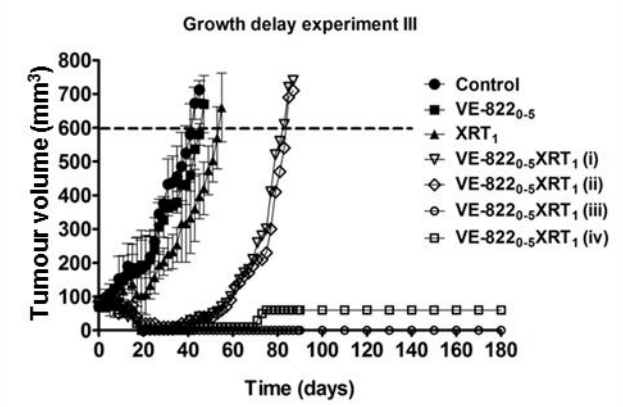
D


Growth delay experiment II
Tumour volume (mm3)
Time (days)
Control
VE-8220-5
XRT1-5
VE-8220-5XRT1-5

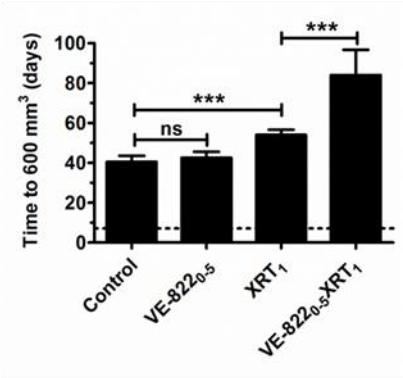
E


TV600 (days)
ns
*
***
Control
VE-8220-5
XRT1-5
VE-8220-5XRT1-5

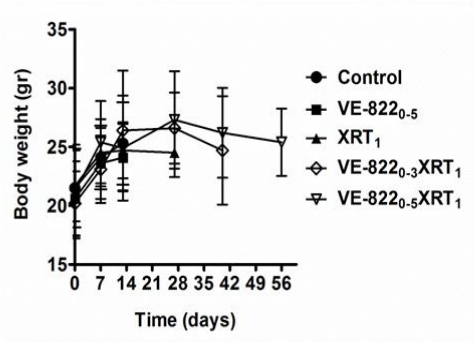
F


Growth delay experiment III
Tumour volume (mm3)
Time (days)
Control
VE-8220-5
XRT1
VE-8220-5XRT1 (i)
VE-8220-5XRT1 (ii)
VE-8220-5XRT1 (iii)
VE-8220-5XRT1 (iv)

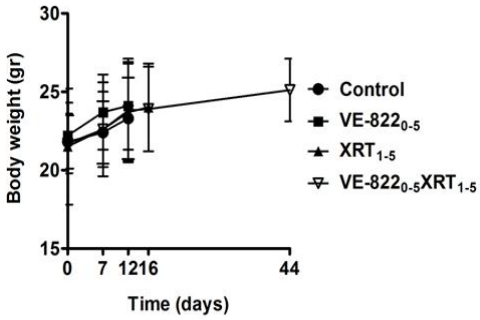
G


Time to 600 mm3 (days)
ns
***
***
Control
VE-8220-5
XRT1
VE-8220-5XRT1

H


Body weight (gr)
Time (days)
Control
VE-8220-5
XRT1
VE-8220-3XRT1
VE-8220-5XRT1

I


Body weight (gr)
Time (days)
Control
VE-8220-5
XRT1-5
VE-8220-5XRT1-5

J

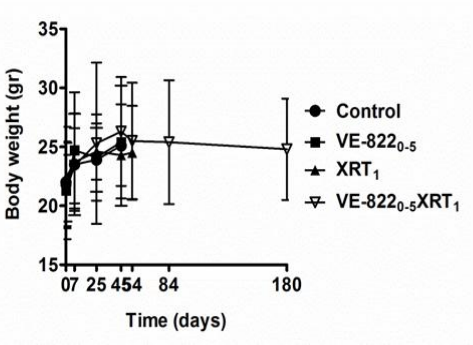
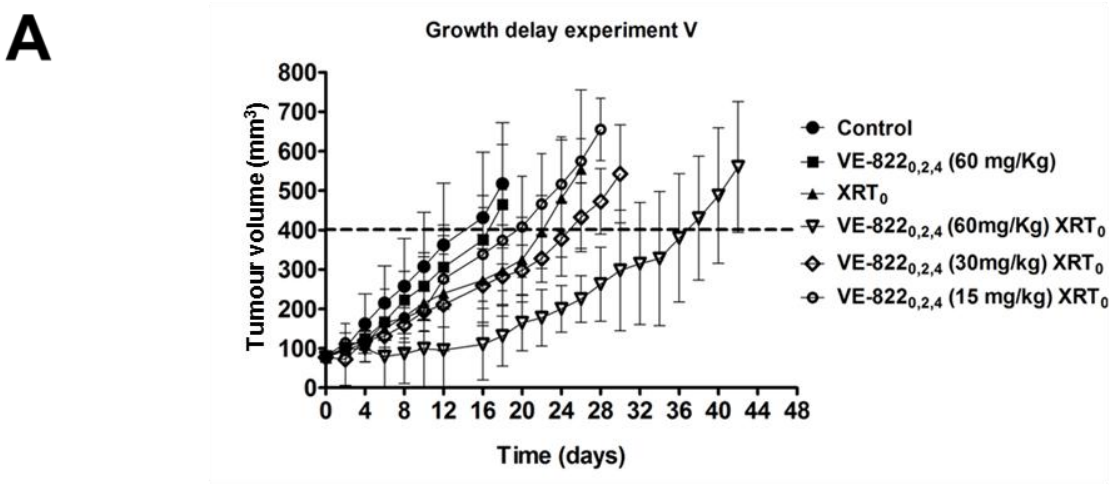

Body weight (gr)
Time (days)
Control
VE-8220-5
XRT1
VE-8220-5XRT1

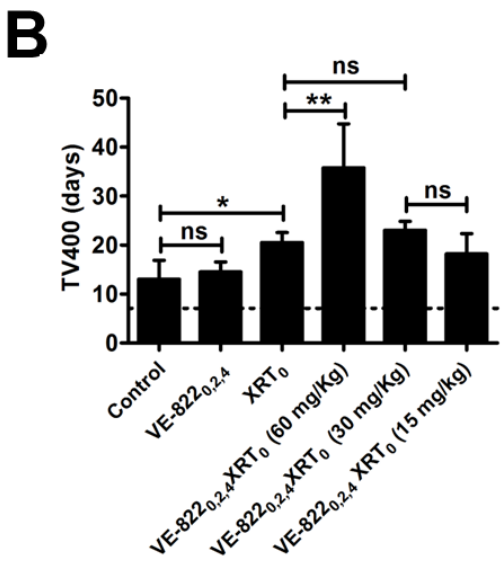
**Figure 6.** VE-822 enhances the therapeutic efficacy of radiation (XRT) in MiaPaCa-2 and PSN-1 xenograft models**.** ***A***, Mice bearing PSN-1 tumours (volume ~ 300 $mm^3$) were treated with VE-822 (60 mg/kg; day 0 and 1), and/or gemcitabine (100 mg/kg; day 0), and/or XRT (6 Gy; day 1). Tumours were harvested 2 h post-XRT. Chk1 phosphorylation (Ser345) was examined by immunoblot in tumour homogenates. Blots were also stained with β-actin and total Chk1, as indicated. ***B,*** When tumours reached a volume of ~80 $mm^3$, designated as day 0, mice were treated as indicated. Growth delay experiment I: mice bearing PSN-1 tumours (n=4-5) were treated daily with either vehicle (control), VE-822 (60 mg/kg) from day 0 to 5 ($VE\text{-}822_{0\text{-}5}$), 6 Gy at day 1 ($XRT_1$), or VE-822 plus 6 Gy by administering the drug for either 4 days ($VE\text{-}822_{0\text{-}3}XRT_1$) or 6 days ($VE\text{-}822_{0\text{-}5}XRT_1$). ***C,*** Time in days, from day 0, to reach a tumour volume of 600 $mm^3$ (TV600) were 11.0 (95% CI = 9.47 to 12.52; control), 11.4 (95% CI = 10.29 to 12.51; $VE\text{-}822_{0\text{-}5}$), 22.4 (95% CI = 19.54 to 25.26; $XRT_1$), 40.20 (95% CI = 38.58 to 41.82; $VE\text{-}822_{0\text{-}3}XRT_1$) and 52.50 (95% CI = 47.22 to 57.78; $VE\text{-}822_{0\text{-}5}XRT_1$). ***D,*** Growth delay experiment II: mice bearing PSN-1 tumours (n=4) were treated with vehicle (control), VE-822 from day 0 to 5 ($VE\text{-}822_{0\text{-}5}$), fractionated XRT using five daily doses of 2 Gy from day 1 to day 5 ($XRT_{1\text{-}5}$) or the combination of VE-822+fractionated XRT ($VE\text{-}822_{0\text{-}5}XRT_{1\text{-}5}$). ***E,*** Time from day 0 to TV600 was 10.7 (95% CI = 9.95 to 11.55; control) and 10.8 ± 0.5 (95% CI = 9.95 to 11.60; $VE\text{-}822_{0\text{-}5}$.), 21.5 (95% CI = 12.90 to 15.77; $XRT_{1\text{-}5}$) and 39.7 (95% CI = 33.93 to 45.40; $VE\text{-}822_{0\text{-}5}XRT_{1\text{-}5}$). ***F,*** Growth delay experiment III: mice bearing MiaPaCa-2 xenograft tumours (n=4) were treated as in (B) with the difference that only one VE-822+XRT combination was tested ($VE\text{-}822_{0\text{-}5}XRT_1$). The volumes of tumours in the combined VE-822+XRT group are plotted individually [$VE\text{-}822_{0\text{-}5}XRT_1$ (i, ii, iii and iv)]. ***G,*** Time in days, from day 0, to TV600 was 40.50 (95% CI = 37.45 to 43.55; control), 42.5 ± 1.9 (95% CI = 39.45 to 45.55; $VE\text{-}822_{0\text{-}5}$), 54.00 ± 1.6 (95% CI = 51.40 to 56.60; $XRT_1$) and 84.0 ± 1.4 days (95% CI = 71.29 to 96.71; $VE\text{-}822_{0\text{-}5}XRT_1$). Of note, the TV600 in the $VE\text{-}822_{0\text{-}5}XRT_1$ group was estimated based only on the two tumours with re-growth ($VE\text{-}822_{0\text{-}5}XRT_1$ (i) and (ii)). The growth curves were plotted until mice were sacrificed. ***H-J,*** Effect of VE-822 on weight of mice treated with single and fractionated radiation. The weight of the mice employed in growth delay experiment I ***(H)***, II ***(I)*** and III ***(J)*** was measured to assess treatment-related toxicity. In ***B, D*** and ***F***, points show the mean of tumour volume ($mm^3$) of each treatment group (n=4-5). In ***C, E*** and ***G***, c*olumns* show mean time to TV600 in days; In H-J, points show the mean values; *bars*, 95% CI. ns, not significant; *, $p<0.05$; ***, $p<0.001$.(Fig. 6A is courtesy of Dr Remko Prevo).

## 5.1.7 VE-822-mediated tumour radiosensitisation *in vivo* is dose-dependent

Intermittent VE-822 dosing (days 0, 2, 4) was tested for radiosensitisation and tolerance at three different doses (15, 30, 60 mg/kg). Intermittent dosing was also chosen to prepare triple combination with chemoradiotherapy (**Growth delay experiment IV**; Fig. 7A). Sixty mg/kg of VE-822 plus XRT was equally well tolerated as lower doses (Fig 7C) and prolonged radiation-induced growth delay, whereas lower doses were markedly

less effective (Fig. 7B). These results show that intermittent dosing of VE-822 is also radiosensitising but dose-dependent.



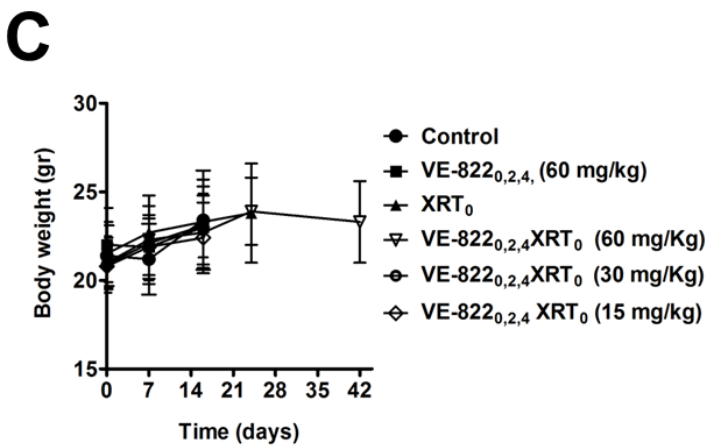



**Figure 7.** Effect of VE-822 dose reduction on radiosensitisation of PSN-1 tumour xenograft. ***A,*** Growth delay experiment IV. When tumours reached a volume of ~80 $mm^3$, mice were randomized into different groups and treated as indicated in the subscripts: control (vehicle), VE-822 (60 mg/kg at day 0, 2 and 5 by oral gavage), 6 Gy single radiation (XRT; day 0) or XRT combined with VE-822 using three different doses (60, 30 and 15 mg/kg, respectively). The different treatments are indicated in the subscripts. The growth curves were plotted until mice were sacrificed. Points, mean of tumour volume ($mm^3$) of each treatment group (n=4-5); bars, 95% CI**.** ***B,*** VE-822-mediated radiosensitisation in PSN-1 tumours is dose-dependent. The average time for tumour volumes to reach a volume of 400 $mm^3$ (TV400) was estimated in days. There was no significant difference in TV400 between the control (control (13; 95% CI = 9.10 to 16.90) and VE-$822_{0,2,4}$ group (14.5; 95% CI = 12.45 to 16.55) . XRT prolonged TV400 as compared to control (20.5; 95% CI = 18.45 to 22.55; $p<0.05$). TV400 was 35.75 (95% CI = 26.71 to 44.79) at thrice 60 mg/kg ($p<0.01$ vs $XRT_0$) compared with 23.15 (95% CI = 21.16 to 24.84) and 18.20 (95% CI = 14.04 to 22.36) at thrice 30 and 15 mg/kg, respectively. *Columns,* mean time to TV400; *bars*, 95% CI. ns, not significant; *, $p<0.05$; **, $p<0.01$.

## 5.1.8 VE-822 increases gemcitabine-mediated radiosensitisation in pancreatic tumour xenografts

Since gemcitabine-based neoadjuvant chemoradiation is frequently used in patients with borderline resectable PDAC [3, 4], the combination of VE-822 plus XRT (**Growth delay experiment V**; Fig. 8A-B) was tested. Gemcitabine (100 mg/kg) was given at day 0 ($Gem_0$), XRT on d1 ($XRT_1$) and VE-822 (60 mg/kg) on d1,3,5 (VE-$822_{1,3,5}$). Treatment with XRT led to a significant increase in TV400 ($p<0.05$) compared to control. $Gem_0$ at this dose did not alter tumour growth significantly. Adding gemcitabine to either VE-822 ($Gem_0$VE-$822_{1,3,5}$) did not significantly increase TV400 compared to gemcitabine alone ($p>0.05$) under the conditions of this experiment. Adding XRT to gemcitabine ($Gem_0XRT_1$) increased tumour growth delay compared to Gem0 ($p<0.05$). Similarly, the tumour growth delay in the VE-$822_{1,3,5}$XRT1 group was significantly longer compared to the XRT1 group ($p<0.05$). VE-822 added to the combination of gemcitabine+XRT ($Gem_0XRT_1$VE-$822_{1,3,5}$) substantially prolonged the tumour growth delay compared to the $Gem_0XRT_1$ group ($p<0.001$). In addition, no weight loss was observed throughout the

experiment (Fig. 8C). These results underscore the potential of VE-822 as a sensitiser to gemcitabine-based chemoradiation therapy for PDAC.

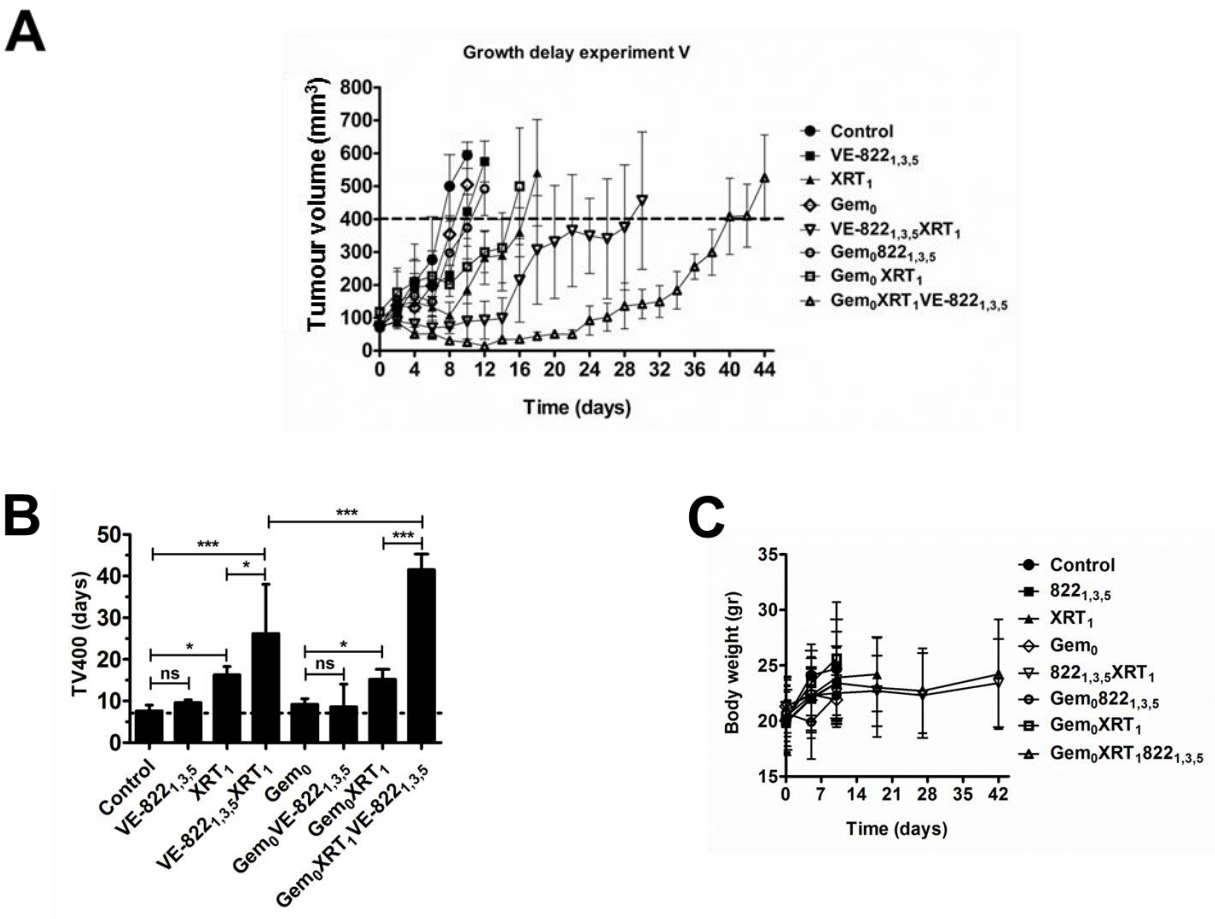
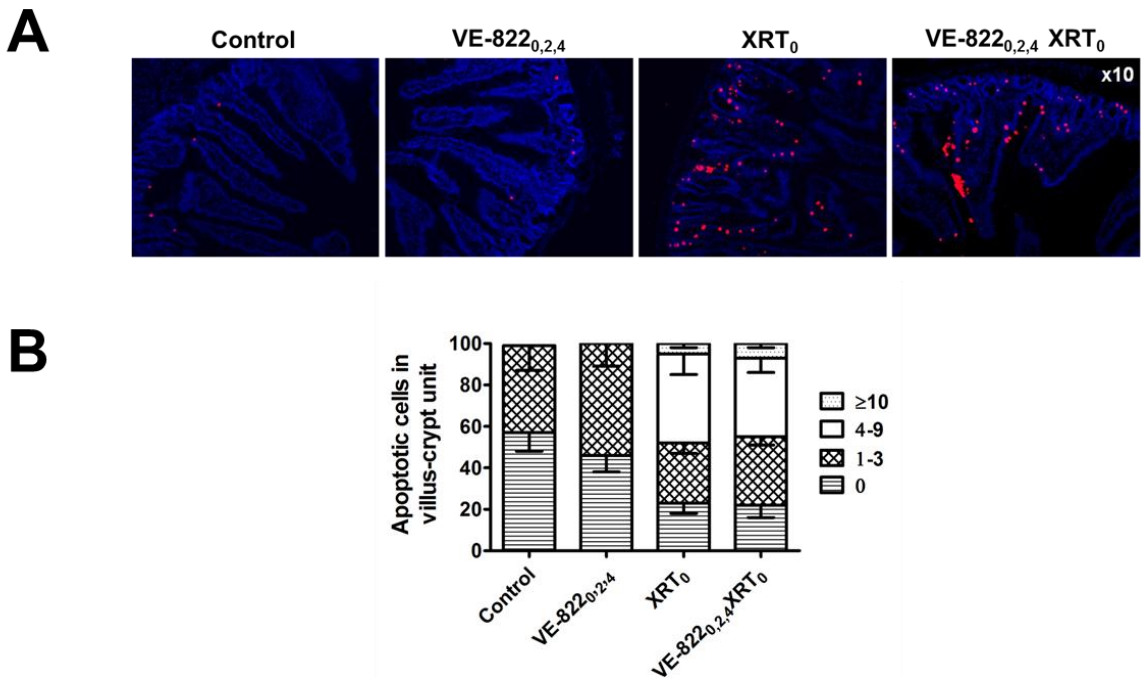



**Figure 8.** VE-822 enhances tumour response in combination with XRT and gemcitabine in in PSN-1 xenograft model. ***A,*** Growth delay experiment V: when tumours reached a volume of ~80 $mm^3$, treatment with VE-822 (60 mg/kg), XRT (6 Gy) and/or gemcitabine (100 mg/kg) was started. Mice were treated from day 0 as indicated. Mean of tumour volume ($mm^3$) of each treatment group (n=4-5); bars, 95% CI. ***B,*** the average time (days) for tumours to reach a volume of 400 $mm^3$ (TV400) from day 0 was: 7.6 (95% CI = 6.18 to 9.01; control), 9.6 (95% CI = 8.920 to 10.28; VE-$822_{1,3,5}$ ), 9.2 (95% CI= 7.840 to 10.56; $Gem_0$), 15.2 (95% CI = ; $Gem_0XRT_1$); 8.6 (95% CI = 3.14 to 14.05; $Gem_0$VE-$822_{1,3,5}$) [ns vs $XRT_1$ and $Gem_0$]; 26.2 (95% CI= 14.37 to 38.03; VE-$822_{1,3,5}XRT_1$), [$p<0.05$ vs $XRT_1$]; 41.5 (95% CI = 37.71 to 45.29; $Gem_0XRT_1$VE-$822_{1,3,5}$); [$p<0.001$ vs VE-$822_{1,3,5}XRT_1$]. *Columns*, mean time to TV600 in days; *bars*, 95% CI. ns, not significant; *, $p<0.05$; **, $p<0.01$; ***, $p<0.001$. ***C***, weight of mice throughout the experiment. Column/*points*, mean; *bars*, 95% CI. ns, not significant; *, $p<0.05$; **, $p<0.01$.

## 5.1.9 VE-822 does not increase tissue toxicity *in vivo*

Since the dose-limiting toxicity for XRT in PDAC is damage to the gastrointestinal tract, we assessed the effect of VE-822 on intestinal damage after abdominal XRT. Apoptosis of the intestine, loss of villus tip and villus length have been used as monitors of radiation damage to the intestine [32, 33]. VE-822 combined with abdominal XRT did not significantly increase the number of apoptotic jejunal cells compared to XRT alone (Fig. 9A-B), as shown by equal numbers of TUNEL-positive cells. Furthermore, VE-822 administered with XRT did not increase villus tip loss or villi shortening when compared with XRT alone (Fig. 9C-E). In keeping with these findings, equivalent body weight loss was observed in the combination and XRT-only groups (Fig. 9F). Thus, in the present toxicity model, no evidence for enhancement of early XRT-induced gastrointestinal damage by VE-822 was found.



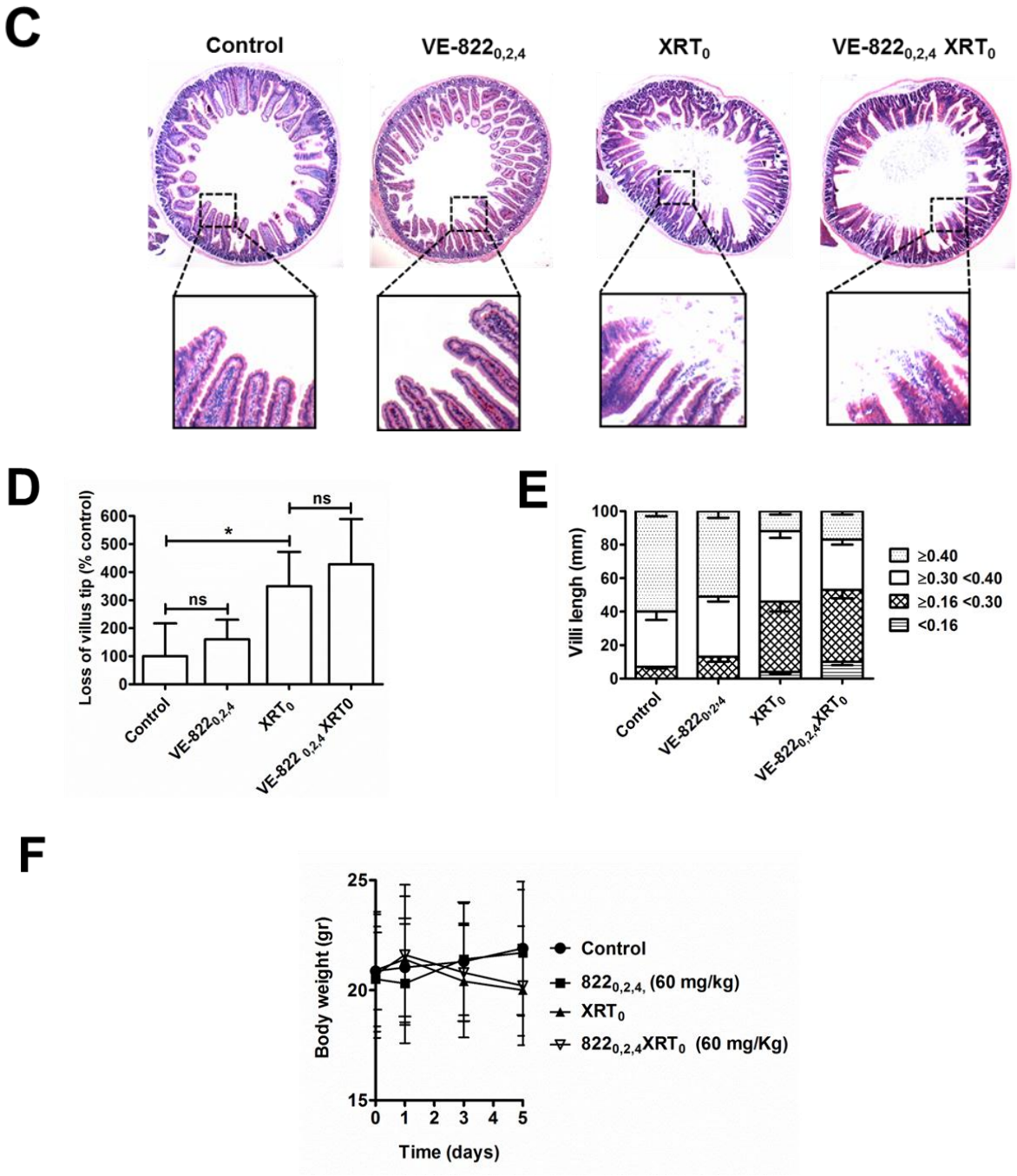
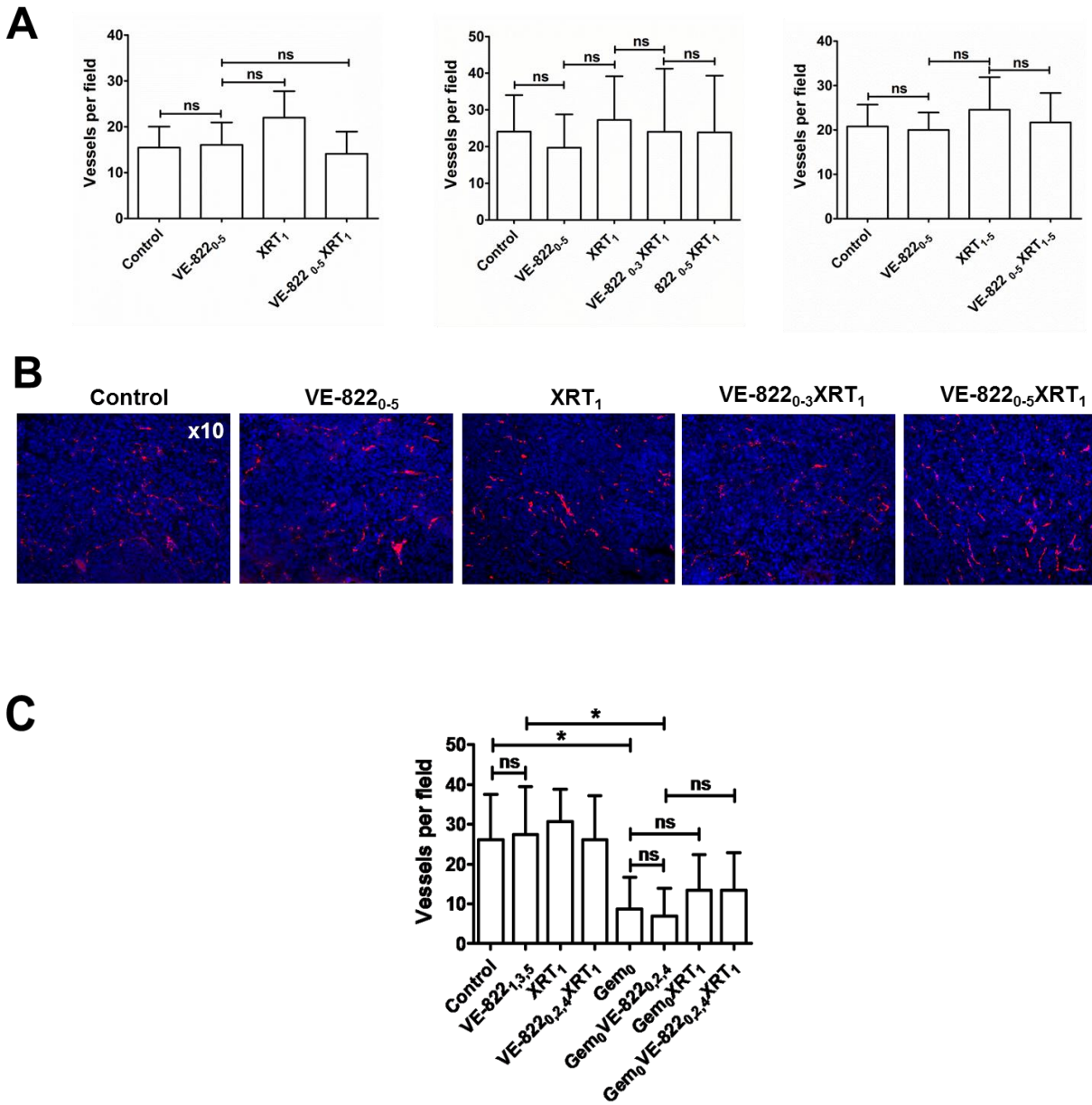



**Figure 9.** VE-822 does not increase normal intestinal cell radiosensitivity *in vivo*. ***A-B,*** Mice (n=3-4) were treated with VE-822 (60 mg/kg) at day 0, 2, and 4 and/or abdominal XRT (6 Gy; day 0), as indicated in the subscripts. VE-822 was started 2 h before XRT. At day 5 mice were killed, and pieces of proximal jejunum were removed and fixed in 3% formaline/PBS for histological examinations. Frequency histograms of apoptotic cells per villus-crypt unit is shown here. ***C-E,*** villus tip loss and villi length was counted and compared between the different groups. ns, not significant. Data shown (means ± 95% CI) are means from 6-8 sections each obtained from different mice. Approximately 100 crypt-villus units were scored per group. ***F,*** weight in mice treated as indicated. Column*/points,* mean; *bars*, 95% CI. ns, not significant; *, $p<0.05$.

## 5.1.10 The effect of VE-822 on tumour vessel density

The effect of VE-822 in tumour vessel density was assessed. CD31 immunostaining was used as a measure of angiogenesis (Fig. 11). In growth delay experiments I-III, VE-822 therapy, alone or with XRT, did not alter vessel density (Fig. 11A-B). In growth delay experiment V, a significantly reduced vessel density was observed after therapy with gemcitabine while addition of VE-822 and/or XRT to the latter did not alter vessel density significantly (Fig. 11C-D).



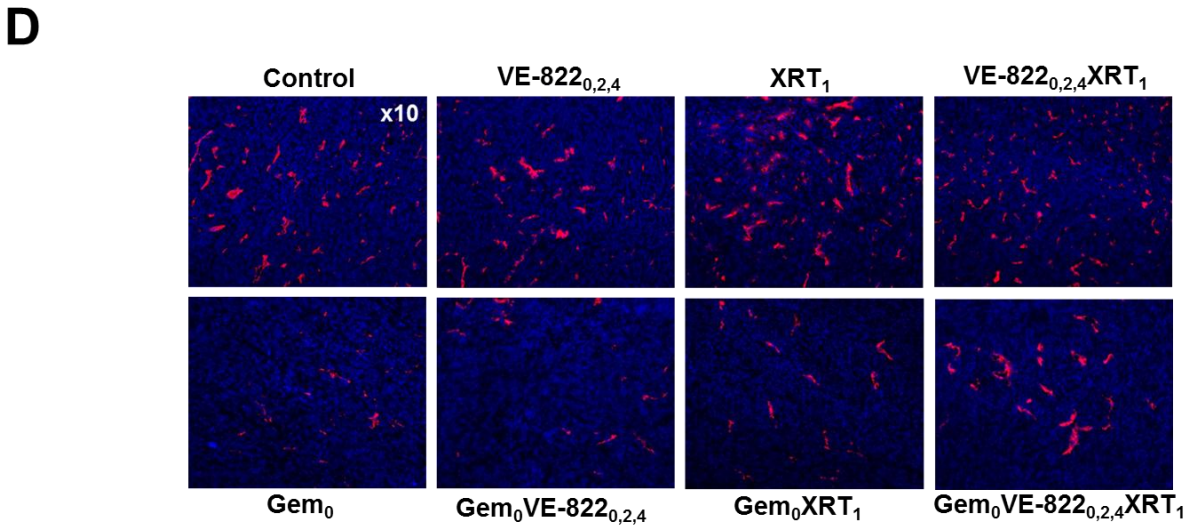
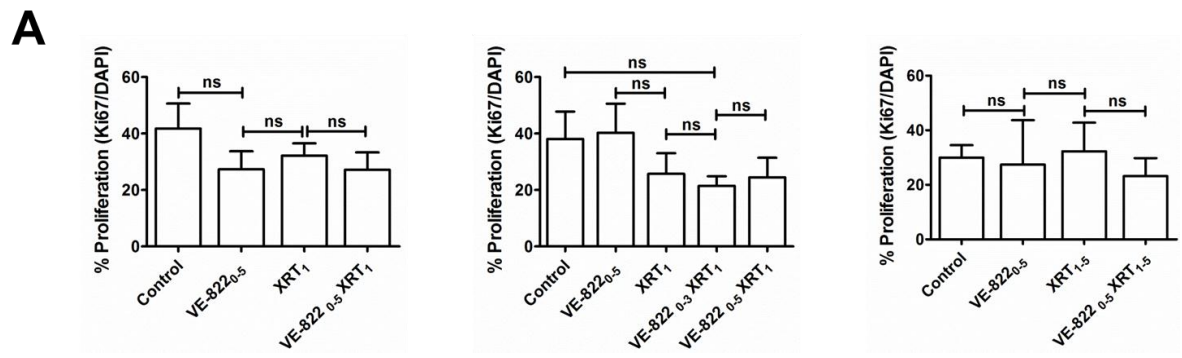



**Figure 11.** VE-822 treatment does not alter vessel density. At the end of the growth delay experiments I-III and V, mice were sacrificed, tumours were excised and immunfluorescent staining with anti-CD31 was performed. The different treatments are indicated in the subscripts. Vascular density in growth delay experiment I (*left panel*), II (*middle*), III (*right panel*) ***(A)*** and V ***(C)***, quantified as the number of blood vessels/field in 5 random viable fields per tumour (n=4-5). In ***(C)***, the mean vessel density was: 26.15 (95% CI = 14.75 to 37.55; control), 27.47 (95% CI = 15.41 to 39.52; VE-822$_{1,3,5}$ ; [ns vs control]), 8.7 (95% CI= 0.69 to 16.71; Gem$_0$; [$p<0.05$ vs control]), 13.44 (95% CI = 4.52 to 22.37; Gem$_0$XRT$_1$), 6.9 (95% CI = -0.058 to 13.86; Gem$_0$VE-822$_{1,3,5}$; [ns vs VE-822$_{1,3,5}$]), 26.2 (95% CI= 15.12 to 37.28; VE-822$_{1,3,5}$XRT$_1$) and 13.5 (95% CI = 4.12 to 22.88; Gem$_0$XRT$_1$VE-822$_{1,3,5}$; [ns vs Gem$_0$VE-822$_{1,3,5}$]). Representative images from experiment I ***(B)*** and V ***(D)*** are shown. CD31 (red), DAPI nuclei (blue). Magnification, x10. *Columns*, mean; *bars*, 95% CI. ns, not significant; *, $p<0.05$.

## 5.1.11 The effect of VE-822 on tumour proliferation

Even though a trend towards lower proliferation was observed in the combination groups in growth delay experiments I-III and V, there was no significant difference in the proportion of Ki67-positive cells (Fig. 12A-D).



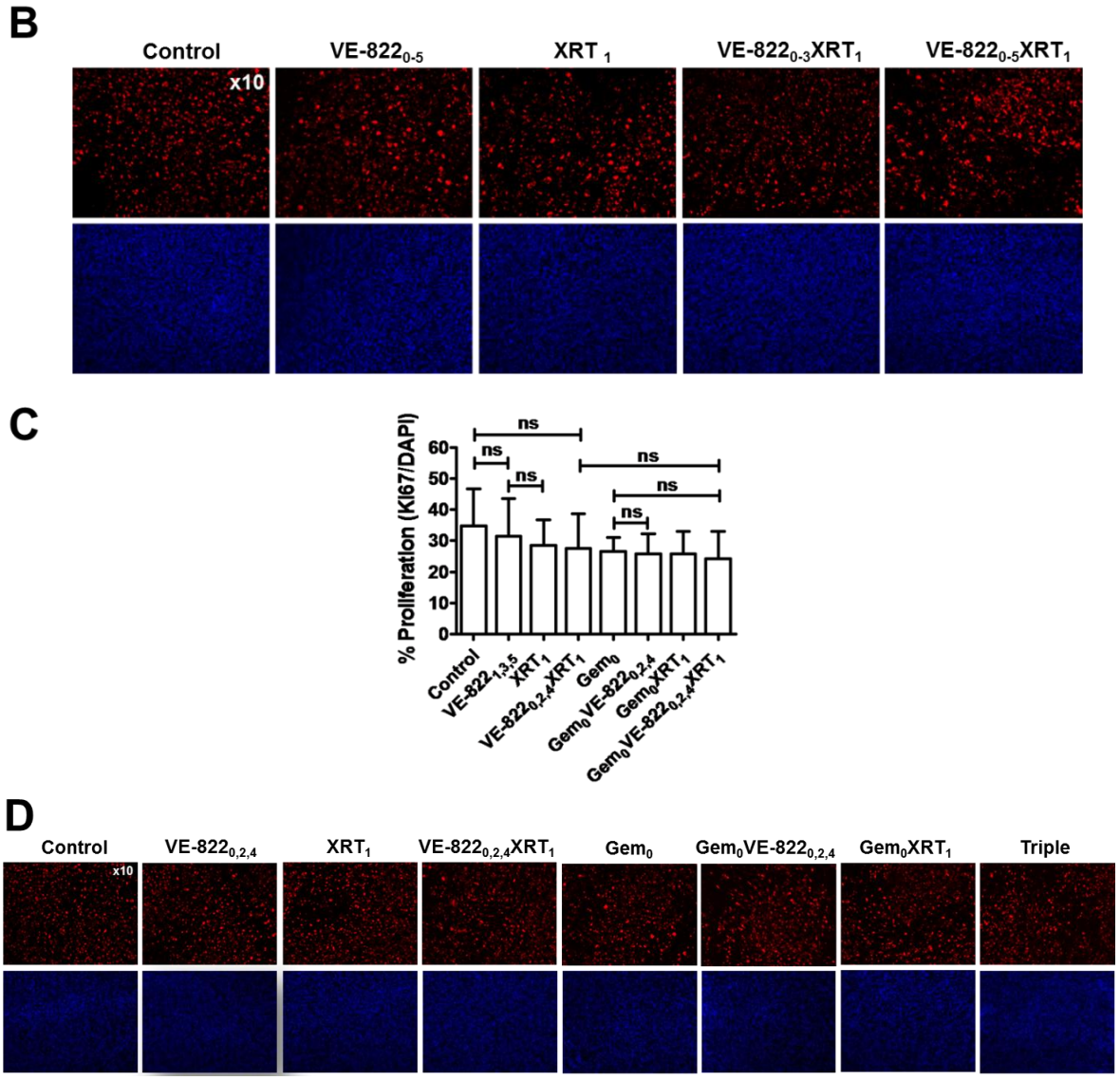



**Figure 12.** Proliferation in pancreatic tumour xenografts following VE-822 treatment. At the end of the growth delay experiments I-III and V, mice were sacrificed, tumours were excised and immunofluorescent staining with anti-Ki-67 was performed. The different treatments are indicated in the subscripts. ***A,*** proliferation in growth delay experiment I (*left panel*), II (*middle*), III (*right panel*) and IV ***(C),*** quantified as the proportion of Ki-67 positive area to DAPI in 5 random viable fields per tumour (n=4-5). Representative images from experiment II ***(B)*** and IV ***(D)*** are shown. Ki-67 (red), DAPI nuclei (blue). Magnification, x10. *Columns*, mean; *bars*, 95% CI. ns, not significant.

## 5.2 DISCUSSION

In the present study the potential of VE-822, a potent ATR inhibitor, to sensitise pancreatic tumour cells and xenografts to XRT and gemcitabine was studied. VE-822 resulted in profound sensitisation of pancreatic cancer cells to radiotherapy both *in vitro* and in xenografts, to the extent that the combination of VE-822 and XRT prevented MiaPaCa-2 tumour regrowth in some mice. VE-822 is a potent, close analogue of the previously reported selective ATR inhibitor, VE-821 [251, 318] with >100-fold cellular selectivity for ATR over ATM and DNA-PK (Table 1 and 2) and effective inhibition of ATR (ATR Ki 200 pM, where Ki is the binding affinity of the drug). VE-822 blocked XRT and gemcitabine-induced Chk1 Ser345 phosphorylation in pancreatic cancer cells and tumours, as well as in normal cell fibroblasts, confirming its ability to disrupt ATR signalling. Of most relevance to the clinical setting, VE-822 sensitised tumours to fractionated XRT. In addition to sensitising tumours to XRT, we found that VE-822 profoundly sensitised tumours to gemcitabine-based chemoradiation. Here, VE-822's demonstrated efficacy remained effective even with doses of gemcitabine that alone had no effect on tumour growth. In accordance with studies that showed that the ATR pathway has a net anti-apoptotic effect in the cellular response to replication inhibitors and XRT [319-321], addition of VE-822 to XRT and/or gemcitabine treatment resulted in increased early and late apoptosis in pancreatic cancer cell cultures.

HRR-deficient cells are more radiosensitive in comparison to HRR-proficient cells [322], whilst enhancing HRR by overexpression of Rad51, a major mediator of HRR, is associated with resistance to radiation [323]. In the present study, VE-822 decreased Rad51 foci in irradiated tumour cells showing that VE-822-mediated radiosensitivity was associated with inhibition of HRR. As expected, VE-822 caused increased persistence of residual γH2AX expression after XRT in pancreatic cancer cells *in vitro*. By promoting a

strong S-phase arrest, the addition of gemcitabine to XRT in current treatments for PDAC may further enhance dependence on ATR-mediated HRR for DSB repair and cancer cell survival. This model would be consistent with the dramatic anticancer effects we observed for the triple combination of VE-822, XRT and gemcitabine *in vivo*. Notably, VE-822 additionally led to abrogation of the XRT-induced G2 checkpoint *in vitro*, which could also contribute to the sensitisation of pancreatic tumour cells to radiotherapy. VE-822 did not affect vascular density in PDAC tumour xenografts in any of the experiments conducted. Interestingly, a decrease in vascular density in the gemcitabine-incorporating groups, which is in line to a previous report [324].

VE-822 did not sensitise MRC5 or HFL-1 normal human fibroblast cell lines, nor HDMECs, to XRT or gemcitabine, despite inhibiting XRT- or gemcitabine-induced Chk1 phosphorylation. This is consistent with the behaviour of the VE-821, the prototype inhibitor produced by Vertex Pharmaceuticals, *in vitro*, as lack of normal cell toxicity has been reported recently [251] and was well tolerated from animals. Furthermore, since damage to the small intestine is commonly dose-limiting during radiotherapy for PDAC [270, 325], we specifically quantified the effect of VE-822 on bowel radiosensitivity. Notably, addition of VE-822 to XRT did not further enhance the jejunal apoptosis or villus damage observed with XRT alone, in agreement with a recent study showing that ATR suppression minimally affects normal tissue homeostasis [249]. Collectively, these data indicate that ATR inhibition is not cytotoxic to normal tissue and, furthermore, we failed to find any evidence of enhanced gastrointestinal epithelial tract damage associated with XRT.

It has been reported that 50-70% of pancreatic cancers harbour mutations in ATM and p53-mediated signalling [216, 217]. Accumulating data based on ATR depletion or kinase-dead expression reveal that inhibiting ATR activity can strongly enhance DNA

damage-induced tumour cell killing and suggest that the frequent loss of ATM-p53 signalling may be an important determinant of this finding [43-45]. ATR depletion can strongly enhance DNA damage-induced tumour cell killing and suggest that the frequent loss of ATM-p53 signalling may be an important determinant of this finding [220, 242, 251, 326]. Moreover, prolonged disruption of the ATR pathway can exacerbate the levels of replication stress in oncogene-driven murine tumours to promote cell killing [247, 248, 313, 316]. These observations provide an explanation for the tumour selective effects of ATRi by VE-822.

Locally advanced PDAC remains an incurable disease and the overall survival rate is typically less than 1 year [216, 260]. Gemcitabine-based radiochemotherapy can increase local control rates and improve progression-free survival but is associated with normal tissue toxicity, which limits its therapeutic utility [270, 325]. The present data show that VE-822 can dramatically sensitise PDAC cancer cells to radiochemotherapy both *in vitro* and *in vivo*. Thus ATRi, and specifically VE-822, represents a very promising candidate for combination with radiation and gemcitabine.

## 5.3 CONCLUSION

The present work demonstrated that ATR inhibition by VE-822 profoundly radiosensitises pancreatic tumours cells and xenografts, and increases the growth delay induced by XRT combined with gemcitabine in pancreatic xenografts, without causing enhanced toxicity to normal cells and tissues. The tumour selectivity shown by VE-822 provides strong evidence that ATR inhibition represents a promising new approach to markedly increase the efficacy of the current therapies for pancreatic cancer.

# CHAPTER 6

## Summary and Future Perspectives

# 6.1 Introduction

Radiotherapy is an important and effective therapeutic modality and it is prescribed either alone or in combination with other treatments, mainly cytotoxic agents [11, 309]. Considerable technological improvements have been recorded during the last decades in the field of radiotherapy with the advent of more sophisticated software and imaging modalities that allow better tumour targeting, more precise dose delivery and minimisation of the dose delivered to the surrounding normal tissue. Despite this progress in the field of radiation oncology, some patients still fail to respond to radiotherapy or they develop a recurrence and some others present more severe side effects, warranting further improvement of radiotherapy efficacy [11, 309]. This can be done by exploiting either the potential of modern technological advances or the radiobiological aspect of malignant tumours. The second approach focuses on making tumour cells more sensitive to radiation without affecting the radiosensitivity of normal cells. One way to achieve this is by using novel agents designed to inhibit targets and signalling cascades important for the tumour cell's survival after radiation. For this thesis, two main pathways were targeted, the PI3K/mTOR pathway and the ATR/Chk1 pathway.

## 6.1.1 Therapeutic targeting of the PI3K/Akt/mTOR pathway

The PI3K/mTOR signalling cascade plays an important role in tumour cell proliferation, cell cycle, apoptosis and survival [86, 97]. This pathway is frequently deregulated in cancer due to tumour-associated mutations affecting its upstream regulators [86, 97]. Different components of the PI3K signalling pathway such as EGF/EGFR have been targeted for development of specific inhibitors with antitumour activity [96]. Gefitinib and erlotinib have been used in patients with NSCLC that harbour EGFR mutations but their efficacy is limited by the development of drug resistance [327]. Rapamycin analogues have exhibited promising activity in preclinical models [97].

However, blockade of mTOR signalling by rapalogs alone can lead to paradoxical phosphorylation of Akt and feedback activation of the PI3K and other prosurvival signalling pathways, such as MAPK, than can limit the therapeutic potential of single PI3K or mTOR inhibitors and compromise radiation efficacy [97, 283, 328]. This provided the rationale for designing dual PI3K/mTOR inhibitors. We and others have previously demonstrated the importance of oncogenic signalling in determining the response of tumours to radiotherapy, as blockade of oncogenic targets results in increased killing of tumour cells to radiation [6, 88, 91, 278].

In **Chapter 2**, the effect of dual PI3K/mTOR inhibition on the radiation response of tumour and endothelial cells was investigated using two novel dual pan-class I PI3K, mTORC1 and mTORC2 inhibitors, BEZ235 and BGT226, provided by Novartis Pharma.. Both agents reduced oncogenic signalling through the PI3K pathway and resulted in profound radiosensitisation of tumours cells with EGFR overexpression or Ras mutation, without significantly affecting their plating efficiency. BEZ235 was the most potent of the two and was hence investigated further. Importantly, BEZ235 also radiosensitised tumour cells under conditions of oxygen deprivation. Furthermore, BEZ235 increased the persistence of DNA damage and G2 cell cycle phase delay in irradiated tumours cells. In endothelial cells, BEZ235 blocked VEGF- and IR-induced Akt phosphorylation in enhanced endothelial cell killing after irradiation. The impact of BEZ235 on apoptosis of tumours and endothelial cells was variable, showing only a modest increase in apoptosis in one of the cells lines tested.

The results of this study provided useful insight on how these drugs possibly sensitise tumour cells. Based on these results of the *in vitro* study, which showed that only about 10% of the cells are apoptotic at 48h after radiation, it appears that apoptosis plays a minor role in the therapeutic outcome upon treatment of tumour cells with radiation, at

least in the cell lines examined. In contrast, the G1-induced cell cycle arrest that BEZ235 alone induces could have made tumour cells more vulnerable to radiation since the absence of checkpoints in tumour cells can affect the redistribution of cells at time-points after various cytotoxic treatments. Similarly, the profound G2/M cell cycle phase arrest observed in the BEZ235 plus radiation group probably contributed majorly to the decreased clonogenicity post-irradiation. Interestingly, Kastan and colleagues have previously shown that radiosensitivity does not result from S-phase checkpoint defects or [192] or abrogation of the irradiation-induced G1 checkpoint [329]. The increased accumulation of cells in the G2/M phase, as seen in the BEZ235 plus irradiation group, could have contributed to decreased clonogenicity by not allowing cells to proliferate [330], impairing in this way their ability to form colonies.

Similarly, the enhanced persistence of γH2AX foci observed when BEZ235 was added to radiation could have affected to the outcome after radiation but whether γH2AX is a quantifiable predictive marker of radiation survival has been controversially discussed. Olive and colleagues investigated the correlation between clonogenic survival and γH2AX expression in tumour cells derived from monolayers or xenografts, at 24 h post-irradiation [331]. The fraction of γH2AX remaining 24 h post-irradiation relative to peak levels 1 h after exposure was correlated with radiosensitivity in 18 human tumour cell lines. The fraction of tumour cells with <3 γH2AX foci was predictive of clonogenic surviving fraction for both monolayer cells and cells from xenograft tumours of irradiated mice [331]. Similar results were reported from Menegakis *et al*. in human squamous cell carcinoma cell lines [332]. Mahrhofer *et al.* studied the levels and decay kinetics of γH2AX in tumour and primary skin fibroblasts lines with a diverse range of radiosensitivity [333]. In contrast to other groups, it was not possible to predict clonogenic cell survival for the cell lines studied from the radiation-induced γH2AX intensity or decay

kinetics. Single agent toxicity could not have contributed majorly to the outcome as the decrease in plating efficiency observed in the tumour cells exposed to BEZ235 for short time (18 h) was not substantial, compared to the DMSO-treated group.

Attention should be also paid to the specificity of the compounds that were tested in the *in vitro* study. BEZ235 and BGT226 have been designed from Novartis Pharmaceutical to specifically block PI3K/Akt and mTOR. In a recent study, though, Toledo *et al.* employed a cell-based screening strategy to identify novel compounds with ATR inhibitory activity in the nanomolar range [313]. Surprisingly, one of the compounds found to possess ATR-inhibiting activity was BEZ235. Apart from ATR, BEZ235 was also very potent against ATM and the catalytic subunit of DNA-PK. A more recent study confirmed these findings [334]. It is known that inhibition of ATR, ATM and DNA-PK can sensitise cells to radiation [189, 191, 335]. Hence, inhibition of these targets could have contributed to the radiosensitising effect of BEZ235 observed both *in vitro* and *in vivo*. In regards to the latter, a speculation can be made, based on the effect observed in the VE-822 plus radiation group. It is highly likely that the improvement of the TME parameters observed after prolonged treatment of tumour xenografts with BEZ235, both before and after radiotherapy ($BEZ235_{0\text{-}58}XRT_7$ group), must have enhanced the cytotoxic effect of radiation *in vivo*, as improvement in tumour oxygenation is known to increase radiosensitivity [43]. However, it can be speculated that the tumour growth delay effect could be, in part, due to the ATR inhibitory effect of BEZ235 reported by Capetillo and colleagues [219]. This is because when the selective ATR inhibitor VE-822 was given for in total six days ($VE\text{-}822_{0\text{-}5}XRT_1$ group) in combination with radiation, tumour growth delay was significantly longer than when administered for four days ($VE\text{-}822_{0\text{-}3}XRT_1$ group) in PDAC xenografts. Therefore, the continued administration of BEZ235 for long time post-irradiation (up to day 58 post-irradiation, when tumour xenograft were

harvested) could have played a role in the outcome observed in a manner analogous to the VE-822 agent. Ideally, in the tumour growth delay study conducted using BEZ235 plus radiation, an additional treatment group would have been randomized, whereby BEZ235 would have been given from day 0 up to day 7. Such a group would have enabled to better differentiate the contribution of the improvement in TME effect vs the inhibition of DNA damage repair effect in the radiosensitisation of tumour xenografts. However, at the time when the tumour growth delay assay was performed, the DNA-PK-/ATM-/ATR-inhibitory potential of BEZ235 was unknown. Cross-inhibition of ATM and DNA-PK by an inhibitor designed to block the PI3K/mTOR pathway might not be very surprising because these kinases have homologous catalytic domains [336].

A relatively recent concept in cancer biology and radiobiology is that of stem cells. Based on that theory, small fractions of tumour cells are self-renewing cancer stem cells that are radioresistant and can be responsible for tumour relapse after the bulk of non-stem cancer cells have been eradicated by radiotherapy [337]. The tumour perivascular niche has described as the home of cancer stem cells and it has been shown that tumour endothelial cells could supply growth factors to maintain the stemness of these cells [338, 339]. The role of PI3K/mTOR pathway in the survival of cancer stem cells and its relevance to radiation outcome remain largely unexplored. In a recent study using a medulloblastoma model, Hambardzumyan *et al.* demonstrated that the nestin-expressing perivascular stem cells survive radiation, activate the PI3K/Akt pathway, undergo p53-dependent cell cycle arrest, and re-enter the cell cycle after irradiation [340]. Inhibition of PI3K/Akt signalling sensitised stem cells in the perivascular region to radiation-induced apoptosis and improved the outcome after radiotherapy. This study suggests that cancer stem cells rely on PI3K signalling for their survival and that inhibition of this pathway

could hence lead to tumour eradication. However, more studies are needed to better elucidate the role of this pathway in cancer stem cell-mediated response to radiotherapy.

The PI3K/Akt/mTOR pathway regulates angiogenesis both in normal tissues and in cancers [106, 115]. In **Chapter 4**, we demonstrated that single PI3K and dual PI3K/mTOR blockade by BKM120 and BEZ235, respectively, significantly increased tumour oxygenation and perfusion in two tumour xenograft models. These occurred in a dose-dependent manner and were associated with changes in tumours blood vessel morphology that are consistent with the concept of vascular normalisation. Interestingly, tumour growth itself was unaffected and a moderate decrease in the tumour level of VEGF-A was detected. We further explored these changes in TME by testing different radiation-drug scheduling combinations to better elucidate the contribution of the different effects (intrinsic vs extrinsic) on tumour radiosensitisation. Administration of BEZ235 shortly before irradiation radiosensitised tumours without affecting tumour oxygenation. However, the radiosensitisation was significantly greater when radiation was applied after vascular normalisation was established. Only a marginal growth delay was observed when BEZ235 was initiated three days post-irradiation. Importantly, the improvements in TME were prolonged, even though alterations in hypoxia, perfusion and vascular morphology were observed towards the end of the study, without reaching the baseline levels (day 0). Notably, the effect of BKM120 and BEZ235 on TME appears to be dose-dependent, as a strong anti-vascular effect with extensive vessel leakage was observed when the drugs were administered at very high doses. The data provided evidence on the potential of oncogenic signalling inhibition to modify the TME and improve radiation response.

Although our results are based on studies using xenograft tumour models, we believe that our findings have several important clinical implications. First, the sensitisation to radiation that is conferred by PI3K/mTOR inhibitors after changing the

TME appears to be larger compared to the sensitisation after blockade of the oncogenic signalling itself i.e. intrinsic radiosensitivity. In addition, it seems that changes in tumour hypoxia and vasculature occur within a week of treatment with PI3K/mTOR inhibitors. Therefore, if patients are to benefit from this additional sensitisation effect, then our studies suggest that the signalling inhibitors should be administered at least 7 days before initiation of radiotherapy. Notably, in some studies testing inhibitors of oncogenic signalling, decreased hypoxia and normalisation of tumour vasculature occurred without a significant tumour growth delay, implying that modification of TME might play a principal role in determining the therapeutic outcome for such drugs [150, 173]. Thus, the treatment should be guided by imaging methods relevant to the changes in TME such as FMISO-PET (tumour hypoxia) and DCE-MRI and Angio-CT (tumour blood flow) to test the preclinical hypothesis.

Notably, the Gray Institute for Radiation Oncology and Biology, Oxford University (principal investigator: Geoffrey S. Higgins; co-investigator W. Gillies McKenna) has recently received approval to conduct a phase I trial to test BKM120 plus radiotherapy in the clinical treatment of patients with advanced, inoperable NSCLC. The trial will be funded by the New Agents Committee (NAC) of Cancer Research-UK and it will be supported by Novartis Pharmaceuticals. In this trial, together with the safety of the combination regimen, different parameters of the TME such as tumour hypoxia using FMISO-PET will be investigated.

Second, special attention should be paid in designing a possible future clinical trial based on the data of vascular normalisation after treatment with PI3K/mTOR inhibitors. We observed that this effect is strictly dose-dependent. Furthermore, preclinical studies have demonstrated that administration of PI3K and mTOR inhibitors at high dose results in a strong antivascular effect [341, 342]. On the other hand, phase I clinical trials aim to

test the MTD, even though new studies use the inhibition of downstream drug targets as surrogate markers to examine the efficacy of novel agents in order to confirm that the drug targets are blocked at the concentrations tested. Thus, the administration of oncogenic signalling inhibitors at high doses can, in theory, be counterproductive as vessel regression can result in hypoxia and reduced radiation efficacy. This could compromise the outcome of a future clinical study using chemoradiation in combination with dual PI3K/mTOR inhibitors. Hence, this information should be taken into account.

Third, it appears that, oncogenic signalling inhibitors might have potential advantages over the classical antiangiogenic agents. Our findings and previous data indicate that these agents can, dose-dependently, lead to a more prolonged vascular normalisation than that achieved after treatment with anti-VEGF agents, which would theoretically result in higher radiation and/or chemotherapy efficacy [150, 173]. The latter could be attributed to the partial suppression of excessive VEGF production, as mediated by the oncogenes, rather than complete VEGF blockade from anti-VEGF therapy, which eventually leads to extensive regression of tumour vasculature [23].

Fourth, especially in regards to radiation, this concept was tested using a relatively small total dose of radiation (6 Gy) and it remains to be seen whether this strategy will be applicable in the clinical setting, where multiple fractions (in many cases at least 28 fractions of 1.8-2 Gy) are applied, or even in hypofractionated regimens. The dose-dependent improvement of blood flow observed in tumours treated with PI3K/mTOR inhibitors can play important role in the radiotherapy outcome. However, the effects of radiation on blood vessels can, theoretically, pose a significant challenge in achieving a prolonged vascular normalisation after treatment with PI3K/mTOR inhibitors.

To understand the complexity and the impact that a possible combination of radiotherapy plus PI3K/mTOR inhibitors can have in vascular functionality, a detailed

knowledge of the way radiation affects blood vessels is needed. Radiation of endothelial cells *in vitro* has a direct antivascular effect, resulting in decreased cell survival, proliferation, tube formation and migration, in a dose-dependent manner [57-59]. BEZ235-mediated inhibition of DNA-PK but also ATM [313] would be expected to increase radiation-induced killing of normal cells [19], as observed in endothelial cells in our study. Radiation, dose-dependently causes a variety of vascular lesions [343, 344] that can affect tumour growth but also increase side effects [2]. Short-term after treatment, it most often affects microvessels (capillaries, sinusoids) producing capillary rupture. Long-term after treatment, medium-size vessels show neointimal proliferation, fibrinoid necrosis, thrombosis while damage in large vessels is less common [343, 344]. The importance of tumour blood perfusion in the response of tumours to radiotherapy was first reported in 1936 by Mottram [22], who observed that the well-perfused tumour areas were more vulnerable to radiation than poorly-perfused regions. Following that, studies showed that oxygen supply greatly affects tumour cell radiosensitivity and prompted investigators to study the impact of radiation on tumour vasculature using different tumour models and techniques [23]. These studies showed that fractionated radiotherapy induces an increase in blood perfusion early post-irrradiation that returns to the pre-irradiation levels or even declines to levels lower than before treatment [24-27].

Ng *et al*. examined vascular changes in human NSCLC after irradiation using 4.5 Gy fractions to a total dose of 9, 18 and 27 Gy. Similarly, Fokas *et al.* have shown that tumour xenograft irradiation can improve vessel functionality early post-irradiation, resulting in decreased hypoxia [345]. Blood vessels in the peripheral rim presented increased blood flow while only a small improvement in functional vascularity was observed in the tumour centre [28]. Radiotherapy using high single doses such as 10 Gy or higher can cause vascular damage and alter oxygenation levels in both human tumour

xenografts and animal tumours [29, 30] and animal tumours [31-34]. Irradiation of Walker 256 carcinoma of rats with a single dose of 30 Gy resulted in a series of changes [35]. The tumour weight or size increased for 7 days post-irradiation and then decreased until 15 days after irradiation. The vascular volume was decreased from day 1 up to 12 days post-irradiation and then began to recover. Vascular permeability increased early post-irradiation but declined until 12 days after and thereafter began to recover. Interestingly, tumour vasculature began to recover 2-3 days prior to recovery of tumour size, indicating a correlation between tumour cell proliferation and vasculature recovery. As expected, parts of vascular networks that provide blood supply to tumour periphery are normal tissue blood vessels and these might be more resistant to radiation as compared to the newly formed tumour blood vessels in the tumour core [346]. Kio *et al*. reported that high radiation doses results in vessel regression and found that vascular regrowth after irradiation occurs due to vasculogenesis [30]. The rapid decrease in blood flow after high radiation doses could be due to death of endothelial cells undergo ceramide-mediated apoptosis soon after irradiation of the tumours with doses higher than 8–10 Gy [61]. The tumour shrinkage observed after such radiation doses could also result in vessel disorganisation [347].

Denekamp demonstrated that one endothelial cell is responsible for blood supply of a segment of a tumour cord containing as many as 2000 tumour cells. Because the blood vessels are serial tissues, injury even at a single focal point of vessels could impair or even completely stop blood flow resulting in inadequate blood supply of tumour cells and even death [348] and also lead increase toxicity of normal tissues [2]. However, this issue still remains controversial [61, 63, 64]. Similarly, in tissue samples of patients previously exposed to chemotherapy, similar changes in blood vessel morphology has been described but they are more relevant to patients treated with multi-drug regimens, such as leukemia

and lymphoma [349, 350]. Unfortunately, the precise time point that these morphological vessel changes occur has not been well characterised. These effects of radiation on blood vessels can, theoretically, pose an additional challenge in achieving a prolonged vascular normalisation after treatment with PI3K/mTOR inhibitors. Thus, careful consideration should be paid in regards to the possible impact of radiotherapy and chemotherapy on vascular morphology before conducting a clinical study that exploits tumour vasculature changes with oncogenic signalling inhibitors. Nevertheless, the findings of our studies remain promising. Altogether, the pharmacological inhibition of the PI3K/mTOR pathway has shed light on its beneficial role in TME and radiotherapy.

Last but not least, the potential use of biomarkers in studies using PI3K and PI3K/mTOR inhibitors needs to be considered carefully. In oncology, biomarkers are measurable characteristics of pathological states and are increasingly used in the field of new drug development to determine the optimal biological use, distinguish responders from non-responders, confirm blockade of the drug target, predict drug sensitivity and optimise patient selection. Some examples include human epidermal growth factor receptor 2 (HER-2) overexpression in patients with breast cancer to predict response to trastuzumab [351] and Kras mutation evaluation in patients with CRC to predict resistance to anti-EGFR agents [352]. The use of biomarkers reflecting PI3K and mTOR pathway activity is currently under investigation. In a phase I study of the mTOR inhibitor RAD001 (Everolimus) inhibition of mTOR in tumour and skin, as reflected by pS6 and peIF-4G levels, presented a strong correlation, indicating that skin might serve as a useful surrogate tissue [353]. In a different clinical trial using neoadjuvant rapamycin in patients with PTEN-negative recurrent glioblastomas the level of mTOR inhibition was associated with reduced proliferation while Akt activation, secondary to reduced feedback inhibition, was correlated with a shorter time to progression [354].

It is known that PIK3CA mutations can affect response to PI3K inhibitors [86]. Examination of CRC samples showed that PIK3CA mutations and PTEN loss independently predict for resistance to the EGFR targeting agents cetuximab and panitumumab [355, 356]. Notably, this was also observed in Kras wild-type tumours and thus additional assessment of PI3K activity might be necessary before administering EGFR targeting agents. A large-scale RNA interference screen reported that PTEN and the combined analysis with PIK3CA mutation status can be used as an independent prognostic factor in breast cancer patients receiving trastuzumab [357]. O'Brienn *et al.* showed that breast cancer models harbouring mutations in PIK3CA, amplification of human EGFR 2, or dual alterations in two pathway components were extremely sensitive to the antitumour effects of the PI3K inhibitor GDC-0941 [358]. In a phase I, dose-escalation study of BKM120 in patients with advanced solid tumours, BKM120 demonstrated dose-dependent pharmacodynamic effects on [(18)F]FDG-PET, fasting C-peptide, fasting blood glucose, and phosphorylated S6 in skin biopsies [359]. This study demonstrated feasibility and proof-of-concept of class I PI3K inhibition in patients with advanced cancers and provided clear evidence of target inhibition. In a similar phase I study of MK-2206, an allosteric pan-Akt inhibitor, was tested in n=33 patients with advanced cancers. MK-2206 was well tolerated while phosphorylated Akt declined in all tumour biopsies assessed and was suppressed in hair follicles at 6 hours, day 7 and day 15, providing evidence of Akt blockade [360]. Although no clinical data have been reported on BEZ235 to date, it is known that many ongoing trials using this drug incorporate phosphorylation of Akt as a potential biomarker (clinicaltrials.gov). Hair follicles appear to be a useful surrogate tissue not only due to the simplicity of obtaining sample material but also due to the high basal PI3K/mTOR pathway activity [96]. Translational research aimed at validating potential biomarkers in clinical trials testing PI3K and PI3K/mTOR inhibitors is ongoing. Many of

the current trials also aim to conduct analyses of the mutational status of PI3K and PTEN. The implementation such evaluations prospectively in the future may achieve enriched patient populations and greater chance for success with PI3K pathway inhibitors.

## 6.1.2 Therapeutic targeting of the ATR/Chk1 pathway

An important determinant of the response of tumour cell to radiation is its ability to repair DNA damage [189]. The most important pathways of DDR include those that mediate repair of base damages, SSBs and DSBs. These include key biological processes such as the two pathways involved in repairing DSBs i.e. HRR and non-homologous end-joining (NHEJ), together with base excision repair (BER) and the single-strand break repair pathway (SSBR). Less often, radiotherapy leads to the formation of DNA–DNA and DNA–protein crosslinks, as it happens in conditions of oxygen deprivation. A great amount of preclinical studies with novel radiosensitisers and, more important, clinical evidence from cytotoxic chemotherapeutics [308] have showed that interfering with the ability of cells to repair DNA damage can make cells more sensitive to radiation. These lesions, if remain unrepaired will ultimately lead to cell death through diverse biological processes such as mitotic catastrophe, cell cycle arrest and apoptosis [189]. However, although such modalities can increase sensitivity to treatment, they often radiosensitise normal cells to radiation [308]. Hence, alternative strategies should be explored to spare normal tissue from the cytotoxic effect of radiotherapy.

Some degree of selectivity can be enabled by targeting rapidly proliferating tumour cells in organs whereby tumour cell proliferation is rapid but normal cell proliferation is slow, such as brain tumours [361]. A similar paradigm constitutes the use of HRR inhibitors that augment replication stress that occurs post-irradiation and aggravates DNA damage. PARP inhibitors are particularly toxic to HRR-deficient cells [362]. PARP mediates BER and SSBR and PARP inhibitors have been shown to enhance damage by

converting unrepaired SSBs to DSBs during replication, resulting in increased radiosensitivity [246, 362]. Utilising the concept of synthetic lethality, PARP inhibitors have been intensively investigated in the treatment of tumours with BRAC1/2 deficiency as they result in tumour but normal cell death [244, 362].

Targeting ATR might be an alternative approach for selective tumour cell killing [224]. ATR is activated in response to DSBs and/or DNA replication intermediates and activates cellular survival responses [194]. During the last decade, ATR has drawn significant attention as a potential target for novel therapeutic agents in order to potentiate the cytotoxic effect of radiation and chemotherapy [191]. Preclinical evidence has shown that blockade of the ATR/Chk1 pathway might be selective for tumour cells. Reaper *et al.* demonstrated that ATR inhibition by the novel drug VE-821 can kill tumour cells with defective ATM/p53 signalling and hence ATR inhibition could have broad application in cancer therapy. However, there has been a lack of ATR inhibitors available for *in vivo* use in animals and human, possibly due to the challenges in accessing active ATR protein to design effective and selective compounds.

Evidence suggests that chemoradiation could benefit patients with PDAC by improving resectability but this is associated with gastrointestinal toxicity [267, 270]. Thus, a selective radiosensitising agent would be applicable to this tumour entity. In **Chapter 6**, *in vivo* data on a highly potent and selective ATR inhibitor, VE-822, in pancreatic tumour cells and xenograft models were presented. ATR inhibition by VE-822 blocked Chk1 phosphorylation induced by radiation and gemcitabine, both *in vitro* and *in vivo*. VE-822 enhanced persistence of DNA damage, inhibited HRR and lead to abrogation of cell cycle checkpoints after gemcitabine-based chemoradiation. Importantly, VE-822 presented tumour selectivity as it decreased clonogenicity of PDAC cells but not normal fibroblasts or endothelial cells. *In vivo*, VE-822 strongly enhanced radiation-induced

tumour growth delay in two xenograft models, both after single and fractionated radiation. ATR inhibition by VE-822 did not augment radiation-induced gastrointestinal tract epithelial damage, at least in our abdominal irradiation model. To summarize, we provided substantial evidence that VE-822 profoundly sensitises pancreatic cancer cells and tumour models to chemoradiation without increasing normal cell or tissue toxicity.

These data show that ATR inhibition by VE-822 is an exciting new therapeutic approach which might improve the outcome of patients with pancreatic cancer treated with chemoradiotherapy. The next challenge will be to detect possible biomarkers that will enable optimization of drug-radiation scheduling in order to maximize the possibility of clinical success. Could phosphorylation of S345 Chk1 be used a potential biomarker for monitoring VE-822 activity? Chk1 is the immediate downstream target of ATR and is activated in response to DNA damage and/or replication stress resulting in cell cycle arrest [196]. Chk1 plays a role in HRR, as DNA damage-induced HRR is dependent on Chk1-mediated Rad51 phosphorylation. Furthermore, Chk1 is involved in replication fork stabilisation, mitotic spindle checkpoint and inhibition of caspase-3-mediated apoptosis [196]. Based on these known functions of Chk1, it would be predicted that ATR inhibition would affect several possible pharmacodynamic responses. In the *in vivo* study conducted, analysis of Chk1 phosphorylation, as induced by radiation and/or gemcitabine, confirmed efficient blockade of the ATR/Chk1 pathway by VE-822. The incorporation of a biomarker, such as phosphorylation of Chk1, to predict efficacy and response of patients with pancreatic cancer after treatment with VE-822 and chemoradiation might enable careful dosing and minimize side effects.

Hypoxia could be an additional reason why ATR targeting treatments could have broader application in cancer treatment. Severe levels of hypoxia (<0.1% $O_2$) can induce a DDR that is characterised by a rapid replication arrest [56, 363].This is probably mediated

by the enzyme ribonucleotide reductase [364]. The latter is highly dependent on the availability of cellular oxygen for its function and a recent study reported a rapid decline in its levels in response to hypoxia [365]. ssDNA regions accumulate at stalled replication forks in hypoxia and are coated with RPA [366]. This, in turn, leads to phosphorylation of ATR in hypoxia, which upon reoxygenation results into phosphorylation of ATM [367]. Hammond *et al.* have shown that ATR acts to protect stalled replication forks during hypoxia exposure and inhibition of ATR leads to increased killing of tumour cells during hypoxia/reoxygenation that often occur in tumours [366]. Therefore, sensitisation of tumour cells to hypoxia and/or reoxygenation by inhibition of members of the DRR, such as ATR, may be of particular therapeutic importance because hypoxic cells are often associated with increased recurrence [368] and worse prognosis following radiotherapy [56]. In this way, ATR inhibitors appear very promising as apart from radiosensitising tumour cells, they could result in increased killing of radioresistant hypoxic cells, similarly to the concept of hypoxia cytotoxins [369]. It remains unclear for how long the ATR inhibitor VE-822 will have to be administered to result in tumour regression as the drug alone did not result in regression in PDAC tumour xenografts.

A limitation of this work is the use of xenografts. This is particularly important in the context of human PDAC, which is characterised by a strong desmoplastic reaction consisting of pancreatic cancer stellate cells (PSCs). Tuveson and colleagues used a GEM model that closely resembled human PDAC. Tumours were poorly perfused and poorly vascularised and presented impaired delivery of gemcitabine, due to the presence of desmoplastic stroma [264, 265]. In contrast, in the tumour xenograft model, the perfusion was better and tumours were more chemosensitive compared to the GEM mouse model [264]. This study underlined how the TME i.e. desmoplasia contributes to the poor therapeutic response of PDAC. In addition, Brunner and colleagues recently demonstrated

that PSCs promote radioprotection and stimulate proliferation of PDAC cells and tumours [265]. The findings of these studies are important and should be taken into consideration when interpreting our findings. Ideally, we would have tested the radiosensitising potential of VE-822 using a tumour model similar to the GEM, as reported by Tuveson and colleagues [264]. However, the technological characteristics and precision of the animal microirradiators that are currently available make irradiation of such tumour models extremely challenging, if not impossible.

Special attention should be paid in regards to the effect of VE-822 on radiation-induced normal cell and tissue damage. In the experiments that we conducted, VE-822 did not enhance radiation-induced toxicity *in vitro* (fibroblasts and endothelial cells) or *in vivo* (murine abdominal XRT model). Importantly, no weight loss was observed in any of the mice throughout the tumour xenograft delay experiments. In the murine abdominal irradiation model, VE-822 did not augment radiation-induced gastrointestinal tract epithelial damage but this effect of was only examined early post-XRT, as prolonged monitoring after XRT was not possible because of animal welfare issues [370]. At 5 days post-XRT, there was no difference in weight loss between the XRT-alone and XRT plus VE-822 groups in our experiment but no diarrhoea was observed up to this time point. Hence, it remains to be seen whether VE-822 will not augment late XRT-induced abdominal gastrointestinal damage, similarly to our findings early post-XRT. Submucosal fibrosis and mucosal and submucosal lymphangiectasia have been described together with gastrointestinal malabsorption as late complications after radiotherapy [371]. However, these side effects are less common today and the advent of modern radiotherapy techniques, such as IMRT and IGRT, has improved sparing of normal tissue for PDAC [267, 270]. Nevertheless, the strong radiosensitising potential combined with the high tumour selectivity make VE-822 a promising agent for the treatment of PDAC.

In summary, in the present thesis, we explored the targeting of two distinct pathways in combination with radiation and chemoradiation. Inhibition of PI3K/mTOR and ATR/Chk1 signalling might constitute promising targeting strategies to increase response of tumours to radiotherapy. Our findings have considerable translational implications and future clinical trials should aim to validate these observations.

## 6.1.3 References


1. Delaney G, Jacob S, Featherstone C, Barton M: The role of radiotherapy in cancer treatment: estimating optimal utilization from a review of evidence-based clinical guidelines. Cancer 2005, 104:1129-1137.
2. Chera BS, Jackson M, Mazur LM, Adams R, Chang S, Deschesne K, Cullip T, Marks LB: Improving quality of patient care by improving daily practice in radiation oncology. Semin Radiat Oncol 2012, 22:77-85.
3. Verellen D, De Ridder M, Linthout N, Tournel K, Soete G, Storme G: Innovations in image-guided radiotherapy. Nat Rev Cancer 2007, 7:949-960.
4. Bucci MK, Bevan A, Roach M, 3rd: Advances in radiation therapy: conventional to 3D, to IMRT, to 4D, and beyond. CA Cancer J Clin 2005, 55:117-134.
5. Khan FM GB: Treatment Planning in Radiation Oncology. Lippincott Williams & Wilkins; 3rd edition, 2011.
6. Kim DW, Huamani J, Fu A, Hallahan DE: Molecular strategies targeting the host component of cancer to enhance tumour response to radiation therapy. Int J Radiat Oncol Biol Phys 2006, 64:38-46.
7. Begg AC, Stewart FA, Vens C: Strategies to improve radiotherapy with targeted drugs. Nat Rev Cancer 2011, 11:239-253.
8. Harrington KJ, Billingham LJ, Brunner TB, Burnet NG, Chan CS, Hoskin P, Mackay RI, Maughan TS, Macdougall J, McKenna WG, et al: Guidelines for preclinical and early phase clinical assessment of novel radiosensitisers. Br J Cancer 2011, 105:628-639.
9. Withers R: The 4 R's of radiotherapy. In: JT Lett and H Alder (eds), Advances in Radiation Biology, New York: Academic Press, 1975, Vol. 5.

10. Steel GG, McMillan TJ, Peacock JH: The 5Rs of radiobiology. Int J Radiat Biol 1989, 56:1045-1048.

11. Hall EJ GA: Radiobiology for the radiologist, ed 6, Philadelphia, 2006, Lippincott Williams & Wilkins.

12. Barnett GC, West CM, Dunning AM, Elliott RM, Coles CE, Pharoah PD, Burnet NG: Normal tissue reactions to radiotherapy: towards tailoring treatment dose by genotype. Nat Rev Cancer 2009, 9:134-142.

13. Bentzen SM: Preventing or reducing late side effects of radiation therapy: radiobiology meets molecular pathology. Nat Rev Cancer 2006, 6:702-713.

14. Gray LH, Conger AD, Ebert M, Hornsey S, Scott OC: The concentration of oxygen dissolved in tissues at the time of irradiation as a factor in radiotherapy. Br J Radiol 1953, 26:638-648.

15. Thomlinson RH: Tumour anoxia and the response to radiation. Sci Basis Med Annu Rev 1965:74-90.

16. Harris AL: Hypoxia--a key regulatory factor in tumour growth. Nat Rev Cancer 2002, 2:38-47.

17. Bertout JA, Patel SA, Simon MC: The impact of O2 availability on human cancer. Nat Rev Cancer 2008, 8:967-975.

18. Coleman CN: Hypoxia in tumours: a paradigm for the approach to biochemical and physiologic heterogeneity. J Natl Cancer Inst 1988, 80:310-317.

19. Hockel M, Vaupel P: Tumour hypoxia: definitions and current clinical, biologic, and molecular aspects. J Natl Cancer Inst 2001, 93:266-276.

20. Semenza GL: Hypoxia-inducible factors in physiology and medicine. Cell 2012, 148:399-408.

21. Vaupel P, Kelleher DK, Hockel M: Oxygen status of malignant tumours: pathogenesis of hypoxia and significance for tumour therapy. Semin Oncol 2001, 28:29-35.

22. Folkman J: Angiogenesis. Annu Rev Med 2006, 57:1-18.

23. Kerbel RS: Tumour angiogenesis. N Engl J Med 2008, 358:2039-2049.

24. Carmeliet P, Jain RK: Molecular mechanisms and clinical applications of angiogenesis. Nature 2011, 473:298-307.

25. Potente M, Gerhardt H, Carmeliet P: Basic and therapeutic aspects of angiogenesis. Cell 2011, 146:873-887.

26. Vaupel P, Mayer A, Hockel M: Impact of hemoglobin levels on tumour oxygenation: the higher, the better? Strahlenther Onkol 2006, 182:63-71.

27. Spivak JL: The anaemia of cancer: death by a thousand cuts. Nat Rev Cancer 2005, 5:543-555.

28. Vaupel P, Mayer A: Hypoxia in cancer: significance and impact on clinical outcome. Cancer Metastasis Rev 2007, 26:225-239.

29. Carmeliet P, Jain RK: Principles and mechanisms of vessel normalization for cancer and other angiogenic diseases. Nat Rev Drug Discov 2011, 10:417-427.

30. Tatum JL, Kelloff GJ, Gillies RJ, Arbeit JM, Brown JM, Chao KS, Chapman JD, Eckelman WC, Fyles AW, Giaccia AJ, et al: Hypoxia: importance in tumour biology, noninvasive measurement by imaging, and value of its measurement in the management of cancer therapy. Int J Radiat Biol 2006, 82:699-757.

31. Carmeliet P: Angiogenesis in life, disease and medicine. Nature 2005, 438:932-936.

32. Virchow RH, Berlin, 1863. The first report that vascular structures in tumours are abnormal.

33. Goldmann E: The Growth of Malignant Disease in Man and the Lower Animals, with special reference to the Vascular System. Proc R Soc Med 1908, 1:1-13.

34. Folkman J: Tumour angiogenesis: therapeutic implications. N Engl J Med 1971, 285:1182-1186.

35. Bergers G, Benjamin LE: Tumourigenesis and the angiogenic switch. Nat Rev Cancer 2003, 3:401-410.

36. Hicklin DJ, Ellis LM: Role of the vascular endothelial growth factor pathway in tumour growth and angiogenesis. J Clin Oncol 2005, 23:1011-1027.

37. Ferrara N: VEGF and the quest for tumour angiogenesis factors. Nat Rev Cancer 2002, 2:795-803.

38. Hanahan D, Weinberg RA: Hallmarks of cancer: the next generation. Cell 2011, 144:646-674.

39. Duda DG, Jain RK: Premetastatic lung "niche": is vascular endothelial growth factor receptor 1 activation required? Cancer Res 2010, 70:5670-5673.

40. Shaked Y, Voest EE: Bone marrow derived cells in tumour angiogenesis and growth: are they the good, the bad or the evil? Biochim Biophys Acta 2009, 1796:1-4.

41. Bertolini F, Shaked Y, Mancuso P, Kerbel RS: The multifaceted circulating endothelial cell in cancer: towards marker and target identification. Nat Rev Cancer 2006, 6:835-845.

42. Brown JM, Wilson WR: Exploiting tumour hypoxia in cancer treatment. Nat Rev Cancer 2004, 4:437-447.

43. Vaupel P: Tumour microenvironmental physiology and its implications for radiation oncology. Semin Radiat Oncol 2004, 14:198-206.

44. Wouters BG, Brown JM: Cells at intermediate oxygen levels can be more important than the "hypoxic fraction" in determining tumour response to fractionated radiotherapy. Radiat Res 1997, 147:541-550.

45. Brown JM: Tumour hypoxia in cancer therapy. Methods Enzymol 2007, 435:297-321.

46. Alper T, Howard-Flanders P: Role of oxygen in modifying the radiosensitivity of E. coli B. Nature 1956, 178:978-979.

47. Hall EJ RfR, J.P. Lippincot Company, Philadelphia, PA, Second Edition, p. 87.

48. Grau C, Overgaard J: Effect of cancer chemotherapy on the hypoxic fraction of a solid tumour measured using a local tumour control assay. Radiother Oncol 1988, 13:301-309.

49. Tredan O, Galmarini CM, Patel K, Tannock IF: Drug resistance and the solid tumour microenvironment. J Natl Cancer Inst 2007, 99:1441-1454.

50. Teicher BA, Lazo JS, Sartorelli AC: Classification of antineoplastic agents by their selective toxicities toward oxygenated and hypoxic tumour cells. Cancer Res 1981, 41:73-81.

51. Moulder JE, Rockwell S: Tumour hypoxia: its impact on cancer therapy. Cancer Metastasis Rev 1987, 5:313-341.

52. Giaccia AJ: Hypoxic Stress Proteins: Survival of the Fittest. Semin Radiat Oncol 1996, 6:46-58.

53. Rohwer N, Cramer T: Hypoxia-mediated drug resistance: novel insights on the functional interaction of HIFs and cell death pathways. Drug Resist Updat 2011, 14:191-201.

54. Hunter A, Hendrikse A, Renan M, Abratt R: Does the tumour microenvironment influence radiation-induced apoptosis? Apoptosis 2006, 11:1727-1735.

55. Graeber TG, Osmanian C, Jacks T, Housman DE, Koch CJ, Lowe SW, Giaccia AJ: Hypoxia-mediated selection of cells with diminished apoptotic potential in solid tumours. Nature 1996, 379:88-91.

56. Bristow RG, Hill RP: Hypoxia and metabolism. Hypoxia, DNA repair and genetic instability. Nat Rev Cancer 2008, 8:180-192.

57. Abdollahi A, Lipson KE, Han X, Krempien R, Trinh T, Weber KJ, Hahnfeldt P, Hlatky L, Debus J, Howlett AR, Huber PE: SU5416 and SU6668 attenuate the angiogenic effects of radiation-induced tumour cell growth factor production and amplify the direct anti-endothelial action of radiation in vitro. Cancer Res 2003, 63:3755-3763.

58. Imaizumi N, Monnier Y, Hegi M, Mirimanoff RO, Ruegg C: Radiotherapy suppresses angiogenesis in mice through TGF-betaRI/ALK5-dependent inhibition of endothelial cell sprouting. PLoS One 2010, 5:e11084.

59. Park HJ, Griffin RJ, Hui S, Levitt SH, Song CW: Radiation-Induced Vascular Damage in Tumours: Implications of Vascular Damage in Ablative Hypofractionated Radiotherapy (SBRT and SRS). Radiat Res 2012.

60. Chung CH, Wong S, Ang KK, Hammond EH, Dicker AP, Harari PM, Le QT: Strategic plans to promote head and neck cancer translational research within the radiation therapy oncology group: a report from the translational research program. Int J Radiat Oncol Biol Phys 2007, 69:S67-78.

61. Garcia-Barros M, Paris F, Cordon-Cardo C, Lyden D, Rafii S, Haimovitz-Friedman A, Fuks Z, Kolesnick R: Tumour response to radiotherapy regulated by endothelial cell apoptosis. Science 2003, 300:1155-1159.

62. Paris F, Fuks Z, Kang A, Capodieci P, Juan G, Ehleiter D, Haimovitz-Friedman A, Cordon-Cardo C, Kolesnick R: Endothelial apoptosis as the primary lesion initiating intestinal radiation damage in mice. Science 2001, 293:293-297.

63. Brown M, Bristow R, Glazer P, Hill R, McBride W, McKenna G, Muschel R: Comment on "Tumour response to radiotherapy regulated by endothelial cell apoptosis" (II). Science 2003, 302:1894; author reply 1894.

64. Suit HD, Willers H: Comment on "Tumour response to radiotherapy regulated by endothelial cell apoptosis" (I). Science 2003, 302:1894; author reply 1894.

65. Kirsch DG, Santiago PM, di Tomaso E, Sullivan JM, Hou WS, Dayton T, Jeffords LB, Sodha P, Mercer KL, Cohen R, et al: p53 controls radiation-induced gastrointestinal syndrome in mice independent of apoptosis. Science 2010, 327:593-596.

66. Udagawa T, Birsner AE, Wood M, D'Amato RJ: Chronic suppression of angiogenesis following radiation exposure is independent of hematopoietic reconstitution. Cancer Res 2007, 67:2040-2045.

67. Ahn GO, Brown JM: Matrix metalloproteinase-9 is required for tumour vasculogenesis but not for angiogenesis: role of bone marrow-derived myelomonocytic cells. Cancer Cell 2008, 13:193-205.

68. Zips D, Eicheler W, Geyer P, Hessel F, Dorfler A, Thames HD, Haberey M, Baumann M: Enhanced susceptibility of irradiated tumour vessels to vascular endothelial growth factor receptor tyrosine kinase inhibition. Cancer Res 2005, 65:5374-5379.

69. Okunieff P, Dols S, Lee J, Singer S, Vaupel P, Neuringer LJ, Beshah K: Angiogenesis determines blood flow, metabolism, growth rate, and ATPase

kinetics of tumours growing in an irradiated bed: 31P and 2H nuclear magnetic resonance studies. Cancer Res 1991, 51:3289-3295.

70. Chung YL, Jian JJ, Cheng SH, Tsai SY, Chuang VP, Soong T, Lin YM, Horng CF: Sublethal irradiation induces vascular endothelial growth factor and promotes growth of hepatoma cells: implications for radiotherapy of hepatocellular carcinoma. Clin Cancer Res 2006, 12:2706-2715.

71. Ahn GO, Tseng D, Liao CH, Dorie MJ, Czechowicz A, Brown JM: Inhibition of Mac-1 (CD11b/CD18) enhances tumour response to radiation by reducing myeloid cell recruitment. Proc Natl Acad Sci U S A 2010, 107:8363-8368.

72. Kioi M, Vogel H, Schultz G, Hoffman RM, Harsh GR, Brown JM: Inhibition of vasculogenesis, but not angiogenesis, prevents the recurrence of glioblastoma after irradiation in mice. J Clin Invest 2010, 120:694-705.

73. Kozin SV, Duda DG, Munn LL, Jain RK: Is vasculogenesis crucial for the regrowth of irradiated tumours? Nat Rev Cancer 2011, 11:532.

74. Liu SK, Bham SA, Fokas E, Beech J, Im J, Cho S, Harris AL, Muschel RJ: Delta-like ligand 4-notch blockade and tumour radiation response. J Natl Cancer Inst 2011, 103:1778-1798.

75. Minchinton AI, Tannock IF: Drug penetration in solid tumours. Nat Rev Cancer 2006, 6:583-592.

76. Di Paolo A, Bocci G: Drug distribution in tumours: mechanisms, role in drug resistance, and methods for modification. Curr Oncol Rep 2007, 9:109-114.

77. Heldin CH, Rubin K, Pietras K, Ostman A: High interstitial fluid pressure - an obstacle in cancer therapy. Nat Rev Cancer 2004, 4:806-813.

78. Stohrer M, Boucher Y, Stangassinger M, Jain RK: Oncotic pressure in solid tumours is elevated. Cancer Res 2000, 60:4251-4255.

79. Milosevic M, Fyles A, Hedley D, Hill R: The human tumour microenvironment: invasive (needle) measurement of oxygen and interstitial fluid pressure. Semin Radiat Oncol 2004, 14:249-258.

80. Hagendoorn J, Tong R, Fukumura D, Lin Q, Lobo J, Padera TP, Xu L, Kucherlapati R, Jain RK: Onset of abnormal blood and lymphatic vessel function and interstitial hypertension in early stages of carcinogenesis. Cancer Res 2006, 66:3360-3364.

81. Butcher DT, Alliston T, Weaver VM: A tense situation: forcing tumour progression. Nat Rev Cancer 2009, 9:108-122.

82. Bru A, Albertos S, Luis Subiza J, Garcia-Asenjo JL, Bru I: The universal dynamics of tumour growth. Biophys J 2003, 85:2948-2961.

83. Jain RK, Tong RT, Munn LL: Effect of vascular normalization by antiangiogenic therapy on interstitial hypertension, peritumour edema, and lymphatic metastasis: insights from a mathematical model. Cancer Res 2007, 67:2729-2735.

84. Jain RK: Transport of molecules in the tumour interstitium: a review. Cancer Res 1987, 47:3039-3051.

85. Jain RK: Delivery of molecular medicine to solid tumours: lessons from in vivo imaging of gene expression and function. J Control Release 2001, 74:7-25.

86. Engelman JA: Targeting PI3K signalling in cancer: opportunities, challenges and limitations. Nat Rev Cancer 2009, 9:550-562.

87. McKenna WG, Muschel RJ, Gupta AK, Hahn SM, Bernhard EJ: The RAS signal transduction pathway and its role in radiation sensitivity. Oncogene 2003, 22:5866-5875.

88. Prevo R, Deutsch E, Sampson O, Diplexcito J, Cengel K, Harper J, O'Neill P, McKenna WG, Patel S, Bernhard EJ: Class I PI3 kinase inhibition by the

pyridinylfuranopyrimidine inhibitor PI-103 enhances tumour radiosensitivity. Cancer Res 2008, 68:5915-5923.

89. Pore N, Gupta AK, Cerniglia GJ, Jiang Z, Bernhard EJ, Evans SM, Koch CJ, Hahn SM, Maity A: Nelfinavir down-regulates hypoxia-inducible factor 1alpha and VEGF expression and increases tumour oxygenation: implications for radiotherapy. Cancer Res 2006, 66:9252-9259.

90. Kim IA, Bae SS, Fernandes A, Wu J, Muschel RJ, McKenna WG, Birnbaum MJ, Bernhard EJ: Selective inhibition of Ras, phosphoinositide 3 kinase, and Akt isoforms increases the radiosensitivity of human carcinoma cell lines. Cancer Res 2005, 65:7902-7910.

91. Brunner TB, Cengel KA, Hahn SM, Wu J, Fraker DL, McKenna WG, Bernhard EJ: Pancreatic cancer cell radiation survival and prenyltransferase inhibition: the role of K-Ras. Cancer Res 2005, 65:8433-8441.

92. Konstantinidou G, Bey EA, Rabellino A, Schuster K, Maira MS, Gazdar AF, Amici A, Boothman DA, Scaglioni PP: Dual phosphoinositide 3-kinase/mammalian target of rapamycin blockade is an effective radiosensitising strategy for the treatment of non-small cell lung cancer harboring K-RAS mutations. Cancer Res 2009, 69:7644-7652.

93. Shinohara ET, Cao C, Niermann K, Mu Y, Zeng F, Hallahan DE, Lu B: Enhanced radiation damage of tumour vasculature by mTOR inhibitors. Oncogene 2005, 24:5414-5422.

94. Manegold PC, Paringer C, Kulka U, Krimmel K, Eichhorn ME, Wilkowski R, Jauch KW, Guba M, Bruns CJ: Antiangiogenic therapy with mammalian target of rapamycin inhibitor RAD001 (Everolimus) increases radiosensitivity in solid cancer. Clin Cancer Res 2008, 14:892-900.

95. Engelman JA, Luo J, Cantley LC: The evolution of phosphatidylinositol 3-kinases as regulators of growth and metabolism. Nat Rev Genet 2006, 7:606-619.

96. Courtney KD, Corcoran RB, Engelman JA: The PI3K pathway as drug target in human cancer. J Clin Oncol 2010, 28:1075-1083.

97. Zoncu R, Efeyan A, Sabatini DM: mTOR: from growth signal integration to cancer, diabetes and ageing. Nat Rev Mol Cell Biol 2011, 12:21-35.

98. Wullschleger S, Loewith R, Hall MN: TOR signalling in growth and metabolism. Cell 2006, 124:471-484.

99. Cantley LC: The phosphoinositide 3-kinase pathway. Science 2002, 296:1655-1657.

100. Shaw RJ, Cantley LC: Ras, PI(3)K and mTOR signalling controls tumour cell growth. Nature 2006, 441:424-430.

101. Samuels Y, Wang Z, Bardelli A, Silliman N, Ptak J, Szabo S, Yan H, Gazdar A, Powell SM, Riggins GJ, et al: High frequency of mutations of the PIK3CA gene in human cancers. Science 2004, 304:554.

102. Huang CH, Mandelker D, Schmidt-Kittler O, Samuels Y, Velculescu VE, Kinzler KW, Vogelstein B, Gabelli SB, Amzel LM: The structure of a human p110alpha/p85alpha complex elucidates the effects of oncogenic PI3Kalpha mutations. Science 2007, 318:1744-1748.

103. Tozer GM, Kanthou C, Baguley BC: Disrupting tumour blood vessels. Nat Rev Cancer 2005, 5:423-435.

104. Shaked Y, Tang T, Woloszynek J, Daenen LG, Man S, Xu P, Cai SR, Arbeit JM, Voest EE, Chaplin DJ, et al: Contribution of granulocyte colony-stimulating factor to the acute mobilisation of endothelial precursor cells by vascular disrupting agents. Cancer Res 2009, 69:7524-7528.

105. Ferrara N, Mass RD, Campa C, Kim R: Targeting VEGF-A to treat cancer and age-related macular degeneration. Annu Rev Med 2007, 58:491-504.

106. Cook KM, Figg WD: Angiogenesis inhibitors: current strategies and future prospects. CA Cancer J Clin 2010, 60:222-243.

107. Lee CG, Heijn M, di Tomaso E, Griffon-Etienne G, Ancukiewicz M, Koike C, Park KR, Ferrara N, Jain RK, Suit HD, Boucher Y: Anti-Vascular endothelial growth factor treatment augments tumour radiation response under normoxic or hypoxic conditions. Cancer Res 2000, 60:5565-5570.

108. Gorski DH, Beckett MA, Jaskowiak NT, Calvin DP, Mauceri HJ, Salloum RM, Seetharam S, Koons A, Hari DM, Kufe DW, Weichselbaum RR: Blockage of the vascular endothelial growth factor stress response increases the antitumour effects of ionizing radiation. Cancer Res 1999, 59:3374-3378.

109. Hurwitz H, Fehrenbacher L, Novotny W, Cartwright T, Hainsworth J, Heim W, Berlin J, Baron A, Griffing S, Holmgren E, et al: Bevacizumab plus irinotecan, fluorouracil, and leucovorin for metastatic colorectal cancer. N Engl J Med 2004, 350:2335-2342.

110. Tong RT, Boucher Y, Kozin SV, Winkler F, Hicklin DJ, Jain RK: Vascular normalization by vascular endothelial growth factor receptor 2 blockade induces a pressure gradient across the vasculature and improves drug penetration in tumours. Cancer Res 2004, 64:3731-3736.

111. Winkler F, Kozin SV, Tong RT, Chae SS, Booth MF, Garkavtsev I, Xu L, Hicklin DJ, Fukumura D, di Tomaso E, et al: Kinetics of vascular normalization by VEGFR2 blockade governs brain tumour response to radiation: role of oxygenation, angiopoietin-1, and matrix metalloproteinases. Cancer Cell 2004, 6:553-563.

112. Jain RK: Normalization of tumour vasculature: an emerging concept in antiangiogenic therapy. Science 2005, 307:58-62.

113. Ebos JM, Kerbel RS: Antiangiogenic therapy: impact on invasion, disease progression, and metastasis. Nat Rev Clin Oncol 2011, 8:210-221.

114. Maity A, Bernhard EJ: Modulating tumour vasculature through signalling inhibition to improve cytotoxic therapy. Cancer Res 2010, 70:2141-2145.

115. Castellino RC, Durden DL: Mechanisms of disease: the PI3K-Akt-PTEN signalling node--an intercept point for the control of angiogenesis in brain tumours. Nat Clin Pract Neurol 2007, 3:682-693.

116. Kerbel RS, Viloria-Petit A, Klement G, Rak J: 'Accidental' anti-angiogenic drugs. anti-oncogene directed signal transduction inhibitors and conventional chemotherapeutic agents as examples. Eur J Cancer 2000, 36:1248-1257.

117. Liu L, Zhu S, Gong Z, Low BC: K-ras/PI3K-Akt signalling is essential for zebrafish hematopoiesis and angiogenesis. PLoS One 2008, 3:e2850.

118. Jiang BH, Zheng JZ, Aoki M, Vogt PK: Phosphatidylinositol 3-kinase signalling mediates angiogenesis and expression of vascular endothelial growth factor in endothelial cells. Proc Natl Acad Sci U S A 2000, 97:1749-1753.

119. Lelievre E, Bourbon PM, Duan LJ, Nussbaum RL, Fong GH: Deficiency in the p110alpha subunit of PI3K results in diminished Tie2 expression and Tie2(-/-)-like vascular defects in mice. Blood 2005, 105:3935-3938.

120. Serban D, Leng J, Cheresh D: H-ras regulates angiogenesis and vascular permeability by activation of distinct downstream effectors. Circ Res 2008, 102:1350-1358.

121. Graupera M, Guillermet-Guibert J, Foukas LC, Phng LK, Cain RJ, Salpekar A, Pearce W, Meek S, Millan J, Cutillas PR, et al: Angiogenesis selectively requires

the p110alpha isoform of PI3K to control endothelial cell migration. Nature 2008, 453:662-666.

122. Luo J, McMullen JR, Sobkiw CL, Zhang L, Dorfman AL, Sherwood MC, Logsdon MN, Horner JW, DePinho RA, Izumo S, Cantley LC: Class IA phosphoinositide 3-kinase regulates heart size and physiological cardiac hypertrophy. Mol Cell Biol 2005, 25:9491-9502.

123. Jiang BH, Jiang G, Zheng JZ, Lu Z, Hunter T, Vogt PK: Phosphatidylinositol 3-kinase signalling controls levels of hypoxia-inducible factor 1. Cell Growth Differ 2001, 12:363-369.

124. Belaiba RS, Bonello S, Zahringer C, Schmidt S, Hess J, Kietzmann T, Gorlach A: Hypoxia up-regulates hypoxia-inducible factor-1alpha transcription by involving phosphatidylinositol 3-kinase and nuclear factor kappaB in pulmonary artery smooth muscle cells. Mol Biol Cell 2007, 18:4691-4697.

125. Chachami G, Simos G, Hatziefthimiou A, Bonanou S, Molyvdas PA, Paraskeva E: Cobalt induces hypoxia-inducible factor-1alpha expression in airway smooth muscle cells by a reactive oxygen species- and PI3K-dependent mechanism. Am J Respir Cell Mol Biol 2004, 31:544-551.

126. Zhong H, Chiles K, Feldser D, Laughner E, Hanrahan C, Georgescu MM, Simons JW, Semenza GL: Modulation of hypoxia-inducible factor 1alpha expression by the epidermal growth factor/phosphatidylinositol 3-kinase/PTEN/AKT/FRAP pathway in human prostate cancer cells: implications for tumour angiogenesis and therapeutics. Cancer Res 2000, 60:1541-1545.

127. Skinner HD, Zheng JZ, Fang J, Agani F, Jiang BH: Vascular endothelial growth factor transcriptional activation is mediated by hypoxia-inducible factor 1alpha,

HDM2, and p70S6K1 in response to phosphatidylinositol 3-kinase/AKT signalling. J Biol Chem 2004, 279:45643-45651.

128. Carver DJ, Gaston B, Deronde K, Palmer LA: Akt-mediated activation of HIF-1 in pulmonary vascular endothelial cells by S-nitrosoglutathione. Am J Respir Cell Mol Biol 2007, 37:255-263.

129. Lee KS, Kim SR, Park SJ, Min KH, Lee KY, Choe YH, Park SY, Chai OH, Zhang X, Song CH, Lee YC: Mast cells can mediate vascular permeability through regulation of the PI3K-HIF-1alpha-VEGF axis. Am J Respir Crit Care Med 2008, 178:787-797.

130. Mazure NM, Chen EY, Laderoute KR, Giaccia AJ: Induction of vascular endothelial growth factor by hypoxia is modulated by a phosphatidylinositol 3-kinase/Akt signalling pathway in Ha-ras-transformed cells through a hypoxia inducible factor-1 transcriptional element. Blood 1997, 90:3322-3331.

131. Trisciuoglio D, Iervolino A, Zupi G, Del Bufalo D: Involvement of PI3K and MAPK signalling in bcl-2-induced vascular endothelial growth factor expression in melanoma cells. Mol Biol Cell 2005, 16:4153-4162.

132. Hu L, Hofmann J, Jaffe RB: Phosphatidylinositol 3-kinase mediates angiogenesis and vascular permeability associated with ovarian carcinoma. Clin Cancer Res 2005, 11:8208-8212.

133. Xia C, Meng Q, Cao Z, Shi X, Jiang BH: Regulation of angiogenesis and tumour growth by p110 alpha and AKT1 via VEGF expression. J Cell Physiol 2006, 209:56-66.

134. Fang J, Ding M, Yang L, Liu LZ, Jiang BH: PI3K/PTEN/AKT signalling regulates prostate tumour angiogenesis. Cell Signal 2007, 19:2487-2497.

135. Hamada K, Sasaki T, Koni PA, Natsui M, Kishimoto H, Sasaki J, Yajima N, Horie Y, Hasegawa G, Naito M, et al: The PTEN/PI3K pathway governs normal vascular development and tumour angiogenesis. Genes Dev 2005, 19:2054-2065.

136. Sun JF, Phung T, Shiojima I, Felske T, Upalakalin JN, Feng D, Kornaga T, Dor T, Dvorak AM, Walsh K, Benjamin LE: Microvascular patterning is controlled by fine-tuning the Akt signal. Proc Natl Acad Sci U S A 2005, 102:128-133.

137. Yuan TL, Choi HS, Matsui A, Benes C, Lifshits E, Luo J, Frangioni JV, Cantley LC: Class 1A PI3K regulates vessel integrity during development and tumourigenesis. Proc Natl Acad Sci U S A 2008, 105:9739-9744.

138. Morales-Ruiz M, Fulton D, Sowa G, Languino LR, Fujio Y, Walsh K, Sessa WC: Vascular endothelial growth factor-stimulated actin reorganization and migration of endothelial cells is regulated via the serine/threonine kinase Akt. Circ Res 2000, 86:892-896.

139. Fulton D, Gratton JP, McCabe TJ, Fontana J, Fujio Y, Walsh K, Franke TF, Papapetropoulos A, Sessa WC: Regulation of endothelium-derived nitric oxide production by the protein kinase Akt. Nature 1999, 399:597-601.

140. Phung TL, Ziv K, Dabydeen D, Eyiah-Mensah G, Riveros M, Perruzzi C, Sun J, Monahan-Earley RA, Shiojima I, Nagy JA, et al: Pathological angiogenesis is induced by sustained Akt signalling and inhibited by rapamycin. Cancer Cell 2006, 10:159-170.

141. Schnell CR, Stauffer F, Allegrini PR, O'Reilly T, McSheehy PM, Dartois C, Stumm M, Cozens R, Littlewood-Evans A, Garcia-Echeverria C, Maira SM: Effects of the dual phosphatidylinositol 3-kinase/mammalian target of rapamycin inhibitor NVP-BEZ235 on the tumour vasculature: implications for clinical imaging. Cancer Res 2008, 68:6598-6607.

142. Qayum N, Muschel RJ, Im JH, Balathasan L, Koch CJ, Patel S, McKenna WG, Bernhard EJ: Tumour vascular changes mediated by inhibition of oncogenic signalling. Cancer Res 2009, 69:6347-6354.

143. Cohen-Jonathan E, Evans SM, Koch CJ, Muschel RJ, McKenna WG, Wu J, Bernhard EJ: The farnesyltransferase inhibitor L744,832 reduces hypoxia in tumours expressing activated H-ras. Cancer Res 2001, 61:2289-2293.

144. Delmas C, End D, Rochaix P, Favre G, Toulas C, Cohen-Jonathan E: The farnesyltransferase inhibitor R115777 reduces hypoxia and matrix metalloproteinase 2 expression in human glioma xenograft. Clin Cancer Res 2003, 9:6062-6068.

145. Xue Q, Hopkins B, Perruzzi C, Udayakumar D, Sherris D, Benjamin LE: Palomid 529, a novel small-molecule drug, is a TORC1/TORC2 inhibitor that reduces tumour growth, tumour angiogenesis, and vascular permeability. Cancer Res 2008, 68:9551-9557.

146. Zhang Q, Bindokas V, Shen J, Fan H, Hoffman RM, Xing HR: Time-course imaging of therapeutic functional tumour vascular normalization by antiangiogenic agents. Mol Cancer Ther 2011, 10:1173-1184.

147. Weppler SA, Krause M, Zyromska A, Lambin P, Baumann M, Wouters BG: Response of U87 glioma xenografts treated with concurrent rapamycin and fractionated radiotherapy: possible role for thrombosis. Radiother Oncol 2007, 82:96-104.

148. Guba M, von Breitenbuch P, Steinbauer M, Koehl G, Flegel S, Hornung M, Bruns CJ, Zuelke C, Farkas S, Anthuber M, et al: Rapamycin inhibits primary and metastatic tumour growth by antiangiogenesis: involvement of vascular endothelial growth factor. Nat Med 2002, 8:128-135.

149. Warburton C, Dragowska WH, Gelmon K, Chia S, Yan H, Masin D, Denyssevych T, Wallis AE, Bally MB: Treatment of HER-2/neu overexpressing breast cancer xenograft models with trastuzumab (Herceptin) and gefitinib (ZD1839): drug combination effects on tumour growth, HER-2/neu and epidermal growth factor receptor expression, and viable hypoxic cell fraction. Clin Cancer Res 2004, 10:2512-2524.

150. Cerniglia GJ, Pore N, Tsai JH, Schultz S, Mick R, Choe R, Xing X, Durduran T, Yodh AG, Evans SM, et al: Epidermal growth factor receptor inhibition modulates the microenvironment by vascular normalization to improve chemotherapy and radiotherapy efficacy. PLoS One 2009, 4:e6539.

151. Bernsen HJ, Rijken PF, Peters JP, Bakker JH, Boerman RH, Wesseling P, van der Kogel AJ: Suramin treatment of human glioma xenografts; effects on tumour vasculature and oxygenation status. J Neurooncol 1999, 44:129-136.

152. Izumi Y, Xu L, di Tomaso E, Fukumura D, Jain RK: Tumour biology: herceptin acts as an anti-angiogenic cocktail. Nature 2002, 416:279-280.

153. Sodir NM, Swigart LB, Karnezis AN, Hanahan D, Evan GI, Soucek L: Endogenous Myc maintains the tumour microenvironment. Genes Dev 2011, 25:907-916.

154. Shannon AM, Telfer BA, Smith PD, Babur M, Logie A, Wilkinson RW, Debray C, Stratford IJ, Williams KJ, Wedge SR: The mitogen-activated protein/extracellular signal-regulated kinase kinase 1/2 inhibitor AZD6244 (ARRY-142886) enhances the radiation responsiveness of lung and colorectal tumour xenografts. Clin Cancer Res 2009, 15:6619-6629.

155. Ding Y, Boguslawski EA, Berghuis BD, Young JJ, Zhang Z, Hardy K, Furge K, Kort E, Frankel AE, Hay RV, et al: Mitogen-activated protein kinase kinase

signalling promotes growth and vascularization of fibrosarcoma. Mol Cancer Ther 2008, 7:648-658.

156. Ansiaux R, Baudelet C, Jordan BF, Beghein N, Sonveaux P, De Wever J, Martinive P, Gregoire V, Feron O, Gallez B: Thalidomide radiosensitises tumours through early changes in the tumour microenvironment. Clin Cancer Res 2005, 11:743-750.

157. Segers J, Di Fazio V, Ansiaux R, Martinive P, Feron O, Wallemacq P, Gallez B: Potentiation of cyclophosphamide chemotherapy using the anti-angiogenic drug thalidomide: importance of optimal scheduling to exploit the 'normalization' window of the tumour vasculature. Cancer Lett 2006, 244:129-135.

158. McGee MC, Hamner JB, Williams RF, Rosati SF, Sims TL, Ng CY, Gaber MW, Calabrese C, Wu J, Nathwani AC, et al: Improved intratumoural oxygenation through vascular normalization increases glioma sensitivity to ionizing radiation. Int J Radiat Oncol Biol Phys 2010, 76:1537-1545.

159. Hamzah J, Jugold M, Kiessling F, Rigby P, Manzur M, Marti HH, Rabie T, Kaden S, Grone HJ, Hammerling GJ, et al: Vascular normalization in Rgs5-deficient tumours promotes immune destruction. Nature 2008, 453:410-414.

160. Rolny C, Mazzone M, Tugues S, Laoui D, Johansson I, Coulon C, Squadrito ML, Segura I, Li X, Knevels E, et al: HRG inhibits tumour growth and metastasis by inducing macrophage polarization and vessel normalization through downregulation of PlGF. Cancer Cell 2011, 19:31-44.

161. Skuli N, Monferran S, Delmas C, Favre G, Bonnet J, Toulas C, Cohen-Jonathan Moyal E: Alphavbeta3/alphavbeta5 integrins-FAK-RhoB: a novel pathway for hypoxia regulation in glioblastoma. Cancer Res 2009, 69:3308-3316.

162. Mazzone M, Dettori D, Leite de Oliveira R, Loges S, Schmidt T, Jonckx B, Tian YM, Lanahan AA, Pollard P, Ruiz de Almodovar C, et al: Heterozygous deficiency of PHD2 restores tumour oxygenation and inhibits metastasis via endothelial normalization. Cell 2009, 136:839-851.

163. Hansen-Algenstaedt N, Stoll BR, Padera TP, Dolmans DE, Hicklin DJ, Fukumura D, Jain RK: Tumour oxygenation in hormone-dependent tumours during vascular endothelial growth factor receptor-2 blockade, hormone ablation, and chemotherapy. Cancer Res 2000, 60:4556-4560.

164. Jain RK, Safabakhsh N, Sckell A, Chen Y, Jiang P, Benjamin L, Yuan F, Keshet E: Endothelial cell death, angiogenesis, and microvascular function after castration in an androgen-dependent tumour: role of vascular endothelial growth factor. Proc Natl Acad Sci U S A 1998, 95:10820-10825.

165. Wildiers H, Guetens G, De Boeck G, Verbeken E, Landuyt B, Landuyt W, de Bruijn EA, van Oosterom AT: Effect of antivascular endothelial growth factor treatment on the intratumoural uptake of CPT-11. Br J Cancer 2003, 88:1979-1986.

166. Dickson PV, Hamner JB, Sims TL, Fraga CH, Ng CY, Rajasekeran S, Hagedorn NL, McCarville MB, Stewart CF, Davidoff AM: Bevacizumab-induced transient remodelling of the vasculature in neuroblastoma xenografts results in improved delivery and efficacy of systemically administered chemotherapy. Clin Cancer Res 2007, 13:3942-3950.

167. Willett CG, Boucher Y, di Tomaso E, Duda DG, Munn LL, Tong RT, Chung DC, Sahani DV, Kalva SP, Kozin SV, et al: Direct evidence that the VEGF-specific antibody bevacizumab has antivascular effects in human rectal cancer. Nat Med 2004, 10:145-147.

168. Willett CG, Duda DG, di Tomaso E, Boucher Y, Ancukiewicz M, Sahani DV, Lahdenranta J, Chung DC, Fischman AJ, Lauwers GY, et al: Efficacy, safety, and biomarkers of neoadjuvant bevacizumab, radiation therapy, and fluorouracil in rectal cancer: a multidisciplinary phase II study. J Clin Oncol 2009, 27:3020-3026.

169. Williams KJ, Telfer BA, Brave S, Kendrew J, Whittaker L, Stratford IJ, Wedge SR: ZD6474, a potent inhibitor of vascular endothelial growth factor signalling, combined with radiotherapy: schedule-dependent enhancement of antitumour activity. Clin Cancer Res 2004, 10:8587-8593.

170. Williams KJ, Telfer BA, Shannon AM, Babur M, Stratford IJ, Wedge SR: Combining radiotherapy with AZD2171, a potent inhibitor of vascular endothelial growth factor signalling: pathophysiologic effects and therapeutic benefit. Mol Cancer Ther 2007, 6:599-606.

171. Abdollahi A, Griggs DW, Zieher H, Roth A, Lipson KE, Saffrich R, Grone HJ, Hallahan DE, Reisfeld RA, Debus J, et al: Inhibition of alpha(v)beta3 integrin survival signalling enhances antiangiogenic and antitumour effects of radiotherapy. Clin Cancer Res 2005, 11:6270-6279.

172. Huber PE, Bischof M, Jenne J, Heiland S, Peschke P, Saffrich R, Grone HJ, Debus J, Lipson KE, Abdollahi A: Trimodal cancer treatment: beneficial effects of combined antiangiogenesis, radiation, and chemotherapy. Cancer Res 2005, 65:3643-3655.

173. Qayum N, Im J, Stratford MR, Bernhard EJ, McKenna WG, Muschel RJ: Modulation of the tumour microvasculature by phosphoinositide-3 kinase inhibition increases doxorubicin delivery in vivo. Clin Cancer Res 2012, 18:161-169.

174. Fokas E, Im JH, Hill S, Yameen S, Stratford M, Beech J, Hackl W, Maira SM, Bernhard EJ, McKenna WG, Muschel RJ: Dual inhibition of the PI3K/mTOR pathway increases tumour radiosensitivity by normalizing tumour vasculature. Cancer Res 2012, 72:239-248.

175. Zhang M, Kleber S, Rohrich M, Timke C, Han N, Tuettenberg J, Martin-Villalba A, Debus J, Peschke P, Wirkner U, et al: Blockade of TGF-beta signalling by the TGFbetaR-I kinase inhibitor LY2109761 enhances radiation response and prolongs survival in glioblastoma. Cancer Res 2011, 71:7155-7167.

176. Kozin SV, Boucher Y, Hicklin DJ, Bohlen P, Jain RK, Suit HD: Vascular endothelial growth factor receptor-2-blocking antibody potentiates radiation-induced long-term control of human tumour xenografts. Cancer Res 2001, 61:39-44.

177. Zhou Q, Gallo JM: Differential effect of sunitinib on the distribution of temozolomide in an orthotopic glioma model. Neuro Oncol 2009, 11:301-310.

178. Zhou Q, Guo P, Gallo JM: Impact of angiogenesis inhibition by sunitinib on tumour distribution of temozolomide. Clin Cancer Res 2008, 14:1540-1549.

179. Matsumoto S, Batra S, Saito K, Yasui H, Choudhuri R, Gadisetti C, Subramanian S, Devasahayam N, Munasinghe JP, Mitchell JB, Krishna MC: Antiangiogenic agent sunitinib transiently increases tumour oxygenation and suppresses cycling hypoxia. Cancer Res 2011, 71:6350-6359.

180. Liu J, Liao S, Huang Y, Samuel R, Shi T, Naxerova K, Huang P, Kamoun W, Jain RK, Fukumura D, Xu L: PDGF-D improves drug delivery and efficacy via vascular normalization, but promotes lymphatic metastasis by activating CXCR4 in breast cancer. Clin Cancer Res 2011, 17:3638-3648.

181. Teicher BA, Dupuis NP, Robinson MF, Emi Y, Goff DA: Antiangiogenic treatment (TNP-470/minocycline) increases tissue levels of anticancer drugs in mice bearing Lewis lung carcinoma. Oncol Res 1995, 7:237-243.

182. Ma J, Pulfer S, Li S, Chu J, Reed K, Gallo JM: Pharmacodynamic-mediated reduction of temozolomide tumour concentrations by the angiogenesis inhibitor TNP-470. Cancer Res 2001, 61:5491-5498.

183. Nakahara T, Norberg SM, Shalinsky DR, Hu-Lowe DD, McDonald DM: Effect of inhibition of vascular endothelial growth factor signalling on distribution of extravasated antibodies in tumours. Cancer Res 2006, 66:1434-1445.

184. Kurozumi K, Hardcastle J, Thakur R, Yang M, Christoforidis G, Fulci G, Hochberg FH, Weissleder R, Carson W, Chiocca EA, Kaur B: Effect of tumour microenvironment modulation on the efficacy of oncolytic virus therapy. J Natl Cancer Inst 2007, 99:1768-1781.

185. Dings RP, Loren M, Heun H, McNiel E, Griffioen AW, Mayo KH, Griffin RJ: Scheduling of radiation with angiogenesis inhibitors anginex and Avastin improves therapeutic outcome via vessel normalization. Clin Cancer Res 2007, 13:3395-3402.

186. Ansiaux R, Baudelet C, Cron GO, Segers J, Dessy C, Martinive P, De Wever J, Verrax J, Wauthier V, Beghein N, et al: Botulinum toxin potentiates cancer radiotherapy and chemotherapy. Clin Cancer Res 2006, 12:1276-1283.

187. Singh Jaggi J, Henke E, Seshan SV, Kappel BJ, Chattopadhyay D, May C, McDevitt MR, Nolan D, Mittal V, Benezra R, Scheinberg DA: Selective alpha-particle mediated depletion of tumour vasculature with vascular normalization. PLoS One 2007, 2:e267.

188. Harper JW, Elledge SJ: The DNA damage response: ten years after. Mol Cell 2007, 28:739-745.

189. Jackson SP, Bartek J: The DNA-damage response in human biology and disease. Nature 2009, 461:1071-1078.

190. O'Connor MJ, Martin NM, Smith GC: Targeted cancer therapies based on the inhibition of DNA strand break repair. Oncogene 2007, 26:7816-7824.

191. Smith J, Tho LM, Xu N, Gillespie DA: The ATM-Chk2 and ATR-Chk1 pathways in DNA damage signalling and cancer. Adv Cancer Res 2010, 108:73-112.

192. Kastan MB, Lim DS: The many substrates and functions of ATM. Nat Rev Mol Cell Biol 2000, 1:179-186.

193. Keith CT, Schreiber SL: PIK-related kinases: DNA repair, recombination, and cell cycle checkpoints. Science 1995, 270:50-51.

194. Cimprich KA, Cortez D: ATR: an essential regulator of genome integrity. Nat Rev Mol Cell Biol 2008, 9:616-627.

195. Wagner JM, Kaufmann SH. Prospects for the Use of ATR Inhibitors to Treat CancerPharmaceuticals 2010, 3, 1311-1334.

196. Dai Y, Grant S: New insights into checkpoint kinase 1 in the DNA damage response signalling network. Clin Cancer Res 2010, 16:376-383.

197. Zou L, Elledge SJ: Sensing DNA damage through ATRIP recognition of RPA-ssDNA complexes. Science 2003, 300:1542-1548.

198. Zou L, Cortez D, Elledge SJ: Regulation of ATR substrate selection by Rad17-dependent loading of Rad9 complexes onto chromatin. Genes Dev 2002, 16:198-208.

199. Delacroix S, Wagner JM, Kobayashi M, Yamamoto K, Karnitz LM: The Rad9-Hus1-Rad1 (9-1-1) clamp activates checkpoint signalling via TopBP1. Genes Dev 2007, 21:1472-1477.

200. Mordes DA, Cortez D: Activation of ATR and related PIKKs. Cell Cycle 2008, 7:2809-2812.

201. Kumagai A, Lee J, Yoo HY, Dunphy WG: TopBP1 activates the ATR-ATRIP complex. Cell 2006, 124:943-955.

202. Ellison V, Stillman B: Biochemical characterization of DNA damage checkpoint complexes: clamp loader and clamp complexes with specificity for 5' recessed DNA. PLoS Biol 2003, 1:E33.

203. Liu Q, Guntuku S, Cui XS, Matsuoka S, Cortez D, Tamai K, Luo G, Carattini-Rivera S, DeMayo F, Bradley A, et al: Chk1 is an essential kinase that is regulated by Atr and required for the G(2)/M DNA damage checkpoint. Genes Dev 2000, 14:1448-1459.

204. Sorensen CS, Syljuasen RG, Falck J, Schroeder T, Ronnstrand L, Khanna KK, Zhou BB, Bartek J, Lukas J: Chk1 regulates the S phase checkpoint by coupling the physiological turnover and ionizing radiation-induced accelerated proteolysis of Cdc25A. Cancer Cell 2003, 3:247-258.

205. Kumagai A, Dunphy WG: Claspin, a novel protein required for the activation of Chk1 during a DNA replication checkpoint response in Xenopus egg extracts. Mol Cell 2000, 6:839-849.

206. Kemp MG, Akan Z, Yilmaz S, Grillo M, Smith-Roe SL, Kang TH, Cordeiro-Stone M, Kaufmann WK, Abraham RT, Sancar A, Unsal-Kacmaz K: Tipin-replication protein A interaction mediates Chk1 phosphorylation by ATR in response to genotoxic stress. J Biol Chem 2010, 285:16562-16571.

207. Chen J: Ataxia telangiectasia-related protein is involved in the phosphorylation of BRCA1 following deoxyribonucleic acid damage. Cancer Res 2000, 60:5037-5039.

208. Ashwell S, Zabludoff S: DNA damage detection and repair pathways--recent advances with inhibitors of checkpoint kinases in cancer therapy. Clin Cancer Res 2008, 14:4032-4037.

209. Cuadrado M, Martinez-Pastor B, Murga M, Toledo LI, Gutierrez-Martinez P, Lopez E, Fernandez-Capetillo O: ATM regulates ATR chromatin loading in response to DNA double-strand breaks. J Exp Med 2006, 203:297-303.

210. Casper AM, Nghiem P, Arlt MF, Glover TW: ATR regulates fragile site stability. Cell 2002, 111:779-789.

211. Pichiorri F, Ishii H, Okumura H, Trapasso F, Wang Y, Huebner K: Molecular parameters of genome instability: roles of fragile genes at common fragile sites. J Cell Biochem 2008, 104:1525-1533.

212. Khadaroo B, Teixeira MT, Luciano P, Eckert-Boulet N, Germann SM, Simon MN, Gallina I, Abdallah P, Gilson E, Geli V, Lisby M: The DNA damage response at eroded telomeres and tethering to the nuclear pore complex. Nat Cell Biol 2009, 11:980-987.

213. d'Adda di Fagagna F, Reaper PM, Clay-Farrace L, Fiegler H, Carr P, Von Zglinicki T, Saretzki G, Carter NP, Jackson SP: A DNA damage checkpoint response in telomere-initiated senescence. Nature 2003, 426:194-198.

214. Lopez-Contreras AJ, Fernandez-Capetillo O: The ATR barrier to replication-born DNA damage. DNA Repair (Amst), 9:1249-1255.

215. Mukhopadhyay UK, Senderowicz AM, Ferbeyre G: RNA silencing of checkpoint regulators sensitises p53-defective prostate cancer cells to chemotherapy while sparing normal cells. Cancer Res 2005, 65:2872-2881.

216. Hidalgo M: Pancreatic cancer. N Engl J Med, 362:1605-1617.

217. Jones S, Zhang X, Parsons DW, Lin JC, Leary RJ, Angenendt P, Mankoo P, Carter H, Kamiyama H, Jimeno A, et al: Core signalling pathways in human pancreatic cancers revealed by global genomic analyses. Science 2008, 321:1801-1806.

218. Tao Y, Leteur C, Yang C, Zhang P, Castedo M, Pierre A, Golsteyn RM, Bourhis J, Kroemer G, Deutsch E: Radiosensitisation by Chir-124, a selective CHK1 inhibitor: effects of p53 and cell cycle checkpoints. Cell Cycle 2009, 8:1196-1205.

219. Toledo LI, Murga M, Zur R, Soria R, Rodriguez A, Martinez S, Oyarzabal J, Pastor J, Bischoff JR, Fernandez-Capetillo O: A cell-based screen identifies ATR inhibitors with synthetic lethal properties for cancer-associated mutations. Nat Struct Mol Biol 2011.

220. Sangster-Guity N, Conrad BH, Papadopoulos N, Bunz F: ATR mediates cisplatin resistance in a p53 genotype-specific manner. Oncogene.

221. Ruzankina Y, Schoppy DW, Asare A, Clark CE, Vonderheide RH, Brown EJ: Tissue regenerative delays and synthetic lethality in adult mice after combined deletion of Atr and Trp53. Nat Genet 2009, 41:1144-1149.

222. Hurley PJ, Wilsker D, Bunz F: Human cancer cells require ATR for cell cycle progression following exposure to ionizing radiation. Oncogene 2007, 26:2535-2542.

223. Nghiem P, Park PK, Kim Y, Vaziri C, Schreiber SL: ATR inhibition selectively sensitises G1 checkpoint-deficient cells to lethal premature chromatin condensation. Proc Natl Acad Sci U S A 2001, 98:9092-9097.

224. Toledo LI, Murga M, Fernandez-Capetillo O: Targeting ATR and Chk1 kinases for cancer treatment: a new model for new (and old) drugs. Mol Oncol 2011, 5:368-373.

225. Toledo LI, Murga M, Gutierrez-Martinez P, Soria R, Fernandez-Capetillo O: ATR signalling can drive cells into senescence in the absence of DNA breaks. Genes Dev 2008, 22:297-302.

226. Rodriguez-Bravo V, Guaita-Esteruelas S, Salvador N, Bachs O, Agell N: Different S/M checkpoint responses of tumour and non tumour cell lines to DNA replication inhibition. Cancer Res 2007, 67:11648-11656.

227. Sarkaria JN, Busby EC, Tibbetts RS, Roos P, Taya Y, Karnitz LM, Abraham RT: Inhibition of ATM and ATR kinase activities by the radiosensitising agent, caffeine. Cancer Res 1999, 59:4375-4382.

228. Nishida H, Tatewaki N, Nakajima Y, Magara T, Ko KM, Hamamori Y, Konishi T: Inhibition of ATR protein kinase activity by schisandrin B in DNA damage response. Nucleic Acids Res 2009, 37:5678-5689.

229. Plunkett W, Huang P, Xu YZ, Heinemann V, Grunewald R, Gandhi V: Gemcitabine: metabolism, mechanisms of action, and self-potentiation. Semin Oncol 1995, 22:3-10.

230. Karnitz LM, Flatten KS, Wagner JM, Loegering D, Hackbarth JS, Arlander SJ, Vroman BT, Thomas MB, Baek YU, Hopkins KM, et al: Gemcitabine-induced activation of checkpoint signalling pathways that affect tumour cell survival. Mol Pharmacol 2005, 68:1636-1644.

231. Parsels LA, Morgan MA, Tanska DM, Parsels JD, Palmer BD, Booth RJ, Denny WA, Canman CE, Kraker AJ, Lawrence TS, Maybaum J: Gemcitabine

sensitisation by checkpoint kinase 1 inhibition correlates with inhibition of a Rad51 DNA damage response in pancreatic cancer cells. Mol Cancer Ther 2009, 8:45-54.

232. Jardim MJ, Wang Q, Furumai R, Wakeman T, Goodman BK, Wang XF: Reduced ATR or Chk1 expression leads to chromosome instability and chemosensitisation of mismatch repair-deficient colorectal cancer cells. Mol Biol Cell 2009, 20:3801-3809.

233. Ganzinelli M, Carrassa L, Crippa F, Tavecchio M, Broggini M, Damia G: Checkpoint kinase 1 down-regulation by an inducible small interfering RNA expression system sensitised in vivo tumours to treatment with 5-fluorouracil. Clin Cancer Res 2008, 14:5131-5141.

234. Pommier Y: Topoisomerase I inhibitors: camptothecins and beyond. Nat Rev Cancer 2006, 6:789-802.

235. Flatten K, Dai NT, Vroman BT, Loegering D, Erlichman C, Karnitz LM, Kaufmann SH: The role of checkpoint kinase 1 in sensitivity to topoisomerase I poisons. J Biol Chem 2005, 280:14349-14355.

236. Cliby WA, Lewis KA, Lilly KK, Kaufmann SH: S phase and G2 arrests induced by topoisomerase I poisons are dependent on ATR kinase function. J Biol Chem 2002, 277:1599-1606.

237. Wagner JM, Karnitz LM: Cisplatin-induced DNA damage activates replication checkpoint signalling components that differentially affect tumour cell survival. Mol Pharmacol 2009, 76:208-214.

238. Lewis KA, Lilly KK, Reynolds EA, Sullivan WP, Kaufmann SH, Cliby WA: Ataxia telangiectasia and rad3-related kinase contributes to cell cycle arrest and survival after cisplatin but not oxaliplatin. Mol Cancer Ther 2009, 8:855-863.

239. Fu D, Calvo JA, Samson LD: Balancing repair and tolerance of DNA damage caused by alkylating agents. Nat Rev Cancer 2012, 12:104-120.

240. Caporali S, Levati L, Starace G, Ragone G, Bonmassar E, Alvino E, D'Atri S: AKT is activated in an ataxia-telangiectasia and Rad3-related-dependent manner in response to temozolomide and confers protection against drug-induced cell growth inhibition. Mol Pharmacol 2008, 74:173-183.

241. Caporali S, Falcinelli S, Starace G, Russo MT, Bonmassar E, Jiricny J, D'Atri S: DNA damage induced by temozolomide signals to both ATM and ATR: role of the mismatch repair system. Mol Pharmacol 2004, 66:478-491.

242. Wilsker D, Bunz F: Loss of ataxia telangiectasia mutated- and Rad3-related function potentiates the effects of chemotherapeutic drugs on cancer cell survival. Mol Cancer Ther 2007, 6:1406-1413.

243. Chan DA, Giaccia AJ: Harnessing synthetic lethal interactions in anticancer drug discovery. Nat Rev Drug Discov 2011, 10:351-364.

244. Helleday T: The underlying mechanism for the PARP and BRCA synthetic lethality: clearing up the misunderstandings. Mol Oncol 2011, 5:387-393.

245. Shaheen M, Allen C, Nickoloff JA, Hromas R: Synthetic lethality: exploiting the addiction of cancer to DNA repair. Blood 2011, 117:6074-6082.

246. Calabrese CR, Almassy R, Barton S, Batey MA, Calvert AH, Canan-Koch S, Durkacz BW, Hostomsky Z, Kumpf RA, Kyle S, et al: Anticancer chemosensitisation and radiosensitisation by the novel poly(ADP-ribose) polymerase-1 inhibitor AG14361. J Natl Cancer Inst 2004, 96:56-67.

247. Gilad O, Nabet BY, Ragland RL, Schoppy DW, Smith KD, Durham AC, Brown EJ: Combining ATR suppression with oncogenic Ras synergistically increases

genomic instability, causing synthetic lethality or tumourigenesis in a dosage-dependent manner. Cancer Res 2010, 70:9693-9702.

248. Murga M, Campaner S, Lopez-Contreras AJ, Toledo LI, Soria R, Montana MF, D'Artista L, Schleker T, Guerra C, Garcia E, et al: Exploiting oncogene-induced replicative stress for the selective killing of Myc-driven tumours. Nat Struct Mol Biol 2011, 18:1331-1335.

249. Schoppy DW, Ragland RL, Gilad O, Shastri N, Peters AA, Murga M, Fernandez-Capetillo O, Diehl JA, Brown EJ: Oncogenic stress sensitises murine cancers to hypomorphic suppression of ATR. J Clin Invest 2011.

250. Murga M, Bunting S, Montana MF, Soria R, Mulero F, Canamero M, Lee Y, McKinnon PJ, Nussenzweig A, Fernandez-Capetillo O: A mouse model of ATR-Seckel shows embryonic replicative stress and accelerated aging. Nat Genet 2009, 41:891-898.

251. Reaper PM, Griffiths MR, Long JM, Charrier JD, Maccormick S, Charlton PA, Golec JM, Pollard JR: Selective killing of ATM- or p53-deficient cancer cells through inhibition of ATR. Nat Chem Biol 2011, 7:428-430.

252. Morgan MA, Parsels LA, Zhao L, Parsels JD, Davis MA, Hassan MC, Arumugarajah S, Hylander-Gans L, Morosini D, Simeone DM, et al: Mechanism of radiosensitisation by the Chk1/2 inhibitor AZD7762 involves abrogation of the G2 checkpoint and inhibition of homologous recombinational DNA repair. Cancer Res 2010, 70:4972-4981.

253. Mitchell JB, Choudhuri R, Fabre K, Sowers AL, Citrin D, Zabludoff SD, Cook JA: In vitro and in vivo radiation sensitisation of human tumour cells by a novel checkpoint kinase inhibitor, AZD7762. Clin Cancer Res 2010, 16:2076-2084.

254. Lara PN, Jr., Mack PC, Synold T, Frankel P, Longmate J, Gumerlock PH, Doroshow JH, Gandara DR: The cyclin-dependent kinase inhibitor UCN-01 plus cisplatin in advanced solid tumours: a California cancer consortium phase I pharmacokinetic and molecular correlative trial. Clin Cancer Res 2005, 11:4444-4450.

255. Edelman MJ, Bauer KS, Jr., Wu S, Smith R, Bisacia S, Dancey J: Phase I and pharmacokinetic study of 7-hydroxystaurosporine and carboplatin in advanced solid tumours. Clin Cancer Res 2007, 13:2667-2674.

256. Welch S, Hirte HW, Carey MS, Hotte SJ, Tsao MS, Brown S, Pond GR, Dancey JE, Oza AM: UCN-01 in combination with topotecan in patients with advanced recurrent ovarian cancer: a study of the Princess Margaret Hospital Phase II consortium. Gynecol Oncol 2007, 106:305-310.

257. Jimeno A, Rudek MA, Purcell T, Laheru DA, Messersmith WA, Dancey J, Carducci MA, Baker SD, Hidalgo M, Donehower RC: Phase I and pharmacokinetic study of UCN-01 in combination with irinotecan in patients with solid tumours. Cancer Chemother Pharmacol 2008, 61:423-433.

258. Kortmansky J, Shah MA, Kaubisch A, Weyerbacher A, Yi S, Tong W, Sowers R, Gonen M, O'Reilly E, Kemeny N, et al: Phase I trial of the cyclin-dependent kinase inhibitor and protein kinase C inhibitor 7-hydroxystaurosporine in combination with Fluorouracil in patients with advanced solid tumours. J Clin Oncol 2005, 23:1875-1884.

259. Li D, Xie K, Wolff R, Abbruzzese JL: Pancreatic cancer. Lancet 2004, 363:1049-1057.

260. Raimondi S, Maisonneuve P, Lowenfels AB: Epidemiology of pancreatic cancer: an overview. Nat Rev Gastroenterol Hepatol 2009, 6:699-708.

261. Landi S: Genetic predisposition and environmental risk factors to pancreatic cancer: A review of the literature. Mutat Res 2009, 681:299-307.

262. Samuel N, Hudson TJ: The molecular and cellular heterogeneity of pancreatic ductal adenocarcinoma. Nat Rev Gastroenterol Hepatol 2012, 9:77-87.

263. Mahadevan D, Von Hoff DD: Tumour-stroma interactions in pancreatic ductal adenocarcinoma. Mol Cancer Ther 2007, 6:1186-1197.

264. Olive KP, Jacobetz MA, Davidson CJ, Gopinathan A, McIntyre D, Honess D, Madhu B, Goldgraben MA, Caldwell ME, Allard D, et al: Inhibition of Hedgehog signalling enhances delivery of chemotherapy in a mouse model of pancreatic cancer. Science 2009, 324:1457-1461.

265. Mantoni TS, Lunardi S, Al-Assar O, Masamune A, Brunner TB: Pancreatic Stellate Cells Radioprotect Pancreatic Cancer Cells through {beta}1-Integrin Signalling. Cancer Res, 71:3453-3458.

266. Jafari M, Abbruzzese JL: Pancreatic cancer: future outlook, promising trials, newer systemic agents, and strategies from the Gastrointestinal Intergroup Pancreatic Cancer Task Force. Surg Oncol Clin N Am 2004, 13:751-760, xi.

267. Ben-Josef E, Lawrence TS: Radiotherapy: the importance of local control in pancreatic cancer. Nat Rev Clin Oncol 2012, 9:9-10.

268. Lim KH, Chung E, Khan A, Cao D, Linehan D, Ben-Josef E, Wang-Gillam A: Neoadjuvant therapy of pancreatic cancer: the emerging paradigm? Oncologist 2012, 17:192-200.

269. Loehrer PJ, Sr., Feng Y, Cardenes H, Wagner L, Brell JM, Cella D, Flynn P, Ramanathan RK, Crane CH, Alberts SR, Benson AB, 3rd: Gemcitabine alone versus gemcitabine plus radiotherapy in patients with locally advanced pancreatic

cancer: an Eastern Cooperative Oncology Group trial. J Clin Oncol 2011, 29:4105-4112.

270. Brunner TB, Scott-Brown M: The role of radiotherapy in multimodal treatment of pancreatic carcinoma. Radiat Oncol 2010, 5:64.

271. Klautke G, Brunner TB: Radiotherapy in pancreatic cancer. Strahlenther Onkol 2008, 184:557-564.

272. Martin NE, Brunner TB, Kiel KD, DeLaney TF, Regine WF, Mohiuddin M, Rosato EF, Haller DG, Stevenson JP, Smith D, et al: A phase I trial of the dual farnesyltransferase and geranylgeranyltransferase inhibitor L-778,123 and radiotherapy for locally advanced pancreatic cancer. Clin Cancer Res 2004, 10:5447-5454.

273. Kisucka J, Butterfield CE, Duda DG, Eichenberger SC, Saffaripour S, Ware J, Ruggeri ZM, Jain RK, Folkman J, Wagner DD: Platelets and platelet adhesion support angiogenesis while preventing excessive hemorrhage. Proc Natl Acad Sci U S A 2006, 103:855-860.

274. Bernhard EJ, Stanbridge EJ, Gupta S, Gupta AK, Soto D, Bakanauskas VJ, Cerniglia GJ, Muschel RJ, McKenna WG: Direct evidence for the contribution of activated N-ras and K-ras oncogenes to increased intrinsic radiation resistance in human tumour cell lines. Cancer Res 2000, 60:6597-6600.

275. Gupta AK, Bakanauskas VJ, Cerniglia GJ, Cheng Y, Bernhard EJ, Muschel RJ, McKenna WG: The Ras radiation resistance pathway. Cancer Res 2001, 61:4278-4282.

276. Kim IA, Fernandes AT, Gupta AK, McKenna WG, Bernhard EJ: The influence of Ras pathway signalling on tumour radiosensitivity. Cancer Metastasis Rev 2004, 23:227-236.

277. Rudner J, Ruiner CE, Handrick R, Eibl HJ, Belka C, Jendrossek V: The Akt-inhibitor Erufosine induces apoptotic cell death in prostate cancer cells and increases the short term effects of ionizing radiation. Radiat Oncol 2010, 5:108.

278. Cengel KA, Voong KR, Chandrasekaran S, Maggiorella L, Brunner TB, Stanbridge E, Kao GD, McKenna WG, Bernhard EJ: Oncogenic K-Ras signals through epidermal growth factor receptor and wild-type H-Ras to promote radiation survival in pancreatic and colorectal carcinoma cells. Neoplasia 2007, 9:341-348.

279. Li HF, Kim JS, Waldman T: Radiation-induced Akt activation modulates radioresistance in human glioblastoma cells. Radiat Oncol 2009, 4:43.

280. McKenna WG, Muschel RJ, Gupta AK, Hahn SM, Bernhard EJ: Farnesyltransferase inhibitors as radiation sensitisers. Semin Radiat Oncol 2002, 12:27-32.

281. Bonner JA, Harari PM, Giralt J, Azarnia N, Shin DM, Cohen RB, Jones CU, Sur R, Raben D, Jassem J, et al: Radiotherapy plus cetuximab for squamous-cell carcinoma of the head and neck. N Engl J Med 2006, 354:567-578.

282. Seeliger H, Guba M, Kleespies A, Jauch KW, Bruns CJ: Role of mTOR in solid tumour systems: a therapeutical target against primary tumour growth, metastases, and angiogenesis. Cancer Metastasis Rev 2007, 26:611-621.

283. Carracedo A, Ma L, Teruya-Feldstein J, Rojo F, Salmena L, Alimonti A, Egia A, Sasaki AT, Thomas G, Kozma SC, et al: Inhibition of mTORC1 leads to MAPK pathway activation through a PI3K-dependent feedback loop in human cancer. J Clin Invest 2008, 118:3065-3074.

284. Abid MR, Guo S, Minami T, Spokes KC, Ueki K, Skurk C, Walsh K, Aird WC: Vascular endothelial growth factor activates PI3K/Akt/forkhead signalling in endothelial cells. Arterioscler Thromb Vasc Biol 2004, 24:294-300.

285. Wang X, Yue P, Chan CB, Ye K, Ueda T, Watanabe-Fukunaga R, Fukunaga R, Fu H, Khuri FR, Sun SY: Inhibition of mammalian target of rapamycin induces phosphatidylinositol 3-kinase-dependent and Mnk-mediated eukaryotic translation initiation factor 4E phosphorylation. Mol Cell Biol 2007, 27:7405-7413.

286. Maira SM, Stauffer F, Brueggen J, Furet P, Schnell C, Fritsch C, Brachmann S, Chene P, De Pover A, Schoemaker K, et al: Identification and characterization of NVP-BEZ235, a new orally available dual phosphatidylinositol 3-kinase/mammalian target of rapamycin inhibitor with potent in vivo antitumour activity. Mol Cancer Ther 2008, 7:1851-1863.

287. Cho DC, Cohen MB, Panka DJ, Collins M, Ghebremichael M, Atkins MB, Signoretti S, Mier JW: The efficacy of the novel dual PI3-kinase/mTOR inhibitor NVP-BEZ235 compared with rapamycin in renal cell carcinoma. Clin Cancer Res 2010, 16:3628-3638.

288. Liu TJ, Koul D, LaFortune T, Tiao N, Shen RJ, Maira SM, Garcia-Echevrria C, Yung WK: NVP-BEZ235, a novel dual phosphatidylinositol 3-kinase/mammalian target of rapamycin inhibitor, elicits multifaceted antitumour activities in human gliomas. Mol Cancer Ther 2009, 8:2204-2210.

289. Marone R, Erhart D, Mertz AC, Bohnacker T, Schnell C, Cmiljanovic V, Stauffer F, Garcia-Echeverria C, Giese B, Maira SM, Wymann MP: Targeting melanoma with dual phosphoinositide 3-kinase/mammalian target of rapamycin inhibitors. Mol Cancer Res 2009, 7:601-613.

290. Manara MC, Nicoletti G, Zambelli D, Ventura S, Guerzoni C, Landuzzi L, Lollini PL, Maira SM, Garcia-Echeverria C, Mercuri M, et al: NVP-BEZ235 as a new therapeutic option for sarcomas. Clin Cancer Res 2010, 16:530-540.

291. Chiarini F, Grimaldi C, Ricci F, Tazzari PL, Evangelisti C, Ognibene A, Battistelli M, Falcieri E, Melchionda F, Pession A, et al: Activity of the novel dual phosphatidylinositol 3-kinase/mammalian target of rapamycin inhibitor NVP-BEZ235 against T-cell acute lymphoblastic leukemia. Cancer Res 2010, 70:8097-8107.

292. Budach W, Taghian A, Freeman J, Gioioso D, Suit HD: Impact of stromal sensitivity on radiation response of tumours. J Natl Cancer Inst 1993, 85:988-993.

293. Cengel KA, McKenna WG: Molecular targets for altering radiosensitivity: lessons from Ras as a pre-clinical and clinical model. Crit Rev Oncol Hematol 2005, 55:103-116.

294. Carmeliet P: Angiogenesis in health and disease. Nat Med 2003, 9:653-660.

295. Baumann M, Krause M, Zips D, Eicheler W, Dorfler A, Ahrens J, Petersen C, Bruchner K, Hilberg F: Selective inhibition of the epidermal growth factor receptor tyrosine kinase by BIBX1382BS and the improvement of growth delay, but not local control, after fractionated irradiation in human FaDu squamous cell carcinoma in the nude mouse. Int J Radiat Biol 2003, 79:547-559.

296. Gurtner K, Deuse Y, Butof R, Schaal K, Eicheler W, Oertel R, Grenman R, Thames H, Yaromina A, Baumann M, Krause M: Diverse effects of combined radiotherapy and EGFR inhibition with antibodies or TK inhibitors on local tumour control and correlation with EGFR gene expression. Radiother Oncol 2011, 99:323-330.

297. Krause M, Prager J, Zhou X, Yaromina A, Dorfler A, Eicheler W, Baumann M: EGFR-TK inhibition before radiotherapy reduces tumour volume but does not improve local control: differential response of cancer stem cells and nontumourigenic cells? Radiother Oncol 2007, 83:316-325.

298. Zips D. Tumour growth and response to radiation. In: Joiner M vdKA, editors. Basic Clinical Radiobiology. London: Hodder Arnold; 2009. P. 78-101

299. Jain RK, Finn AV, Kolodgie FD, Gold HK, Virmani R: Antiangiogenic therapy for normalization of atherosclerotic plaque vasculature: a potential strategy for plaque stabilization. Nat Clin Pract Cardiovasc Med 2007, 4:491-502.

300. Fukumura D, Jain RK: Tumour microvasculature and microenvironment: targets for anti-angiogenesis and normalization. Microvasc Res 2007, 74:72-84.

301. Sorensen AG, Batchelor TT, Zhang WT, Chen PJ, Yeo P, Wang M, Jennings D, Wen PY, Lahdenranta J, Ancukiewicz M, et al: A "vascular normalization index" as potential mechanistic biomarker to predict survival after a single dose of cediranib in recurrent glioblastoma patients. Cancer Res 2009, 69:5296-5300.

302. Pluda JM: Tumour-associated angiogenesis: mechanisms, clinical implications, and therapeutic strategies. Semin Oncol 1997, 24:203-218.

303. Hanahan D, Folkman J: Patterns and emerging mechanisms of the angiogenic switch during tumourigenesis. Cell 1996, 86:353-364.

304. Carmeliet P, Collen D: Transgenic mouse models in angiogenesis and cardiovascular disease. J Pathol 2000, 190:387-405.

305. Folkman J, Hanahan D: Switch to the angiogenic phenotype during tumourigenesis. Princess Takamatsu Symp 1991, 22:339-347.

306. Matthews DJ, Yakes FM, Chen J, Tadano M, Bornheim L, Clary DO, Tai A, Wagner JM, Miller N, Kim YD, et al: Pharmacological abrogation of S-phase

checkpoint enhances the anti-tumour activity of gemcitabine in vivo. Cell Cycle 2007, 6:104-110.

307. Stathis A, Moore MJ: Advanced pancreatic carcinoma: current treatment and future challenges. Nat Rev Clin Oncol, 7:163-172.

308. Helleday T, Petermann E, Lundin C, Hodgson B, Sharma RA: DNA repair pathways as targets for cancer therapy. Nat Rev Cancer 2008, 8:193-204.

309. Begg AC, Stewart FA, Vens C: Strategies to improve radiotherapy with targeted drugs. Nat Rev Cancer, 11:239-253.

310. Negrini S, Gorgoulis VG, Halazonetis TD: Genomic instability--an evolving hallmark of cancer. Nat Rev Mol Cell Biol 2010, 11:220-228.

311. Ansari D, Rosendahl A, Elebro J, Andersson R: Systematic review of immunohistochemical biomarkers to identify prognostic subgroups of patients with pancreatic cancer. Br J Surg 2011, 98:1041-1055.

312. Okazaki T, Javle M, Tanaka M, Abbruzzese JL, Li D: Single nucleotide polymorphisms of gemcitabine metabolic genes and pancreatic cancer survival and drug toxicity. Clin Cancer Res, 16:320-329.

313. Toledo LI, Murga M, Zur R, Soria R, Rodriguez A, Martinez S, Oyarzabal J, Pastor J, Bischoff JR, Fernandez-Capetillo O: A cell-based screen identifies ATR inhibitors with synthetic lethal properties for cancer-associated mutations. Nat Struct Mol Biol 2011, 18:721-727.

314. Sangster-Guity N, Conrad BH, Papadopoulos N, Bunz F: ATR mediates cisplatin resistance in a p53 genotype-specific manner. Oncogene 2011, 30:2526-2533.

315. Nghiem P, Park PK, Kim Ys YS, Desai BN, Schreiber SL: ATR is not required for p53 activation but synergizes with p53 in the replication checkpoint. J Biol Chem 2002, 277:4428-4434.

316. Schoppy DW, Ragland RL, Gilad O, Shastri N, Peters AA, Murga M, Fernandez-Capetillo O, Diehl JA, Brown EJ: Oncogenic stress sensitises murine cancers to hypomorphic suppression of ATR. J Clin Invest 2012, 122:241-252.

317. Hammond EM, Giaccia AJ: The role of ATM and ATR in the cellular response to hypoxia and re-oxygenation. DNA Repair (Amst) 2004, 3:1117-1122.

318. Charrier J-D, Durrant S, Kay D, Knegtel R, MacCormick S, Mortimore M, .et al. Pyrazine derivatives useful as inhibitors of ATR kinase and their preparation and use in the treatment of diseases., WO 2010071837.

319. Rodriguez R, Meuth M: Chk1 and p21 cooperate to prevent apoptosis during DNA replication fork stress. Mol Biol Cell 2006, 17:402-412.

320. Sidi S, Sanda T, Kennedy RD, Hagen AT, Jette CA, Hoffmans R, Pascual J, Imamura S, Kishi S, Amatruda JF, et al: Chk1 suppresses a caspase-2 apoptotic response to DNA damage that bypasses p53, Bcl-2, and caspase-3. Cell 2008, 133:864-877.

321. Myers K, Gagou ME, Zuazua-Villar P, Rodriguez R, Meuth M: ATR and Chk1 suppress a caspase-3-dependent apoptotic response following DNA replication stress. PLoS Genet 2009, 5:e1000324.

322. Frankenberg-Schwager M, Gebauer A, Koppe C, Wolf H, Pralle E, Frankenberg D: Single-strand annealing, conservative homologous recombination, nonhomologous DNA end joining, and the cell cycle-dependent repair of DNA double-strand breaks induced by sparsely or densely ionizing radiation. Radiat Res 2009, 171:265-273.

323. Vispe S, Cazaux C, Lesca C, Defais M: Overexpression of Rad51 protein stimulates homologous recombination and increases resistance of mammalian cells to ionizing radiation. Nucleic Acids Res 1998, 26:2859-2864.

324. Harikumar KB, Kunnumakkara AB, Sethi G, Diagaradjane P, Anand P, Pandey MK, Gelovani J, Krishnan S, Guha S, Aggarwal BB: Resveratrol, a multitargeted agent, can enhance antitumour activity of gemcitabine in vitro and in orthotopic mouse model of human pancreatic cancer. Int J Cancer 2010, 127:257-268.

325. Huguet F, Andre T, Hammel P, Artru P, Balosso J, Selle F, Deniaud-Alexandre E, Ruszniewski P, Touboul E, Labianca R, et al: Impact of chemoradiotherapy after disease control with chemotherapy in locally advanced pancreatic adenocarcinoma in GERCOR phase II and III studies. J Clin Oncol 2007, 25:326-331.

326. Peasland A, Wang LZ, Rowling E, Kyle S, Chen T, Hopkins A, Cliby WA, Sarkaria J, Beale G, Edmondson RJ, Curtin NJ: Identification and evaluation of a potent novel ATR inhibitor, NU6027, in breast and ovarian cancer cell lines. Br J Cancer 2011, 105:372-381.

327. Wheeler DL, Dunn EF, Harari PM: Understanding resistance to EGFR inhibitors-impact on future treatment strategies. Nat Rev Clin Oncol 2010, 7:493-507.

328. Zitzmann K, Ruden J, Brand S, Goke B, Lichtl J, Spottl G, Auernhammer CJ: Compensatory activation of Akt in response to mTOR and Raf inhibitors - a rationale for dual-targeted therapy approaches in neuroendocrine tumour disease. Cancer Lett 2010, 295:100-109.

329. Slichenmyer WJ, Nelson WG, Slebos RJ, Kastan MB: Loss of a p53-associated G1 checkpoint does not decrease cell survival following DNA damage. Cancer Res 1993, 53:4164-4168.

330. Kastan MB, Bartek J: Cell-cycle checkpoints and cancer. Nature 2004, 432:316-323.

331. Klokov D, MacPhail SM, Banath JP, Byrne JP, Olive PL: Phosphorylated histone H2AX in relation to cell survival in tumour cells and xenografts exposed to single and fractionated doses of X-rays. Radiother Oncol 2006, 80:223-229.

332. Menegakis A, Yaromina A, Eicheler W, Dorfler A, Beuthien-Baumann B, Thames HD, Baumann M, Krause M: Prediction of clonogenic cell survival curves based on the number of residual DNA double strand breaks measured by gammaH2AX staining. Int J Radiat Biol 2009, 85:1032-1041.

333. Mahrhofer H, Burger S, Oppitz U, Flentje M, Djuzenova CS: Radiation induced DNA damage and damage repair in human tumour and fibroblast cell lines assessed by histone H2AX phosphorylation. Int J Radiat Oncol Biol Phys 2006, 64:573-580.

334. Mukherjee B, Tomimatsu N, Amancherla K, Camacho CV, Pichamoorthy N, Burma S: The dual PI3K/mTOR inhibitor NVP-BEZ235 is a potent inhibitor of ATM- and DNA-PKCs-mediated DNA damage responses. Neoplasia 2012, 14:34-43.

335. Choudhury A, Cuddihy A, Bristow RG: Radiation and new molecular agents part I: targeting ATM-ATR checkpoints, DNA repair, and the proteasome. Semin Radiat Oncol 2006, 16:51-58.

336. Liu P, Cheng H, Roberts TM, Zhao JJ: Targeting the phosphoinositide 3-kinase pathway in cancer. Nat Rev Drug Discov 2009, 8:627-644.

337. Baumann M, Krause M, Hill R: Exploring the role of cancer stem cells in radioresistance. Nat Rev Cancer 2008, 8:545-554.

338. Calabrese C, Poppleton H, Kocak M, Hogg TL, Fuller C, Hamner B, Oh EY, Gaber MW, Finklestein D, Allen M, et al: A perivascular niche for brain tumour stem cells. Cancer Cell 2007, 11:69-82.

339. Brunner TB, Kunz-Schughart LA, Grosse-Gehling P, Baumann M: Cancer stem cells as a predictive factor in radiotherapy. Semin Radiat Oncol 2012, 22:151-174.

340. Hambardzumyan D, Becher OJ, Rosenblum MK, Pandolfi PP, Manova-Todorova K, Holland EC: PI3K pathway regulates survival of cancer stem cells residing in the perivascular niche following radiation in medulloblastoma in vivo. Genes Dev 2008, 22:436-448.

341. Kong D, Okamura M, Yoshimi H, Yamori T: Antiangiogenic effect of ZSTK474, a novel phosphatidylinositol 3-kinase inhibitor. Eur J Cancer 2009, 45:857-865.

342. Garlich JR, De P, Dey N, Su JD, Peng X, Miller A, Murali R, Lu Y, Mills GB, Kundra V, et al: A vascular targeted pan phosphoinositide 3-kinase inhibitor prodrug, SF1126, with antitumour and antiangiogenic activity. Cancer Res 2008, 68:206-215.

343. Fajardo LF: The pathology of ionizing radiation as defined by morphologic patterns. Acta Oncol 2005, 44:13-22.

344. Fajardo LF: Is the pathology of radiation injury different in small vs large blood vessels? Cardiovasc Radiat Med 1999, 1:108-110.

345. Fokas E, Hanze J, Kamlah F, Eul BG, Lang N, Keil B, Heverhagen JT, Engenhart-Cabillic R, An H, Rose F: Irradiation-dependent effects on tumour perfusion and endogenous and exogenous hypoxia markers in an A549 xenograft model. Int J Radiat Oncol Biol Phys 2010, 77:1500-1508.

346. Song CW, Levitt SH: Quantitative study of vascularity in Walker carcinoma 256. Cancer Res 1971, 31:587-589.

347. Song CW, Sung JH, Clement JJ, Levitt SH: Vascular changes in neuroblastoma of mice following x-irradiation. Cancer Res 1974, 34:2344-2350.

348. Denekamp J: Vascular endothelium as the vulnerable element in tumours. Acta Radiol Oncol 1984, 23:217-225.

349. Shahab N, Haider S, Doll DC: Vascular toxicity of antineoplastic agents. Semin Oncol 2006, 33:121-138.

350. Torrisi JM, Schwartz LH, Gollub MJ, Ginsberg MS, Bosl GJ, Hricak H: CT findings of chemotherapy-induced toxicity: what radiologists need to know about the clinical and radiologic manifestations of chemotherapy toxicity. Radiology 2011, 258:41-56.

351. Slamon DJ, Leyland-Jones B, Shak S, Fuchs H, Paton V, Bajamonde A, Fleming T, Eiermann W, Wolter J, Pegram M, et al: Use of chemotherapy plus a monoclonal antibody against HER2 for metastatic breast cancer that overexpresses HER2. N Engl J Med 2001, 344:783-792.

352. Allegra CJ, Jessup JM, Somerfield MR, Hamilton SR, Hammond EH, Hayes DF, McAllister PK, Morton RF, Schilsky RL: American Society of Clinical Oncology provisional clinical opinion: testing for KRAS gene mutations in patients with metastatic colorectal carcinoma to predict response to anti-epidermal growth factor receptor monoclonal antibody therapy. J Clin Oncol 2009, 27:2091-2096.

353. Saal LH, Johansson P, Holm K, Gruvberger-Saal SK, She QB, Maurer M, Koujak S, Ferrando AA, Malmstrom P, Memeo L, et al: Poor prognosis in carcinoma is associated with a gene expression signature of aberrant PTEN tumour suppressor pathway activity. Proc Natl Acad Sci U S A 2007, 104:7564-7569.

354. Cloughesy TF, Yoshimoto K, Nghiemphu P, Brown K, Dang J, Zhu S, Hsueh T, Chen Y, Wang W, Youngkin D, et al: Antitumour activity of rapamycin in a Phase I trial for patients with recurrent PTEN-deficient glioblastoma. PLoS Med 2008, 5:e8.

355. Sartore-Bianchi A, Martini M, Molinari F, Veronese S, Nichelatti M, Artale S, Di Nicolantonio F, Saletti P, De Dosso S, Mazzucchelli L, et al: PIK3CA mutations in colorectal cancer are associated with clinical resistance to EGFR-targeted monoclonal antibodies. Cancer Res 2009, 69:1851-1857.

356. Perrone F, Lampis A, Orsenigo M, Di Bartolomeo M, Gevorgyan A, Losa M, Frattini M, Riva C, Andreola S, Bajetta E, et al: PI3KCA/PTEN deregulation contributes to impaired responses to cetuximab in metastatic colorectal cancer patients. Ann Oncol 2009, 20:84-90.

357. Berns K, Horlings HM, Hennessy BT, Madiredjo M, Hijmans EM, Beelen K, Linn SC, Gonzalez-Angulo AM, Stemke-Hale K, Hauptmann M, et al: A functional genetic approach identifies the PI3K pathway as a major determinant of trastuzumab resistance in breast cancer. Cancer Cell 2007, 12:395-402.

358. O'Brien C, Wallin JJ, Sampath D, GuhaThakurta D, Savage H, Punnoose EA, Guan J, Berry L, Prior WW, Amler LC, et al: Predictive biomarkers of sensitivity to the phosphatidylinositol 3' kinase inhibitor GDC-0941 in breast cancer preclinical models. Clin Cancer Res 2010, 16:3670-3683.

359. Bendell JC, Rodon J, Burris HA, de Jonge M, Verweij J, Birle D, Demanse D, De Buck SS, Ru QC, Peters M, et al: Phase I, dose-escalation study of BKM120, an oral pan-Class I PI3K inhibitor, in patients with advanced solid tumours. J Clin Oncol 2012, 30:282-290.

360. Yap TA, Yan L, Patnaik A, Fearen I, Olmos D, Papadopoulos K, Baird RD, Delgado L, Taylor A, Lupinacci L, et al: First-in-man clinical trial of the oral pan-AKT inhibitor MK-2206 in patients with advanced solid tumours. J Clin Oncol 2011, 29:4688-4695.

361. Van Meir EG, Hadjipanayis CG, Norden AD, Shu HK, Wen PY, Olson JJ: Exciting new advances in neuro-oncology: the avenue to a cure for malignant glioma. CA Cancer J Clin 2010, 60:166-193.

362. Chalmers AJ, Lakshman M, Chan N, Bristow RG: Poly(ADP-ribose) polymerase inhibition as a model for synthetic lethality in developing radiation oncology targets. Semin Radiat Oncol 2010, 20:274-281.

363. Hammond EM, Kaufmann MR, Giaccia AJ: Oxygen sensing and the DNA-damage response. Curr Opin Cell Biol 2007, 19:680-684.

364. Nordlund P, Reichard P: Ribonucleotide reductases. Annu Rev Biochem 2006, 75:681-706.

365. Pires IM, Bencokova Z, Milani M, Folkes LK, Li JL, Stratford MR, Harris AL, Hammond EM: Effects of acute versus chronic hypoxia on DNA damage responses and genomic instability. Cancer Res 2010, 70:925-935.

366. Hammond EM, Dorie MJ, Giaccia AJ: Inhibition of ATR leads to increased sensitivity to hypoxia/reoxygenation. Cancer Res 2004, 64:6556-6562.

367. Hammond EM, Dorie MJ, Giaccia AJ: ATR/ATM targets are phosphorylated by ATR in response to hypoxia and ATM in response to reoxygenation. J Biol Chem 2003, 278:12207-12213.

368. Harada H, Inoue M, Itasaka S, Hirota K, Morinibu A, Shinomiya K, Zeng L, Ou G, Zhu Y, Yoshimura M, et al: Cancer cells that survive radiation therapy acquire HIF-1 activity and translocate towards tumour blood vessels. Nat Commun 2012, 3:783.

369. Overgaard J: Hypoxic radiosensitisation: adored and ignored. J Clin Oncol 2007, 25:4066-4074.

370. Workman P, Aboagye EO, Balkwill F, Balmain A, Bruder G, Chaplin DJ, Double JA, Everitt J, Farningham DA, Glennie MJ, et al: Guidelines for the welfare and use of animals in cancer research. Br J Cancer 2010, 102:1555-1577.

371. Trier JS, Browning TH: Morphologic response of the mucosa of human small intestine to x-ray exposure. J Clin Invest 1966, 45:194-204.